# UNIVERSITA' DEGLI STUDI DI NAPOLI FEDERICO II

## XXXIII CICLO DEL DOTTORATO DI RICERCA IN BIOLOGIA

# Response and tolerance to pollutants by plants: perspectives in biomonitoring and phytoremediation

Settore scientifico-disciplinare:
BIO/01 - BOTANICA GENERALE


DOTTORANDO
**Maria Cristina Sorrentino**

COORDINATORE
**Prof.re Salvatore Cozzolino**

SUPERVISORE DI TESI
**Prof.ssa Valeria Spagnuolo**

# INDEX

Ecological Indicators 108 (2020) 105727
https:// doi.org/10.1016/j.ecolind.2019.105727.

# Abstract

Environmental pollution represents one of the modern challenges for scientific community; researchers should indeed, increase resources to improve green and low-cost technologies for monitoring compromised ecosystems, and developing new eco-friendly methodologies for their recovery. Plant organs and associated microbiota interact with pollutants in the phyllosphere and rhizosphere to remediate (or mitigate the effects) of contaminants not only in soils but also in the air. This makes phytoremediation one of the possible green technique in the control of air pollution. Phytoremediation is indeed not only considered as a method to return soils to agriculture for food and feed production, but also as a technique to control air pollution by avoiding the resuspension of contaminated PM (Particulate Matter). This consideration makes it clear that phytoremediation and air biomonitoring represent two interconnected aspects in the framework of plant-abiotic stress interaction. These two related aspects represent the research area of my Ph.D. project.

As for soil phytoremediation I carried out several experiments on *Cynara cardunculus* L. var. *altilis* DC. Particularly, three cultivars were grown on a gardening soil added with Cd and Pb, on industrial soil containing Cd and Pb, and in hydroponics contaminated with the same metals. Different behaviors were observed under metal stress compared to the control plants, with some cultivar-specific responses. Although all cultivars could uptake significant amounts of metals, only *C. cardunculus* cv Spagnolo counteracted metal stress preserving chloroplast ultrastructure and cell morphology. Moreover, the same cultivar showed a significant increase in stomata number, with subsequent enhancement of gas exchanges and net photosynthesis. By contrast, in the other cultivars analyzed, Cd and Pb uptake were coupled to severe ultrastructural alterations, a decrease in life span, pigment content, stomata number and photosynthetic activity. Finally, the sequential elution technique on the three cultivars grown in hydroponics was carried out to establish the amount of metal fractions in the apoplast and symplast compartments. The results indicated that a low fraction of Cd and Pb was chelated by EDTA; therefore, a high quantity of metals could potentially reach the cytoplasm inducing all observed responses. Furthermore, a lower translocation factor for both metals was calculated in hydroponics compared to soil; this result support the idea that root hairs, developed in hydroponics only under metal stress, act as metal sequestration sites.

Regarding air biomonitoring, the aim of my PhD project was to investigate new applicative aspects of the moss- and lichen-bags technique. Since numerous contributions exist focused on metal uptake, but few were directed to organic pollutants so far, I tested the ability of moss and lichen transplants exposed alive or oven-devitalized, to entrap PAHs (Polycyclic Aromatic Hydrocarbons) in summer and winter. The results indicate that lichen performed better than moss due to its thallus morphology storing and preserving the low molecular weight PAH fraction (not linked to PM) from photodegradation, especially in summer. In addition, oven devitalization did not affect PAH accumulation, since both biomonitors spent their life mainly in cryptobiosis, even

when exposed alive and sprayed with water; by contrast, devitalization, lowering PAH pre-exposure content allowed to estimate even low pollution levels.
The other experiments on biomonitoring of air quality were carried out at Antwerp University, in the laboratory of prof. Roeland Samson. Moss bags have been used since '70s, and are regarded as a useful, versatile tool for biomonitoring of air quality, but almost all published papers concern exposure in fixed points in open air. Therefore, the novelty of my research was to investigate indoor metal pollution and metal uptake in moss-bags exposed in moving systems (bicycles). In both experiments I evaluated moss metal contents by ICP-MS (Inductively Coupled Plasma-Mass Spectrometry) and magnetic properties of moss by saturated isothermal remanent magnetization (SIRM). The indoor-outdoor moss-bags exposure, carried out in parallel at Naples and Antwerp, showed outdoor element concentrations were significantly higher than indoors, and that most of indoor pollution derived from outdoor sources, even if some elements (e.g., Ni and Ti) were related to specific indoor fonts (e.g., cooking and house cleaning products). The short residence time (8-12h), prevalent in Belgium, lowered the ventilation frequency by opening windows, preserving indoor environments from outdoor metal contamination. Bike experiments carried out by six volunteers plus me in Antwerp, demonstrated that moss bags could entrap PM and related elements, when exposed in moving systems. Their well-known ability to discriminate specific land use classes was confirmed, since different metal uptakes and fluxes were observed along green, urban and industrial routes. Furthermore, daily flux calculation evidenced an exposure to air metal pollution 10-25 folds higher in moving systems compared to fixed positions (comparison with fixed outdoor exposure points). In both experimental designs, SIRM proved a useful, sample-conservative method for predicting metal-pollution level before chemical analysis. The evaluation of air quality outdoors, indoors and in fixed and moving conditions can provide a complete picture of human exposure to atmospheric elemental pollution.

## Riassunto

L'inquinamento ambientale rappresenta una delle sfide moderne per la comunità scientifica; i ricercatori dovrebbero infatti aumentare le risorse per migliorare le tecnologie verdi e a basso costo per il monitoraggio degli ecosistemi compromessi e sviluppare nuove metodologie eco-compatibili per il loro recupero. Gli organi delle piante e il microbiota associato interagiscono con gli inquinanti sia nella fillosfera che nella rizosfera realizzando sistemi di biorimedio o mitigazione sia nei suoli che in atmosfera; in quest'ottica, il fitorisanamento si inquadra come una delle possibili tecniche verdi nel controllo dell'inquinamento atmosferico. Il fitorisanamento, infatti, non è solo considerato come un metodo per restituire i suoli all'agricoltura per la produzione di alimenti e mangimi, ma anche come una tecnica per controllare l'inquinamento atmosferico evitando la risospensione del PM contaminato. Questa considerazione rende chiaro come il fitorisanamento e il biomonitoraggio dell'aria siano

due aspetti interconnessi nell'ambito delle interazioni piante-stress abiotici. Questi due aspetti correlati rappresentano l'area di analisi del mio progetto di dottorato di ricerca.
Per quanto riguarda il fitorisanamento, ho effettuato diversi esperimenti su *Cynara cardunculus* L. var. *altilis* DC. Tre cultivar sono state coltivate su un terreno da giardinaggio con l'aggiunta di Cd e Pb, su terreno industriale contenente elevate quantità di Cd e Pb, e in idroponica contaminata con gli stessi metalli. Sono stati osservati comportamenti diversi in condizione di stress indotto da metalli rispetto alle piante di controllo, con alcune risposte cultivar specifiche. Sebbene tutte le cultivar fossero in grado di assorbire quantità significative di metalli, solo *C. cardunculus* cv Spagnolo contrastava lo stress metallico preservando l'ultrastruttura dei cloroplasti e la morfologia cellulare. Inoltre, la stessa cultivar ha mostrato un aumento significativo del numero di stomi, con conseguente potenziamento degli scambi gassosi e fotosintesi netta. Al contrario, nelle altre cultivar analizzate, l'assorbimento di Cd e Pb era accoppiato a gravi alterazioni ultrastrutturali, diminuzione della durata della vita, del contenuto di pigmenti e del numero di stomi, con conseguente riduzione dell'attività fotosintetica. Infine, mediante la tecnica di eluizione sequenziale sulle tre cultivar coltivate in idroponica, è stato possibile stabilire la distribuzione del Cd e del Pb nei compartimenti apoplasto e simplasto. I risultati hanno indicato che una bassa frazione di Cd e Pb era chelata con EDTA; pertanto, un'elevata quantità di metalli, poteva muoversi via simplasto, e quindi nel citoplasma inducendo tutte le risposte osservate. Inoltre, è stato calcolato un fattore di traslocazione inferiore per entrambi i metalli in coltura idroponica rispetto al suolo; questo risultato supporta l'idea che i peli radicali, sviluppati in coltura idroponica solo in presenza del metallo, possano agire come siti di sequestro del metallo stesso.
Per quanto riguarda il biomonitoraggio della qualità dell'aria, l'obiettivo del mio progetto di dottorato è stato quello di indagare nuovi aspetti applicativi della tecnica delle moss- e lichen-bags. Dato che molti lavori trattano l'accumulo di metalli, e relativamente pochi l'accumulo di inquinanti organici, ho testato la capacità di muschi e licheni esposti idratati o devitalizzati in bags, di intrappolare gli IPA (Idrocarburi Policiclici Aromatici) in estate e in inverno. I risultati indicano che il lichene mostrava accumuli significativamente maggiori del muschio grazie al tallo pluristratificato, in grado di conservare la frazione di IPA non legata al PM (cioè quelli a basso peso molecolare). L'accumulo era molto maggiore in inverno, poiché le temperature basse e l'irraggiamento scarso limitano la fotodegradazione di questi composti. Inoltre, la devitalizzazione in stufa non influenzava l'accumulo di IPA, poiché entrambi i biomonitor trascorrono la maggior parte del tempo in criptobiosi, anche quando esposti vivi e spruzzati con acqua. La devitalizzazione, in più, abbassando il contenuto di IPA nel materiale pre-esposizione, consente la possibilità di rilevare livelli anche bassi di inquinamento.
Gli altri esperimenti sul biomonitoraggio della qualità dell'aria sono stati effettuati all'estero, presso l'Università di Anversa, nel laboratorio del prof. Roeland Samson. La tecnica delle moss bags, nonostante sia utilizzata sin dagli anni '70, è stata finora applicata essenzialmente seguendo un protocollo che prevede l'esposizione in punti fissi all'aria aperta. L'aspetto innovativo della mia ricerca è stato quello di utilizzare le moss-bags per studiare l'inquinamento da metalli in ambienti indoor e in sistemi in movimento

(biciclette); in entrambi i modelli di esposizione ho valutato il contenuto elementale dei muschi mediante ICP-MS (Inductively Coupled Plasma-Mass Spectrometry) e le proprietà magnetiche del muschio mediante magnetizzazione isotermica residua di saturazione (SIRM). L'esposizione indoor-outdoor delle moss-bags, effettuata in parallelo a Napoli e Anversa, ha mostrato che in entrambe le città gli accumuli outdoor erano significativamente maggiori di quelli indoor; la maggior parte dell'inquinamento indoor derivava da fonti esterne, anche se alcuni elementi (es. Ni e Ti) erano legati a specifiche fonti interne (es. pulire casa, cucinare). Il breve tempo di residenza giornaliero (8-12h), prevalente in Belgio, riduceva la frequenza di ventilazione, preservando gli ambienti interni dalla contaminazione elementale esterna. Nell'esperimento con le biciclette, tre moss-bags riempite con *Hypnum cupressiforme* sono state trasportate da sei volontari più me ad Anversa lungo percorsi urbani, industriali e "verdi". I risultati dimostrano che le moss-bags legate alle bici, erano in grado di intercettare il PM e gli elementi ad esso legati. La loro ben nota capacità di discriminare specifiche classi di uso del suolo è stata confermata, poiché sono stati osservati accumuli e flussi giornalieri degli elementi crescenti a partire dai percorsi verdi, poi urbani e infine industriali. Inoltre, il calcolo del flusso giornaliero ha evidenziato un'esposizione all'inquinamento atmosferico da metalli 10-25 volte maggiore nel sistema in movimento (cioè la bicicletta) rispetto alle posizioni fisse (punti fissi di esposizione all'aperto). In entrambi gli esperimenti, il SIRM si è dimostrato un metodo conservativo e utile per prevedere il livello di inquinamento da metalli prima dell'analisi chimica. La valutazione della qualità dell'aria all'esterno, all'interno e in condizioni fisse e in movimento può aiutarci a fornire un quadro più completo dell'esposizione umana all'inquinamento da metalli.

# Introduction

During the last three decades, the World is experiencing an extraordinary growth, especially in the urban human population, which is expected to increase 2.3% per year up to 2030 (Brockerhoff, 2000; United Nations, 2000, 2004; UNFPA, 2004). Population growth coupled with rapid economic development involves an increase in energy consumption and in environmental pollution (Gurjar et al., 2012). This growing urbanization, accompanied by the development of technologies aimed at expanding the economies of nations, has caused severe environmental problems (Lee et al. 2020). Urbanization involves industrialization and massive vehicular traffic, both of which release pollutants to air, soil, and water. Parallel to the population growth, farmland activities have also seen an increasingly massive use of mineral fertilizers, herbicides, and additives for animal feeds, and in some cases contaminated water for irrigation, with a global increase of the pollution level in all ecosystems (Foley et al., 2005; Motuzova et al., 2014). The massive human intervention creates unfavourable or stressful conditions for the growth and development of living organisms, including plants (Zhu, 2016). Among the adverse environmental conditions the plants face, are biotic stress, such as pathogen infections or herbivore attacks, and abiotic stress, such as drought, radiation, extreme temperatures, nutrient deficiency, and xenobiotic substances, such as heavy metals. Environmental pollutants are therefore regarded as abiotic stressors for living organisms. It has been demonstrated that climate changes, which often appear as a continuous swing between extreme weather conditions, intensify abiotic stresses (Fedoroff et al., 2010).

Based on all above, tackling environmental pollution represents one of the modern challenges for the scientific community; researchers should increase resources and dedicate projects to improve green and low-cost technologies for monitoring compromised ecosystems to develop new eco-friendly methodologies for their recovery. In this perspective, plants have a prominent role, as they possess unique and winning characteristics both for detecting and facing environmental pollution. The sessile habit, in addition to their natural ability to absorb nutrients from the soil or to intercept them by the air through dry and wet depositions, thanks to the wide surface exposed to atmosphere, make them particularly suitable in the remediation of polluted soils (and growth matrices) and in the assessment of air quality. For example, the absence of roots and a leaf cuticle,

and the ability to intercept PM (e.g., Di Palma et al., 2017), make the cryptogams well suited as biomonitors of air quality, particularly for PM-linked pollutants, (e.g., Capozzi et al., 2021). On the other hand, in vascular plants, the hydrophobic waxes and cuticle of the leaves can accumulate airborne organic pollutants, whereas stomata represent a further route for both gaseous and PM-linked atmospheric pollutants towards the mesophyll (Desalme et al., 2013). Roots can absorb/adsorb pollutants from soil, or simply entrap soil particles, avoiding their resuspension, and thus reducing the level of atmospheric pollution. As plants are sessile, they cannot escape from environmental contamination; therefore, they have developed a variety of mechanisms to overcome biotic and abiotic stresses by avoidance and/or adaptation.

All these considerations prove that plants can be profitably used in phytoremediation, as well as in biomonitoring.

*Phytoremediation*

In a broad sense, the use of plants to remediate pollutants from water, soil, and air is commonly referred to as phytoremediation (Cunningham et al., 1995). However, in a more shared point of view, phytoremediation is a set of agronomic techniques to decrease or degrade pollutants in soils using plants, soil amendments and microbial associations (Nedjimi, 2021). Soil is regarded as non-renewable resource, since the time between its consumption and regeneration is very long; this justifies the attention of the scientific community to all issues concerning the protection of this resource and the recovery of polluted or degraded soils. Differently from physical-chemical techniques, phytoremediation does not alter soil properties and its microflora; therefore, it represents a green technology to recover soil fertility, especially in low polluted soils, or limit the expansion of contaminated areas, or avoid polluted soil and dust resuspension (Lee et al., 2020). The most common type of phytoremediation is phytoextraction, the success of which depends on several plant characteristics, being the most important ones the ability to produce large quantities of biomass and the capacity to accumulate large amounts of pollutants in the shoot tissue without visible symptoms. Plants that can accumulate high concentrations of a given pollutants in their shoots are called hyperaccumulators. These plants should not include food crops; moreover, they should have high tolerance to a given pollutant, and resistance to diseases and pests; also, they should be unattractive to

animals, minimizing the risk of transferring the pollutant to higher trophic levels of the food chain (Thangavel and Subhuram, 2004).

Among pollutants, heavy metals are becoming a serious issue worldwide with increasing industrialization and subsequent alteration of the natural biogeochemical cycles. Elements can be released to the atmosphere by natural sources, soil erosion and volcanic emissions; but they can also derive from anthropogenic sources. Unlike organic substances, heavy metals are essentially non-biodegradable and therefore accumulate in the environment posing a risk to the environmental and human health. Moreover, their accumulation in the tissues of living organisms (bio- accumulation) is followed by an increase in their concentrations while passing from lower to higher trophic levels (biomagnification) (Khan et al., 2015). Cadmium (Cd) and lead (Pb) are among the most widespread metal pollutants worldwide (Su et al., 2014). Their increase in the environment results from many human activities including exploitation of metal-ores (i.e., mineral mines) and soil-applied chemicals, such as fertilizers (Alloway, 1995; Sanità di Toppi and Gabbrielli, 1999). Pb naturally occurs in soils with concentrations between 20 and 50 mg $kg^{-1}$ (Nriagu, 1978); however, soils containing less than 100 mg $kg^{-1}$ Pb are regarded as non-polluted soils (Meggeson and Hall, 1999).

In plants, the exposition to heavy metals, and especially Cd, results in a severe reduction of plant growth and development because of a decline of photosynthetic activity (Arena et al., 2017). This damage my occur both directly, i.e., through alteration of photosystems, and by indirect mechanisms, e.g., through alteration of stomata function, damages to chloroplasts ultrastructure, decrease in pigment content, variation of thylakoid composition (Chandra and Kang, 2016; Molas, 2002; Skórzyńska-Polit and Baszyński, 1997). In addition to growth pattern and photosynthesis alterations, metals in plants can induce genotoxicity (e.g., Al-Qurainy et al., 2010; Sorrentino et al., 2017), as they intercalate with DNA bases, and oxidative stress (León et al. 2002; Boominathan and Doran, 2003).

The selection of a plant species for phytoremediation of metal polluted soils involves a deep knowledge of the mechanisms at the basis of plant resistance against metal stress.

Among plants used in phytoremediation, *C. cardunculus* L. is a perennial species, belonging to the family of Asteraceae, particularly well adapted to the Mediterranean environment (Zohary and Basnizki, 1975; Raccuia et al., 2004). In particular, *C. cardunculus* L. var. *altilis* DC. (leafy or domestic cardoon), is characterized by an intensive growth with a high production of epigeal biomass, roots and seed used for green

chemistry (bioenergy and biofuel) (e.g., Raccuia and Melilli, 2007, 2010; Toscano et al.2016). Based on these traits, and experimental trials carried out on a panel of species known for their resistance under metal stress, cardoon was chosen for the experiments performed during my PhD project.

*Biomonitoring*

Nowadays air quality assessment is among the most pressing topics of the applied research, to be addressed by scientists to the development of appropriate and reliable methodologies and protocols, on which ground new specific policies. In fact, human health is strongly related to air pollution, especially in industrialized and emerging countries. World Health Organization (WHO) showed that air pollution exposure produced 7 million deaths in 2012 (WHO, 2014). The WHO (2014) affirmed that air pollution is the world's largest environmental health risk, highly responsible of heart diseases, lung cancer, and respiratory pathologies. Although air pollution sources might be from natural sources most of the pollution derives from anthropogenic fonts such as industrial processes, burning of fossil fuel, waste treatment, construction, and farmland activity (Sharma et al., 2018) Regardless their origin, air pollutants consist of primary and secondary pollutants. The first are emitted as such into the atmosphere, directly from a source; for example, particulate matter (PM), carbon monoxide (CO) and sulphur dioxide ($SO_2$). Secondary pollutants derive from the reaction of the primary ones with other compounds present in the atmosphere; for example, oxygen, which can produce ozone ($O_3$), carbon dioxide ($CO_2$) and sulphur trioxide ($SO_3$) (Sitaras and Siskos, 2008). Monitoring of air quality is inherently difficult to achieve because the composition of the air changes according to spatial and temporal dynamics that are often sudden and unpredictable. Air monitoring is currently carried out by automatic devices; however, they can measure only few kinds of pollutants and due to the high costs, a dense network of monitoring stations is practically impossible to implement. Plant biomonitors, and particularly cryptogams, have been successfully used since 70s, both as bioindicators and as bioaccumulators of airborne pollutants. Mosses and lichens are well suited to air biomonitoring, since they lack roots and cuticle and therefore, they absorb nutrients in form of wet and dry atmospheric depositions through the entire thallus surface. In addition, these organisms have high capacity to intercept and retain particulate matter

and PM-linked pollutants, such as elements and high molecular weight PAHs (Capozzi et al., 2021). They allow to set up dense monitoring webs and measure numerous pollutants. Besides, they prove a versatile tool, providing the opportunity to choose flexible experimental designs by using either native or transplanted plant species (i.e., passive or active biomonitoring). The use of transplants has given a significant boost to biomonitoring, allowing the measurement of air pollution level in highly impacted areas, such as those in proximity of industrial plants (De Agostini et al., 2020) where spontaneous cryptogams are usually absent, and even in confined environments (Vuković et al., 2014). In the last decades, biomonitoring by cryptogams has achieved remarkable innovation and several aspects have been clarified regarding the traits of a good biomonitor and the exposure conditions of transplants.

The international team participating in the FP7 Mossclone project (www.mossclone.eu) selected the moss *Sphagnum palustre* L. among some candidate species, based on its element uptake capacity; then grew and characterized a *S. palustre* clone to be used in several active biomonitoring surveys. Several parameters were tested during the exposure of the moss bags (i.e., exposure height and time, moss density in the bag, the shape of the bag and mesh size). The results showed that only exposure time and moss density significantly affected element uptake. Some tests were also performed to evaluate the uptake of polycyclic aromatic hydrocarbons (PAHs), showing that *S. palustre* clone could accumulate all the ring-based classes of PAHs (Aboal et al., 2020). Compared to metals, organic pollutants have been scantly analyzed so far (e.g., Dolegowska and Migaszewski, 2011; Ötvös et al., 2004); among the organic pollutants, PAHs are widely distributed and considered as persistent organic contaminants in the environment (Ravindra et al., 2008). Although a small fraction of PAHs can move from the soil to plant tissue, most of airborne PAHs enter vascular plants through the leaf surface, via stomata or via cuticle waxes (Desalme et al., 2013).

Another intriguing issue related to the moss-bag approach is the effect of the exposure conditions. While a large body of literature exist on moss-bags ability to intercept PM and related pollutants when exposed in open air and fixed positions, only a few studies deal with moss or lichen bags exposed indoors and none concerns the uptake ability of moss-bags exposed in mobile system, such as a bicycle or a motorcycle.

It is a common idea that indoor environments are clean and healthy, but scientific evidence has shown that indoor air can be more seriously polluted than expected, sometimes even more than outdoor air of large industrialized cities (WHO, 2014).

Moreover, an approach based exclusively on the assessment of outdoor air pollution shows a limited effectiveness, since people spend most of their time indoors (Bo et al., 2017; Maertens et al., 2004). The assessment of indoor air contamination in work and life environments is important to evaluate the total risk of exposure for humans and to estimate the contribution of the inner pollution sources, such as cleaning products, cooking, and smoking.

A recent paper investigating the wind effect on element uptake capacity of mosses exposed in bags reported that moss bags tied to weathervanes accumulated greater quantities of elements than mosses exposed in fixed positions (Garcie-Seoane et al., 2019). These results not only suggest that moss bags could be profitably used for air biomonitoring in moving systems, but also, that the magnitude of the exposure to air pollution is greater in mobile systems, which encourages the set-up of air biomonitoring experiments in these conditions. In many cities in fact, people reach workplace or school by bikes or motorcycles to escape vehicular traffic and overcrowded public transport, even more in the last year, due to the Covid 19 pandemic. Exploring the magnitude of human exposure to air pollution in all condition (indoor, outdoor, mobile) could open new perspectives in data acquisition for a global evaluation of the health risks related to air pollution.

*Aims and synopsis of the PhD thesis*

In the framework of plant-pollutant interaction in phytoremediation, aims of the present work was to deepen the knowledge of the morphophysiological responses observed in cardoon plants under metal stress, particularly Cd and Pb. By using different culture conditions and three cardoon cultivars, I considered the effects of these heavy metals on several traits, as the growth pattern, root and leaf morphology and ultrastructure, the element uptake capacity and element repartition between symplast and apoplast, the antioxidant power, the protein pattern related to photosynthesis and the photosynthetic efficiency. Among common and cultivar-specific responses, the study also evidenced new parameters that can be efficiently used in the selection of candidate species for phytoremediation. The results of the relative experiments are presented in the form of three published papers here enclosed as chapters 1 to 3 of the present dissertation.

In the paper of Chapter 1, three cardoon cultivars (Siciliano, Sardo, Spagnolo) were grown on a metal-polluted industrial soil, or on gardening soil as a control. Growth

pattern, leaf damages and ultrastructure, Rubisco content and photosynthesis efficacy were evaluated; the results indicated a better performance of *Cynara cardunculus* var. *altilis* cv Spagnolo grown under metal stress, compared to the other cultivars.

In the article of Chapter 2 the three cardoon cultivars were grown on the same industrial soil, highly contaminated by heavy metals, particularly Cd and Pb. Two growth cycles were carried out, followed by chemical analyses of plant shoots and roots, as well as soil, to evaluate the phytoextraction potential of the three cultivars. In addition, other parameters were considered, such as fresh and dry weight, tolerance index, life span, nitrogen content, promptly available and potentially available metal fractions in the soil. The results indicated that all the three cultivars showed high uptake capacity, with Cd translocation higher than Pb; however, Sardo and Siciliano cultivars coupled metal accumulation with water stress and a decrease in growth and lifespan.

In the third article (Chapter 3) the same three cardoon cultivars were grown in hydroponics under metal stress, to evaluate root morphology; in addition, stomata development in relation to gas exchange, and antioxidant power were considered in treated and control plants. The results indicated that root hairs developed only under metal stress and could act as storage sites for these pollutants; stomata increased their size or their number under metal stress, affecting gas exchange and net photosynthesis; three different responses were observed in the cultivars, concerning the antioxidant power. Once again, only *Cynara cardunculus* var. *altilis* cv Spagnolo could implement such responses to neutralize metal stress.

As for the interaction between plants and pollutants in biomonitoring, aim of this work was to provide new applicative insights into the moss-bag approach. Particularly, PAH uptake by moss and lichen bags was considered to examine methodological aspects specifically related to the biomonitoring of these organic pollutants. Moreover, the efficacy of the moss-bags to detect airborne element pollution was tested both in indoor environments and in mobile systems (i.e., moss-bags carried by bicycles). These latter experiments were carried out in Antwerp (Belgium), at the Laboratory of Environmental and Urban Ecology of the Department of Bioscience Engineering of the University of Antwerp, under the supervision of Prof. Roeland Samson. All the results relative to biomonitoring are presented in form of a published paper and two manuscripts enclosed as chapters 4 to 6 of this dissertation.

The Chapter 4 presents a methodological paper in which the effects of the biomonitor vitality and season (summer vs. winter) on PAH uptake ability were evaluated in moss

and lichen transplanted in bags. The vitality did not affect PAH uptake since both biomonitors exposed alive rapidly lost water and entered a state of cryptobiosis (ascertained by measuring photochemical efficiency). By contrast, exposure season was important; PAH uptake was indeed lower in summer due to photodegradation of these pollutants. Lichen performed better than moss since its multi-layered thallus preserved low molecular weight PAHs and showed higher accumulation ability.

In the Chapter 5 an experiment is described, concerning the indoor (i.e., houses)-outdoor exposure of moss bags in parallel in the urban areas of Antwerp and Naples. Chemical and SIRM analyses of the moss materials highlighted that outdoor air pollution was significantly higher than indoor one in both cities; most indoor pollution derived from outdoor environment, even if for some elements, abundant indoors, specific indoor sources could be suggested. Finally, life habits could affect the level and quality of indoor air pollution.

In the Chapter 6 a manuscript is presented, focused of the ability of "mobile" moss bags to intercept, and retain airborne pollutants. The moss bags were analyzed by ICP-MS and SIRM after the exposure on bicycles commuting in Antwerp along routes characterized by different land use. Although the experiment evidenced some critical issue leading to reconsider the exposure design, the mobile moss bags were able to intercept airborne pollutants and distinguish among industrial, urban, and green routes; the exposure magnitude was significantly higher in mobile system than in static position.

# Chapter 1

## Performance of three cardoon cultivars in an industrial heavy metal-contaminated soil: Effects on morphology, cytology and photosynthesis

M.C. Sorrentino, F. Capozzi, C. Amitrano, S. Giordano, C. Arena*, V. Spagnuolo

*Dipartimento di Biologia, Università degli Studi di Napoli Federico II, via Cinthia 4, 80126, Napoli, Italy*

***Journal of Hazardous Materials 351 (2018) 131–137***
***https://doi.org/10.1016/j.jhazmat.2018.02.044***

**Graphical abstract**

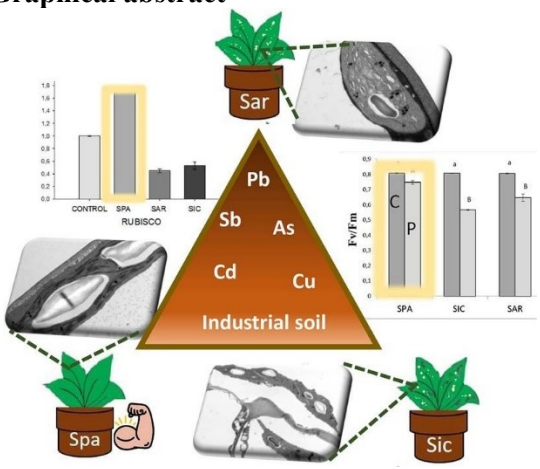


*Keywords:*
D1 and rubisco Heavy-metal stress Metal tolerance Photochemistry TEM

### Abstract

In the present work the cytomorphological and physiological effects on three cardoon cultivars –Sardo, Siciliano, Spagnolo - grown in a metal-polluted soil, were investigated, to assess the traits concurring to the high tolerance to metal stress observed in cv. Spagnolo compared to the other two cultivars. The plants were grown for one month on a real polluted soil collected at a dismantling battery plant, highly enriched by heavy metals, especially Cd and Pb, and their leaves were analyzed by a multidisciplinary approach. TEM observations highlighted severe ultrastructural damage in Sardo and Siciliano and preserved cytological traits in Spagnolo. Both pigment content and photochemistry indicated a decline in photosynthesis in Sardo and Sicilano and a substantial stability of the same parameters in Spagnolo. Protein analysis indicated a decrease in D1 level in all cultivars; in Spagnolo the D1 decrease was more pronounced and associated to a significant increase in Rubisco, a pattern likely preserving photosynthetic efficiency and high biomass production. In conclusion, Spagnolo cardoon was able to face metal stress through a prompt, multiple response balancing structural and functional traits.

∗ Corresponding author. E-mail address: carmen.arena@unina.it (C. Arena).
https://doi.org/10.1016/j.jhazmat.2018.02.044. Received 11 December 2017; Received in revised form 21 February 2018; Accepted 23 February 2018 Available online 01 March 2018 0304-3894/

## 1. Introduction

Heavy metals can be released into various environmental matrices due to the anthropic activities, and although heavy metals are naturally occurring throughout the earth's crust, their excessive use and sub- sequent release represents a serious ecological issue for ecosystems and human health [1,2]. Among heavy metals, lead (Pb) and Cadmium (Cd) represent the most common contaminants that accumulate in soils and sediments [3]. Even if these elements are not essential for plant growth, they may be taken up by plants from both air and soil. When the ab- sorption is from soil, the element can be translocated through roots into the leaves. Limitation in plant growth and biomass production are common responses in heavy metal polluted areas, due to alteration in many metabolic pathways such as photosynthesis. Several studies have shown that the photosynthetic efficiency of many species is deeply affected by the presence of heavy metals in soils [4–6]. Trace elements may also act indirectly on the photosynthetic activity by decreasing the level of photosynthetic pigments or damaging the structure of chloroplasts [7]. A depletion in the chlorophyll and carotenoid content re- presents an early symptom of metal toxicity [8–11]. In addition, disturbance in the uptake of metals and their consequent distribution in plant may lead to premature senescence of leaves and consequently to the reduction of leaf lamina expansion [12]. Even so, changes in these parameters strictly depend on the harshness and the duration of metal stress, but also on plant species.

Since heavy metals are non-biodegradable, they accumulate in plant tissues and may enter the food chain. As so, this contamination re- presents a serious hazard not only to plants and the environment but also to human health [13,14].

Phytoremediation consists of several agronomic techniques with the aim to decrease or degrade contaminants in soils using plants, soil amendments and microbial consortia [15–17]. Differently from physical-chemical techniques, phytoremediation does not alter soil properties and its microflora; [18] therefore, it represents a green technology to recover soil fertility, especially in low polluted soils, or reduce the risk of expanding contaminated areas. Whatever the technique purpose while planning a phytoremediation action, it is of paramount importance a complete knowledge of the plant response to pollutants, not only in terms of accumulation, but also in relation to biomass production, tolerance, influence on plant development, morphology and physiology.

In a parallel study [19] the performance of three cardoon cultivars Sardo, Siciliano and Spagnolo was evaluated on an industrial, highly metal-polluted soil, by measuring metal

content in plant tissues and in soil after two culture rounds. We found that Spagnolo could balance considerable metal uptake ability versus good growth parameters, showing the longest life span and the smallest reduction in biomass, when grown on polluted soil.

In the present work, the cytomorphological and physiological effects induced by the metal-polluted soil on the three cardoon cultivars were studied to assess the plant traits mostly concurring to the high metal tolerance observed in cv Spagnolo. In particular, we considered i) morphological characteristics, such as the occurrence of leaf chlorosis and necrosis, changes of leaf area and cell ultrastructure; ii) alterations of physiological traits, namely pigments and proteins involved in photosynthesis, and photosystem photochemical efficiency.

## 2. Materials and methods

### *2.1. Plant material and experimental design*

The species tested in this study was *Cynara cardunculus* var *altilis*; we used three cultivars: Siciliano, Sardo and Spagnolo. The seeds were germinated to primary roots on wet filter paper for five days at 25 °C in the dark. Since the seedlings directly cultured on polluted soil were unable to grow up, for a first culture step, twenty seedlings for each cultivar were transferred to a standard gardening soil into 10 cm dia- meter pots and irrigated three times a week for 30 days with MS liquid culture medium [20] (Murashige and Skoog Basal Salt MiXture, Sigma Life Science M5524-50L, 2.2 g $L^{-1}$). Afterward, ten plants for each cultivar were transferred on a polluted industrial soil and watered with MS liquid medium, while other ten were transplanted in fresh gardening soil as control plants. The polluted soil here used was collected at a battery dismantling plant, with Cd and Pb concentrations ranging from hundreds to thousands ppm [21]; in a parallel study we found that metals were mostly present as potentially bioavailable fraction and only in a limited proportion as promptly available fraction; in addition, metal bioavailability increased during successive cardoon growth cycles [19]. All plants were grown under semi controlled conditions in greenhouse with Photosynthetic Photon FluX Density (PPFD) at the top of the canopy, of 450–550 µmol photons $m^{-2}$ $s^{-1}$, air temperature 22 ± 2 °C, relative humidity (RH) 55–65%.

After 30-day growth period, plant material was collected to estimate the following parameters: i) morphology and ultrastructure of the leaves; ii) level of proteins involved in photosynthesis; iii) pigment content in leaves; iv) photosynthetic activity.

*2.2. Morphology of the three cultivars*

Morphological traits were visually assessed 15 days after transplant onto polluted/control soils (leaf morphology and presence/absence of chlorosis and necrosis); at the end of the treatment, leaf area (LA) and total necrotic area were measured by ImageJ software on ten leaves for each sample. We assessed these parameters since the exposure to toXic metals may determine a competition in metal uptake, which results in an altered uptake of essential nutrient; this condition may lead to premature senescence of leaves (i.e., necrosis) and the reduction in leaf lamina [12].

*2.3. TEM observation*

We investigated cell ultrastructure to put in evidence if toXic effects of metals altered the structure of chloroplasts and photosynthetic apparatus, as observed in other plants [4,7]. Samples of the three cultivars, grown in control conditions and in polluted soil, at the end of the treatment, were prepared for TEM observations; 2–3 mm leaf specimens were fiXed with 3% glutaraldehyde, dehydrated with ethanol up to propylene oXide and embedded in Spurr's epoXy medium. Ultrathin sections (50-60 nm thick) were collected on copper grids and stained by UAR (Electron Microscopy Sciences, EMS Catalog #22409) following the manufacturer's instructions. A FEI EM 208S Transmission Electron Microscope (TEM), with an accelerating voltage of 80 kV, was used for observations.

*2.4. Protein extraction and western blot analysis*

Photosynthetic protein analysis was carried out because protein pattern may be severely affected by heavy metal contamination altering photosynthetic plant capability [32]. Protein extraction of leaves was carried out on plants after 1-month growth on polluted/control soil, according to Wang et al. [22] and Bertolde et al. [23] using 0.3 g of plant material for each sample. An SDS-PAGE (10%) was performed by using Dual Color Protein Standard (Bio-Rad) as marker and Laemmli loading buffer added to samples in order to follow protein separation. Western blot analysis on leaf and root samples were performed using a blocking solution (100 mM Tris-HCl pH 8.0, 150 mM NaCl, 0,1% Tween 20, 5% BSA) and primary antibodies (Agrisera) to reveal different proteins: Rubisco (anti-RbcL, rabbit polyclonal serum), D1 (anti-PsbA, hen polyclonal), and Actin (anti-ACT, rabbit polyclonal serum) as loading control. The immunorevelation was performed using the kit for chemiluminescence (Westar

Supernova, Cyanagen) by ChemiDoc System (Bio-Rad). Densitometry analysis was performed using ImageJ software (Rasband, W.S., U.S. NIH, Bethesda, Maryland, USA, 1997-2012) normalizing each band value with the corresponding actin band value. Results were expressed as percentages of the control set to 100%.

### *2.5. Chlorophyll and carotenoid determination*

The pigment composition, namely chlorophylls and carotenoids, were analyzed to assess the occurrence of potential damages in light harvesting by the photosynthetic apparatus [7-9]. Chlorophylls and carotenoids were extracted from n = 5 leaves for treatment and determined following the procedure reported by Lichtenthaler [24]. More specifically, pigments were extracted from a frozen leaf disk of 0.283 cm2 using a mortar and a pestle in ice-cold 100% acetone. Then, the solution has been centrifuged at 3000 rpm for 7'. Chlorophyll a, b and carotenoids were quantified by spectrophotometer (Cary 100 UV-VIS, Agilent Technologies, Santa Clara, CA, USA) at 662, 630 and 470 nm wavelengths.

### *2.6. Fluorescence emission measurements*

Chlorophyll a fluorescence measurements were carried out on leaves from each treatment by means of a portable pulse amplitude modulated fluorometer (FluorPen FP100, Photon System Istruments, CZ). Fluorescence emission analysis allows a non-invasive evaluation of photosynthetic performance in plants, related to plant light conversion capacity to the reaction centers. Photochemical parameters in the dark and in the light, were calculated. For measurement in the dark, leaves were darkened for 30 min to determine the maximal photo- chemical efficiency (Fv/Fm) following Kitajimae Butler [25]. The quantum yield of PSII electron transport (ΦPSII), was expressed according to Genty et al. [26]. Later, ΦPSII was used for the calculation of linear electron transport rate (ETR) according to Krall and Edwards [27] and, overall, photosynthetic capacity in vivo. Thermal dissipation of excess absorbed light was expressed by non-photochemical quenching (NPQ) and calculated according to Bilger e Björkman [28].

### *2.7. Statistical analysis*

Data were processed with one-way ANOVA using Sigma Stat 3.5 software (Jandel Scientific, San Rafael, CA, USA). Multiple comparison tests were performed with

Duncan coefficient using < 0.05 as the level of probability. The Kolmogorov–Smirnov and Shapiro–Wilk tests were performed to check for normality.

## 3. Results and discussion

### *3.1. Morphology*

Plant morphology is illustrated in Fig. 1s and Table 1; Fig. 1s refers to plants 15-d after transplant, while data reported in Table 1 refer to the end of the treatment (i.e., 30-d after transplant). Chlorosis and necrosis in C. cardunculus cvs Sardo and Siciliano, were already evident 15 days after their transplant on polluted soil (Fig. 1s, b and d respectively); whereas Spagnolo plants grown on polluted soil (f) were like the control (e). Differently from treated plants, control plants of cardoon Siciliano showed lobate leaves (Fig. 1s, c), a trait characteristic of a late stage of leaf differentiation in all cultivars; this indicates a slowdown of leaf development occurring in Siciliano under metal stress. At the end of the treatment the leaf area was strongly reduced in Sardo and Spagnolo cultivars (Table 1); leaf area reduction can be easily interpreted as a response to metal stress. This result was also observed in Beta vulgaris L. in a soil containing Cd, Cr, Cu, Ni, Pb and Zn [29]. No area reduction was observed in Siciliano leaves, but in this cultivar necrotic areas covered a good 26%, about three times the necrotic areas observed in Sardo (9%). At the end of treatments, cardoon Spagnolo did not show different morphology compared to control (i.e., absence of chlorosis and necrosis), apart from the reduced leaf area (Table 1).

Table 1
Plant morphology (mean ± SD) of cardoon Sardo, Siciliano and Spagnolo after 30 days growt h on polluted and control soils. LA: leaf area. For each treatment n = 10.

| Cultivar | Treatment | LA ($cm^2$) | % necrosis | Chlorosis |
|---|---|---|---|---|
| SAR | Control | 219 ± 7 | 0 | – |
| | Polluted | 169 ± 7 | 9 ± 1 | + |
| SIC | Control | 143 ± 8 | 0 | – |
| | Polluted | 146 ± 6 | 26 ± 3 | + |
| SPA | Control | 220 ± 6 | 0 | – |
| | Polluted | 181 ± 9 | 0 | – |

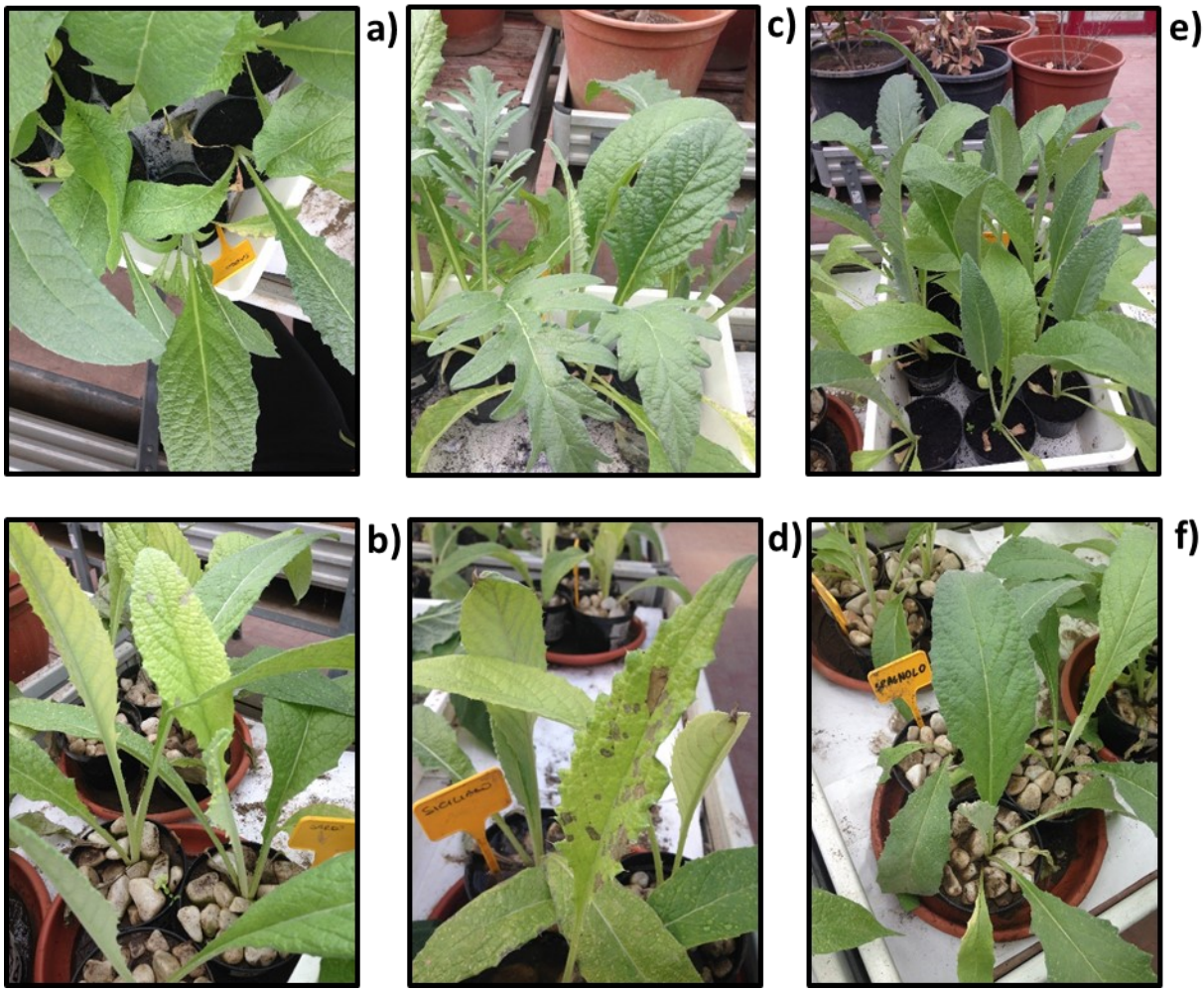


Figure 1s. Plants of *C. cardunculus* grown on control and polluted soil 45 days after planting (45 d on gardening soil for control plants; 30 d on gardening soil + 15 d on polluted soil for treated plants). *a* and *b*) cv Sardo: chlorosis and small necrotic areas in plants grown 15 d on polluted soil (*b*) compared to control (*a*). *c* and *d*) cv Siciliano: leaves of treated plants (*d*) showing necrosis more evident than in Sardo. *e* and *f*) cv Spagnolo: control and treated plants showing similar morphology.

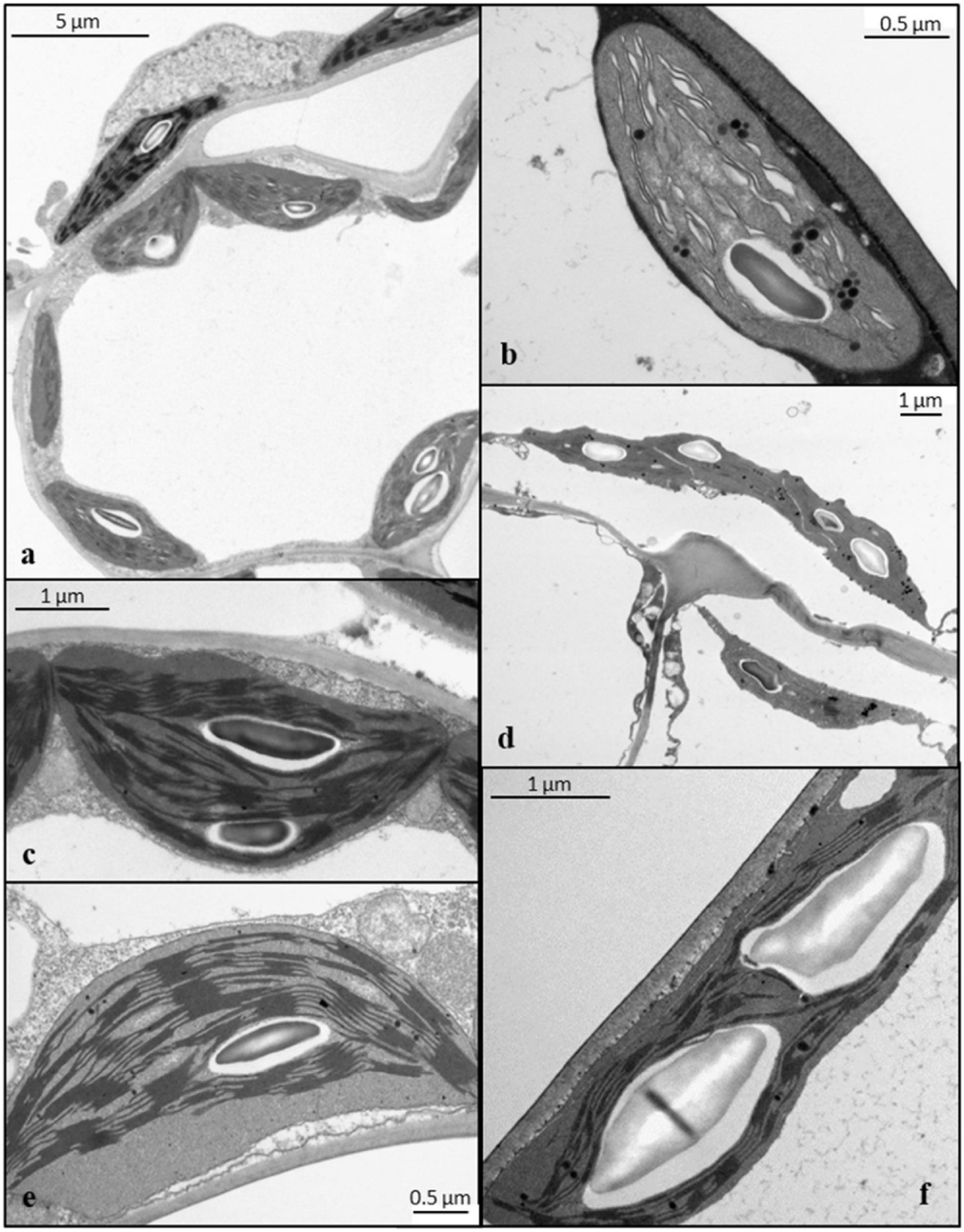


Fig. 1. TEM microphotographs of leaf tissue of
*Cynara cardunculus* cultivars: Sardo (*a* and *b*);
Siciliano (*c* and *d*); Spagnolo (*e* and *f*) grown on control (*a*, *c* and *e*) and polluted (*b, d* and *f*) s
oil.

### *3.2. TEM observations*

TEM observations refer at the end of the treatment and are illustrated in Fig. 1. Control leaf samples of all the three cultivars (a, c and e for Sardo, Siciliano and Spagnolo, respectively) highlighted the presence of well-preserved cells, showing several chloroplasts, with nu- merous grana having regularly packed thylakoids and 1 or 2 large starch granules. Cell wall and cytoplasm showed a regular organization, with ribosomes, endomembranes and organelles in the latter; a large central limpid vacuole was generally observed. Leaf samples from cardoon cultivars grown on polluted soil (Fig. 1b, d and f for Sardo, Siciliano and Spagnolo, respectively) showed evident cytological alterations, particularly severe in Sardo and Siciliano. Here, the chloroplasts lost their typical organization: thylakoid membranes appeared frequently swollen (Sardo, Fig. 1b), or even not distinguishable (Siciliano, Fig. 1d). The cell wall, as well as the cytoplasm were often more electrondense than the control (d); the vacuole often showed inclusions (Fig. 1b, d and f); all these traits could be related to the presence of metals [30,31]. Leaf cells of cardoon Siciliano were often plasmolyzed (Fig. 1d), in agreement with the relevant percentage of necrosis observed in this cultivar. Arena et al. [32] found that *C. cardunculus* cultured in the presence of Cd or Pb for 90 days had well preserved chloroplast ultrastructure like control plants, but metal concentrations employed in that study were very much lower than those characterizing the polluted soil of the present work. Surprisingly, despite the high level of metal concentration of the tested soil, at the end of the treatment, the plants of cv. Spagnolo kept ultrastructural traits typical of the control; the only sign of cell stress observed in this cultivar was the reduction of thylakoid number packed in each granum (Fig. 1e and f).

### *3.3. Photosynthetic pigment content*

Total chlorophyll and carotenoid contents are reported in Fig. 2. All cultivars showed similar pigment concentrations when grown on control soil, whereas significant decrease ($P < 0.05$) in chlorophylls and carotenoids was observed in cultivars grown on polluted soil. However, while in Spagnolo pigment concentrations helved, a more drastic re- duction occurred in Sardo and Siciliano. This inhibitory effect could be the consequence of Cd accumulation, which is known to be delivered through plant organs more easily than other heavy metals [33].

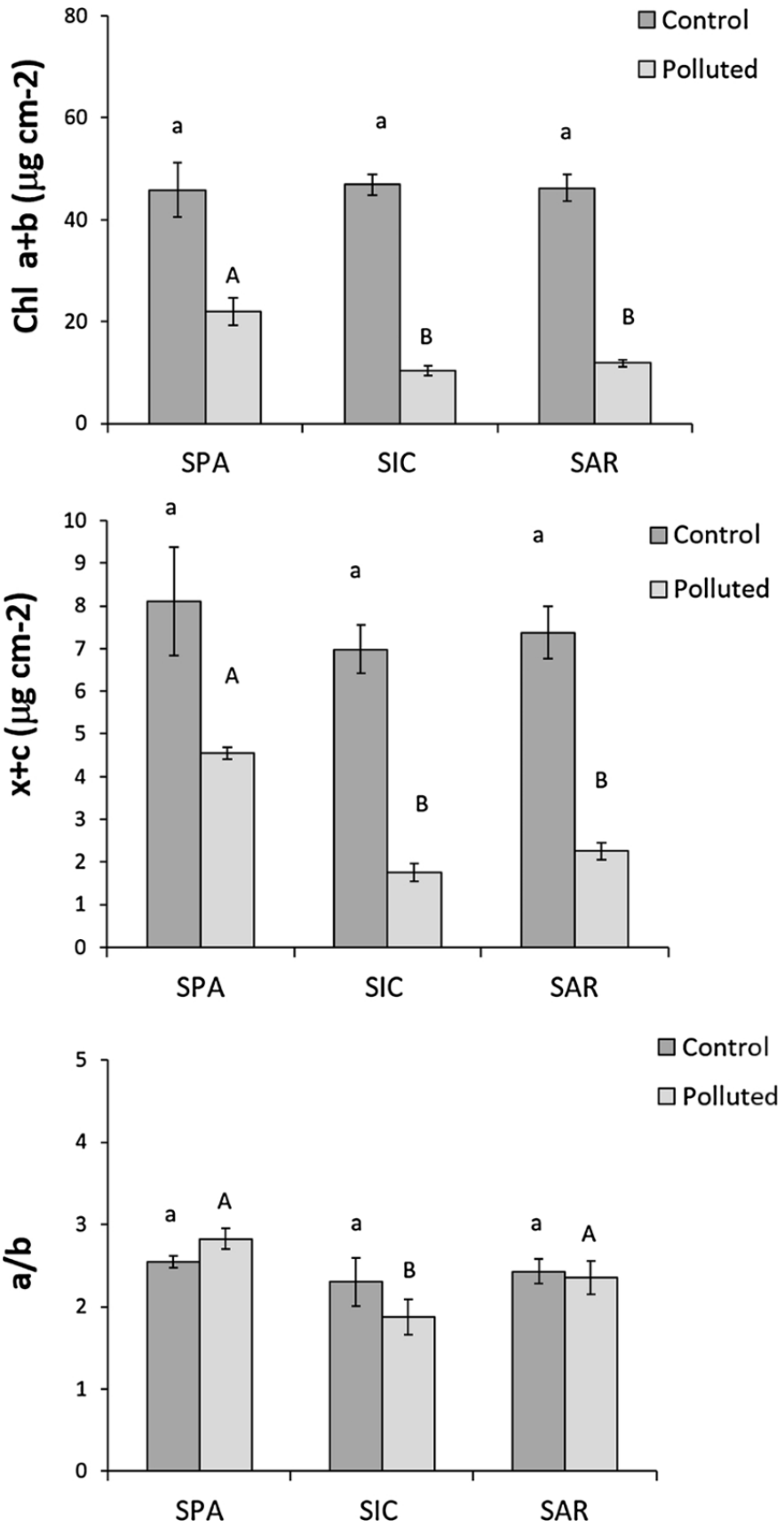


Fig. 2. Total chlorophyll (Chl a + b), total carotenoid (Car x + c) content and chlorophyll a/b ratio in three different *Cynara cardunculus* cultivars: Spagnolo (SPA), Siciliano (SIC) and Sardo (SAR) grown on Control and Polluted soil. Each value represents the mean ± SE (n = 5). Different letters

correspond to significantly different values according to multiple comparison tests ($P < 0.05$). Small and capital letters refer to control and polluted plants, respectively.

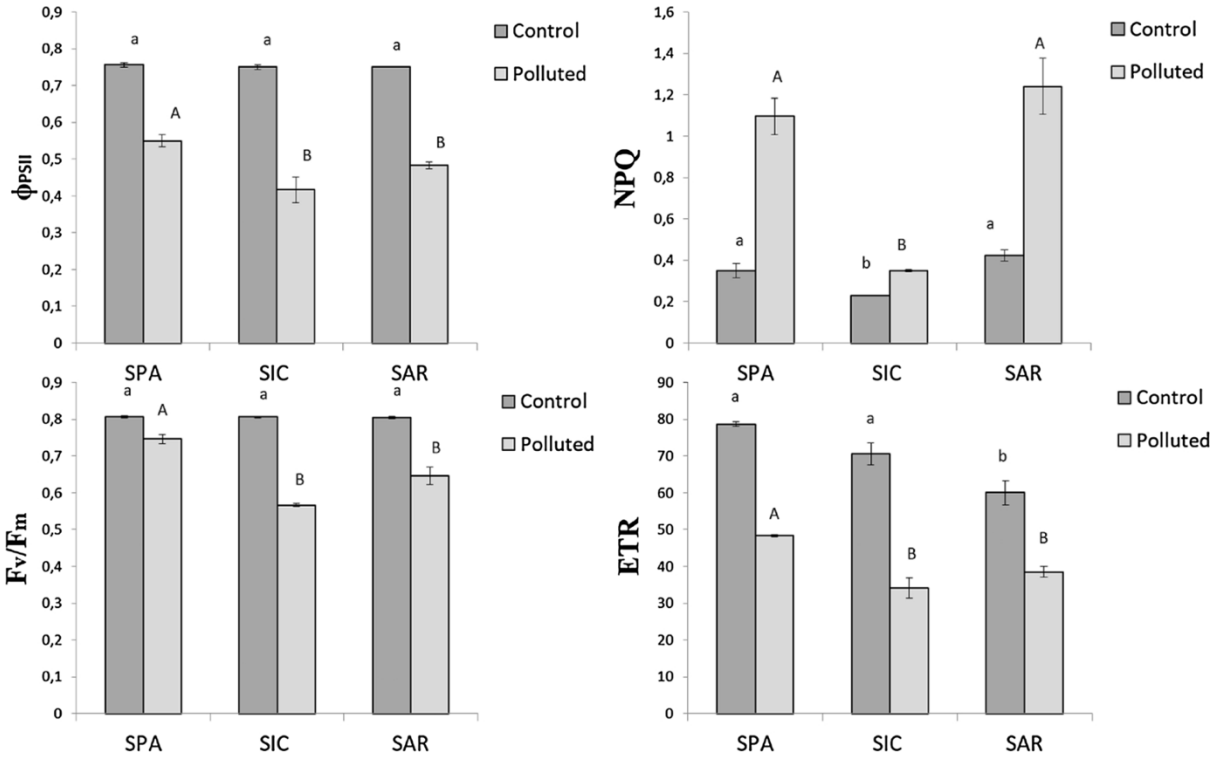


Fig.3. Quantum yield of PSII electron transport (ΦPSII), non-photochemical quenching (NPQ), maximal photochemical efficiency (Fv/Fm), and linear electron transport rate (ETR) in three different *Cynara cardunculus* cultivars: Spagnolo (SPA), Siciliano (SIC) and Sardo (SAR) grown on Control and Polluted soil. Each value represents the mean ± SE (n = 5). Different letters indicate significantly different values according to multiple comparison tests ($P < 0.05$). Small and capital letters refer to control and polluted plants, respectively.

Furthermore, the excess of heavy metals could decrease the pigment concentration indirectly by lowering the transport rate of Fe to the leaves [34]. Iron is involved in the synthesis of pigments, which could therefore be affected by its decrement. Additionally, this decrement could subsequently affect the photosynthetic reactions and chloroplast structure, in line with TEM observations of cvs. Sardo and Siciliano. No significant difference was detected among controls in chl a/b ratio (Fig. 2). Among treated plants, cv. Spagnolo exhibited the highest value of the chl a/b ratio, whereas the lowest ($P < 0.05$) was observed in Siciliano. This could be attributed to the more rapid degradation of Chl a compared to Chl b, with detrimental effect in the reaction centers. This hypothesis is consistent with the significant decrease ($P < 0.05$) of maximal PSII photochemical efficiency of cvs. Siciliano and Sardo (see paragraph below). It is also noticeable that, leaves of cv. Siciliano showed the greatest percentage of necrosis, compared to the other cultivars that displayed less pronounced toxicity symptoms.

*3.4. Photochemistry*

The quantum yield of PSII electron transport (ϕPSII) and the max- imum PSII photochemical efficiency (Fv/Fm) were significantly higher

in control plants compared to respective plant grown on polluted soil (Fig.3). About controls, no significant difference among cultivars was detected. Conversely, the growth on polluted soil affected PSII photo- chemical activity. It is likely that the higher heavy metal concentration in leaf tissue, can affect significantly the photosystem capability to convert light energy, determining a decline of photochemistry, com- pared to unpolluted controls. However, despite this reduction, cv. Spagnolo showed the highest values of ΦPSII and Fv/Fm, compared to the other two cultivars, indicating a strong intrinsic capacity to tolerate and face this kind of stress. In cultivar Siciliano the significant reduction of ΦPSII could be determined by the low production of ATP and NADPH, with negative outcome on the dark phase of photosynthesis. This is consistent with the lowest biomass content found in this cultivar (19 Capozzi et al. unpublished). The significant reduction ($P < 0.05$) of photochemical efficiency of plants in polluted soil, occurred with a

significant rise ($P < 0.05$) of non-photochemical quenching, except for cv. Siciliano which exhibited the lowest value of NPQ. However, as the lowest NPQ occurred not only on polluted soil, but also in control, it is likely that this cultivar has a low capability to thermally dissipate the excess of absorbed light not utilized in photochemistry, exposing itself to the higher risk of photodamage under metal stress. This result is consistent with leaf necrosis and Chl a degradation observed in cultivar Siciliano.

*3.5. Western blot analysis*

The western blot analysis evidenced a significant decrease of D1 content, the key protein of photosystem II, in cv. Spagnolo grown on polluted soil (Fig. 4) compared to unpolluted control. Conversely, in Siciliano and Sardo the D1 reduction is less evident. The changes in photosynthetic protein levels may be interpreted as a consequences of metal contamination. Several published papers showed indeed, de- crease or increase of photosynthetic protein concentrations, and even expression, in response to metal stress [35,36]. However, a precise comparison is not possible since the studies carried out so far only considered laboratory experiments with a single metal [32,37], a condition very different from a real soil; but it is noticeable that the cultivars Sardo and Siciliano (i.e.,

nontolerant cultivars) once again gave similar response, also in term of photosynthetic protein production. The less pronounced D1 reduction observed in cvs. Siciliano and Sardo can be considered a way to compensate for their reduced photochemistry. On the other hand, cv. Spagnolo kept a higher photochemical efficiency despite the lowest D1 protein level. The decrease in D1, i.e., the key protein of photosystem II, found in cv. Spagnolo well fits the chloroplast ultrastructure, showing grana with a reduced number of thylakoids and partitions, compared to control plants (i.e., the lower partition number, the lower D1 level); this indicates that Spagnolo can give a combined response involving both structure and function. As for Rubisco, it is reported the lack of a generalized pattern under heavy metal toxicity in soil [38,39,40] and most of the results are related to Cd-induced stress [41]. In our study Rubisco protein level exhibited a striking difference among cultivars, showing the highest concentration ($P < 0.01$) in cv. Spagnolo grown on polluted soil and a significant decrease in the other two cultivars. The overproduction of Rubisco compared to control, is consistent with the large starch granules and the highest photo- chemistry and biomass production observed in this cultivar, confirming its better photosynthetic capacity under stress. As reported in Kosovà et al. [42], indeed, hyperaccumulators generally show an up regulation of photosynthetic proteins, including Rubisco, while sensitive plants exhibit the opposite behavior. Unexpectedly, we found that, although all the tested cultivars acted as hyperaccumulators (19 -Capozzi et al., unpublished), only Spagnolo upregulated the production of Rubisco.

Moreover, a different mechanism could be related to Rubisco hyperproduction, supporting the stability observed in cv. Spagnolo under metal stress; indeed, most pollutants, including heavy metals, enhance oxidative processes, determining plant tissue damage by increasing ROS production [43]. However, due to its well-known oxygenase activity, Rubisco could have determined a slowing down of the oxidative processes, with positive effect on structure (i.e., absence on chlorosis and necrosis, preserved ultrastructure) and function, preserving life traits of cv. Spagnolo grown on polluted soil. Nowadays there is a lack of information about the effects of heavy metals on Rubisco. Studies made on single heavy metals, such as Cd, Mn, Fe, Al, showed that detrimental effects on both activity and concentration of Rubisco de- pend on the nature of the element and its concentration [44]. Our data suggest that the observed changes in Rubisco levels in the different cardoon cultivars, could also depend on the possible synergic effects of the metal cocktail present in the polluted soil.

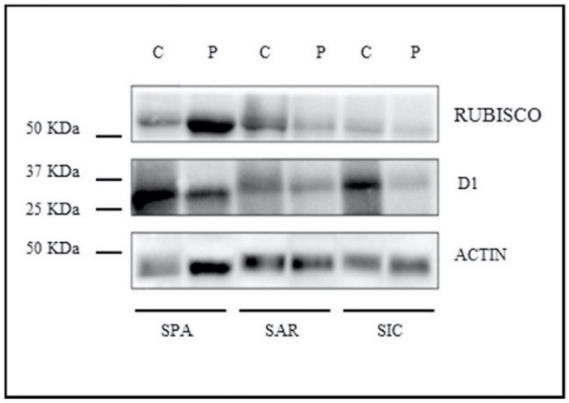


a)

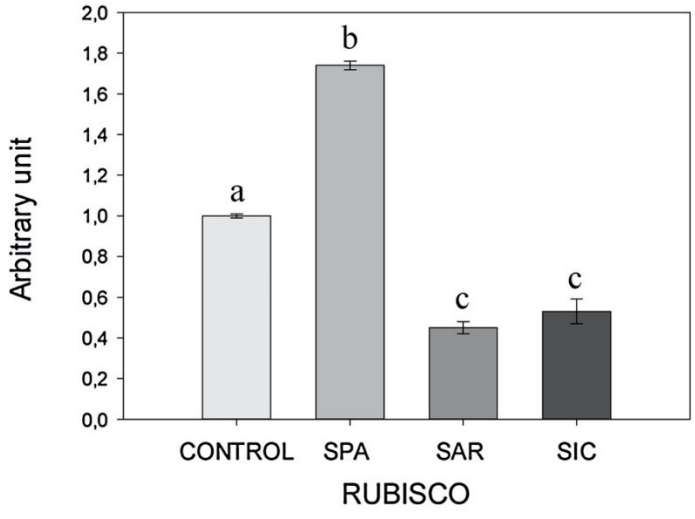


b)

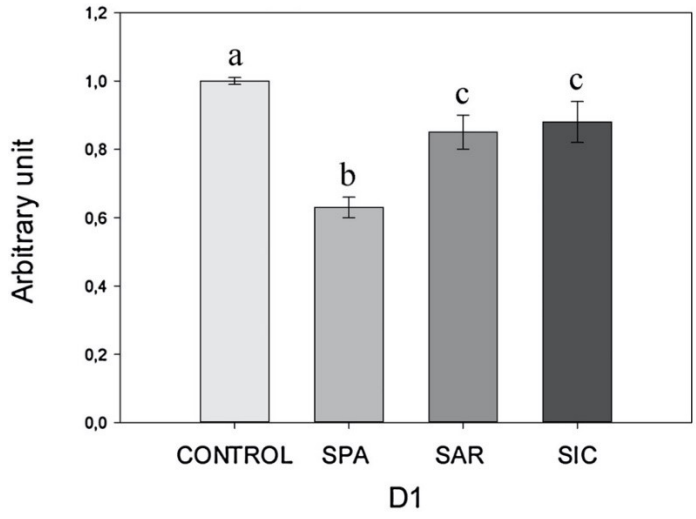


c)

Fig. 4. Western blot analysis (a) and densitometric analysis of Rubisco (b) and D1 (c) proteins in the three cultivars of *Cynara cardunculus* (Spagnolo, Sardo and Siciliano) in control and treated plants. The bar diagrams represent pixel volumes of Rubisco and D1 proteins in samples. The bands were normalized to the appropriate actin band. Each value represents the mean ± SE (n = 3) considering control sample value as 1 (100%). Different letters indicate statistically significant differences among treatments according to multiple comparison tests ($P < 0.05$).

## 4. Conclusions

In this study, morphological and physiological parameters were evaluated in three cultivars of C. cardunculus grown on a real metal contaminated soil. Among the tested cultivars, Spagnolo showed the best performance under metal stress condition, operating a prompt, multiple response at morphological and physiological levels. This has been achieved by balancing of structural and functional traits, with a global positive impact on plant tolerance and growth. It is likely to suppose that this response depends on the activation of detoxification mechanisms, e.g., the complexation of metals by metal-chelating agents, or their immobilization in low-metabolism cell compartments. Further investigations are needed to support these hypotheses.

This experiment is the first study aimed to assess the outcomes of plant growth on a real metal-polluted soil at multiscale level, without the influence of other environmental parameters. In a future field experiments, other factors should be considered, such as the variations of temperature, humidity and nutrient availability, affecting plant photosynthesis and growth. In addition, the influence of air pollutants from neighboring areas should be considered too. These contaminants, in fact, could modify soil properties (e.g., organic matter, water capacity, pH and cationic exchange capacity) or enter the plant, affecting its growth and metabolism.

Acknowledgements

This work was supported by grant from the MIUR (Italian Ministry of University and Research) “Development of green technologies for production of BIOchemicals and their use in preparation and industrial application of POLImeric materials from agricultural biomasses cultivated in a sustainable way in Campania region (BioPoliS)”, project code PON03PE_00107_1, funded in the frame of Operative National Programme Research and Competitiveness 2007–2013 D. D. Prot. N. 713/Ric. 29/10/2010.

We would like to thank Dr. Riccardo Riccardi, as a member of Arca 2010, an enterprise participating in BioPolis, for providing us cardoon seeds, and Dr. Sergio Sorbo for TEM analysis.

## References


1. A. Cristaldi, G. Oliveri Conti, E.H. Jho, P. Zuccarello, A. Grasso, C. Copat, M. Ferrante, Phytorem ediation of contaminated soils by heavy metals and PAHs. A brief review, Environmental Technolo gy & Innovation 8 (2017) 309–326.
2. P.B. Tchounwou, C.G. Yedjou, A.K. Patlolla, D.J. Sutton, Heavy Metals Toxicity and the Environm ent. NIH Public Access, (2014).
3. I.V. Seregin, V.B. Ivanov Physiological aspects of cadmium and lead toxic effects on higher plants Russ. J. Plant Physiol., 48 (2001), pp. 523-544
4. Z. Krupa, T. Baszyński, Some aspects of heavy metals toxicity towards photo- synthetic apparatus – direct and indirect effects on light and dark reactions, Acta Physiol. Plant. 17 (1995) 177–199.
5. B. Myśliwa-
   Kurdziel, M.N.V. Prasad, K. Strzałtka, Photosynthesis in heavy metal stressed plants, in: M.N.V. Pr asad (Ed.), Heavy Metal Stress in Plants. Springer, Berlin, Heidelberg, 2004.
6. M. Bertrand, I. Poirier, Photosynthetica 43 (2005) 345, http://dx.doi.org/10.1007/ s11099-005-0058-2.
7. J. Molas, Changes of chloroplast ultrastructure and total chlorophyll concentration in cabbage leaves caused by excess of organic Ni(II) complex, Environ. Exp. Bot. 47 (2002) 115–126.
8. R.P. Singh, S. Dabas, A. Choudhary, Recovery of $Pb^{2+}$ caused inhibition of chlorophyll biosynthesis in leaves of Vigna radiata (L.) Wilczej by inorganic salts, Indian J. Exp. Biol. 34 (1996) 1129–1132.
9. E. Masarovičová, M. Holubová, Effect of copper on growth and chlorophyll content of some herbs, Rostl. Výr. 44 (1998) 261–265.
10. A. Emamverdian, Y. Ding, F. Mokhberdoran, Y. Xie, Heavy metal stress and some mechanisms of plant defense response, Sci. World J. (2015) 18, http://dx.doi.org/ 10.1155/2015/756120.
11. B.A. Ghnaya, G. Charles, A. Hourmant, B.J. Hamida, M.C.R. Branchard, Physiological behaviou r of four rapeseed cultivar (Brassica napus L.) submitted to metal stress, Physiology 332 (2009) 363 –370.
12. B. Myśliwa-Kurdziel, M.N.V. Prasad, K. Strzałka, Heavy metal influence on the light phase of photosynthesis, Physiology and Biochemistry of Metal Toxicity and Tolerance in Plants, Springer, Netherlands, 2002, pp. 229–255.
13. M.A. Conceição Gomes, R.A. Hauser-
    Davis, A. Nunes de Souza, A.P. Vitória, Metal phytoremediation: general strategies, genetically mo dified plants and applications in metal nanoparticle contamination, Ecotoxicol. Environ. Saf. 134 (2 016) 133–147.
14. A. Horta, B. Malone, U. Stockmann, B. Minasny, T.F.A. Bishop, A.B. McBratney, R. Pallasser, L. Pozza, Potential of integrated field
    spectroscopy and spatial analysis for enhanced assessment of soil contamination: A prospective revi ew, Geoderma 241–242 (2015) 180–209.
15. S. Greipsson, Phytoremediation, Nat. Educ. Knowl. 3 (2011) 7.
16. H. Ali, E. Khan, M.A. Sajad, Phytoremediation of heavy metals
    concepts and applications, Chemosphere. 91 (2013) 869–881.

17. Ecoremed Operative Handbook, (2017) (Accessed 31 October 2017), http://www. ecoremed.it/images/stories/FinalReport/LIFE%20ECOREMED%20Handbook.pdf.
18. X. Zhang, Y.G. Zhu, Y.B. Zhang, Y.X. Liu, S.C. Liu, J.W. Guo, R.D. Li, S.L. Wu, B.D. Chen, Growth and metal uptake of energy sugarcane (Saccharum spp.) in different metal mine tailings with soil amendments, J. Environ. Sci-China 26 (2014) 1080–1089.
19. F. Capozzi, M.C. Sorrentino, A.G. Caporale, N. Fiorentino, S. Giordano, V. Spagnuolo, Metal phytoextraction from an industrial contaminated soil: a screening of three cultivars of *Cynara cardunculus*. (Under review), (2018).
20. T. Murashige, F. Skoog, A revised medium for rapid growth and bio assays with tobacco tissue cultures, Physiol. Plant. 15 (1962) 473–497.
21. N. Fiorentino, V. Ventorino, C. Rocco, V. Cenvinzo, D. Agrelli, L. Gioia, I. Di Mola, P. Adamo, O. Pepe, M. Fagnano, Giant reed growth and effects on soil biological fertility in assisted phytoremediation of an industrial polluted soil, Sci. Total Environ. 575 (2017) 1375–1383.
22. W. Wang, R. Vignani, M. Scali, M. Cresti, A universal and rapid protocol for protein extraction from recalcitrant plant tissues for proteomic analysis, Electrophoresis 27 (2006) 2782–2786.
23. F.Z. Bertolde, A.A.F. Almeida, F.A. Silva, T.M. Oliveira, C.P. Pirovani, Efficient method of protein extraction from Theobroma cacao L. roots for two-dimensional gel electrophoresis and mass spectrometry analyses, Genet. Mol. Res. 13 (2014) 5036–5047.
24. H.K. Lichtenthaler, Chlorophylls and carotenoids, pigments of photosynthetic biomembranes, Method. Enzymol. 148 (1987) 350–382.
25. M. Kitajima, W.L. Butler, Quenching of chlorophyll fluorescence and primary photochemistry in chloroplasts by dibromothymoquinone, Biochim. Biophys. Acta 376 (1) (1975) 105–115.
26. B. Genty, J.M. Briantais, N.R. Baker, The relationship between the quantum yield of photosynthetic electron transport and quenching of chlorophyll fluorescence, Biochim. Biophys. Acta 90 (1989) 87–92.
27. J.P. Krall, G.E. Edwards, Relationship between photosystem II activity and CO2 fixation in leaves, Physiolo. Plant. 86 (1992) 180–187.
28. W. Bilger, O. Björkman, Role of xanthophyll cycle and energy dissipation in dif- ferently oriented faces of light–induced absorbance changes, fluorescence and photosynthesis in Hedera canariensis, Photosynt. Res. 25 (1990) 173–185.
29. R.P. Singh, M. Agrawal, Effects of sewage sludge amendment on heavy metal ac- cumulation and consequent responses of Beta vulgaris plants, Chemosphere 67 (2007) 2229–2240.
30. A. Basile, S. Giordano, G. Cafiero, V. Spagnuolo, R. Castaldo-Cobianchi, Tissue and cell localization of experimentally supplied lead in Funaria hygrometrica (Hedw) using X-ray SEM and TEM microanalys, J. Bryol. 18 (1994) 69–81.
31. V. Spagnuolo, M. Zampella, S. Giordano, P. Adamo, Cytological stress and element uptake in moss and lichen exposed in bags in urban area, Ecotoxicol. Environ. Safe. 74 (2011) 1434–1443.
32. C. Arena, F. Figlioli, M.C. Sorrentino, L.G. Izzo, F. Capozzi, S. Giordano, V. Spagnuolo, Ultrastructural, protein and photosynthetic alterations induced by Pb and Cd in *Cynara*

*carduncul*us L., and its potential for phytoremediation, Ecotoxicol. Environ. Safe. 145 (2017) 83–89.

33. J.U. Nwosu, A.K. Harding, G. Linder, Cadmium and lead uptake by edible crops grown in a silt loa m soil, Bull. Environ. Contam. Toxicol. 54 (1995) 570–578.
34. A. Siedlecka, Z. Krupa, Cd/Fe interaction in higher plants its consequences for the photosynthetic apparatus, Photosynthetica 36 (1999) 321–331.
35. P. Kieffer, J. Dommes, L. Hoffmann, J.F. Hausman, J. Renaut, Quantitative changes in protein expression of cadmium-exposed poplar plants, Proteomics 8 (2008) 2514–2530.
36. I. Duquesnoy, P. Goupil, I. Nadaud, G. Branlard, A. Piquet-Pissaloux, G. Ledoigt, Identification of Agrostis tenuis leaf proteins in response to As (V) and As (II I) in- duced stress using a proteomics approach, Plant Sci. 176 (2009) 206–213.
37. F. Pietrini, M.A. Iannelli, S. Pasqualini, A. Massacci, Interaction of cadmium with glutathione and p hotosynthesis in developing leaves and chloroplasts of Phragmites australis (Cav.) Trin. ex Steudel, Plant Phys. 133 (2003) 829–837.
38. C. Chaffei, K. Pageau, A. Suzuki, H. Gouia, M.H. Ghorbel, C. Masclaux-Daubresse, Cadmium toxicity induced changes in nitrogen management in Lycopersicon es- culentu m leading to a metabolic safeguard through an amino acid storage strategy, Plant. Cell. Physiol. 45 ( 2004) 1681–1693.
39. B. Dhir, P. Sharmila, P. Pardha Saradhi, P. Sharma, R. Kumar, D. Mehta, Heavy metal induced ph ysiological alterations in Salvinia natans, Ecotox. Environ. Safe. 74 (2011) 1678–1684.
40. R.R. Ying, R.L. Qiu, Y.T. Tang, P.J. Hu, H. Qiu, H.R. Chen, T.H. Shi, Cadmium tolerance of carbon assimilation enzymes and chloroplast in Zn/Cd hyper- accumulator Picris divaricate, J. Plant Physiol. 167 (2010) 81–87.
41. J. Galmés, I. Aranjuelo, H. Medrano, J. Flexas, Variation in Rubisco content and activity under vari able climatic factors, Photosynth. Res. 117 (2013) 73–90.
42. K. Kosová, P. Vítámvás, I.T. Prášil, J. Renaut, Plant proteome changes under abiotic stress—contribution of proteomics studies to understanding plant stress response, J. Proteomics 74 (2011) 1 301–1322.
43. H. Bothe, Plants in heavy metal soils, in: I. Sherameti, A. Varma (Eds.), Detoxification of Heavy M etal, Springer Publisher, 2011, pp. 35–57.
44. J. Galmés, I. Aranjuelo, H. Medrano, J. Flexas, Variation in Rubisco content and activity under vari able climatic factors, Photosynt. Res. 117 (2013) 73–90.

# Chapter 2

## Exploring the phytoremediation potential of *Cynara cardunculus*: a trial on an industrial soil highly contaminated by heavy metals

Fiore Capozzi[1], Maria Cristina Sorrentino[1], Antonio Giandonato Caporale[2], Nunzio Fiorentino[2], Simonetta Giordano[1]*, Valeria Spagnuolo[1]

[1]*Dipartimento di Biologia, Università degli Studi di Napoli Federico II, via Cinthia 26, 80126 NAPOLI*
[2]*Dipartimento di Agraria, Università degli Studi di Napoli Federico II, via Università 100, 80055 Portici, (NA)*

***Environmental Science and Pollution Research 27 (2020) 9075–9084 https://doi.org/10.1007/s11356-019-07575-9***

**Abstract**

Metal-uptake capacity and growth patterns of three cardoon cultivars (Sardo, Siciliano and Spagnolo) were investigated for phytoremediation in a metal-contaminated soil.
Metal concentrations after one and two growth rounds were measured in soil and plants by ICP-MS. Potentially and promptly available metal fractions were estimated by EDTA and ammonium nitrate. Plant weight, water and nitrogen content and life-span were considered as growth parameters.
After the first growth cycle, a significant accumulation of all elements was observed in roots, whereas only Cd, Cu, Fe, Pb and Sb were significantly translocated to the shoots. After the second growth cycle, a further significant increase, especially in roots, was observed in all cultivars and for all elements considered. High percentages of the potentially available fraction were found for As, Cd, Cu, Pb and Sb. Metal concentrations in plants were far higher than the promptly available fraction, indicating an increase of metal bioavailability during culture rounds. A severe decrease of weight and life span was observed in Sardo and Siciliano grown on polluted soil, along with an increase in N content.
The cultivar Spagnolo, harmonizing a high ability of metal uptake and tolerance, proved the most efficient cultivar in metal phytoremediation.

Key Words: *cardoon*; metal pollution; metal bioavailability; phytoremediation; translocation factor

Corresponding author: giordano@unina.it

## Introduction

Soil contamination by heavy metals (HM) is a complex and pressing problem deeply felt at a global scale, particularly in densely populated and industrialized areas, since soil keeps for a long time the pollution footprint and is therefore considered a non-renewable resource. In 2008, the European Environment Information and Observation Network for soil (EIONET-SOIL) estimated 2.5 million potentially contaminated sites in Europe, of which about 342,000 have already been identified as contaminated, including several thousand in Italy (Ecoremed Operative handbook 2017; Panagos et al. 2013)

Heavy metals are non-biodegradable pollutants accumulating in the environment as consequence of natural and anthropogenic activities, as rock weathering, volcanic emissions, metal-ore exploitation, industrial activities, and waste disposal, increasing urbanization of land and agricultural practices. They can poison the atmosphere through the rise in HM-enriched particulate matter (PM) (Capozzi et al. 2016; Di Palma et al. 2017; Iodice et al. 2016), and can contaminate water bodies, sediments and particularly soils, where the residence time of HM is significantly longer than in other environmental compartments (Alloway 1995). Heavy metals accumulate in living organisms along the food chain, posing at serious risk the top trophic levels, including man. In Italy, an inventory of HM polluted areas compiled by the Ministry of the Environment since 1998 lead to a figure of 57 priority interest sites at national scale (SIN), 6 of which in Campania Region for a total of 345.000 ha of land potentially hazardous; these areas mainly represent the result of the dismantling of industrial plants and the illegal contaminated waste disposal on soils previously devoted to agriculture (di Gennaro 2014; Legislative Decree no. 152 of April 2006). So, the clean-up of HM polluted soils represents nowadays a crucial challenge to minimize the hazard for the ecosystem. Many physical, chemical and biological approaches were attempted so far to cope with this problem with different outcomes. Physical and chemical methods are generally expensive, and their application gives back soils that lost most of their biological properties, destroyed the original microflora, and sometimes produced new wastes. The use of plants and associated soil microbes in restoring polluted soils (phytoremediation) is an effective and eco-friendly restoration emerging method and is receiving increasing attention by researchers and stakeholders. It consists of a pool of agricultural techniques aimed at reducing the concentration of organic and inorganic pollutants or the risk related to their presence by using plants, soil amendments and microbial consortia (Ali et al. 2013). It is cost effective compared to physical and chemical methods, efficient in soils with low and

diffuse contamination, solar-driven and generally well accepted by public opinion. High biomass yield, root to shoot metal translocation and high tolerance to heavy-metal toxicity are among the plant features valuable for phytoremediation; but the suitability of individual plant species should be harmonized to the contingent environmental conditions of use and the specific agricultural demands (e.g. nutrients, water, average temperature) of the species. So far, many species have been tested in controlled conditions or in real field tests for their suitability in phytoextraction or phytostabilization purposes, some with promising results (e.g., Fiorentino et al. 2013 and 2016; Meers et al. 2010; Liu et al. 2000). In the framework of the projects BioPoliS (PON03PE_00107_1) and Ecoremed (Life11/ ENV_IT_275), both focused on the development of new guidelines in phytoremediation of metal-contaminated soils and new green technologies to produce biochemicals from plants, several species were tested, including *Cynara cardunculus* L. var. *altilis* DC. This species is widespread in Mediterranean area (Wiklund 1992); it showed a good tolerance to HM stress and high ability to accumulate a suite of metals, administered as solutions, in laboratory experiments (Arena et al. 2017; Hernández-Allica et al. 2007; Llugany et al. 2012; Papazoglou 2011). The further step of the research was to test the response of this species in a real polluted soil in a greenhouse experiment, prior to pass to a clean-up trial in open field. Therefore, the aims of the present work were: i) to test HM tolerance of three cardoon cultivars (Siciliano, Sardo, Spagnolo) in terms of plant life span and biomass production; ii) to assess uptake ability of the three cultivars and the respective root to shoot translocation factor for a suite of potentially toxic metals; iii) to evaluate the suitability of cardoon for phytoextraction or phytostabilization; iv) to evaluate metal concentrations in the rhizosphere after one and two consecutive plant growth cycles. All tests were performed by using a real industrial polluted soil collected at a battery dismantling plant, with Cd and Pb concentrations ranging from hundreds to thousands ppm (Visconti et al. 2018).

## Materials and Methods

### *Soil collection*

The soil was collected in a site located in the industrial area of the municipality of Marcianise (Campania, southern Italy: 41° 00’ 48.9” N - 14° 17’ 49.7” E) in the western part of the Campanian plain (Visconti et al. 2018). The area, characterized by a typical Mediterranean climate with long and dry summer, is located next to an industrial plant

for recycling car electric batteries; it was classified by the regional authorities as potentially contaminated by Cd and Pb due to past storage of waste from the industrial plant itself. To prevent soil particles resuspension in the collection area, a phytoremediation project was approved, using the ECOREMED protocol (2017) based on planting of poplar stands and permanent meadows.

*Plant material and experimental design*

The species tested in this study was *Cynara cardunculus* L. var. *altilis* DC. and its three cultivars: Siciliano, Sardo, Spagnolo. The seeds were germinated to primary roots on wet filter paper for five days at 25°C in the dark. After germination, the seedlings were all transferred to a standard gardening soil into pots and irrigated three times a week for 30 days with MS liquid culture medium (Murashige and Skoog 1962) (Murashige and Skoog Basal Salt Mixture, Sigma Life Science M5524-50L, 2.2 g $L^{-1}$). Then, twenty plants for each cultivar were transplanted into polluted soil (see below), whereas other twenty, were transplanted into fresh standard gardening soil and used as control. After 30 days ten plants for each cultivar were kept on contaminated soil until death, to evaluate their life span in comparison with control plants, while the other plants were collected to perform the following analyses: biomass production (fresh weight FW and dry weight DW), water and nitrogen content, multielemental content in roots, shoots and rhizosphere soil. Afterword, newly germinated plants were used for a second 30-day growth cycle on the same soil samples, and relative multielemental analyses of root, shoot and rhizosphere soil were carried out to evaluate possible different metal extraction ability in comparison with the first growth cycle.

All the experiments were performed under semi controlled conditions in greenhouse: more specifically, the Photosynthetic Photon Flux Density (PPFD) at the top of the canopy, during the whole growth period was 450-550 µmol photons $m^{-2}s^{-1}$, air temperature 22±2 °C, relative humidity (RH) 55-65 %.

*Chemical analyses*

*Soil*

Soil samples (n=10 for each experimental thesis) were dried to constant weight at 40°C and sieved by a 2 mm mesh sieve. Then, soil fractions (sand, silt and clay) were separated using a pipette and a sieving method, following a pretreatment with $H_2O_2$ to oxidize

organic matter, and dispersion was aided by sodium hexametaphosphate. Soil pH was measured by potentiometry in distilled water (1:2.5 soil/water ratio).

To quantify the total metal contents, 1 g of each soil sample, further sieved through a 20-mesh (0.8 mm) screen, was digested by an acid solution of (2:2:1:1) $H_2O$ - HF - $HClO_4$ - HNO. HCl 50% was added to the residue and heated using a mixing hot block. The concentrations of 13 elements (Al, As, Ba, Cd, Ce, Cr, Cu, Fe, La, Mn, Ni, Pb, Sb) were analyzed for all the sample solutions with a Perkin Elmer Elan 6000 ICP mass spectrometer. To avoid contamination by acid digestion, blanks (mineralization solutions without soil samples) were analyzed as well.

To estimate the promptly (i.e., readily soluble) and potentially bioavailable fractions of the major metal soil contaminants, selected 2-mm sieved soil subsamples were extracted by either 1M $NH_4NO_3$ or 0.05M EDTA at pH 7 (Rauret et al. 2001) respectively. In Germany, indeed, soil extraction by 1M $NH_4NO_3$ is recognized as official standard and recommended by the German Federal Soil Protection and Contaminated Sites Ordinance to assess the risk of transfer of metals from the soil to plants.

*Plants*

For the analysis of the metals in the plants, aliquots of control and treated plants (n=10) were dried to constant weight at 40 °C, separated into roots and shoots, powdered and homogenized using a Retsch PM200 ball miller equipped with agate pockets. An amount of 250 mg plant material was digested with the same protocol used for soil (see above paragraph).

Both for plants and soil, the percentage of recovery ranged for all the elements between 80 % and 110 % and the precision of the ICP-MS analysis was considered acceptable, with the RSD values lower than 10 %.

For total nitrogen content, aerial biomass of the control and treated plants was collected at the end of the experiment and sub-samples were oven-dried at 70 °C till constant weight for chemical analyses. Nitrogen content of plant tissue was measured on fine grounded dry biomass according to the Kjeldahl method.

*Data analysis*

Basic statistics and graphs were computed by Microsoft Excel, 2010. A principal component analysis (PCA) was applied to chemical contents in control and treated plant tissues. Analysis of variance (ANOVA) followed by Tukey's post hoc test was used to

compare growth parameters, as well as element concentration in plant tissues and soils subject to the different treatments ($p<0.05$). All the statistical tests were performed using Statistica software ver. 8.0 (Stat Soft Inc., 2007).

## Results

*Soil physicochemical properties*

The industrial soil under study can be classified as a sandy loam, consisting primarily of medium to coarse size sand particles (~65%). It is moderately alkaline (pH in $H_2O$ around 8.0), even for the variable but not negligible content in carbonates (5.3% on average). It also holds a medium-low content in organic matter (<3%) and its electrical conductivity (<0.4 dS $m^{-1}$) does not reveal a consistent accumulation of soluble salts limiting plant growth.

*Soil and plant elemental content*

The elements analyzed in both soil and plants are reported in Tables 1 and 2. As for the element concentrations in the soil before phytoremediation treatment (Table 1), several thousand ppm of Pb and about 300 ppm of Cd were found.

A general decrease was observed after plant culturing in the rhizosphere soil, significant for most of cases, especially after the second growth cycle (Table 1). Particularly, all the cultivars could significantly reduce the Pb content in the rhizosphere, especially the cv. Sardo, from about 67000 mg $kg^{-1}$ in pre-remediation soil to about 35000 mg $kg^{-1}$ after two growth rounds. This cultivar had indeed the highest ability to reduce metal concentration in the rhizosphere soil compared to the other two cultivars (difference significant for Al, Ce, Cu, La, Sb based on element concentrations measured in the soil after the second growth cycle).

Since after the first growth cycle, in the plants grown on polluted soil (Table 2), a significant increase of most elements was observed in roots, compared to control soil. By contrast, only Cd, Cu, Fe, Pb and Sb significantly increased also in leaves, indicating that these elements were translocated to the shoots.

After the second growth cycle, a further significant increase especially in roots was observed in all cultivars and for all elements considered.

Standardized data on root and shoot contents after the second growth cycle were explored by PCA to evaluate the accumulation trends among the different cultivars and plant organs (Figure 1). The projection of the cases (i.e., root and shoot) and variables

(elements) of the PCA, separated the roots of the treated plants from all other items along the first coordinate accounting for 81% of the total variance. This suggests that roots from plants grown on polluted soil, were particularly enriched in most elements; this trend was especially evident in *C. cardunculus* cv. Sardo. Control roots, control leaves and treated leaves, diverged limitedly along the second axis, which explains about 15% of the total variance.

Based on the total element content (sum of normalized values obtained dividing each element concentration by the maximum value) in the roots after the second growth round (Figure 2), Sardo showed the highest uptake ability, with all element concentrations higher than those found in the other cultivars, except for Cd, which had the highest concentration in Spagnolo. Considering all elements, Siciliano had a total element accumulation of 83% and Spagnolo of 88%, compared to Sardo (fixed to 100%).

Table 1. Elemental content (mean±SD, n=10) in control (pre-remediation polluted soil) and rhizosphere soils (post-remediation) after the 1st and the 2nd growth cycle. Different letters indicate significant differences ($p<0.05$) according to Tukey's post hoc test.

| | | Post-remediation | | | | | |
|---|---|---|---|---|---|---|---|
| | | Sardo | | Siciliano | | Spagnolo | |
| SOIL | Pre-remediation | PS1* | PS2 | PS1 | PS2 | PS1 | PS2 |
| Al | 69233±763a | 64150±919b | 50900±848e | 62200±565c | 59200±141d | 68100±989a | 63350±494bc |
| As | 176±35a | 181±34a | 118±11b | 138±4ab | 140±35ab | 162±29ab | 122±2b |
| Ba | 968±30a | 956±61ab | 735±42d | 925±60ab | 827±53cd | 973±48a | 871±2bc |
| Cd | 314±38a | 266±14b | 254±11b | 270±2b | 278±9ab | 271±34ab | 260±2b |
| Ce | 100.0±3.0a | 93.9±3.0b | 73.2±0.3f | 87.5±2.0cd | 81.3±0.1e | 92.9±5.9bc | 85.9±0.2de |
| Cr | 95.1±15.5a | 84.2±11.3a | 54.5±4.9c | 69.5±0.7abc | 60.3±2.8bc | 78.0±1.4ab | 64.5±2.8bc |
| Cu | 870±40a | 720±56b | 554±11c | 708±15b | 670±27b | 701±33b | 685±23b |
| Fe | 46786±715a | 42400±1979b | 32900±1414c | 40550±1060bc | 36850±1626c | 44850±1202b | 38500±1414c |
| La | 51.9±0.9a | 50.4±0.1ab | 40.5±0.1e | 46.45±1.1cd | 46.1±0.7cd | 48.6±2.9bc | 45.2±1.1d |
| Mn | 1035±20ab | 975±25bc | 791±24e | 905±28cd | 845±18de | 1078±72a | 921±55cd |
| Ni | 96.2±8.5a | 74.1±12.5b | 51.2±4.5d | 62.7±0.3c | 63.3±12.5bc | 75.7±4.4b | 61.2±3.5c |
| Pb | 67300±2778a | 68000±2828a | 34800±707d | 63150±8414ab | 43050±4030c | 59750±1060b | 55850±7990b |
| Sb | 1480±41a | 1380±79a | 912±17c | 1317±7a | 1151±27b | 1230±16b | 1188±4b |

*PS: polluted soil; 1 & 2 stands for first and second growth cycle

*Biomass production, water stress, life span and nitrogen content*

In Table 3 fresh and dry weight (aerial part), water and nitrogen content in plant tissue, as well as life span, are reported for each cultivar grown on control and polluted soil. Despite some differences in the weight depending on the specific cultivar, with a biomass production higher in *C. cardunculus* cv. Spagnolo, no substantial differences among the three cultivars grown on control soil were observed based on fresh weight. By contrast, polluted substrate strongly limited cardoon growth with a different response of the tested cultivars; once again cv. Spagnolo resulted the most adaptable to stress conditions with the lowest biomass reduction in polluted soils (-43% FW vs -53% in Sardo and -66% in Siciliano). Dry weight and water content values highlighted the occurrence of water stress in *C. cardunculus* cv. Siciliano after 1-month growth on polluted soil, with a decrease in water content of about 8% compared to control plants; whereas, Sardo and Spagnolo seemed to better tolerate the growth on polluted soil in terms of water stress.

Comparing plants grown on control and polluted soil (Table 3), nitrogen content in the shoots of Sardo and Siciliano cardoon, was inversely proportional to biomass (DW) production, showing the lowest values in plants with the highest dry biomass, i.e., those grown on unpolluted soil. Nitrogen content recorded in Spagnolo grown on control soil were significantly higher (+50%) than those measured in the other two cultivars and remained unchanged when the plant grew on polluted soil (Table 3). Another trait favoring this cultivar in growing on HM-contaminated soil was represented by the longest life span (18 weeks), recorded in the present experiment (Table 3). All these data indicated the cultivar Spagnolo as the most resistant to metal-stress.

Table 2. Elemental content (mean±SD, n=10) in leaves (L) and roots (R) of cardoon cultivars (Siciliano, Sardo, Spagnolo) in plants grown in unpolluted soil (US), and after the 1st and 2nd growth cycle on polluted soil (PS1, PS2). Different letters indicate significant differences ($p<0.05$) according to Tukey's post hoc test.

| | Sardo | | | | | | Siciliano | | | | | | Spagnolo | | | | | |
|---|---|---|---|---|---|---|---|---|---|---|---|---|---|---|---|---|---|---|
| | US* | | PS1** | | PS2 | | US | | PS1 | | PS2 | | US | | PS1 | | PS2 | |
| | L | R | L | R | L | R | L | R | L | R | L | R | L | R | L | R | L | R |
| **Al** | 83±29f | 400±100d | 467±153d | 8133±977b | 300±264d | 24366±6087a | 167±58e | 567±58d | 500±100d | 2233±602c | 667±404d | 22366±1332a | 200±57e | 300±100e | 533±153d | 2700±307c | 400±100d | 21800±1056a |
| **As** | 0.86±0.70e | 1.56±0.61de | 1.10±0.36e | 19.4±8.0b | 1.10±0.43e | 60.00±17.00a | 1.46±0.15e | 1.66±0.58de | 1.70±0.52de | 7.30±1.76c | 2.96±1.82d | 47.20±23.90a | 0.56±0.20e | 1.13±0.05e | 1.10±0.60e | 9.43±3.02c | 2.26±0.92d | 59.50±22.10a |
| **Ba** | 9.0±0.0d | 7.6±1.5d | 16.0±3.4c | 137±42b | 12.3±4.2c | 350.3±96.2a | 11.3±1.1c | 12.6±1.1c | 16.3±2.0c | 39.6±10.5c | 22.1±9.2c | 333.6±192.8a | 8.6±0.5d | 7.3±2.0d | 16.0±3.4c | 50.3±21.9c | 14.0±2.0c | 314.6±146.8a |
| **Cd** | 0.3±0.1d | 0.17±0.1d | 100±27b | 155±5b | 54±14c | 211±27a | 0.4±0.1d | 0.2±0.1d | 71±30c | 65±26c | 58±4c | 191±70ab | 0.4±0.1d | 0.2±0.1d | 97±11bc | 140±72b | 72±10c | 224±79a |
| **Ce** | 0.15±0.04d | 0.64±0.21d | 0.54±0.16d | 12.52±3.28b | 0.65±0.56d | 36.75±7.52a | 0.22±0.03d | 0.81±0.14d | 0.66±0.13d | 3.50±1.10c | 1.01±0.59d | 32.60±18.10a | 0.22±0.07d | 0.37±0.18d | 0.73±0.24d | 4.11±1.4c | 0.66±0.19d | 32.47±14.92a |
| **Cr** | 2.04±0.01e | 2.10±0.03e | 2.33±0.57e | 10.71±1.82b | 5.70±3.23d | 32.00±7.34a | 2.40±0.01e | 5.06±2.60d | 2.05±0.15e | 3.70±0.60dc | 9.70±1.15bc | 23.33±3.86a | 2.00±0.22e | 2.30±0.34e | 2.30±0.05e | 7.70±3.20c | 7.66±3.78c | 23.00±9.84ab |
| **Cu** | 2.50±0.40d | 5.33±1.09d | 7.73±1.50c | 175.00±19.00b | 8.93±4.23c | 366.00±69.40a | 2.66±0.81d | 7.93±1.07c | 9.16±2.40c | 72.00±30.10b | 16.00±3.90c | 315.00±26.00a | 2.20±0.26d | 5.20±1.80d | 9.53±3.59c | 112.00±63.30b | 9.40±2.16c | 339.00±132.00a |
| **Fe** | 67±39f | 200±100e | 300±100e | 5733±381b | 183±19e | 17200±5650ab | 116±76ef | 333±57e | 300±100e | 1566±404c | 483±51d | 14766±8675ab | 100±19f | 233±58e | 333±58e | 1733±680c | 266±57e | 14667±6551ab |
| **La** | 0.05±0.01c | 0.33±0.15c | 0.33±0.11c | 7.03±0.89b | 0.4±0.26c | 19.9±4.47a | 0.08±0.02c | 0.43±0.05c | 0.36±0.05c | 2.00±0.65c | 0.56±0.30c | 18.20±9.89a | 0.06±0.02c | 0.16±0.11c | 0.40±0.10c | 2.66±1.15c | 0.33±0.11c | 18.00±8.55ab |
| **Mn** | 38.6±4.9c | 24.3±17.3c | 50.6±12.0c | 154.0±42.0b | 26.0±7.0c | 389.0±102.0a | 45.3±43.8c | 41.3±30.9c | 43.0±1.0c | 48.6±5.7c | 39.6±21.3c | 341.0±94.0a | 46.3±22.5c | 16.6±6.4c | 45.0±11.7c | 63.0±19.4c | 57.3±11.7c | 330.0±50.0a |
| **Ni** | 0.86±0.81e | 0.86±0.40e | 1.41±0.26de | 12.00±1.30b | 3.06±1.24d | 31.60±11.90a | 0.56±0.30e | 2.46±1.76d | 1.46±0.51de | 3.96±1.30d | 5.83±1.78c | 24.6±12.1a | 0.46±0.11e | 0.80±0.30e | 1.56±0.55de | 7.10±3.04c | 4.43±1.96c | 30.00±16.90a |
| **Pb** | 5.70±1.46d | 10.30±1.00d | 486±253c | 3480±1292b | 552±189c | 8152±3357a | 7.36±3.45d | 16.80±3.60d | 1395±355c | 3466±1410b | 704±226c | 4632±1498ab | 7.01±0.26d | 16.30±8.61d | 575±103c | 3700±1255b | 628±254c | 5760±2779a |
| **Sb** | 0.31±0.02e | 0.23±0.18e | 5.47±1.86d | 127±34b | 5.20±3.74d | 554±142a | 0.53±0.24e | 0.37±0.19e | 7.18±2.15d | 38.5±8.01c | 12.7±8.56d | 438±248a | 0.58±0.16e | 0.30±0.24e | 7.50±2.88d | 45.50±8.97c | 6.19±1.49d | 471±213a |

*US: Unpolluted soil; **PS: polluted soil; R: Root; L: Leaf; 1 & 2 stands for first and second growth cycle

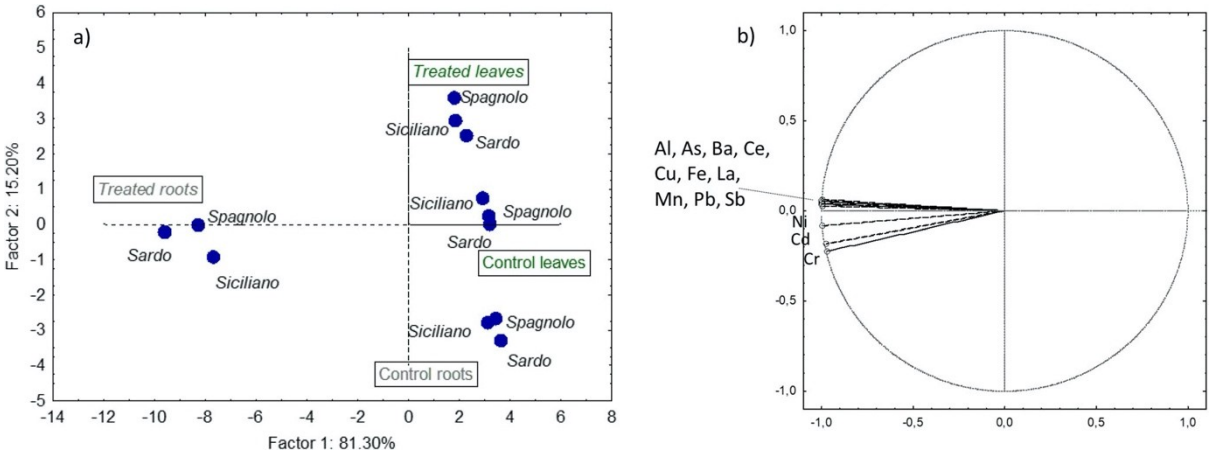


Fig. 1 PCA of the chemical content in plant tissues (leaves and roots after the second growth round) of the three cultivars of C. cardunculus (Sardo, Siciliano, and Spagnolo) grown on gardening soil (control) and polluted soil (treated); projection of cases (a) and variables (b)

*Metal bioavailability, bioconcentration and translocation factors*

In soil, the promptly available fraction of the metals - extracted by ammonium nitrate - was very low, in particular for As, Cu and Pb (<<1% of the total content, Table 4); however, considerable amounts of Cd (62% of the total content), Pb (74%) and Sb (54%) were extracted by EDTA, namely the potentially bioavailable fractions and therefore transferrable to plant tissues (Table 4).

For As, Cu, Cd, Pb and Sb the relation between their content in soil and in plant tissues was investigated by calculating bioconcentration and translocation factors (Ali et al. 2013; Esringü et al. 2014), both reported in Table 5. The results indicate higher metal bioconcentration during the second growth round for all cultivars and elements (Table 5), in agreement with metal content found in plants from the second culture cycle. A high translocation factor was found for Cd (up to 109%), while it was always lower than 25% for the other elements.

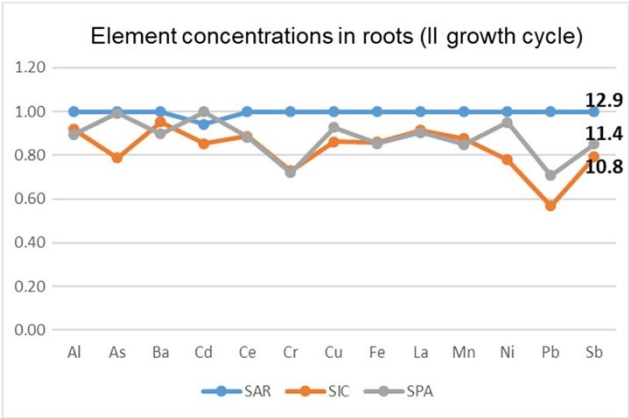


Fig. 2 Normalized element concentrations measured in the roots of the three cultivars after the second growth cycle and their summation (SAR, Sardo; SIC, Siciliano; SPA, Spagnolo)

Table 3 Fresh and dry weight (aerial part), water content, life span, and N content in the shoots of cardoon grown on control (gardening soil), polluted soil

| Cultivar | | FW ± SD (g) | DW ± SD (g) | Water content (%)** | Life span* (weeks) | N (%) |
|---|---|---|---|---|---|---|
| Sardo | Control | 16.16 ± 4.01a | 2.86 ± 0.56a | 82.3% | > 18 | 1.99 ± 0.56b |
| | Polluted | 7.60 ± 3.20c | 1.44 ± 0.17b | 81.1% | 13.7 | 3.08 ± 0.32a |
| Siciliano | Control | 18.09 ± 3.86a | 2.89 ± 0.96a | 84.0% | > 18 | 2.01 ± 0.85b |
| | Polluted | 6.19 ± 2.03c | 1.46 ± 0.31b | 76.4% | 14.5 | 2.98 ± 0.40a |
| Spagnolo | Control | 1 20.95 ± 2.98a | 3.39 ± 0.55a | 83.8% | > 18 | 3.18 ± 0.36a |
| | Poluted | 12.01 ± 2.55b | 1.91 ± 0.24b | 84.1% | 18 | 3.19 ± 0.09a |

Different letters indicate significant differences ($p < 0.05$) according to Tukey's post hoc test. *Life span after transplant to polluted soil or control soil. For all tests, $n = 10$, for nitrogen content, $n = 6$. **Not significantly different
For further details, see the "Materials and methods" sections

Table 4 Percentage of bioavailable EDTA and $NH_4NO_3$ extracted fractions from polluted soil (see Table 1, pre- remediation soil)

| | EDTA (%) | $NH_4NO_3$ (%) |
|---|---|---|
| As | 17 | 0.3 |
| Cd | 62 | 1.5 |
| Cu | 36 | 0.13 |
| Pb | 74 | 0.04 |
| Sb | 54 | 1.0 |

Table 5 Bioconcentration factor (BF) for each considered element in root and shoot of different cultivars of cardoon (Sardo, SA; Siciliano, SI; Spagnolo, SP) after the first and the second growth cycles (1–2).

| BF | Root (%) | Shoot (%) | TF= Cs/Cr (%) |
|---|---|---|---|
| **As** | | | |
| SA_1 | 7.6 | 0.4 | 5.7 |
| SA_2 | 33.2 | 0.6 | 1.8 |
| SI_1 | 2.9 | 0.7 | 23.3 |
| SI_2 | 34.0 | 2.1 | 6.3 |
| SP_1 | 3.7 | 0.4 | 11.7 |
| SP_2 | 36.6 | 1.4 | 3.8 |
| **Cd** | | | |
| SA_1 | 49.3 | 31.8 | 109.0 |
| SA_2 | 71.9 | 21.8 | 25.4 |
| SI_1 | 20.8 | 22.6 | 64.4 |
| SI_2 | 78.0 | 19.8 | 30.3 |
| SP_1 | 44.7 | 30.9 | 69.2 |
| SP_2 | 82.4 | 26.4 | 32.1 |

| | | | |
|---|---|---|---|
| **Cu** | | | |
| SA_1 | 20.2 | 0.9 | 12.7 |
| SA_2 | 50.8 | 1.2 | 5.1 |
| SI_1 | 8.3 | 1.1 | 4.4 |
| SI_2 | 44.6 | 2.3 | 2.4 |
| SP_1 | 13.0 | 1.1 | 8.5 |
| SP_2 | 48.5 | 1.3 | 2.8 |
| **Pb** | | | |
| SA_1 | 12.1 | 0.8 | 15.2 |
| SA_2 | 51.0 | 2.1 | 1.4 |
| SI_1 | 6.9 | 1.0 | 6.8 |
| SI_2 | 55.1 | 0.8 | 4.0 |
| SP_1 | 8.6 | 0.9 | 10.9 |
| SP_2 | 61.9 | 1.0 | 1.6 |
| **Sb** | | | |
| SA_1 | 8.6 | 0.4 | 18.6 |
| SA_2 | 40.2 | 0.4 | 2.9 |
| SI_1 | 2.6 | 0.5 | 4.3 |
| SI_2 | 33.3 | 1.0 | 0.9 |
| SP_1 | 3.1 | 0.5 | 16.5 |
| SP_2 | 38.4 | 0.5 | 1.3 |

For each element, the translocation factor (TF) calculated as the ratio between element concentrations in shoot ($C_s$) and root ($C_r$) is reported in the last column

## Discussion

*Metal uptake, soil clean-up ability and growth pattern*

Element concentrations found in pre-remediation soil were generally in line with those measured in a previous work analyzing the same soil (Visconti et al. 2018), despite the high variability of soil composition highlighted in that article. It is worth noting that metal concentrations in the soil used in the present work were far greater than those measured in the ILVA brownfield site, located in the same region, in the Bagnoli-Fuorigrotta plain, hosting from 1910 to the 1990s one of the largest Italian iron-steel production plants (Fiorentino et al. 2017). However, physical-chemical properties of the present soil, in particular conductivity, evidenced conditions compatible with plant growth. Although all cultivars were able to accumulate significant, large amounts of metals, reducing in parallel the level of metal contamination in the soil, the cultivar Sardo provided the best performance both concerning metal accumulation and soil cleaning-up. Indeed, these results should be considered with caution, due to the extreme variability of soil composition, and especially considering that the ten samples of pre-remediation soil were certainly collected from the entire soil sample after its homogenization, but not from the individual pots, like post-remediation soil samples.

The further reduction of metals in the rhizosphere soil, observed after the second growth round, and significantly higher than the first, supports a role of root exudates in shifting of the chemical equilibrium between insoluble and soluble fractions of each element, enhancing element bioavailability and plant uptake. This shift was likely favored by the acidification of the soil (Salomons 1995); in fact, pH started from a value of 8.0 before the first growth cycle and decreased to 7.5 and 7.0 after the first and the second culture cycles, respectively. It is likely that this acidification could increase metal bioavailability and salt soluble fraction, thereby affecting soil conductivity until reaching condition unfavorable to plant growth, leading to plant death after several weeks of growth on polluted soil (13 weeks in Sardo and 18 in Spagnolo). In addition, the high metal accumulation and reduced growth observed in Sardo could be responsible of its shortest life span on polluted soil.

Biomass production of all cultivars was affected by metal pollution, especially in Sardo and Siciliano; in fact, Spagnolo showed a biomass about two folds that of the other cultivars, when grown on polluted soil. Along with a biomass reduction, the cultivar Siciliano also exhibited water stress; this result is consistent with previous observations evidencing necrosis and plasmolysis occurring in Siciliano (Sorrentino et al. 2018). Moreover, the severe growth reduction observed in Sardo and Siciliano agrees with the increase of N concentration found in their leaves, and likely due to the well-known concentration/dilution effect (Wang et al. 2017). It is worth noting that Spagnolo had constitutively (i.e., while growing on unpolluted soil) a higher concentration of N compared to the other two cultivars and that this concentration remained unchanged in the shoot of Spagnolo grown on polluted soil; this suggests that Spagnolo had the highest mineral-N use efficiency, or a higher root efficiency compared to the other cultivars. These traits could favor this cultivar under limiting growth conditions. All these results well agree with those reported in a previous work (Sorrentino et al. 2018), in which other morpho-physiological parameters were evaluated in these cardoon cultivars grown on the same polluted soil. Particularly, severe ultrastructural damages were observed in the chloroplasts of Sardo and Siciliano, whereas a preserved ultrastructure was found in Spagnolo; accordingly, this latter also exhibited a positive physiological response under metal stress, showing the highest photochemical efficiency and a significant increase in the production of key proteins involved in photosynthesis, like Rubisco.

*Metal bioavailability, bioconcentration and translocation*

Soil analyses showed that the promptly available fraction of metals represented a very limited amount. However, based on the very high metal contents found in pre-remediation soil, even

these low fractions may represent a noticeable risk for plants growing on this soil. Moreover, the fact that considerable amounts of Cd, Pb and Sb were found in the potentially bioavailable fractions (i.e., that extracted by EDTA) and therefore could enter plant tissues, posing a serious risk for environment and biota (Manoucheheri and Bermond 2009; Menzies et al. 2007). Indeed, metals and metalloids occur in soil in a variety of forms; exchangeable fraction is easily bioavailable because it consists of metals weakly bound to colloidal or particulate material, whereas the complexed, precipitated or strongly bound metal species are generally accounted as fractions potentially available to biota. Metals associated to Fe and Mn oxides and organic matter, for instance, are often considered potentially available, while metals occluded in non-siliceous and siliceous minerals result to be poorly available (Rauret et al. 1999). However, since bioavailability is strongly affected by soil chemical properties as pH, even the less bioavailable pool might be partially taken up by the plants. To this regard, we noted that cardoon plants extracted from soil not only the promptly available fraction, but also part of the potentially available fraction. This result indicates these plants as suitable candidate for phytoextraction and confirm the increase of the bioavailable metal fraction during the two culture rounds. In cardoon grown on polluted soil, metal concentrations for most elements reached levels of 1-2 orders higher than those observed in control plants, indicating that *C. cardunculus* acts as a hyperaccumulator species (van der Ent et al. 2015). This seemingly obvious result is not so common; in fact, among plants able to grow on metal polluted soil, the majority are metal excluders (Baker 1987). In addition, in several plant species hyperaccumulation exists as a side effect of acidic root exudates evolved as a P- acquisition mechanism, as observed in *Phytolacca americana* L. growing on Mn mines from China and USA (Lambers et al. 2015).

It is known that hyperaccumulators have BCF greater than 1 (i.e., >100%) (Cluis 2004). However, in soils highly metal polluted, as the one we tested, BCF could result lower than 1 (Ali et al. 2013). Interestingly, the translocation factor was always lower in the second growth round for all considered elements; however, for As, Cu, Pb and Sb these lower TFs corresponded to higher metal contents in leaves (i.e., their percentage values were lower since their content in roots was much higher compared to the first growth round; see also Table 2). By contrast, for Cd this lower TF is associated to a low metal content in leaves from the second growth round (i.e., despite the high amount of Cd accumulated in the second growth round, most remained in the root; see also Table 2). It is likely that the accumulation of Cd in the root is highly dependent on Cd bioavailability, differently from its translocation; therefore, the increased Cd bioavailability after the first growth round could produce a higher accumulation

in root, but not necessarily a higher translocation. These differences in root and shoot accumulation find a possible explanation in the fact that one of the normal functions of roots is to absorb ions from the water solution of the rhizosphere, whereas shoot does not normally play this role (Salt et al. 1997).

## Conclusions

All the three cultivars of cardoon tested in the present experiment proved able to accumulate metals in their tissues when grown on an industrial, highly metal-polluted soil and to significantly reduce metal content in rhizosphere soil after two growth cycles, especially Sardo. *C. cardunculus* acted as a hyperaccumulator since its metal content was higher than promptly available fraction, suggesting that phytoremediation with cardoon could be a viable option in highly contaminated soils. Contaminated plants produced during phytoremediation actions can be further processed for bioharvesting of metals (phytomining) and to produce green energy from organic biomass (e.g. biofuel). A shift between potentially and promptly available fraction occurred, likely favored by pH decrease during the two growth cycles. This can explain the satisfactory performance in metal accumulation, as well as the higher uptake in the second growth round, but likely also the reduced life span of the cultivars grown on polluted soil. In addition, this species proved a good phytoextractant for Cd, being this metal largely translocated to leaves, whereas it can be considered a good phytostabilizer for the other elements here analyzed; however, further investigations could reveal different accumulation/translocation patterns in soils with different level of metal pollution. The severe reductions in biomass production and life span observed in Sardo and Siciliano, suggest a lower resistance of these cultivars under metal stress, despite the best accumulation performance of the first. In conclusion, *C. cardunculus* cv. Spagnolo is recommended in future field experiments, for its ability to couple metal uptake and soil cleaning up with the best growth performance and the longest life span.

**Acknowledgements.**
This work was partly supported by grant from the Ministero dell'Università e della Ricerca Scientifica¬Industrial research project "Development of green technologies for production of BIOchemicals and their use in preparation and industrial application of POLImeric materials from agricultural biomasses cultivated in a sustainable way in Campania region (BioPoliS)" PON03PE_00107_1, funded in the frame of Operative National Programme Research and Competitiveness 2007–2013 D. D. Prot. N. 713/Ric. 29/10/2010; and partly financed by the EU Commission, Project: LIFE/11/ENV/IT/275ECOREMED "Implementation of ecocompatible protocols for agricultural soil remediation in Litorale Domizio-Agro Aversano NIPS". We would like to thank Dr. Riccardo Riccardi, as a member of Arca 2010, an enterprise participating in BioPolis, for providing us cardoon seeds.

**References**

Ali H, Khan E, Sajad MA (2013) Phytoremediation of heavy metals - Concepts and applications. Chemosphere 91:869–881. DOI: 10.1016/j.chemosphere.2013.01.075

Alloway BJ (1995) Heavy metals in soils, 2nd edn, Blackie Academic and Professional, an Imprint of Chapman & Hall, London.

Arena C, Figlioli F, Sorrentino MC, Izzo LG, Capozzi F, Giordano S, Spagnuolo V (2017) Ultrastructural, protein and photosynthetic alterations induced by Pb and Cd in *Cynara cardunculus* L., and its potential for phytoremediation. Ecotox Environ Safe 145:83–89. DOI: 10.1016/j.ecoenv.2017.07.015

Baker AJ (1987) Metal tolerance. New Phytol 106:93–111. https://doi.org/10.1111/j.1469-8137.1987.tb04685.x

Capozzi F, Giordano S, Di Palma A, Spagnuolo V, De Nicola F, Adamo P (2016) Biomonitoring of atmospheric pollution by moss bags: discriminating urban-rural structure in a fragmented landscape. Chemosphere 149:211–218. https://doi.org/10.1016/j.chemosphere.2016.01.065

Cluis C (2004) Junk-greedy greens: phytoremediation as a new option for soil decontamination. Bio Tech J 2:61–67.

di Gennaro A (2014) Per una storia dell'ecosistema metropolitano di Napoli, In: Viella SRL (ed) Meridiana 80. Città metropolitana, pp 105–124.

Di Palma A, Capozzi F, Spagnuolo V, Giordano S, Adamo P (2017) Atmospheric particulate matter intercepted by moss-bags: Relations to moss trace element uptake and land use. Chemosphere 176:361–368. DOI: 10.1016/j.chemosphere.2017.02.120

Esringü A, Turan M, Güne M¸ Karaman RM (2014) Roles of Bacillus megaterium in remediation of boron, lead, and cadmium from contaminated soil. Commun Soil Sci Plan 45:1–19. https://doi.org/10.1080/00103624.2013.875194

Fiorentino N, Fagnano M, Ventorino V, Pepe O, Zoina A, Impagliazzo A (2013) Assisted phytoextraction of heavy metals: compost and Trichoderma effects on giant reed (Arundo donax L.) uptake and soil quality. Ital J Agron 8:244–254. DOI https://doi.org/10.4081/ija.2013.e29

Fiorentino N, Ventorino V, Rocco C, Cenvinzo V, Agrelli D, Gioia L, Di Mola I, Adamo P, Pepe O, Fagnano M (2016) Giant reed growth and effects on soil biological fertility in assisted phytoremediation of an industrial polluted soil. Sci Total Environ 575:1375–1383. DOI: 10.1016/j.scitotenv.2016.09.220

Hernández-Allica J, Garbisu C, Barrutia O, Becerril JM (2007) EDTA-induced heavy metal accumulation and phytotoxicity in cardoon plants. Environ Exp Bot 60:26–32. https://doi.org/10.1016/j.envexpbot.2006.06.006

Iodice P, Adamo P, Capozzi F, Di Palma A, Senatore A, Spagnuolo V, Giordano S (2016) Air pollution monitoring using emission inventories combined with the moss bag approach. Sci Total Environ 541: 1410-1419. DOI: 10.1016/j.scitotenv.2015.10.034

Lambers H, Hayes PE, Laliberté E, Oliveira RS, Turner BL (2015) Leaf manganese accumulation and phosphorus-acquisition efficiency. Trends Plant Sci. 20:83. https://doi.org/10.1016/j.tplants.2014.10.007

Liu D, Jiang W, Liu C, Xin C, Hou W (2000) Uptake and accumulation of lead by roots, hypocotyls and shoots of Indian mustard Brassica juncea (L.). Bioresource Technol 71:273–277. https://doi.org/10.1016/S0960-8524(99)00082-6

Llugany M, Miralles R, Corrales I, BarcelóJ, Poschenrieder C (2012) *Cynara cardunculus* a potentially useful plant for remediation of soils polluted with cadmium or arsenic J Geochem Explor 123:122–127. https://doi.org/10.1016/j.gexplo.2012.06.016

Manouchehri N, Bermond A (2009) EDTA in Soil Science: A Review of Its Application in Soil Trace Metal Investigations. Terr Aquat Environ Technol 3:1–15.

Meers E, Van Slycken S, Adriaensen K, Ruttens A, Vangronsveld J, Du Laing G, Witters N, Thewys T, Tack FMG (2010) The use of bio-energy crops (*Zea mays*) for 'phytoattenuation' of heavy metals on moderately contaminated soils: a field experiment. Chemosphere 78:35–41. DOI: 10.1016/j.chemosphere.2009.08.015

Menzies NW, Donn MJ, Kopittke PM (2007) Evaluation of extractants for estimation of the phytoavailable trace metals in soils. Environ Pollut 145:121–130. https://doi.org/10.1016/j.envpol.2006.03.021.

Murashige T, Skoog F (1962) A revised medium for rapid growth and bio assays with tobacco tissue cultures. Physiol plantarum 15:473–497. https://doi.org/10.1111/j.1399-3054.1962.tb08052.x

Panagos P, Van Liedekerke M, Yigini Y, Montanarella L (2013) Contaminated sites in Europe: review of the current situation based on data collected through a European network. J Environ Public Health, vol. 2013, Article ID 158764, 11 pages. http://dx.doi.org/10.1155/2013/158764.

Papazoglou EG (2011) Responses of *Cynara cardunculus* L. to single and combined cadmium and nickel treatment conditions. Ecotox Environ Safe 74:195–202. DOI: 10.1016/j.ecoenv.2010.06.026

Papoyan A, Piñeros M, KochianLV (2007) Plant Cd2+and Zn2+status effects on root and shoot heavy metal accumulation in Thlaspi caerulescens. New Phytol 175:51–58. DOI: 10.1111/j.1469-8137.2007.02073.x

Rauret G, López-Sánchez JF, Bacon J, Gomez A, Muntau H, Queaviller P (2001) Certification of the contents (mass fraction) of Cd, Cr, Cu, Ni, Pb and Zn in an organic-rich soil following harmonised EDTA and acetic acid extraction procedures, BCR-700, BCR information, reference materials. Report EUR 19774 EN. ISBN: 92-894-0755-7

Rauret G, López-Sánchez JF, Sahuquillo A, Davidson C, Ure A, Quevauviller P (1999) Improvement of the BCR 3-step sequential extraction procedure prior to the certification of new sediment and soil reference materials. J Environ Monit 1:57–61. DOI:10.1039/A807854H

Salomons W (1995) Environmental impact of metals derived from mining activities: Processes, predictions, prevention. J Geochem Explor 52:5–23. https://doi.org/10.1016/0375-6742(94)00039-E

Salt DE, Pickering IJ, Prince RC, Gleba D, Dushenkov S, Smith RD, Raskin I (1997) Metal accumulation by aquacultured seedlings of indian mustard. Environ Sci Technol 31:1636–1644. DOI: 10.1021/es960802n

Sorrentino MC, Capozzi F, Amitrano C, Giordano S, Arena C, Spagnuolo V (2018) Performance of three cardoon cultivars in an industrial heavy metal-contaminated soil: effects

on morphology, cytology and photosynthesis. J Hazard Mater 351:131-137. 10.1016/j.jhazmat.2018.02.044

van der Ent A, Baker AJ, Reeves RD, Pollard AJ, Schat H (2015) Commentary: toward a more physiologically and evolutionarily relevant definition of metal hyperaccumulation in plants. Front Plant Sci (2015) 6:544. https://doi.org/10.3389/fpls.2015.00554

Wang X, Ye T, Ata-Ul-Karim ST, Zhu Y, Liu L, Cao W, Tang L (2017) Development of a critical nitrogen dilution curve based on leaf area duration in wheat. Front Plant Sci 8:1517. DOI: 10.3389/fpls.2017.01517

Wiklund A (1992) The genus *Cynara* L. (Asteraceae-Cardueae). Bot J Linn Soc 109: 75–123.

Xia HP (2004) Ecological rehabilitation and phytoremediation with four grasses in oil shale mined land. Chemosphere 54:345 –353. DOI: 10.1016/S0045-6535(03)00763-X

**Sitography**

BBodSchV (1999). Bodenschutz- und Altlastenverordnung [Federal Soil Protection and Contaminated Sites Ordinance]. 12 July 1999, Germany. http://www.gesetze-im-internet.de/bbodschv/index.html (accessed 13-05-2019)

BS ISO 19730 (2008). Soil quality - Extraction of trace elements from soil using ammonium nitrate solution. ISBN 978 0 580 54932 8, First edition 2008-12-01. https://www.iso.org/standard/41019.html (accessed 13-05-2019)

DIN 19730 (1997). Bodenbeschaffenheit–Extraktion von Spurenelementen mit Ammoniumnitratlösung. Beuth Verlag Berlin. https://www.beuth.de/de/norm/din-iso-19730/117095524 (accessed 13-05-2019)

Ecoremed Operative Handbook.
http://www.ecoremed.it/images/stories/FinalReport/LIFE%20ECOREMED%20Handbook.pdf (accessed 13-05-2019)

Legislative Decree, April 2006, n. 152.
http://www.camera.it/parlam/leggi/deleghe/06152dl6.htm. (accessed 13-05-2019)

# Chapter 3

## Facing metal stress by multiple strategy: morpho-physiological responses of cardoon (*Cynara cardunculus* L.) grown in hydroponics

Maria Cristina Sorrentino[1], Fiore Capozzi[1], Chiara Amitrano[2], Gaetano De Tommaso[3], Carmen Arena*[1], Mauro Iuliano[3], Simonetta Giordano [1], Valeria Spagnuolo[1]*

[1]*Dipartimento di Biologia, Università degli Studi di Napoli Federico II, Complesso Universitario di Monte Sant'Angelo, Cupa Nuova Cintia, 21 - 80126 – Napoli, Italia*
[2]*Dipartimento di Agraria, Università degli Studi di Napoli Federico II, Via Università, 100 – 80055-Portici, Italia.*
[3]*Dipartimento di Scienze Chimiche, Università degli Studi di Napoli Federico II, Complesso Universitario di Monte Sant'Angelo, Cupa Nuova Cintia, 21 - 80126 – Napoli, Italia.*

***Environmental Science and Pollution Research (2021) https://doi.org/10.1007/s11356-021-13242-9***

*corresponding authors: valeria.spagnuolo@unina.it; carmen.arena@unina.it

**Abstract**

The contamination of environments by heavy metals has become an urgent issue causing undesirable accumulations and severe damages to agricultural crops, especially cadmium and lead which are among the most widespread and dangerous metal pollutants worldwide. The selection of proper species is a crucial step in many plant-based restoration approaches; therefore, the aim of the present work was to check for early morpho-physiological responsive traits in three cultivars of *Cynara cardunculus* (Sardo, Siciliano and Spagnolo), helping to select the best performing cultivar for phytoremediation. For all three tested cultivars, our results indicate that cardoon displays some morpho-physiological traits to face Cd and Pb pollution, particularly at root morphology level, element uptake ability and photosynthetic pigment content. Other traits show instead, a cultivar-specific behavior; in fact, stomata plasticity, photosynthetic pattern and antioxidant power provide different responses, but only Spagnolo cv. achieves a successful strategy attaining a real resilience to metal stress. The capacity of Spagnolo plants to modify leaf structural and physiological traits under heavy metal contamination to maintain high photosynthetic efficiency should be considered an elective trait for its use in contaminated environments.

Keywords: Cardoon; Stomata; Root hairs; Gas exchanges; Cadmium; Lead.

## 1 Introduction

Rapid urbanization and agricultural practices can be considered the main responsible for metal pollution of land, water and plants, with a general detrimental effect for all living organisms. Although heavy metals are natural components of soil at trace levels, and some of them (i.e., Cu and Zn) are essential for the normal plant growth and development, the increasing anthropogenic activities have contributed to their accumulations. Urbanization involves industrialization and massive vehicular traffic, which release pollutants to air, soil, and water. Moreover, farmland activities sometimes imply the use of contaminated irrigation water, and mineral fertilizers, herbicides, additives for animal feeds, with global increase of metal pollution. As a consequence of current land-use practices, or activities inducing heavy metal mobilization, many soils are contaminated by these pollutants, especially in form of pesticides and nutrients (Motuzova et al., 2014). In recent time, the soil contamination by heavy metals has become an urgent issue, since it results in a severe loss in agricultural yield and damages on human health, due to metal entrance into the food web and biomagnification of some metals, such as Pb and Cd (He et al., 2015; Su et al., 2014).

The toxicity of heavy metals on plant metabolism has received extensive interest for several decades (Markert, 1993), with particular attention to crops (Chaney, 2015), whose contamination can cause health problems, as these plants are directly related to human diet. Cadmium (Cd) and lead (Pb) are among the most widespread metal pollutants worldwide (Su et al., 2014). Pb naturally occurs in soils but it is present in relatively low concentrations. In uncontaminated soils, Pb is generally in the range of 20-50 mg $kg^{-1}$ (Nriagu, 1978). Non-polluted soils usually contain less than 100 mg $kg^{-1}$ Pb; soils in unpolluted polar areas, buried before the industrial revolution, contain less than 5 mg $kg^{-1}$ (Meggeson and Hall, 1999). In industrialized areas, up to 1000 mg $kg^{-1}$ Pb and above has been recorded (Angelone and Bini, 1992; Capozzi et al., 2020). In recent studies carried out in Southern Italy, aimed to the environmental restoration of metal-contaminated areas, some industrial sites were selected, with Cd and Pb concentrations ranging between 1.6 and 314 mg $kg^{-1}$, and 409 and 100,000 mg $kg^{-1}$, respectively (Capozzi et al., 2020; Visconti et al., 2018).

Cadmium naturally occurs in Zn, Pb, and Cu ores with Zn concentration exceeding 50-200 folds Cd; the mining and smelting of these ores involve Cd contamination of surrounding soils (Chaney, 2015).

In plants, the exposition to heavy metals, and especially Cd, results in a severe reduction of plant growth and development as a consequence of photosynthetic apparatus impairment

(Arena et al., 2014). Photosynthesis is one of the process sensitive to metal toxicity (Arena et al., 2017; Figlioli et al., 2018; Krupa and Baszyński, 1995; Sorrentino et al., 2018). Metals may have multidirectional effects on photosynthesis (for a review see Prasad and Strzałka, 1999). The excess of Cd or Pb, for example, affects the photosynthetic electron transport (Krupa and Baszyński, 1995; Myśliwa-Kurdziel, 2002), as well as the activities of Calvin-Benson cycle enzymes, or the net assimilation of $CO_2$ (Arena et al., 2017; Prasad and Strzałka 1999; Sorrentino et al. 2018). Photosynthetic activity can also be altered indirectly by heavy metals, for example, decreasing the content of photosynthetic pigments, altering chloroplast ultrastructure (Molas 2002; Sorrentino 2018), and lipid and protein composition of thylakoids (Skórzyńska-Polit and Baszyński 1997). Cadmium and Pb accumulation in leaves interferes with the stomata functioning, affecting the overall photosynthesis and transpiration rates (Chandra and Kang, 2016). The plant physiological response against heavy metals is strictly depending on the species, being linked to the plant individual capability to face the stress. Some species are powerful bio-accumulators (Arena et al., 2017a, 2017b) and used in phytoremediation of contaminated soils.

In previous works (Capozzi et al., 2020; Sorrentino et al., 2018) carried out on *Cynara cardunculus* L. var. *altilis* DC., three cultivars were grown on a gardening soil and on industrial soil containing Cd and Pb, and different behaviors were observed under metal stress compared to the control plants. Although all cultivars could uptake significant amounts of metals, only *C. cardunculus* cv Spagnolo counteracted metal stress preserving chloroplast ultrastructure and increasing photosynthetic efficacy. By contrast, in the other cultivars analyzed, Cd and Pb uptake were coupled to decrease in life span, pigment content and photosynthetic activity. The selection of a species for phytoremediation of metal polluted soils involves a deep knowledge of the mechanisms at the basis of plant resistance against metal stress; based on previous experimental evidences, *C. cardunculus*, cv Spagnolo, seems to be an eligible candidate for phytoremediation. We hypothesized that Cd and Pb, provided in hydroponic cultures, could affect other morpho-physiological traits, useful as early proxy of metal stress in the selection of phytoremediation species. Therefore, the aim of the present work was to verify if cultivar-specific responses occurred, considering: i) the number of stomata and the total stomata surface in relation to gas exchanges; ii) root morphology in relation to metal uptake and translocation; iii) pigment content, photochemical efficiency and antioxidant response.

## 2 Materials and methods

### *2.1 Plant material and growth conditions*

The seeds of three cultivars of *Cynara cardunculus* var. *altilis* DC. (provided by Arca 2010 scarl), named Sardo (SAR), Siciliano (SIC) and Spagnolo (SPA), were germinated on wet filter paper for five days in the dark. Once primary roots and cotyledons were fully developed, 15 seedlings of each cultivar were moved to a hydroponic floating system, consisting of polystyrene plug trays floating in plastic tanks containing a constant volume of 5 L of aerated nutrient solution (Hoagland and Arnon, 1950) at pH 5.5. Three tanks were used for the experimental plan: 5 seedlings of each cultivar per tank were exposed to a specific heavy metal or none as control; at two-true-leaf stage, $CdCl_2$ and $Pb(NO_3)_2$ at the concentration of $10^{-5}$ M were supplied to the culture medium. The nutrient solution was renewed twice a week for 30 d. The parameters of growth chamber were constantly monitored to maintain controlled conditions of temperature 24/18 °C, relative humidity (RH) 55-75% (day/night), and a photoperiod of 16 h light per day with a Photosynthetic Photon Flux Density (PPFD) at the top of the canopy of 180–200 μmol photons $m^{-2}$ $s^{-1}$. After 30 d culture, all plants were analysed.

### *2.2 Morphological traits of roots and stomata*

Root tips (5 for each thesis) from controls and metal-treated plants, at the end of the treatment, were cut under a stereomicroscope and observed under LM (Leica DME ICC50W) to estimate the presence of root hair and the extension of hair zone. To determine the stomata size and number, four leaves of each cultivar were collected after the heavy metal exposure. All selected leaves were at the same age and development degree. A gently peeling of the abaxial surface was carried out by scotch tape to remove trichomes. At mid lamina, four surface replicas were obtained by nail topcoat. For each thesis 16 replicas were observed under light microscope (n = 16, total analysed surface = 0.8 $mm^2$ x 16) and images acquired were analysed by ImageJ software (National Institute of Health, MD, USA), (Figure 1 a). Moreover, 20 stomata (i.e., 20 couples of guard cells) were measured for each thesis: both major and minor axes of each stoma were used to calculate its area as an ellipse (Fig. 1b). Then, this area was multiplied per the average stomata number found on a 0.8 $mm^2$ area and this value was assumed as total stomata surface (TSS).

### *2.3 Chemical analysis and Sequential elution technique*

To evaluate the total amounts of intra- and extra-cellular fractions of Cd and Pb, a sequential elution technique was used. Treated samples were divided into two batches: one batch was

directly analysed for the total element content, after dehydration and acid digestion. The second batch was put in 20 mL of 20 mM $Na_2EDTA$ solution for 20 min and then rinsed in deionized water, to remove the extracellular soluble fraction of Cd or Pb, also including that bound to the cell wall (Branquinho and Brown, 1994; Branquinho et al., 1997; Spagnuolo et al., 2011). Specifically, all samples (shoot and root for total element content and only shoot for sequential elution; n=5) were weighted and dried in oven at 40 °C until constant weight. Dehydrated plant materials were ground in an agate mortar for the digestion phase. Samples represented by root or leaf powder of weight between 100 and 250 mg were digested in 5 mL $HNO_3$ 65% (hyperpure, Carlo Erba) and 2.5 mL $H_2O_2$ 30% (Sigma Aldrich) for metal analysis.

The digested samples were diluted to 25 mL in Millipore water and subsequently filtered to analyse Pb and Cd by Flame AAS (Varian Spectra AA 220 FS). All Pb and Cd standards solutions, for calibration curves, were prepared in 0.1 M $HNO_3$ by dilution of $Pb(NO_3)_2$ and $Cd(NO_3)_2$ stock solutions respectively. Lead (II) and Cadmium (II) nitrate stock solutions were prepared by dissolving lead or cadmium metal, 5N8 (Metal Research) with a nitric acid stock solution. The exact metal concentration, in both solutions, was determined by complexometric titration with EDTA. The reference plant material CTA-OTL-1 (oriental tobacco leaves) was also acid-digested and analysed for Cd and Pb concentrations, to determine the recovery percentages of the two elements; they were 92 and 103% respectively.

*2.4 Gas Exchange analysis*

For the gas exchange and fluorescence measurements, fully expanded leaves were collected at 30 d after sowing.

Leaf gas exchanges were measured with a Modular Gas Exchange Measuring System equipped with an infrared gas analyser QUBIT SYSTEMS S151 IRGA $CO_2$ analyzer, (Qubit Systems Inc. Kingston, Ontario, Canada) to measure, at different times, the concentration of $CO_2$ in a gas entering a leaf chamber, and the concentration of $CO_2$ in the same gas after it leaves the chamber. The difference between influx and efflux $CO_2$ concentrations allowed the calculation of photosynthetic $CO_2$ fixation rate. The system included humidity/temperature sensor (Q-S161) which measured relative humidity of the air before and after it has passed through the leaf chamber plus temperature at the RH sensor. The RH differential between influx and efflux gas, the temperature, and the flow rate through the leaf chamber, allowed calculation of leaf transpiration rates.

The youngest full expanded leaves (5 leaves per plant for each treatment) were chosen for the measurements. Each leaf was enclosed in the leaf chamber for about 5-8 minutes to allow the

photosynthesis to reach the steady-state. The environmental parameter fixed into the chamber were: photosynthetic photon flux density (PPFD) of 800 μmol photons $m^{-2}$ $s^{-1}$, temperature of 25°C±1, ambient $CO_2$ concentration of 360 μmol $CO_2$ $mol^{-1}$, RH 50%. The PPFD on cuvette was provided by LED external source (A113, Qubit System) which supplies photosynthetically active radiation to the leaf with minimum heat load. Net photosynthesis ($A_N$), transpiration (E) and stomatal conductance to vapour (gs) were calculated according to the LoggerPro software (Qubit Systems Inc., Canada) as reported in Sengupta et al., 2019.

Using the differential $CO_2$ concentration, which is the difference between the influx and efflux $CO_2$ (dif. $CO_2$), following the molecular flow (MF) rate net-photosynthesis was calculated as follow:

$A_N$ = dif. $CO_2$ × MF Transpiration rate (1)

Where MF = Flow rate/[22.4 × (273 + Tair)/273]/60 × 10,000/ leaf area,

Traspiration (E) was also calculated automatically by the software by using the values of reference and analytical relative humidity (RH) values. Stomatal conductance was calculated as reported:

$g_s$ = E / (ws - Anal. w) (2)

Where ws is the water vapor concentration in saturated Air and Anal. w the analyzed water vapour.

*2.5 Photosynthetic pigment content*

Total chlorophylls and carotenoids were determined at 30 DAS on the same 5 leaves per treatment utilized for gas exchange and fluorescence emission measurements, according to Lichtenthaler (1987). Pigments were extracted from leaf disks of 0.2 $cm^2$ by mortar and pestle in ice-cold 100% acetone and centrifuged at 5000 rpm for 5 min (Labofuge GL, Heraeus Sepatech, Hanau, Germany). The absorbance of supernatants was quantified by spectrophotometer (Cary 100 UV-VIS, Agilent Technologies, Santa Clara, CA, USA) at 470, 645 and 662 nm and pigment concentration expressed in μg $cm^{-1}$.

*2.6 Fluorescence emission measurements*

Fluorescence emission measurements were also performed on five replicates per each treatment, coming from five different plants. A portable FluorPen FP100max fluorometer, equipped with a light sensor (Photon System Instruments, Brno, Czech) was used for measurements, following the procedure reported in Arena et al. (2017a). The ground fluorescence signal, $F_o$, was induced on 30′ dark adapted leaves, by a blue LED internal light of about 1–2 μmol $m^{-2}$ $s^{-1}$. The maximal

fluorescence level in the dark, $F_m$, was induced by a 1s saturating light pulse of 3000 μmol $m^{-2}$ $s^{-1}$. The maximum quantum efficiency of PSII photochemistry, Fv/Fm, was calculated as ($F_m - F_o$)/$F_m$, according to Kitajima and Butler (1975). The fluorescence measurements in the light, were performed utilizing an open leaf-clip suitable for measurements under ambient light. The quantum yield of PSII electron transport ($\Phi_{PSII}$) was determined according to Genty et al. (1989). The linear electron transport rate (ETR) was expressed following Krall and Edwards (1992), whereas the non- photochemical quenching (NPQ) was calculated as described in Bilger and Björkman (1990).

*2.7 Antioxidant capacity determination*

The antioxidant analysis was carried out following the procedure reported in Costanzo et al. 2020, by the Ferric Reducing Antioxidant Power assay (FRAP). More specifically 0.25 g of powdered sample was mixed with 60:40 (v/v) methanol/water solution and centrifuged at 14000 rpm for 15 min at 4 °C. Then an acetate buffer (1:16 300 mM pH 3.6) containing a mix of tripyridyltriazine (TPTZ) (1:1.6 10 mM TPTZ in 40 mM HCl) and $FeCl_3$ (1:16 12 mM $FeCl_3$) was added to the extracts. The absorbance was measured at 593 nm with a spectrophotometer (UV-VIS Cary 100, Agilent Technologies, Palo Alto, CA, USA) after 1 h of incubation at 4 °C, using Trolox (6-hydroxy-2,5,7,8-tetramethylchroman-2-carboxylic acid) as standard. The antioxidant capacity was expressed as μmol Trolox equivalents for mg of sample fresh weight (FW).

*2.8 Statistical analysis*

Basic statistics for morphological parameters: number of stomata, the stomata area (μm²) and the total stomata surface (mean number of stomata found on a surface of 0.8 $mm^2$ x mean stomata area, μm²) were calculated and performed in excel.

Statistically significant differences among treatments were analysed by one-way analysis of variance (ANOVA). Shapiro-Wilk and Kolmogorov-Smirnov tests were performed to check for normality. The Holm- Sidak and Tukey's tests were applied for all multiple comparison procedures based on a significance level of $p<0.05$, for physiological and morphological parameters, respectively. The package Sigma-Plot 11.0 (Jandel Scientific, San Rafael, CA, USA) was used for statistical data processing.

## 3 Results and discussion

*3.1 Responses on stomata.*

Results of stomata counting, and stomata area calculation are reported in Table 1 and Figure 1. Stomata number varied significantly depending on cultivar: control plants, of Sardo cv. had the highest number of stomata for each surface unit (on average 213), almost twice the number of stomata counted in Spagnolo (on average 117, Fig. 1c). In both cardoon Sardo and Siciliano, metal treatments significantly decreased stomata number. Moreover, alterations in stomata shape were occasionally observed in the latter (Fig. 1s - supplementary). A decrease in stomata number was already observed in *Beta vulgaris* in response to an excess of the micronutrient Zn (Sagardoy et al., 2010).

Table 1. Stomata number and area in control and metal-treated cultivars of *C. cardunculus*

| Cv | Treatment | Stomata number§ (N.) | Stomata area ($\mu m^2$) | Total stomata surface § ($\mu m^2$) |
|---|---|---|---|---|
| | | Mean±SD | Mean±SD | Mean±SD |
| **Sardo** | ***C** | 213±19ab | 383±50c | 79921±13794ab |
| | **Cd** | 152±28cd | 531±84ab | 51177±14022b |
| | **Pb** | 145±67cd | 340±73c | 80541±37958ab |
| **Siciliano** | **C** | 170±33bc | 466±125ab | 80213±29975ab |
| | **Cd** | 107±18d | 506±127ab | 62809±18004ab |
| | **Pb** | 100±7d | 583±96a | 47056±6268b |
| **Spagnolo** | **C** | 117±7d | 463±86abc | 54372±12585b |
| | **Cd** | 231±42a | 447±46bc | 92265±25328a |
| | **Pb** | 168±51bc | 385±60c | 71502±26932ab |

*C: Control; SD: standard deviation. Different letters indicate significant differences ($p < 0.05$) among the treatments according to Tukey's post-hoc test. § All parameters were estimated on a surface of 0.8 $mm^2$

By contrast, in Spagnolo cv. grown under metal stress, the number of stomata significantly increased, especially with Cd, where stomata nearly doubled those of control plants. In addition, in Sardo and Siciliano cultivars, a noticeable increase of stomata area was also observed (significant in Sardo treated with Cd). This result can be interpreted as a compensative response of the plants under metal stress, to counteract the decrease of stomata number.

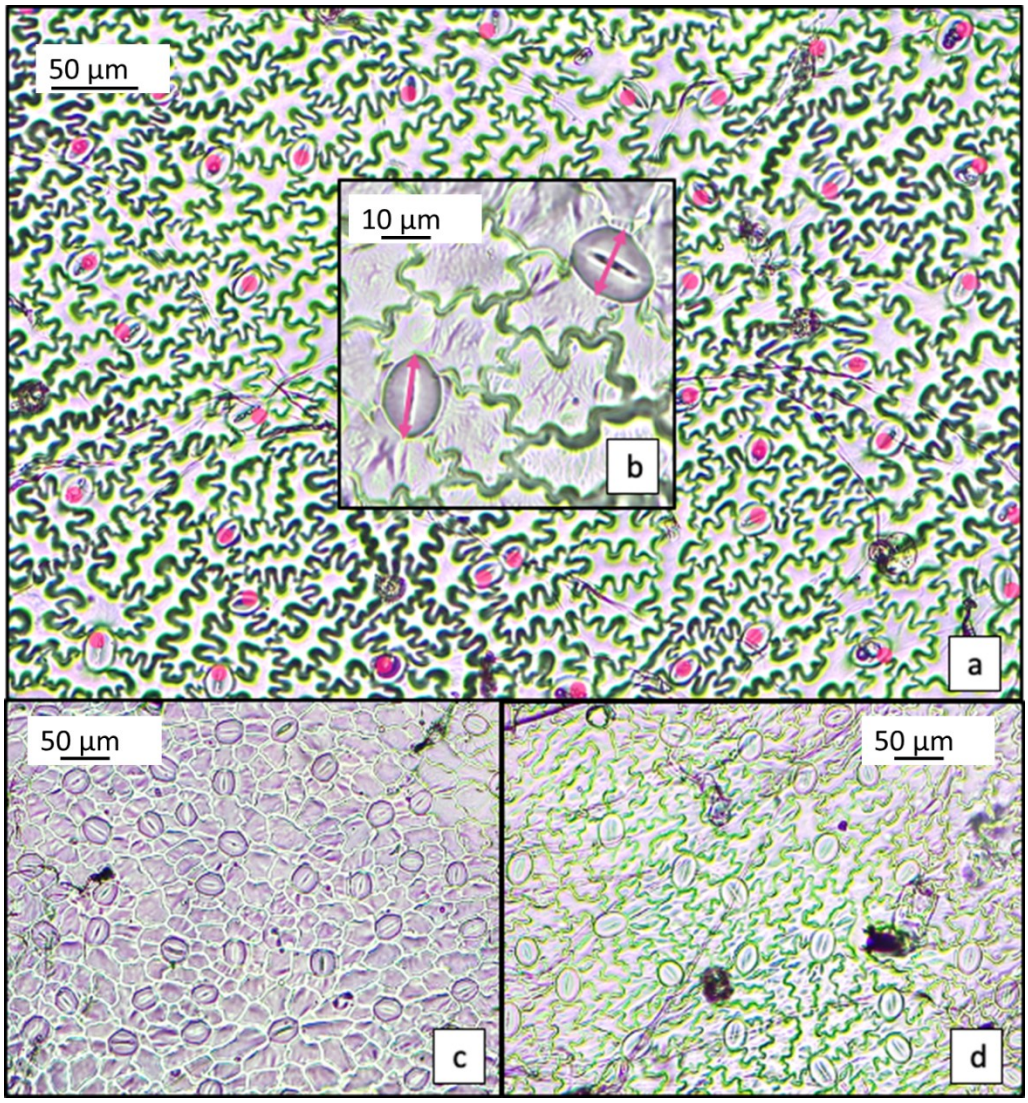


Figure 1 – Example of stomata counting (a) and measuring (b) in a control sample of Spagnolo cardoon. Pb-treated samples of Spagnolo (c) and Siciliano (d) leaf replicas. Note the higher number of smaller stomata in the first; see the paragraph 3.1 for further details.

However, this response seems not enough to cope the reduced number of stomata; in fact, only in the case of Pb-treated plants of Sardo a complete recovery of total stomata surface was achieved. In Spagnolo cardoon, the sole increase of stomata number produced a parallel increase of total stomata surface, with positive effect on gas exchange.

An increase of stomata number in plants grown under metal presence was already observed in the literature; in wheat seedlings grown with Cu and Zn the number of stomata increased with a dose-dependent trend (Stolarska et al., 2007). In soybean seedlings grown in the presence of Pb an increase of stomata number coupled to a reduction in their size, was observed (Weryszko-Chmielewska and Chwil, 2004). In the latter case, the authors suggested that a larger number of epidermal cells enhances detoxification mechanisms. Given that several papers report the

negative effects of heavy metals on plant metabolic pathways, stomata more numerous but reduced in size, could provide a prompt response in gas exchange. This could explain why in cardoon, where stomata undergo a double regulation pattern under metal stress (i.e., in number and size), stomata number is more important than size for gas exchanges and photosynthesis.

*3.2 Responses on roots: morphology, element uptake and translocation*

The observation of root apparatus after 30 d of culture (Fig. 2) highlighted the presence of 3-6 roots, similarly, developed in control and metal-treated plants; however, the observation of the root tip under a light microscope evidenced the absence of root hairs in control plants, and the development of numerous root hairs in metal-treated plants, especially with Pb, where the hairy zone was about twice that of Cd-treated plants (7-8 mm vs. 3-4). The presence of root hairs could be interpreted as a plant response to metal stress, overall enhancing the root surface, cell wall binding sites for cations, and likely element absorption/ adsorption and sequestration in the walls (Krzesłowska, 2011; Parrotta et al., 2015).

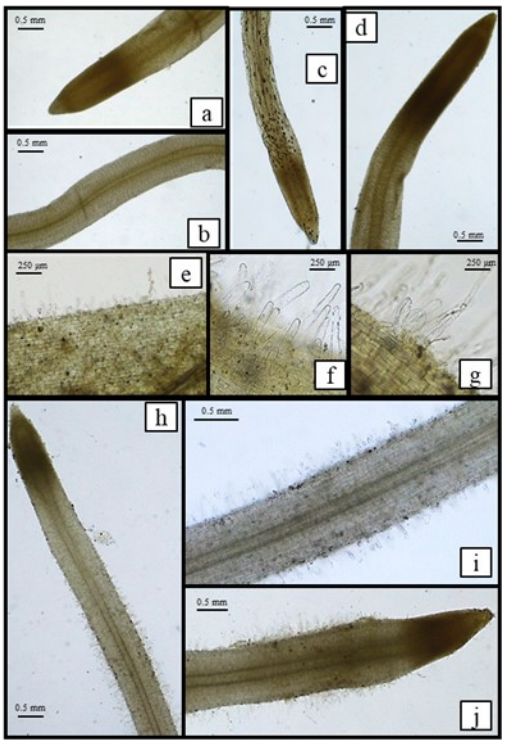


Figure 2 – Roots of control plants of Spagnolo (a, b), Siciliano (c) and Sardo (d) cardoon cultivars. Roots of Cd-treated plants of Sardo, Siciliano and Spagnolo (e, f, and g respectively). Roots of Pb-treated plants of of Sardo, Siciliano and Spagnolo (h, i and j). See paragraph 3.2 for details.

Cadmium and Pb concentrations and their translocation factors (TF) in plants are reported in Table 2. Element concentrations were below detection limit (BDL) in control plants. Significant differences were observed between different organs (i.e., root vs leaves) and between EDTA-

treated and untreated leaves. The EDTA washing demonstrate that a conspicuous part of Cd and Pb does not belong to the extracellular soluble fraction (removed by EDTA) but is likely located inside the cells. This could explain the noticeable physiological and ultrastructural alterations observed in a previous work in which cardoon plants were cultured under metal stress in an industrial soil (Sorrentino et al., 2018). By contrast, no significant difference was observed between cultivars; these results agree with previous findings, showing that the same three cultivars did not display significant differences in their element uptake when grown on an industrial soil (Capozzi et al., 2020). Moreover, in the present experiment Cd and Pb concentrations in shoot and root resulted higher than those measured in a previous experiment carried out on gardening soil watered with metal solutions (Arena et al., 2017), at parity of metal concentration ($10^{-5}$ M) and growth period (30 d). This result is consistent in the two cases reflecting the amounts of metals received; in fact, the plants grown in gardening soil received about 600 mL metal solution each, whereas in hydroponics every plant received about 1.5 L metal solution ($10^{-5}$ M) in 30 d. In addition, the metals in solution could become partly inaccessible when supplied to the soil by irrigation; soil is indeed a complex matrix able to bind temporarily or stably metal ions, whereas they could preserve their bioavailability in hydroponics. Further, comparing the two experiments (gardening soil vs. hydroponics), in the first, translocation factors of 199% and 74% were calculated for Cd and Pb, values far long higher than those calculated in hydroponics (26-29% for Cd and 5-6% for Pb). All the same, it is confirmed the higher value of TF for Cd. It is reported, indeed, that plant nutrients and Cd compete for the same transporters; therefore, Cd can be easily absorbed and translocated to the shoot (Nazar et al., 2012). This discrepancy could be due to the presence of root hairs, which develop only in metal-treated plants grown in hydroponics; root hairs could indeed provide a large surface for metal sequestration. The lack of root hairs in hydroponic control can be considered as an expected trait; in fact, root hairs develop to increase root surface ensuring an adequate water supply, even in very small spaces, as between soil particles. The development of root hairs in Cd and Pb contaminated hydroponics could be a response to metal stress and especially to Pb, since the hairy zone was particularly developed in these plants and was coupled to a very low TF to the shoot.

Table 2. Element concentrations (ppm on dry weight, mean±SD, n=5) in leaf (L and L+ EDTA), root (R) and relative translocation factor (TF) in the three cardoon cultivars.

| | **Sardo** | **Siciliano** | **Spagnolo** |
|---|---|---|---|
| **Cd** | | | |
| **L** | 183±17b | 152±19b | 184±81b |
| **L+EDTA** | 138±10c | 102±14c | 146±62c |
| **R** | 693±53a | 573±59a | 642±75a |
| **TF** | 0.26 | 0.26 | 0.29 |
| **Pb** | | | |
| **L** | 63±13b | 48±11b | 57±8b |
| **L+EDTA** | 47±14c | 29±6c | 31±12c |
| **R** | 824±102a | 891±31a | 1110±182a |
| **TF** | 0.06 | 0.05 | 0.05 |

Different letters indicate statistical differences according to Tukey's post hoc test ($p<0.05$).

*3.3 Gas exchanges*

Leaf gas-exchanges measurements are reported in Fig. 3. It is evident how Sardo and Siciliano cardoon showed the same trend of response in the measurements, being higher in control plants and lower in Cd and Pb; whereas Spagnolo showed a different physiological behaviour, with no difference in net photosynthesis among control and treated plants (Fig. 3 a) and a significant increase of transpiration and stomatal conductance in polluted plants (Fig. 3 b, c). More specifically, Sardo presented the highest net photosynthesis and stomata conductance in non-polluted plants, values which significantly decrease in Cd and Pb contaminated plants (Fig. 3 a, b). These data are in agreement with those of the stomatal counting. Indeed, the highest presence of stomata could allow a higher stomata conductance, which in turn accounts for an enhanced photosynthesis. Conversely, in Spagnolo grown under metal stress, increased both transpiration and stomatal conductance compared to control (Fig. 3 b, c). Once again, these data agree with stomatal counting, where Spagnolo grown in presence of Pb and Cd increase the stomata number. Indeed, gas exchanges in leaves are recognized to be controlled by several anatomical traits (i.e., stomatal number, size, aperture), affecting the stomatal conductance and the diffusion through the mesophyll (Haworth et al., 2016; Xiong et al., 2017). From our results it is also worth mentioning that Cd reduced stomata conductance and evapotranspiration more than Pb in the cultivars Sardo and Siciliano (Fig. 3).

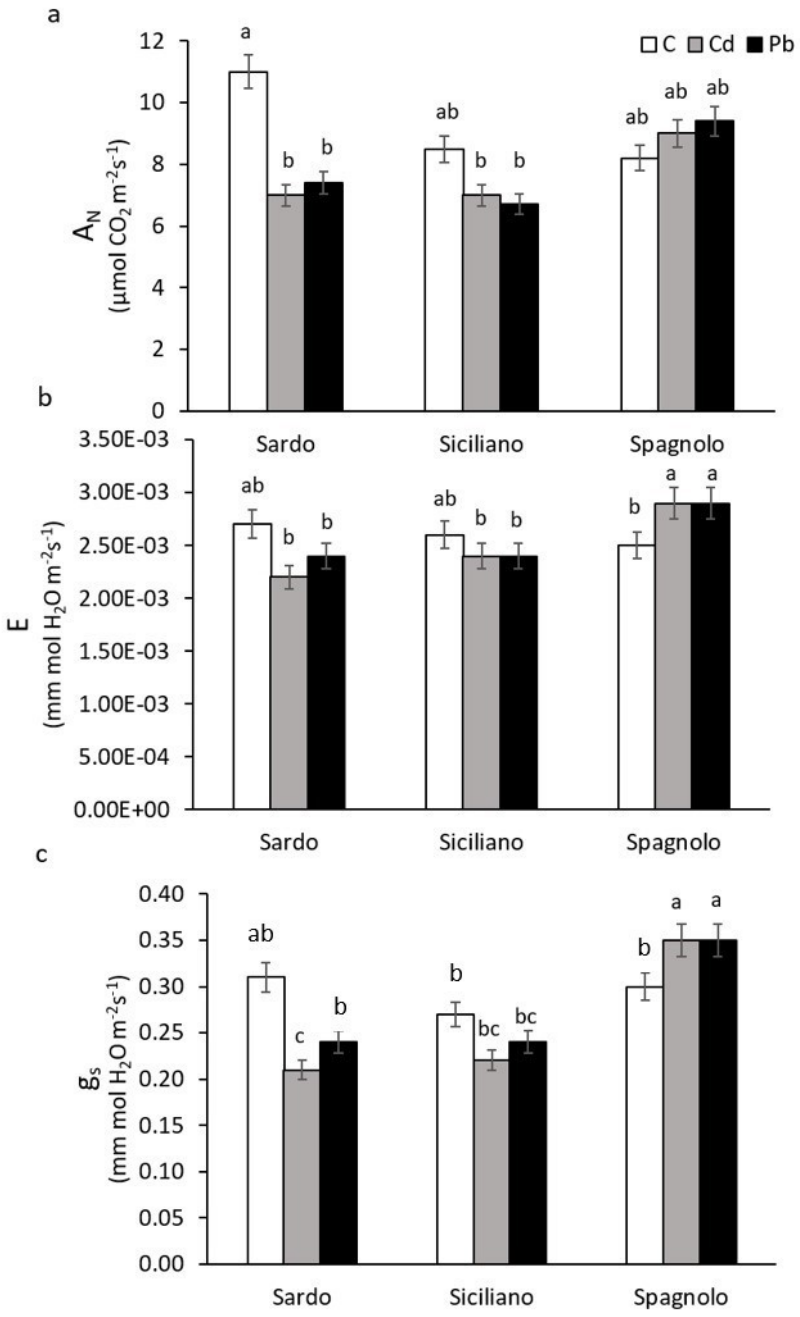


Figure 3 – Net Photosynthesis, AN (a), Transpiration rate, E (b) and Stomatal conductance, gs (c) measured on control (C), Cd-treated and Pb-treated Sardo, Siciliano and Spagnolo cultivar. Data are mean±SD, n=5. Different letters indicate significant differences among the treatments, according to Tukey's post-hoc test ($p<0.05$).

*3.4 Photosynthetic pigment content*

Photosynthetic pigment content represents a suitable proxy for the detection of damages to photosynthetic apparatus. In our experiment, Spagnolo and Sardo, showed a higher content of photosynthetic pigments (Fig 4) in control and Pb plants, differently from Siciliano cultivar in

which the pigment amount was significantly reduced under Cd and Pb treatments compared to control.

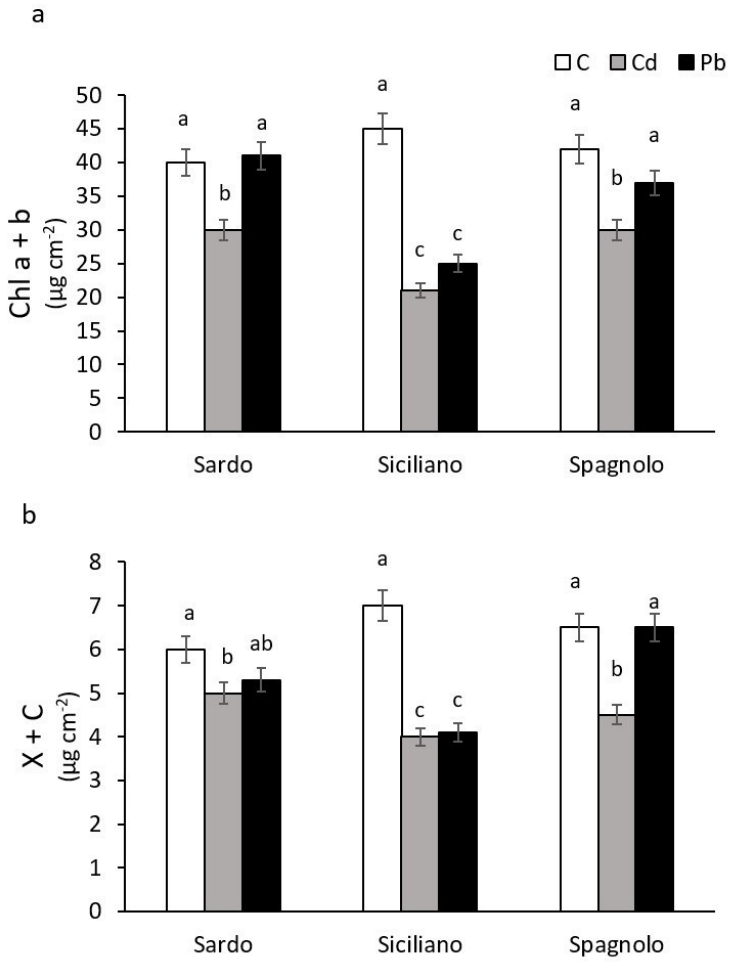


Figure 4 – Total chlorophylls, Chl a+b (a), Total carotenoids, x+c (b) determined on control (C), Cd-treated and Pb-treated Sardo, Siciliano and Spagnolo cultivar. Data are mean±SD, n=5. Different letters indicate significant differences among the treatments, according to Tukey's post-hoc test ($p<0.05$).

These results indicate a higher sensitivity to Cd, compared to Pb, in Spagnolo and Sardo cardoon, and an overall vulnerability of Siciliano cultivar to both metals regards pigments. The reduction of chlorophylls and carotenoids due to heavy metal contamination has often been reported as a damage occurring at the enzymatic level during the chlorophyll synthesis or by inducing oxidative stress that results harmful for the biosynthetic pathways of photosynthetic pigments (Parajapat and Tripathi, 2008; De Micco et al., 2019). One of the most common results of injuries by heavy metal contamination is chlorosis. Metals interfere with pigment and influence the Chl content in plants as $Mg^{2+}$ in chlorophyll is substituted by $Cu^{2+}$, $Zn^{2+}$, $Cd^{2+}$,

$Hg^{2+}$, $Pb^{2+}$, or $Ni^{2+}$ (Kupper et al. 1996). In our study pigment content is significatively affected by heavy metals in Siciliano plants (Fig. 4) with repercussion on the net photosynthesis (Fig. 3 a).

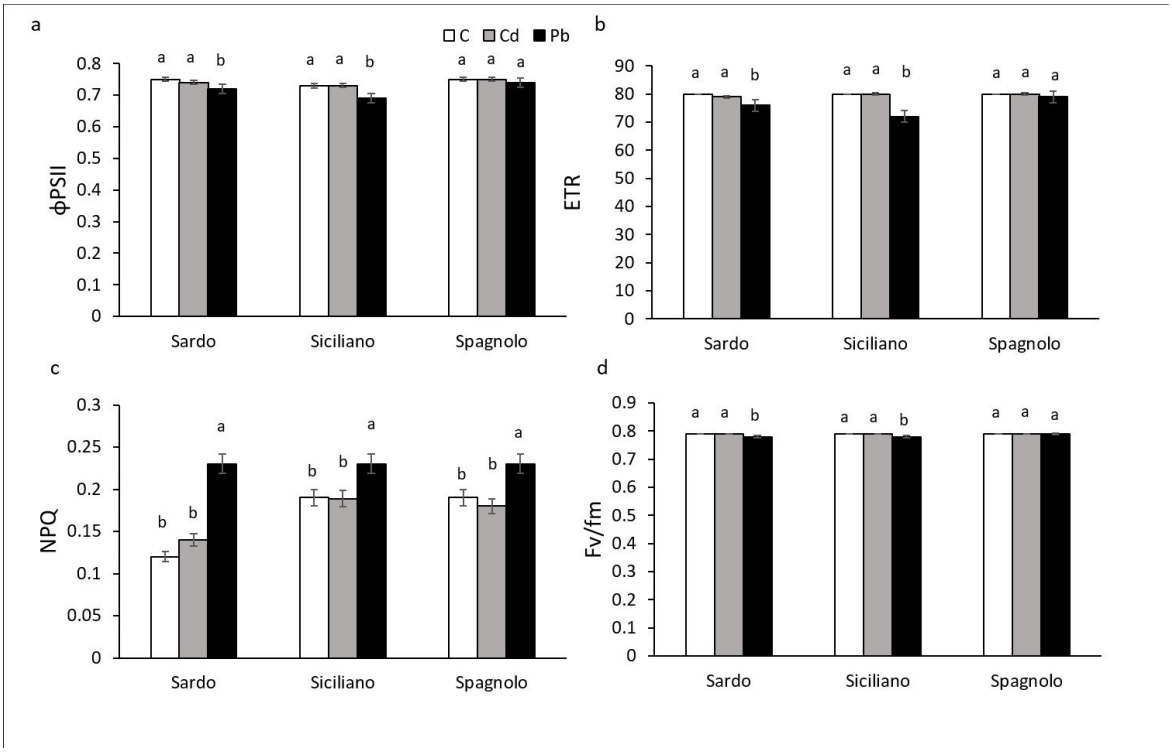


Figure 5 – Quantum yield of PSII electron transport, ΦPSII (a), Electron transport rate, ETR (b) Non-Photochemical Quenching, NPQ (c), PSII Maximum quantum yield, Fv/Fm, measured on control (C), Cd-treated and Pb-treated Sardo, Siciliano and Spagnolo cultivar. Data are mean±SD, n=5. Different letters indicate significant differences among the treatments, according to Tukey's post-hoc test ($p<0.05$).

Various authors have reported similar decreases in pigment content under heavy metal stress (Zengin and Munzuroglu, 2006; Arena et al., 2014), whereas only a few have found enhanced concentrations of photosynthetic pigments after the exposure to metals (Devi Prasad, 1982). These contradictory results are probably due to the effects of mixed heavy metals in the soil water medium, which compete with each other. Furthermore, in Sardo and Spagnolo both chlorophyll and carotenoids decreased when treated with Cd but not with Pb. A significant inhibitory effect on photosynthetic pigments was found in our previous study with cardoon plants grown on polluted soil and was ascribed to the major presence of Cd (Sorrentino et al., 2018). This result confirms that cadmium is harmful to pigments probably because of its fasted deliver through plants and accumulation in leaves compared to other heavy metals (Nwosu et al., 1995; John et al., 2009).

*3.5 Fluorescence emission measurements*

Cd and Pb exert different effects on the diverse components of photosynthetic apparatus; Cd seems to be more deleterious than Pb on light-harvesting pigments, but photosystem efficiency is more affected by Pb, even if the outcomes depend on intrinsic sensitivity of the different cardoon cultivars, The chlorophyll *a* fluorescence emission analyses showed that the quantum yield of PSII electron transport (ϕPSII), the electron transport rate (ETR) and the maximum PSII photochemical efficiency (Fv/Fm) where negatively affected only by Pb, in Sardo and Siciliano cultivars. Conversely no effect following both metal treatment was detected in Spagnolo, confirming the highest capability of this cultivar to face the metal stress (Fig. 5, a, b, c)). The non-photochemical quenching (NPQ) significantly rises under Pb treatment, in all cultivars, compared to Cd and control, indicating that under Cd treatment photosynthetic apparatus promotes the thermal dissipation of energy not utilized in photochemistry (Fig. 5 d), (Arena et al 2017a; 2017b). The higher photochemical efficiency of Spagnolo, compared to Sardo and Siciliano, is in accordance with the highest net photosynthetic rates measured in this cultivar under Cd and Pb treatments. From our data it is evident that for the cultivars Sardo and Siciliano the gas exchanges are more responsive than PSII photochemistry to metal stress, because the treatment with both Cd and Pb determines a significant reduction of net photosynthesis, together with a decline of stomatal number and photosynthetic pigment content. We suggest that the higher resistance of Spagnolo cultivar to Cd and Pb, depends on an elevated capability to harvest and convert light in photochemistry, also in addition to a strong stomatal regulation allowing plants to carry out a fine-tuning of light and dark processes of photosynthesis.

*3.6 Antioxidant response*

The three cultivars showed a different antioxidant power both in control plants and in response to metal injuries (Fig. 2s). It has been demonstrated that in natural ecosystems, the plant antioxidant production depends on several factors such as climate, soil, geographic location where plants grow and, of course, species (George et al., 2004; Lebasky et al., 2001; Ogaya et al., 2011); this could explain the different antioxidant power observed in the three cultivars also in control condition. Particularly, the significantly lower value ($p<0.01$) of antioxidant capacity in Spagnolo control plants compared to Sardo and Siciliano could indicate a reduced need to develop a strong antioxidant system in this cultivar due to its intrinsic capacity to withstand the metal stress.

Whereas in Sardo no variation in antioxidant capacity among control and treated plants was found, in Siciliano Cd- and Pb-treated plants this parameter significantly decreased compared to control, indicating a negligible role of the antioxidants under heavy metal stress in this cultivar (Fig. 2s). In addition, the Siciliano cultivar, although the higher constitutive antioxidant capacity, is not able to face the injuries under metal stress, as demonstrated by the sporadic occurrence of damaged stomata (Fig. 1s) and chloroplasts (Sorrentino et al., 2018).

Conversely, compared to control, Spagnolo cultivar showed a significant increase of antioxidant capacity in Cd- and even more in Pb-treated plants (Fig. 2s), suggesting a remarkable contribute of antioxidant compounds in plant defense against Cd and Pb injuries. Our results indicate that heavy metal stress influences antioxidant status, providing three cultivar-specific responses. However, as FRAP assay only measures nonenzymatic (reductants) antioxidants in plant samples, we cannot exclude the occurrence of other effects involving specific enzymatic pathways, such as super oxide dismutase (SOD) or catalase (CAT) (Gjorgieva et al., 2013).

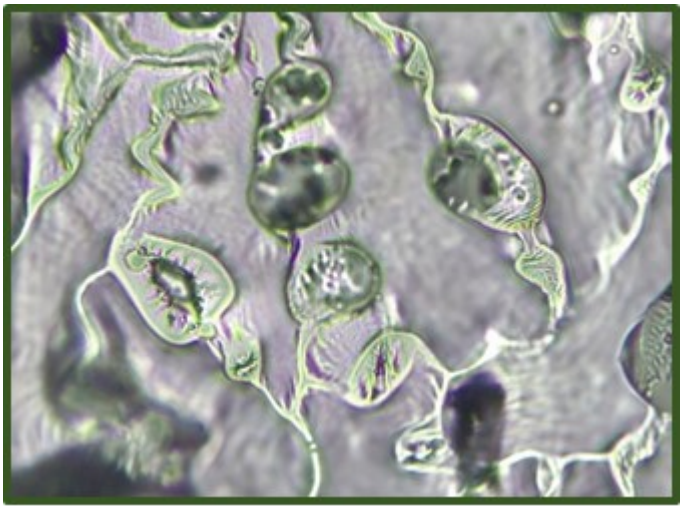

Figure 1S- Altered stomata observed in Cd-treated leaves of Siciliano cultivar

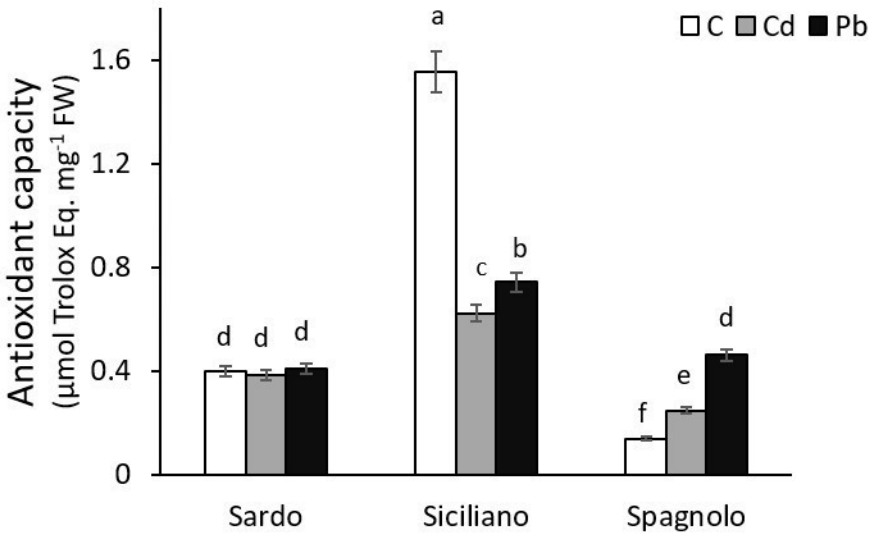


Figure 2s – Antioxidant capacity measured on control (C), Cd-treated and Pb-treated Sardo, Siciliano and Spagnolo cultivars. Data are mean±SD, n=3. Different letters indicate significant differences among the treatments, according to Tukey's post-hoc test ($p<0.05$).

## 4 Conclusions

This work clarifies several strategies of cardoon plants to cope with metal stress. Primarly, the modulation of number and size of the stomata is proposed as a proxy for evaluating the tolerance to metals by potential phytoremediation plants. In fact, the increase of stomata of reduced size enhances gas exchange ability, determining the growth of healthy plants.

Some results indicate that *Cynara cardunculus* plants display and face metal injuries by active morpho-physiological changes, regardless the cultivar; specifically, root hair development and pigment content decrease. Other traits show instead, a cultivar-specific behavior; particularly, photosynthetic pattern and stomata plasticity provide different responses, but only Spagnolo cardoon achieves a successful strategy preserving its morphophysiology. The stomata response follows two different patterns: the increase of stomata area (i.e. Sardo and Siciliano) and the increase of stomata number (i.e. Spagnolo). Only this latter leads to a real resilience to metal stress, by improving the photosynthetic performance both in terms of $CO_2$ absorption and light harvesting and conversion to photosystems. It is likely that the entrance of Cd and Pb into the cells, proved by the chemical analysis, induces a decrease in pigment concentration, which may be a first signal of an impending decline in net photosynthesis. This event, in turn, determines the onset of recovery mechanisms at the stomata level and adjustments in the photochemistry in Spagnolo cardoon. The increase of antioxidant capacity and the ability of Spagnolo plants to

modify leaf structural and physiological traits under heavy metal contamination to maintain high photosynthetic efficiency, should be considered an elective trait for its cultivation in polluted environments.

**Author's contribution:** conceptualization of the experiment: Valeria Spagnuolo and Simonetta Giordano; investigation: Maria Cristina Sorrentino, Fiore Capozzi, Chiara Amitrano, Gaetano De Tommaso; data curation: Valeria Spagnuolo, Carmen Arena, Maria Cristina Sorrentino, Mauro Iuliano; Statistical analysis: Fiore Capozzi, Chiara Amitrano; writing—original draft preparation: Valeria Spagnuolo, Maria Cristina Sorrentino, Carmen Arena; writing—review and editing: all the authors; supervision: Valeria Spagnuolo.

**Ethical Approval:** this study does not involve human participants

**Funding:** This research received no external funding.

**Conflicts of Interest:** The authors declare no conflict of interest and no financial and non-financial competing interests

**Availability of data and materials:** all data supporting the results are included in the manuscript

**Consent to Participate:** this study does not involve human participants nor human data or human tissue

**Consent to Publish:** this manuscript does not contain individual person's data

**Acknowledgements**

We wish to thank Dr. Riccardo Riccardi (Arca 2010 scarl) for providing us *C. cardunculus* seeds.

## References


Angelone, M., Bini, C. 1992. Trace elements concentrations in soils and plants of Western Europe. In: Biogeochemistry of Trace Metals. Lewis publishers, Boca Raton, pp 19–60.

Arena, C., De Maio, A., De Nicola, F., Santorufo, L., Vitale, L., Maisto, G., 2014. Assessment of eco-physiological performance of *Quercus ilex* L. leaves in urban area by an integrated approach. Water Air Soil Poll. 225-1824. https://doi.org/10.1007/s11270-013-1824-6

Arena, C., Santorufo, L., Cataletto, P. R., Memoli, V., Scudiero, R., Maisto, G. 2017a. Eco-physiological and antioxidant responses of holm oak (*Quercus ilex* L.) leaves to Cd and Pb. Water Air Soil Poll. 228-459. https://doi.org/10.1007/s11270-017-3638-4

Arena, C., Figlioli, F., Sorrentino, M.C., Izzo, L.G., Capozzi, F., Giordano, S., Spagnuolo, V. 2017b. Ultrastructural, protein and photosynthetic alteration induced by Pb and Cd in *Cynara cardunculus* L. and its potential for phytoremediation. Ecotox. Environ. Safe. 145, 83–89. https://doi.org/10.1016/j.ecoenv.2017.07.015

Branquinho, C., Brown, D.H. 1994. A method for studying the cellular location of lead in lichens. The Lichenologist. 26, 83-90.

Branquinho, C., Brown, D.H., Catarino, F. 1997. The cellular location of Cu in lichens and its effects on membrane integrity and chlorophyll fluorescence. Environ. Exp. Bot. 38, 165-179. https://doi.org/10.1016/S0098-8472(97)00015-4

Bilger, W., Björkman, O. 1990. Role of xanthophyll cycle and energy dissipation in differently oriented faces of light–induced absorbance changes, fluorescence and photosynthesis in Hedera canariensis, Photosynt. Res. 25, 173–185.

Capozzi, F., Sorrentino, M.C., Caporale, A.G., Fiorentino, N., Giordano, S., Spagnuolo, V. 2020. Exploring the phytoremediation potential of *Cynara cardunculus*: a trial on an industrial soil highly contaminated by heavy metals. Environ. Sci. Poll. Res., 27, 9075-9084. https://doi.org/10.1007/s11356-019-07575-9

Chandra, R., Kang, H. 2016. Mixed heavy metal stress on photosynthesis, transpiration rate, and chlorophyll content in poplar hybrids. Forest Sci. Technol. 12, 55-61. https://doi.org/10.1080/21580103.2015.1044024

Chaney, R. L. 2015. How Does Contamination of Rice Soils with Cd and Zn Cause High Incidence of Human Cd Disease in Subsistence Rice Farmers. Curr. Pollut. Rep. 1, 13-22. https://doi.org/10.1007/s40726-015-0002-4

Costanzo, G., Iesce, M.R., Naviglio, D., Ciaravolo, M., Vitale, E., Arena, C. 2020. Comparative studies on different Citrus cultivars: a revaluation of waste mandarin components. Antioxidants 517, 1-12. https://doi.org/10.3390/antiox9060517

De Micco, V., Amitrano, C., Stinca, A., Izzo, L. G., Zalloni, E., Balzano, A., Barile, R., Conti, P., Arena, C. 2019. Dust accumulation due to anthropogenic impact induces anatomical and photochemical changes in leaves of Centranthus ruber growing on the slope of the Vesuvius volcano. Plant Biology. https://doi.org/10.1111/plb.12966

Devi Prasad, P.V., Devi Prasad, P.S. 1982. Effects of cadmium, lead and nickel on three freshwater green algae. Water Air Soil Poll. 17, 263-268.

Figlioli, F., Sorrentino, M.C., Memoli, V., Arena, C., Maisto, G., Giordano, S., Capozzi, F., Spagnuolo, V. 2019. Overall plant responses to Cd and Pb metal stress in maize: Growth pattern, ultrastructure, and photosynthetic activity. Environ. Sci. Pollut. R. 26, 1781-1790.

Gjorgieva, D., Panovska, T. K., Ruskovska, T., Bačeva, K., Stafilov, T. 2013. Influence of Heavy Metal Stress on Antioxidant Status and DNA Damage in Urtica dioica. BioMed Res. Int. https://doi.org/10.1155/2013/276417

Genty, B., Briantais, J.M., Baker, N.R. 1989. The relationship between the quantum yield of photosynthetic electron transport and quenching of chlorophyll fluorescence. Biochim. Biophys. Acta. 90, 87-92.

George, B., Kaur, C., Khurdiya, D.S., Kapoor, H.C., 2004. Antioxidants in tomato (Lycopersicum esculentum) as a function of genotype. Food Chem. 84, 45–51.

Kaznina, N. M., Titov, A. F., Batova, Yu. V., Laidinen, G. F. 2014. The resistance of plants *Setaria veridis* (L.) Beauv. to the influence of cadmium. Biol. Bull. 5,474-480.

Haworth, M., Killi, D., Materassi, A., Raschi, A., Centritto, M. 2016. Impaired Stomatal Control Is Associated with Reduced Photosynthetic Physiology in Crop Species Grown at Elevated [CO2].

He, Z., Shentu, J., Yang, X., Baligar, V.C., Zhang, T., Stoffella, P.J. 2015. Heavy Metal Contamination of Soils: Sources, Indicators, and Assessment. J. Environ. Ind. 9,17-18.

Hoagland, D.R., Arnon, D.I. 1950. The water culture method for growing plants without soil. Col. Agric. Exp. Stn. Circ. 347, pp. 1-32.

John, R., Ahmad, P., Gadgil, K., Sharma, S. 2009. Heavy metal toxicity: effect on plant growth, biochemical parameters and metal accumulation by Brassica juncea L. Int. J. Plant. Prod. 3, 65-75.

Kitajima, M., Butler, W.L. 1975. Quenching of chlorophyll fluorescence and primary photochemistry in chloroplasts by dibromothymoquinone, Biochim. Biophys. Acta. 376.1, 105–115.

Krall, J.P., Edwards, G.E. 1992. Relationship between photosystem II activity and CO2 fixation in leaves. Physiolo. Plant. 86.1, 180-187.

Krupa, Z., Baszyński, T. 1995. Some aspects of heavy metals toxicity towards photosynthetic apparatus – direct and indirect effects on light and dark reactions. Acta Physiol. Plant. 17: 177-190.

Krzesłowska, M. 2011. The cell wall in plant cell response to trace metals: polysaccharide remodeling and its role in defense strategy. Acta Physiol Plant 33, 35–51. https://doi.org/10.1007/s11738-010-0581-z

Kűpper, H., Kűpper, F., Spiller, M. 1996. Environmental relevance of heavy metal-substituted chlorophyll using the example of water plants. J. exp. Bot. 47, 259-266.

Lebasky, M. J., Sharifi Ashoorabadi, A. 2001. Changes in Hypericin in different habitats of Goli. Research of Iranian Medicinal Plants and Herbs. Res Inst. Fore. Rang. 11, 100–87.

Lichtenthaler, H.K. 1987. Chlorophylls and carotenoids, Pigments of photosynthetic biomembranes. Method. Enzymol. 148, 350-382.

Markert, B. 1993. Plants as biomonitors: indicators for heavy metals in the terrestrial environment. New York, VCH Publishers. 644 p. ISBN 3-52-73000-15.

Meggeson, T.P., Hall, N.W. 1999. An investigation into the spatial and temporal distribution of lead, cadmium and zinc in contemporary soils and paleosols in a high arctic and

an arctic alpine environment. In: Abstracts of 'European Perspectives on Land Contamination Conference' Soc. of the Chem. Ind., London. Land Contamination and Reclamation 7(4).

Motuzova, G.V., Minkina, T.M., Karpova, E.A., Barsova, N.U., Mandzhieva, S.S., 2014. Soil contamination with heavy metals as a potential and real risk to the environment. J. Geochem. Explor., 144, 241-246

Myśliwa-Kurdziel, B., Prasad, M.N.V., Strzalka, K. 2002. Heavy metal influence on the light phase of photosynthesis. Physiology and biochemistry of metal toxicity and tolerance in plants. Dordrecht Kluwer Academic Publishers (pg. 229-255).

Nazar, R., Iqbal, N., Masood, A., Iqbal Khan, R.M., Syeed, S., Khan, N. 2012. Cadmium Toxicity in Plants and Role of Mineral Nutrients in Its Alleviation. Am. J. Plant Sci. 3, 1476-1489 https://doi.org/10.4236/ajps.2012.310178

Nriagu, J.O. 1978. The biogeochemistry of Lead in the environment. Pp 18-88. Amsterdam: Elsevier.

Nwosu, J.U., Harding, A.K., Linder, G. 1995. Cadmium and lead uptake by edible crops grown in a silt loam soil. Bull. Environ. Contam. Toxicol. 54, 570–578.

Ogaya, R., Penuelas, J., Asensio, D., Llusia, J. 2011. Chlorophyll fluorescence responses to temperature and water availability in two co-dominant Mediterranean shrub and tree species in a long-term field experiment simulating climate change. Environ. Exp. Bot. 73, 89–93. https://doi.org/10.1016/j.envexpbot.2011.08.004

Parrotta, L., Guerriero, G., Sergeant, K., Cai, G., Hausman, J.F. 2015. Target or barrier? The cell wall of early- and later-diverging plants vs cadmium toxicity: differences in the response mechanisms. Front. Plant Sci. 6-133. https://doi.org/10.3389/fpls.2015.00133

Prajapati, S.K., Tripathi, B.D. 2008. Seasonal variation of leaf dust accumulation and pigment content in plant species exposed to urban particulates pollution. J. Environ. Qual. 37, 865–870.

Prasad, M.N.V., Strzalka, K. 1999. Impact of heavy metals on photosynthesis. – In: Prasad, M.N.V., Hagemeyer, J. (ed.): Heavy Metal Stress in Plants. Pp. 117-138. Springer, Heidelberg.

Sagardoy, R., Vázquez, S., Florez-Sarasa, I. D., Albacete, A., Ribas-Carbó, M., Flexas, J., Abadía J., Morales, F. 2010. Stomatal and mesophyll conductances to CO2 are the main limitations to photosynthesis in sugar beet (*Beta vulgaris*) plants grown with excess zinc. New Phytologist (2010) 187: 145–158 doi: 10.1111/j.1469-8137.2010.03241.x

Sengupta, D., Marriboina, S., Unnikrishnan, D.K., Reddy A. 2019 Photosynthetic performance and sugar variations during key reproductive stages of soybean under potassium iodide-simulated terminal drought. Photosynthetica. 57, 458-469.Skórzyńska-Polit, E., Baszyński, T. 1997. Differences in sensitivity of the photosynthetic apparatus in Cd-stressed runner bean plants in relation to their age. Plant Science. 128, 11-21. https://doi.org/10.1016/S0168-9452(97)00126-X

Sorrentino, M.C, Capozzi, F., Amitrano, C., Giordano, S., Arena, C., Spanuolo, V. 2018. Performance of three cardoon cultivars in an industrial heavy metal-contaminated soil: effects on morphology, cytology and photosynthesis. J. Hazard. Mater. 351, 131–137.

Spagnuolo, V., Zampella, M., Giordano, S., Adamo, P. 2011. Cytological stress and element uptake in moss and lichen exposed in bags in urban area. Ecotoxicol. Environ. Safe. 74, 1434-1443.

Storalska, A., Wrobel, J., Wozniak, A., Marska, B. 2007. Effect of zinc and copper soil contamination on the transpiration intensity and stomal index of winter crop wheat seedlings. J. Elementol. 12, 79-86.

Su, C., Jiang, L.Q., Zhang, W.J. 2014. A review on heavy metal contamination in the soil worldwide: Situation, impact and remediation techniques. Environmental Skeptics and Critics. 3, 24-38

Visconti, D., Fiorentino, N., Stinca, A., Di Mola, I., Fagnano, M. 2018. Use of the native vascular flora for risk assessment and management of an industrial contaminated soil. Ital. J. Agron. 13, 23–33. https://doi.org/10.4081/ija.2018.1348

Weryszko-Chmielewska, E., Chwil, M. 2005. Lead-induced histological and ultrastructural changes in the leaves of soybean (*Glycine max* (L.) Merr.). Soil Sci. Plant Nutr. 61,203-212.

Xiong, D., Douthe, C., Flexas, J. 2017. Differential coordination of stomatal conductance, mesophyll conductance, and leaf hydraulic conductance in response to changing light across species. Plant Cell Environ. 41, 436–450.

Zengin, F.K., Munzuroglu, O. 2006. Toxic effects of cadmium (CdCC) on metabolism of sunflower (*Helianthus annuus* L.) seedlings. Acta Agriculturae Scandinavica, Section B: Soil & Plant Science. 56, 224-229.

# Chapter 4

## Implication of vitality, seasonality and specific leaf area on PAH uptake in moss and lichen transplanted in bags

Capozzi F.[1,2], Sorrentino M.C.[1], Di Palma A.[2], Mele F.[1], Arena C.[1], Adamo P.[2], Spagnuolo V.[1]*, Giordano S.[1]

[1] *Dipartimento di Biologia, Università di Napoli Federico II, Via Cinthia 26, 80126 Napoli, Italy.*
[2] *Dipartimento di Agraria, Università di Napoli Federico II, Via Università 100, 80055 Portici (NA), Italy.*

***Ecological Indicators 108 (2020) 105727 https:// doi.org/10.1016/j.ecolind.2019.105727.***

Corresponding author: Valeria Spagnuolo valeria.spagnuolo@unina.it

### Graphical abstract

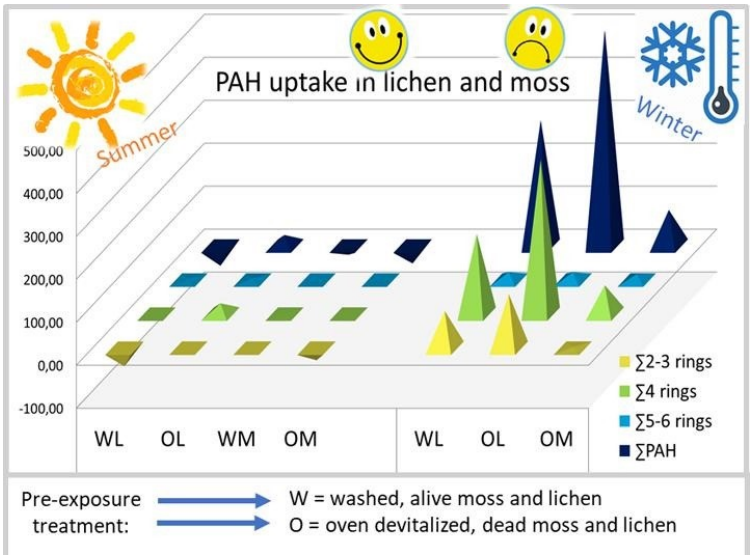


### Abstract

In this work the moss *Hypnum cupressiforme* and the lichen *Pseudevernia furfuracea* were exposed in bags for six weeks alive and oven-devitalized during summer and winter; the content of 24 PAHs was quantified to evaluate the effect of vitality, seasonality and specific leaf area (SLA) on PAH uptake and profiling. Vitality was followed throughout the exposure by measuring PSII maximal photochemical efficiency ($F_v/F_m$). In summer, a limited PAH signal was detected, with no significant increase, or even loss, of these compounds. During winter, a significant increase of PAHs was measured in both biomonitors, especially in those devitalized, with a lower baseline PAH content compared to alive material. This result suggests that PAH uptake mostly relies on passive mechanisms. Accordingly, $F_v/F_m$ demonstrated that moss and lichen exposed alive spent most of the exposure time in cryptobiosis. In both biomonitors 4-rings PAHs prevailed, followed by 2-3-rings in lichen and 5-6-rings in moss. Lichen performed better than moss, due to the ability to entrap PAHs in the body of thalli, preserving these compounds during the exposure. A formula was developed to express the accumulated PAHs

in terms of flux, that resulted higher in lichen than in moss. Oven devitalized lichen exposed in winter provided the highest uptake, indicating that morphology, SLA and seasonality represent key parameters in PAH biomonitoring.

Key words: PAH biomonitoring; moss and lichen transplants; $F_v/F_m$; specific leaf area; daily PAH flux.

## 1. Introduction

Although all industrialized world and emerging countries recognize air pollution as a crucial problem, to be addressed by strategic environmental policies, air monitoring is still insufficiently considered due to the high costs and application restrictions. Further, the variability in air pollution patterns, underline the urgency of feasible approaches aimed to extensive screening of pollutants (De Nicola et al. 2016). Autochthonous and transplanted mosses and lichens have been exploited for several decades as biomonitors of atmospheric pollutants, taking advantage of their thallous structure, allowing the adsorption/absorption of wet and dry atmospheric depositions on the entire surface. For metals and metalloids, it is widely assessed that the uptake ability of mosses and lichens is related to their high surface to mass ratio, their capacity to intercept and retain particulate matter (Di Palma et al. 2017; Spagnuolo et al. 2013) and the specific characteristics of cell walls (Gonzalez and Pokrovsky 2014; Gonzalez et al. 2016). Therefore, moss and lichen vitality does not affect metal uptake (Tretiach et al. 2007), since most of these elements are passively adsorbed to the thalli in form of PM.

Compared to metals, organic pollutants have been poorly investigated so far (e.g., Do1egowska and Migaszewski 2011; Ötvös et al. 2004); among the organic pollutants, PAHs are widely distributed and are regarded as persistent organic contaminants in the environment (Ravindra et al. 2008). Of the total PAH emission into the urban environment, 40% is scavenged by vegetation via dry and wet deposition (Collins and Finnegan 2010; Lehndorff and Schwark 2004). Although a small fraction of PAHs can move from the soil to plant tissue, most of airborne PAHs enter vascular plants via stomata or via cuticle waxes; due to the large surface area, the foliar interface is considered as the main access for organic chemical accumulation (Desalme et al. 2013; Terzaghi et al., 2015). As for PAH detection by mosses and lichens, few, sometime contrasting data are available (Augusto et al. 2013 and 2015; Capozzi et al. 2017; De Nicola et al. 2013; Keyte et al. 2009; Spagnuolo et al. 2017). In a one-year long experiment, Foan et al., (2015) demonstrated that PAH bioconcentration factor in mosses was significantly related to the water solubility (log $K_{OW}$) of these compounds. The absence of stomata and cuticle, in addition to the semi-volatile nature of PAHs (i.e., their partitioning between vapor and particle phases according to their molecular weight, temperature and humidity, and water solubility) make it difficult to predict the entrance routes of these pollutants by the moss and lichen thalli. Moreover, while the recent literature on the cell wall of mosses highlights the presence of several functional groups able to favor metal interception and adsorption (Gonzalez

and Pokrovsky 2014; Gonzalez et al. 2016), PAH interception and retention mechanisms by mosses and lichens could be different due to the prevalent hydrophobic nature of these compounds. Therefore, it appears unclear if mosses and lichens can be efficient biomonitors of atmospheric PAHs, especially when used as transplants.

In a recent study, Capozzi et al. (2017) tested devitalized *H. cupressiforme* exposed in bags in ten sites of southern Italy, set in proximity of random recurrent burnings; they evidenced that moss transplants could uptake high molecular weight (HMW) PAHs, but failed to accumulate low molecular weight (LMW) PAHs. This aspect was likely related to specific morphological features, as the leaves consisting of a single cell layer, and the absence of waxy cuticles, both traits impeding PAH uptake and their preservation in the cells. On the contrary, the ability to accumulate HMW PAHs relied on the well-known capacity of mosses to entrap and passively uptake particulate matter of various composition.

The use of devitalized moss and lichen was developed and applied in many experiments in the recent years (Adamo et al. 2011; Capozzi et al. 2016; De Nicola et al. 2013); this approach, sharing the advantage of bags ready to use, demonstrated highly reproducible and with lower internal variability of replicas, at least for metals and metalloids. But, when used to quantify organic molecules as PAHs, criticism could be raised to the approach with devitalized moss and lichen, which excludes all the uptake mechanisms linked to vitality.

Lichens and mosses have been studied in deep, concerning mechanisms related to desiccation tolerance (Proctor 2000; Kranner et al., 2008). Many bryophytes and lichens can withstand drying to water contents of 5–10% of their dry weight. As soon as water is available, these organisms can recover quickly, within a few minutes or hours, and switch to normal metabolism (Oliver et al., 1998). Chlorophyll fluorescence provides a rapid and non-invasive means of exploring aspects of the behavior of the photosynthetic system during and following environmental stress (Lichtenthaler, 1988; Maxwell and Johnson 2000). To test if devitalized moss and lichen are good biomonitors of air pollution also in the case of PAHs or if, losing vitality, these organisms drop part of their ability to accumulate PAHs, we set up an experiment aimed to: i) test the effect of vitality on the uptake and profiling of PAHs in transplanted moss and lichen; ii) compare PAH uptake in both biomonitors during summer and winter; iii) follow how biomonitor vitality was affected during the exposure duration, using photosynthetic parameters as proxy. Moreover, for comparison with data from physical chemical devices, a formula expressing the accumulated PAHs in terms of flux was implemented.

**Materials and methods**

*2.1 Experimental design, bags preparation and exposure*

The species used for this study were the moss *Hypnum cupressiforme* Hedw. and the lichen *Pseudevernia furfuracea* (L.) Zopf. Moss carpets for summer exposure were collected from tree trunks (*Fagus sylvatica* L.) at Montevergine, (40°59'38.69"N; 14°41'4.53"E - 850-950 m a.s.l. ); moss carpets for winter exposure were collected at Taburno-Camposauro Regional Park on barks of *F. sylvatica* (1000 m a.s.l. - 41°6'18.34"N; 14°35'36.81"E). Lichen thalli were collected from trunks of *Abies alba* Mill. at Monte Matese (41°27'49.14"N; 14°23'5.71"E – 1650 m a.s.l.). The collection sites are proximal natural sites, far, at least 5 km, from known sources of pollution; the collections were completed in a single day.

Moss and lichens were brought to laboratory and manually cleaned; only green and brown-green moss shoots (distal 4-5 cm) were used for bag preparation. Distal lobes of lichen (3-5 cm) were selected and treated as for moss. Moss and lichen were extensively washed and homogenized in distilled water according to Tretiach et al. (2007) and Ares et al (2012), to obtain clean moss and lichen material. At this stage, the two biomonitors were partitioned in two aliquots of approximately 100 g each; one moss and lichen aliquot was devitalized in a dry oven al 100 °C for 24 h to obtain dead moss and lichen (OM and OL, respectively); another aliquot was left alive to obtain (WM and WL, respectively).

Eight samples of dead (oven devitalized, O) and alive (washed, W) moss and lichen materials (OM, OL, WM, WL), were analyzed prior to exposure to assess the baseline PAH contents, and to determine the after-exposure enrichment of moss and lichen with reference to the respective pre-exposure biomaterial.

According to the guidelines for standardization of bag preparation and exposure (Capozzi et al 2016), subspherical bags were prepared with 2.5 g of each bio-material ensuring a density inside the bags of 15 mg $cm^{-1}$. Eight bags of each biomaterial were suspended on a latticework by nylon strings and exposed for 6 weeks in open air, without any artificial shading, on the roof of the Biology Department building in the urban area of Naples city. One additional bag filled with WM and WL was also exposed and used for the evaluation of biomonitor vitality during the exposure, by photochemical measurements (see paragraph below). The exposure started in June 2017 and was repeated for comparison in January 2018, to test how PAH uptake ability was affected by seasonality. Details on meteorological parameters recorded during the two exposure periods in the study area, are given in Table 1.

In the second exposure (winter), based on the results obtained in summer, the experimental design was simplified: lichen was exposed both alive and after oven treatment (WL and OL), while moss was exposed only devitalized (OM). The lichen used for this exposure was a sub-

sample of the spring 2017 collection, stored in cold greenhouse and its vitality was checked as explained below (see paragraph 2.5).

After exposure, moss and lichen materials were removed from bags, dried at 20 °C, manually milled and homogenized with a ceramic mortar and pestle using liquid nitrogen and stored in the dark at 4 °C before the analyses.

Table 1 - Summary of meteorological parameters during the exposure periods.

| | | Summer | Winter |
|---|---|---|---|
| T (°C) | Min | 20.9 | 6.4 |
| | Mean±SD | 27.7±1.8 | 10.5±2.3 |
| | Max | 30.1 | 14.3 |
| Rain | Days | 4 | 25 |
| | mm/day | <10 | >10 |
| Sky | Days | 96% Sunny | 86% Cloudy |
| RH (%) | Mean±SD | 58.4±10.2 | 71.3±9.6 |
| WIND (km/h) | Mean±SD | 9.6±3.2 | 9.1±4.9 |
| | Max | 20.2 | 19.8 |
| | Main direction | SSW | ENE |

*2.2. PAH analyses*

According to the protocols EPA 3550 C 2007 and EPA 8270 D 2014 for PAH analyses, two grams of each biomaterial were sonicated twice by a Falc Sonicator, in 25 mL of dichloromethane for 20 min each. The extracts, purified through activated silica gel, were dried to a volume of 200 mL under a gentle nitrogen stream. Afterwards, the samples were analyzed by GCeMSD (Agilent 5975C with a VF-17MS column) with helium as gas carrier at 1.3 mL $min^{-1}$. The oven temperature program started at 50 °C, increased with ramp rate 30 °C min-1, to 350 °C and held for 9 min. All analyses were performed in selected ion monitoring (SIM). The analyses were performed by the certified Mérieux NutriSciences Company (Resana, Italy). The concentration of the following 24 PAHs were quantified by multi-point calibration curves and labelled internal standards; (2- rings): naphtalene (Naph); 2-methylnaphtalene (2M-Naph); (3-rings): acenaphthene (Ace), acenaphthylene (Acy), fluorene (Flu), phenanthrene (Phen), anthracene (Ant); (4-rings): fluoranthene (Flt), pyrene (Pyr), perylene (Prl), benz[a]anthracene (B[a]A); chrysene (Chrys), (5-rings): benzo[b]fluoranthene (B[b]F), benzo[k]fluoranthene (B[k]F), benzo[j]fluoranthene (B[j]F), benzo[a]pyrene (B[a]P), benzo[e]pyrene (B[e]P), dibenzo[a,h]anthracene (DB[a,h]A), (6-rings): benzo[g,h,i]perylene (B[g,h,i]P), indeno[1,2,3-

c,d]pyrene (IP), dibenzo[a,i]pyrene (DB[a,i]P), dibenzo[a,h]pyrene (DB[a,h]P), dibenzo[a,e]pyrene (DB[a,e]P), dibenzo[a,l]pyrene (DB[a,l]P).

Labelled PAHs (naphthalene D8, acenaphtene D10, phenanthrene D10, chrysene D12, perylene D12) were used as surrogates for the quality control of the procedure and their recovery percentages (from 82% to 120%) were included to correct the concentration of each compound. The minimum detectable PAH concentration was 1 ng $g^{-1}$ d.w. for each compound.

*2.3 Calculation of specific leaf area and deposition flux for moss and lichen*

Twenty individual dry moss shoots were randomly collected and weighted; then, for each shoot the average number of leaves was counted by the aid of a stereomicroscope Leica M8. Afterword, 20 leaves per shoot were randomly selected, photographed, and pictures acquired by a Leica LMD 6500 dissecting light microscope. The photographs were then processed using the free source ImageJ software to calculate the leaf area and the specific leaf area according to the formula:

SLA = Leaf area ($m^2$)/dry weight (g)

For the lichen, 20 dried thalli were selected, individually weighed, and photographed by the aid of a scanner. The acquired pictures were similarly processed by the ImageJ software to calculate SLA.

Here we propose a formula to calculate the pollutant deposition flux, or daily uptake, starting from the data obtained by the biomonitoring (i.e. a mass to mass ratio, usually ppm or ppb, that represents the concentration of a certain pollutant per unit mass of biological tissue) in order to facilitate the comparison with other non-biological monitoring devices.

The flux was calculated using the following formula:

$\mathbf{\Theta_{DF}} = \mathbf{M_{acc}}/(\mathbf{S}*\mathbf{d})$

where $\mathbf{\Theta_{DF}}$ is the deposition flux [$ng*m^{-2}*d^{-1}$]; $\mathbf{M_{acc}}$ is the amount of each pollutant (expressed as *ng*) accumulated during the exposure period, obtained by subtracting the pollutant amount before exposure $M_0$ from that measured after the exposure $M_f$; **S** is the exposed surface of the organism (i.e., leaf area), expressed as $m^2$; **d** is the duration of exposure, expressed as days.

Since **S** is directly linked to the **SLA** (see the above paragraph), the same deposition flux can be quickly obtained by dividing the pollutant concentration $\mathbf{[M]_{acc}}$ (expressed as $ng\ g^{-1}$) by the 2***SLA** ($cm^2g^{-1}$) multiplied for the day of exposure (**d**): $\Theta_{DF} = \mathbf{[M]_{acc}} * (2*\mathbf{SLA}*\mathbf{d})^{-1}$

*2.4 Assessment of vitality in moss and lichen*

The vitality assessment was studied through two experiments carried out during both summer and winter exposures. In the first experiment we built vitality response curves for control (pre-exposed) and for mosses and lichens exposed in bags in open air (WL and WM). Aliquots of control samples, coming from pristine sites, were dried in an oven at 38±2°C for almost one hour until constant weight and then subjected to rehydration dynamics in controlled laboratory conditions in order to assess the intrinsic capability of recovery. The rehydration of samples was obtained in relative humidity (RH%) saturated atmosphere including the lichen lobes and the moss shoots in a closed box filled with wet paper, sprayed with distilled water. The vitality of moss and lichen was measured on fully dried samples (time t = 0) and at different time intervals (2, 5, 12, 20, 30, 40 and 90 min) up to 90 min after rehydration, monitoring the PSII maximal photochemical efficiency ($F_v/F_m$), together with the fresh weight of samples. To measure $F_v/F_m$ on the same spot at each interval of time, the samples were marked with a narrow adhesive ribbon.

To assess the rehydration degree, the samples were weighed at each time, and chlorophyll fluorescence emission measurements were performed. These measurements were considered as a reference for the kinetic of recovery for the samples exposed to open air in moss and lichen bags.

Moss and lichen samples exposed in bags in open air (WM and WL) were periodically collected (after 1, 2, 3, 4 and 5 weeks from exposure) carried in laboratory, immediately weighed, and subjected to fluorescence emission measurements (t =0). After 15, 40, 60, 70, 90 min after rehydration in vapor saturated atmosphere, the samples of both species were again weighed and $F_v/F_m$ measured to assess the vitality. As no difference was found in the kinetics of recovery of $F_v/F_m$ and fresh weight in samples after each week of exposure, a single graph was built considering the behavior of both species during the time of recovery from desiccation.

In the second experiment, the kinetic of dehydration was evaluated; to this aim the rehydrated moss and lichen after each acquisition of $F_v/F_m$ and fresh weight, were put again in their bags and exposed in open air to monitor the time needed for their complete desiccation. The kinetics of dehydration was followed by $F_v/F_m$ and fresh weight measurements until the complete drying of the samples.

The chlorophyll *a* fluorescence emission was measured by means of a Pulse-Amplitude-Modulated fluorometer (Junior-PAM, Walz, Germany) supplied with a monitoring Leaf-Clip JUNIOR-B (Walz, Germany), on 30' dark-adapted samples. The background fluorescence signal, $F_o$, was induced on 30 min dark adapted thalli, by a blue LED internal light of about 2-3 μmol photons·$m^{-2}$ $s^{-1}$, at a frequency of 0.5kHz. The maximal fluorescence level in the dark-

adapted state ($F_m$) was induced by 1s saturating light pulse (8000 μmol photons·$m^{-2}$·$s^{-1}$) at a frequency of 10kHz; the maximal PSII photochemical efficiency ($F_v/F_m$) was calculated as $F_v/F_m = (F_m-F_o)/F_m$ (Maxwell and Johnson 2000).

*2.5 Data analysis*

Microsoft Excel and STATISTICA ver. 8.0 (StatSoft, Inc. 2008) software were used to process the data. Shapiro Wilk's test and Levene's test were used to assess the normality and homogeneity of the variances, respectively. Analysis of Variance (ANOVA) was used to assess the differences among the different theses; in case of rejection of the null hypothesis the Tukey's significance post-hoc test was applied ($p < 0.05$).

## 3. Results

*3.1 PAH contents in lichen and moss in summer and winter exposures*

Average PAH contents in moss and lichen before and after summer and winter exposures are reported in Table 2 and 1s (supplementary table), whereas PAH accumulation in both seasons is showed in Fig 1. Based on the contents, a different PAH profile was observed in the lichen depending on the pre-exposure treatment: WL showed contents of total and 4-rings PAHs significantly higher than OL; oven-devitalization induced a loss of 2-3 and 4-rings PAHs, also affecting the total PAH content (see Table 2, 234 ng g-1 in OL vs. 372 in WL). In summer, a general, but not significant decline of PAHs was observed in WL after the exposure (see Table 2, 372 ng $g^{-1}$ vs. 326 ng $g^{-1}$ and Fig 1), especially concerning 2-3 rings PAHs. By contrast, a moderate not significant increment was observed in OL (see Table 2, 234 ng $g^{-1}$ vs. 260 ng $g^{-1}$ and Fig 1) depending on the increase of 4-6 rings PAHs.

Both PAH profiles and contents were at all comparable in pre-exposure WM and OM (see Table 2 total PAH content 213 and 235 ng $g^{-1}$ respectively), in which 2-3 rings PAHs represented the main fraction, followed by 4-rings and 5-6 rings. In summer, a limited, not significant loss of PAHs was observed after the exposure in both materials (see Table 2, 193 and 194 ng $g^{-1}$ and Fig 1), especially concerning 2-3 rings PAHs.

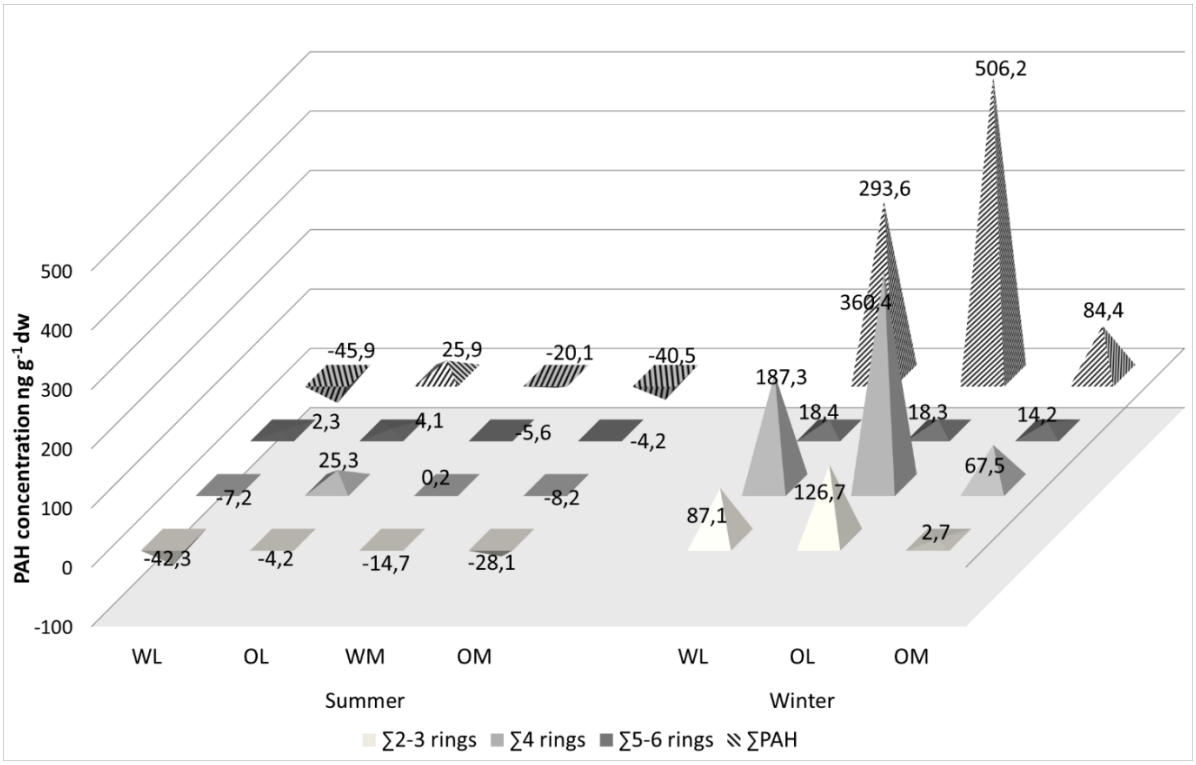


Figure 1. PAH accumulation (post- minus pre-exposure values) in lichen and moss alive (WL, WM) and devitalized (OL, OM) exposed during summer and winter.

In winter, both WL and OL significantly accumulated PAHs during the exposure, particularly the oven-devitalized material, showing a total PAH content of 740 vs. 666 ng $g^{-1}$ found in WL. Oven-devitalized lichen showed contents two folds (for 2-3 rings) and four folds (for 4-rings) higher than pre-exposure contents, while the 6-rings PAHs were substantially unchanged after the exposure (Fig. 1). In OM a significant increase was observed after the exposure (177 vs. 262 ng $g^{-1}$ and Fig 1), specially concerning 4-rings PAHs which doubled their concentration.

Table 2. Average PAH contents (ng $g^{-1}$ DW) in moss and lichen in summer and winter exposure. Each value represents the mean ± SD, n=8. Different letters indicate significant differences among the treatments according to Tukey's post-hoc test.

| | ∑2-3 rings | ∑4 rings | ∑5-6 rings | ∑PAH |
|---|---|---|---|---|
| | **Summer exposure** | | | |
| **WL_pre** | 184.5±12.6b | 178.0±20.6c | 10.8±1.5d | 372.3±22.1c |
| **OL_pre** | 131.5±14.3bc | 91.5±8.5ef | 12.1±2.1cd | 234.3±10.6de |
| **WL_post** | 142.2±16.4bc | 170.8±17.7c | 13.1±2.0cd | 326.4±35.2c |
| **OL_post** | 127.3±15.5bc | 116.8±16.4de | 16.2±1.6cd | 260.2±26.1d |
| **WM_pre** | 120.5±15.8bc | 58.8±7.6f | 34.1±4.6ab | 213.3±7.2de |
| **OM_pre** | 127.1±18.2bc | 68.3±9.8f | 39.5±8.6a | 234.8±30.2de |
| **WM_post** | 105.8±16.3c | 59.0±11.6f | 28.5±5.3ab | 193.2±27.3e |
| **OM_post** | 99.0±16.4c | 60.1±9.0f | 35.3±3.7a | 194.3±25.3e |
| | **Winter exposure** | | | |
| **WL_pre** | 184.5±12.6b | 178.0±20.6c | 10.8±1.5d | 372.3±22.1c |
| **OL_pre** | 131.5±14.3bc | 91.5±8.5ef | 12.1±2.1cd | 234.3±10.6de |
| **WL_post** | 271.6±67.4a | 365.3±11.9b | 29.2±4.3ab | 665.9±39.3b |
| **OL_post** | 258.2±86.4a | 451.9±29.4a | 30.4±5.2ab | 740.5±69.2a |
| **OM_pre** | 77.4±35.4c | 77.35±35.7f | 22.9±3.4bc | 177.6±33.9e |
| **OM_post** | 80.1±22.5c | 144.8±23.5cd | 37.1±3.6a | 262.0±20.1d |

Table 3. PAH accumulation (post- minus pre- exposure contents, ng $g^{-1}$ dw) in OM, WL and OL exposed in winter; maximum values are marked in grey.

| | OM | WL | OL |
|---|---|---|---|
| **Naph** | -8.9 | 51.5 | 77.75 |
| **2-M-Naph** | -1 | 35 | 18.7 |
| **Acy** | -1.7 | -1.5 | 12 |
| **Ace** | 1 | -0.2 | 2.5 |
| **Flu** | -2.9 | -2.1 | -1.3 |
| **Phen** | 16 | 5.3 | 15 |
| **Ant** | 0.3 | -1.5 | 1.8 |
| **Flt** | 25.6 | 48.9 | 127.2 |
| **Pyr** | 29.9 | 117 | 205.4 |
| **B[a]A** | 3.7 | 5.7 | 6.9 |
| **Chrys** | 11.7 | 20.7 | 20.8 |
| **B[b]F** | 2.8 | 5.9 | 4.3 |
| **B[k]F** | 1.1 | 1.8 | 1.6 |
| **B[j]F** | 1.7 | 3.8 | 2.7 |
| **B[e]P** | 4.65 | -2 | -2 |
| **B[a]P** | 0.75 | | |
| **IP** | 1.1 | 2.5 | 2.3 |
| **B[g,h,i]P** | 1.7 | 7.5 | 8.8 |

*3.2 Lichen vs. moss*

The comparison lichen vs. moss was based on the winter exposure, because during the summer, PAH loss prevailed on the accumulation. All the biomaterials showed higher accumulation performances in winter ($p<0.05$); in case of loss of individual PAHs, no significant difference occurred between the pre- and post-exposed contents ($p>0.05$; see Table 1s).

In general, based on PAH content, lichen performed better than moss ($p<0.05$, see Fig. 1; Tables 2 and 1s); the oven-devitalization in lichen, lowered PAH baseline content, (significant for Flu, Phen, Ant, and Flt, $p<0.05$), allowing this biomaterial to measure the highest significant increment during the 6 weeks exposure. Accordingly, based on the average accumulation of the single PAHs (Post-exposure minus pre-exposure contents; Table 3), OM showed the highest accumulation only for two PAHs, WL for 6 and OL for 10 PAHs; therefore, OL had overall the best accumulation performance. Considering the relative percentages of PAH - grouped by rings - accumulated in moss and lichen during the winter (Fig. 2), it is evident that both biomonitors mainly accumulated 4-rings PAHs, 71 and 80% respectively in lichen and moss; conversely, lichen accumulated LMW PAHs (25%), while moss HMW PAHs (17%).


Figure 2. Lichen and moss PAH uptake profile calculated on devitalized materials (OL and OM) exposed in winter. Light grey: 2-3 rings; medium grey: 4- rings; deep grey: 5-6 rings PAHs.

*3.3. SLA and Deposition flux*

The calculation of the SLA for the moss *H. cupressiforme* and the lichen *P. furfuracea* is summarized in Table 4; the deposition flux based on the accumulation of PAH during the exposure (post- minus pre-exposure contents; Table 5) was calculated only on oven devitalized materials exposed in winter, because for these materials a significant accumulation was measured. Deposition flux can be obtained by PAH accumulation for all plant materials and SLA measured in moss and lichen according to the formula reported in the paragraph 2.3; however, to provide a summary picture of PAH flux in the two biomonitors, examples of this calculation for single, illustrative PAHs per each n-ring number type (2- 3- 4- 5- rings), in addition to the summation of each PAH class (2-3 rings, 4 and 5-6 rings) and total PAHs, are given in Table 5.

Table 4- Estimated SLA*2 (expressed as $m^2\ g^{-1}$) for the two biomonitors; n=20.

| **Species** | **Min** | **Mean±SD** | **Max** |
|---|---|---|---|
| ***Hypnum cupressiforme*** | 0.094 | 0.135±0.061 | 0.280 |
| ***Pseudevernia furfuracea*** | 0.021 | 0.026±0.004 | 0.034 |

The SLA mean value of moss was about five folds that of lichen; thus, when considering the deposition flux, all values are far higher (in some cases more than one order of magnitude) for lichen compared to moss.

Table 5- Deposition flux [$\Theta_{DF}$ - $ng*m^{-2}*d^{-1}$] for moss and lichen calculated for some illustrative PAHs, PAHs grouped by rings and total PAHs.

| | **Naph** | **Phen** | **Chrys** | **B(b)F** | **∑2-3 rings** | **∑4 rings** | **∑5-6 rings** | **∑PAH** |
|---|---|---|---|---|---|---|---|---|
| **OM_W** | 0.00 | 2.82 | 2.06 | 0.49 | 0.53 | 11.99 | 2.50 | 14.81 |
| **OL_W** | 71.20 | 13.74 | 19.05 | 3.94 | 116.30 | 250.92 | 16.76 | 463.37 |

*3.4. Assessment of vitality*

Table 6 lists $F_v/F_m$ and fresh weight values measured in fully rehydrated pre-exposed moss and lichen. The monitoring was followed for 90 min. The reference values of $F_v/F_m$ measured before exposure in moss and lichen collected fresh from the field in a pristine area in moist conditions, were respectively 0.729 ± 0.041 and 0.557 ± 0.023, for the same samples the weights in grams were 28.34 ± 2.02 and 11.10 ± 0.92.

Table 6- Moss and lichen fresh weight and maximal PSII photochemical efficiency ($F_v/F_m$) measured in laboratory soon after desiccation in oven at 38±2 °C (t=0) and at different time intervals from rehydration in control healthy individuals. Each value is the mean ± SE (n=3).

| | Moss | | Lichen | |
|---|---|---|---|---|
| Time (min) | Fresh weight (g) | $F_v/F_m$ | Fresh weight (g) | $F_v/F_m$ |
| 0 | 8.16 ± 1.23 | 0.042 ± 0.014 | 3.26 ± 0.65 | 0.011 ± 0.012 |
| 2 | 13.26 ± 1.34 | 0.475 ± 0.031 | 7.27 ± 1.02 | 0.459 ± 0.031 |
| 5 | 13.89 ± 1.13 | 0.489 ± 0.201 | 8.01 ± 0.99 | 0.461 ± 0.041 |
| 12 | 15.88 ± 2.00 | 0.603 ± 0.021 | 8.68 ± 1.00 | 0.498 ± 0.021 |
| 20 | 16.89 ± 1.46 | 0.614 ± 0.031 | 9.10 ± 0.89 | 0.554 ± 0.040 |
| 30 | 18.00 ± 1.87 | 0.625 ± 0.031 | 9.99 ± 1.29 | 0.501 ± 0.031 |
| 40 | 19.02 ± 2.20 | 0.644 ± 0.024 | 10.75 ± 2.12 | 0.545 ± 0.019 |
| 90 | 27.60 ± 2.45 | 0.714 ± 0.031 | 10.81 ± 1.92 | 0.546 ± 0.023 |

The kinetics of rehydration were different in moss and lichen. More specifically, the maximal PSII photochemical efficiency ($F_v/F_m$) was reached after 90 min from moisturizing in the moss (0,714) and just after 20 min in the lichen (0,554). As regards the fresh weight, the original weights were recovered after 30 min in the lichen (9,99 g), and at 90 min in the moss (27,60 g) (Table 6).

Figure 3 shows the values of fresh weight and $F_v/F_m$ measured in dried moss and lichen exposed in bags (WM and WL) in open air soon after sampling and at different times from remoistening. The fresh weight in both species reached the steady state after 40’ from rehydration; in fact, no further increase of fresh weight was observed up to 90’ (Fig. 3, bars). On the contrary, moss and lichen showed different kinetics in $F_v/F_m$: more specifically, in the lichen this parameter recovered after 40’ from rehydration, whereas in the moss it was not restored, even after 90’ (Fig. 3, lines). It is noteworthy that after 24 hrs from rehydration, both species showed a full recovery of $F_v/F_m$ compared to pre-exposed condition (data not showed).

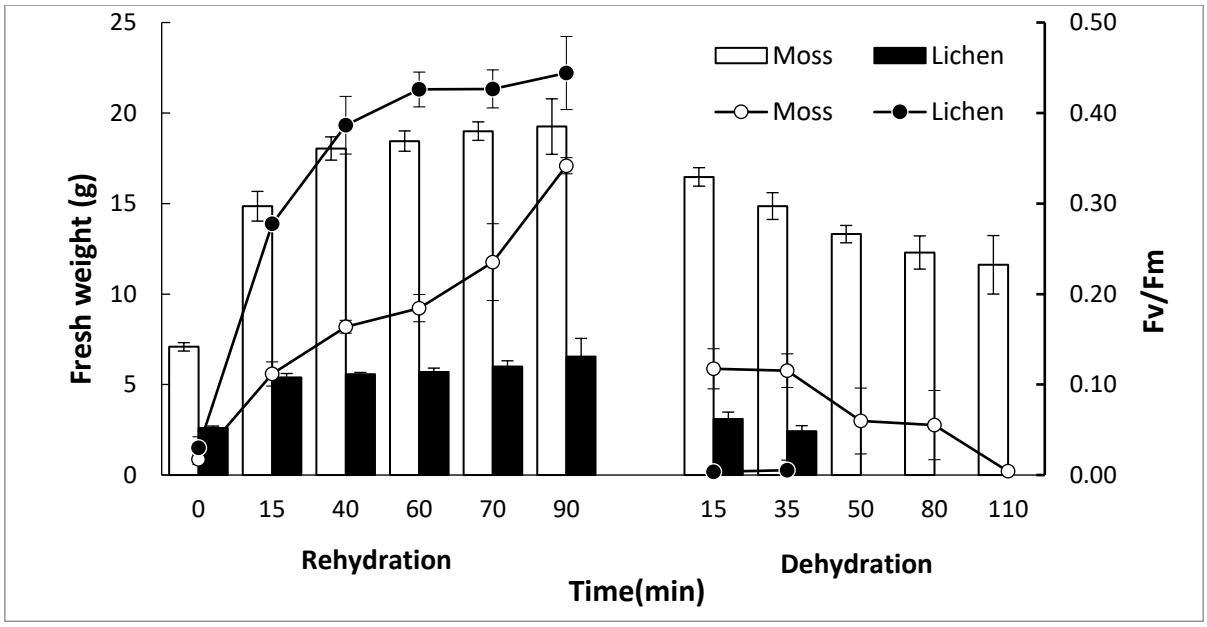


Figure 3. Evaluation of vitality of moss and lichen exposed in bags during rehydration and dehydration cycles, expressed as $F_v/F_m$ (lines) and fresh weight (bars). See text for further details.

The dehydration experiments showed very rapid drop (within 15') of the fresh weight in the lichen compared to the moss (Fig. 3); in parallel also a decline of $F_v/F_m$ was observed. Conversely, the moss remained moistened, with a minimal photochemical activity up to 80', confirming the resistance of this species to desiccation. As for the experiment carried out during the winter exposure, no significant difference was observed in both transplanted species in the kinetics of fresh weight and $F_v/F_m$ (data not showed).

## 4. Discussion

*4.1 PAH accumulation and profile in the two biomonitors*

After emission, PAHs can accumulate in plants through absorption and adsorption mechanisms depending on their availability in the environment, physical chemical properties (e.g., the partitioning between vapor and particle phases, the $K_{OW}$ coefficient), environmental conditions (e.g., temperature, humidity, radiation) and plant traits (Harmens 2013; Loppi et al. 2015). These parameters influence the levels of PAHs and their profile in a variable manner in a given species, even collected in relatively close background areas (Gerdol et al. 2002).

The total PAH pre-exposure contents in our samples were in line with the contents reported by Harmens et al. (2013) for mosses from background areas, in which the average concentration for up to 17 PAHs ranged from ca. 100 to 600 ng $g^1$ dry wt. In addition, according to Gerdol et al (2002), in pre-exposure material collected in pristine sites, the greater fraction was

represented by LMW PAHs. The different content of PAHs in pre-exposed mosses, noticeably higher in those collected in spring at Montevergine (213 ng $g^{-1}$) than in those collected in autumn at Taburno mountain (177 ng $g^{-1}$), could depend on the different deposition rate in the two sites, but also on the different season. The higher PAH content in moss collected in spring could reflect PAHs accumulated during the preceding winter, whereas the lower PAH content in mosses collected in autumn could be affected by PAH degradation and loss occurred in the preceding summer (Harmens et al., 2013). In line with the total PAH content measured in the present work in native lichen, Augusto et al. (2013) found concentrations of 16 EPA-PAHs in lichens between 58 and 556 ng g-1, with the highest values found during the coldest winter months.

The devitalization effect in moss and lichen (OM and OL) produce biomaterials with a lower baseline content of PAHs, compared to the living counterparts (WM and WL), and, thus, higher sensitivity to detect PAH inputs during the exposure period.

Moss and lichen showed different profiles of accumulated PAHs: in both species, the prevalent accumulated fraction is represented by 4-rings PAHs; for the remaining fractions, moss mainly accumulate 5-6 rings while lichen mostly 2-3 rings PAHs. These results agree with previous reports; specifically, for lichens it is known that PAH profile is mostly dominated by 2-3-, and 4-rings PAHs (Augusto et al. 2013). Differences in thallus morphology between the two biomonitors could explain this result; mosses having typically single-cell-layered leaves, do not accumulate 2-3 rings PAHs mainly in vapor phase, but they have the capacity to retain PAHs in particle phase due to their high surface to mass ratio and cell wall chemical properties (Gonzalez and Pokrovsky 2014; Tretiach et al. 2007). In lichens, instead, the structure of cortex and medulla allows for the entrapment and staying of PAHs in vapor phase. This observation well agrees with a previous study based on laboratory experiments, showing that in *Xanthoria parietina* gas phase PAHs easily cross lichen surface and accumulate in the thallus (Augusto et al. 2015). Although the mechanisms of interception of PAHs by plant surface are not completely exploited, a feasible hypothesis could be the adsorption on thallus surface by weak interactions as for example, p-interactions between benzene rings of PAHs and polar molecules of the cell wall, like phenolic compounds and acid polysaccharides (Capozzi et al 2018).

The different PAH profile found in moss and lichen transplanted in bags in urban context seems to conflict with PAH content and profiles reported for species from natural background areas, where both moss and lichen prevalently contain 2-3 rings PAHs. It is assessed that PAHs in the gaseous phase are generally transported to pristine areas, far from pollution sources, while HMW PAHs are generally deposited in larger proportions near emission sources, like urban

and industrial areas (Thomas, 1986). The discrepancy observed between PAH profiles found in native and transplanted biomonitors could depend on the different traits of natural and anthropic environments, the first characterized by climatic conditions preserving the permanence of PAHs in vapor phase, the latter promoting their decomposition due to higher temperature and radiation. This last aspect also affects the different levels of PAHs found in the two exposures, higher in winter compared to summer. Meteorological parameters recorded during the exposure periods support the seasonal variations observed; e.g., mean temperature was more than twice in summer compared to winter, and sunny days were 96% in summer exposure and only 14% in winter exposure (Table 1).

*4.2 Deposition flux*

In this work we suggested a formula to calculate a deposition flux (i.e. a daily uptake normalized to SLA), to provide a conversion of the uptake expressed as mass to mass, into a flux expressed as mass to surface; this step is necessary in view of an intercalibration between bioaccumulators and conventional deposimeters. The values calculated for SLA in *H. cupressiforme* and *P. furfuracea* well agree with those previously reported for the same species (Adamo et al. 2007). The higher values of deposition flux found in the lichen compared to moss depend on the higher thallus thickness (inversely related to SLA), allowing for the accumulation of PAHs (especially LMW) in the body of thalli. Specific leaf area was considered as an ecological trait proportionally linked to uptake of PAHs in vascular plants (Terzaghi et al. 2015). Under this respect, lichen thalli behave as leaves of higher plants; by contrast, moss is loser since its leaves are only one cell thick; this feature can explain the loss of LMW PAHs in moss during the exposure and the consequent null flux for these compounds (e.g. Naph). Of course, fluxes reflect PAH accumulation, with 4-rings PAHs representing the most abundant fraction for both biomonitors. When considering HMW PAHs, their accumulation in strongly dependent on biomonitor surface, significantly higher in moss than in lichen (Adamo et al. 2007) since these compounds are mostly in particle phase.

*4.3 PAH accumulation and vitality*

One of the aims of the present work was to understand if and how the vitality of the two transplanted biomonitors was linked to PAH uptake and accumulation using photochemical efficiency as an indicator of vitality. The fluorescence index maximal PSII photochemical efficiency (Fv/Fm) can be considered a good proxy of the impairment of photosynthetic function following desiccation, and recovery subsequent the rehydration (Seel at al. 1992; Tuba

et al., 1996; Csintalan et al 1999; Tretiach et al., 2007). In parallel, rehydration can be easily evaluated through the measurement of the fresh weight. Surprisingly, these two parameters not only provided different response in moss and lichen, but their kinetics were not synchronized. Our results indicate, indeed, that the completeness and subsequent course of the recovery varied from one species to another. During the rehydration, the moss has a tardive photochemical recovery compared to lichen even if the tissues restore the moisturizing in about 40'. The lichen appears more resilient than moss from a photochemical point of view, showing a substantial restoration of the vitality after 15' rehydration. Notwithstanding, the two species, when exposed in bags, loose their vitality (within few minutes the lichen, less rapidly the moss), entering a cryptobiotic state. In this situation, the uptake and accumulation of PAHs can be considered as a mix of adsorption and absorption, both occurring by passive mechanisms, in which vitality is only marginally involved.

The vitality of these biomonitors is limited to a very narrow time frame, in which humidity conditions due to rain or fog are compatible with photosynthesis; in other words, for most or all exposure time alive cryptogams behave as dead biomonitors, thus not differently from the devitalized material. In agreement with our results, in a previous study Tretiach et al. (2007) found a decline of photosynthetic pigments, chlorophyll fluorescence and $CO_2$ gas exchange in the lichen *Pseudevernia furfuracea* exposed in bags and concluded that transplanted biomonitors are comparable to a "still life". The papers focused on biomonitoring of air quality by "alive" moss and lichen in which bags are periodically sprayed with water (e.g., Sorbo et al. 2008) should be reconsidered in the light of these results, indicating that transplanted moss and lichen spent most or all exposure time in a cryptobiotic steady state even when sprayed.

The decline of vitality parameters in transplanted biomonitors during dehydration is an expected result, considering that even in natural condition many bryophytes and lichens can preserve their vitality by cryptobiosis when their water content is drastically reduced due to drought (Oliver et al. 1998). Surprisingly instead, oven devitalization, which irreversibly stops any active uptake mechanism, does not influence PAH accumulation within the lichen thalli, which results comparable in WL and OL for LMW and HMW PAHs (see Figure 2 and Table 2); this supports the idea that the entrapment and retention of these compounds is principally grounded on mechanisms independent from vitality.

## 5. Conclusions

The above described experiments provide for the first time an overview on PAH accumulation in moss and lichen bags in relation to vitality and morphological traits; the implications of the exposure season and SLA were evaluated as well. The exposure modified PAH profile and determined a loss of PAHs in summer, due to high temperature and radiation; whereas a significant accumulation of PAHs occurred in winter, indicating that cold season is the most appropriate for PAH biomonitoring by transplants, and any comparison between surveys carried out in different seasons should be avoided. Lichens performed better than mosses in terms of accumulation and flux, due to their ability to entrap PAHs in the body of thalli, preserving the most labile fraction (2-3 rings) of PAHs during the exposure. According to morphological traits, lichen PAH profile mainly covers 2-4 rings PAHs (vapor and particle phase), whereas moss prevalently accumulates 4-6 rings PAHs (mostly particle phase). Oven devitalization does not reduce the uptake ability but drops the baseline PAH content enhancing the sensitivity of the biomaterial, allowing PAH detection even at low concentration in the environment. Specific leaf area must be considered as an important feature in the analysis of PAH uptake, since it considers both surface and thickness of thalli, two key traits to clarify accumulation mechanisms of these pollutants. Under this respect, vitality experiments highlighted that PAH accumulation takes place mainly by passive mechanisms, since biomonitors spend most of the exposure time in cryptobiosis, even when exposed alive. Due to the PAH profile found in lichen and moss transplants, partly overlapping, their combined use could be more appropriate for PAH biomonitoring in anthropized environments lacking natural species. Finally, the calculation of the daily deposition flux should be compared to passive samplers to test the real possibility to use transplants to assess PAH deposition and related human health risk.

**Acknowledgements**

The present study was financed by funds from Department of Biology, University Federico II, Naples.

## References

Adamo P., Giordano S., Minganti V., Modenesi P., Monaci F., Pittao E., Tretiach M., Bargagli R. (2007). Lichen and moss bags as monitoring devices in urban areas. Part II: Trace element content in living and dead biomonitors and comparison with synthetic materials. Environ. Pollut., 146, 392-399, DOI 10.1016/j.envpol.2006.03.047.

Adamo P., Giordano S., Sforza A., Bargagli R. (2011). Implementation of airborne trace element monitoring with devitalized transplants of *Hypnum cupressiforme* Hedw.: Assessment of temporal trends and element contribution by vehicular traffic in Naples city. Environ. Pollut., 159 (6) 1620-1628, DOI 10.1016/j.envpol.2011.02.047.

Ares A., Aboal J.R., Carballeira A., Giordano S., Adamo P., Fernández J.A. (2012). Moss bag biomonitoring: A methodological review. Sci. Total Environ., 432, 143-158, DOI 10.1016/j.scitotenv.2012.05.087.

Augusto S., Pereira M.J., Magua, C., Branquinho C. (2013). A step towards the use of biomonitors as estimators of atmospheric PAHs for regulatory purposes. Chemosphere, 92, 626-632, DOI 10.1016/j.chemosphere.2013.03.068.

Augusto S., Sierra J., Nadal M., Schuhmacher M. (2015). Tracking polycyclic aromatic hydrocarbons in lichens: It's all about the algae. Environ. Pollut., 207, 441-445, DOI 10.1016/j.envpol.2015.08.013.

Capozzi F., Giordano S., Aboal J.R., Adamo P., Bargagli R., Boquete T., et al. (2016). Best options for the exposure of traditional and innovative moss bags: a systematic evaluation in three European countries. Environ. Pollut. 214, 362-373. DOI 10.1016/j.envpol.2016.04.043

Capozzi F., Di Palma A., Adamo P., Spagnuolo V., Giordano S. (2017). Monitoring chronic and acute PAH atmospheric pollution using transplants of the moss *Hypnum cupressiforme* and *Robinia pseudacacia* leaves. Atmos. Environ., 150, 45-54. DOI 10.1016/j.atmosenv.2016.11.046.

Capozzi F., Carotenuto R., Giordano S., Spagnuolo V. (2018). Evidence on the effectiveness of mosses for biomonitoring of microplastics in fresh water environment. Chemosphere, 205, 1–7, DOI 10.1016/j.chemosphere.2018.04.074.

Collins C. D., Finnegan, E. Modeling the plant uptake of organic chemicals, including the soil-air-plant pathway. Environ. Sci. Technol. 2010, 44, 998–1003, DOI 10.1021/es901941z.

Csintalan, Z., Proctor M.C.F., Tuba Z. (1999). Chlorophyll Fluorescence during Drying and Rehydration in the Mosses Rhytidiadelphus loreus (Hedw.) Warnst., Anomodon viticulosus (Hedw.) Hook. & Tayl. and Grimmia pulvinata (Hedw.) Sm. Ann. Bot., 84, 235-244, DOI 10.1006/anbo.1999.0919.

De Nicola F., Murena F., Costagliola M.A., Alfani A., Baldantoni D., Prati M.V., Sessa L., Spagnuolo,V., Giordano S. (2013). A multi-approach monitoring of particulate matter, metals and PAHs in an urban street canyon. Environ. Sci. Pollut. Res., 20, 4969–4979, DOI 10.1007/s11356-012-1456-1

De Nicola F.,Adamo P., Giordano S. (2016) Comparison of lichen and moss bags as monitoring devices of airborne trace elements and PAHs. In Biomonitoring of Air Pollution Using Mosses and Lichens, A Passive and Active Approach, State of the Art Research and Perspectives, Aničić Urošević, M., Vuković, G., Tomašević, M., Eds., Nova Science Publishers: New York 2016, chapter 7.

Desalme D., Binet P., Chiapusio G. (2013). Challenges in tracing the fate and effects of atmospheric polycyclic aromatic hydrocarbon deposition in vascular plants. Environ. Sci. Technol., 47, 3967–3981, DOI 10.1021/es304964b.

Di Palma A., Capozzi F., Spagnuolo V., Giordano S., Adamo P. (2017). Atmospheric particulate matter intercepted by moss-bags: relations to moss trace element uptake and land use. Chemosphere, 176, 361-368, DOI 10.1016/j.chemosphere.2017.02.120.

Dolegowska S., Migaszewski Z.M. (2011). PAH concentrations in the moss species Hylocomium splendens (Hedw.) B.S.G. and Pleurozium schreberi (Brid.) Mitt. From the Kielce area (south-central Poland). Ecotox. Environ. Safe., 74, 1636-1644, DOI 10.1016/j.ecoenv.2011.05.011.

Foan L., Domercq M., Bermejo R., Santamaría J.M., Simon V. (2015). Mosses as an integrating tool for monitoring PAH atmospheric deposition: Comparison with total deposition and evaluation of bioconcentration factors. A year-long case-study. Chemosphere, 119, 452–458, DOI 10.1016/j.chemosphere.2014.06.071.

Gerdol R., Bragazza L., Marchesini R., Medici A., Pedrini P., Benedetti S., Bovolenta A., Coppi S. (2002). Use of moss (Tortula muralis Hedw.) for monitoring organic and inorganic air pollution in urban and rural sites in northern Italy. Atmos. Environ., 20, 36, 4069-4075, DOI 10.1016/S1352-2310(02)00298-4.

González A.G., Pokrovsky O.S. (2014). Metal adsorption on mosses: Toward a universal adsorption model. J. Colloid Interface Sci., 415, 169-178, DOI 10.1016/j.jcis.2013.10.028

Gonzalez A.G., Pokrovsky O.S., Beike A.K., Reski R., Di Palma A., Adamo P., Giordano S., Fernandez J.A. (2016). Metal and proton adsorption capacities of natural and cloned Sphagnum mosses. J. Colloid Interface Sci., 461, 326-334, DOI 10.1016/j.jcis.2015.09.012

Harmens H., Foan L., Simon V., Mills G. (2013). Terrestrial mosses as biomonitors of atmospheric POPs pollution: A review. Environ. Pollut., 173, 245-254, DOI 10.1016/j.envpol.2012.10.005.

Keyte I., Wild E., Dent J., Jones K.C. (2009). Investigating the foliar uptake and within-leaf migration of phenanthrene by moss (*Hypnum cupressiforme*) using two-photon excitation microscopy with autofluorescence. Environ. Sci. Technol., 43(15), 5755–5761, DOI 10.1021/es900305c.

Kranner I., Beckett R., Hochman A., Nash T.H. (2008). Desiccation-tolerance in lichens: a review. Bryologist, 111(4), 576-593, DOI 10.1639/0007-2745-111.4.576.

Lehndorff E., Schwark L. (2004). Biomonitoring of air quality in the Cologne Conurbation using pine needles as a passive sampler – Part II: polycyclic aromatic hydrocarbons (PAH). Atmos. Environ., 38, 3793–3808, DOI 10.1016/j.atmosenv.2004.03.065.

Lichtenthaler H.K., Rinderle U. (1988). The role of chlorophyll fluorescence in the detection of stress conditions in plants. CRC Crit. Rev. Anal. Chem., 19 (1), S29–S85, DOI 10.1080/15476510.1988.10401466.

Loppi S., Pozo K., Estellano V.H., Corsolini S., Sardella G., Paoli L. (2015). Accumulation of polycyclic aromatic hydrocarbons by lichen transplants: Comparison with gas-phase passive air samplers. Chemosphere, 134, 39–43, DOI 10.1016/j.chemosphere.2015.03.066.

Maxwell K, Johnson G.N. (2000). Chlorophyll fluorescence – A practical guide. J. Exp. Bot., 51, 659-668, DOI 10.1093/jexbot/51.345.659.

Oliver M.J., Wood A.J., O'Mahony P. (1998). 'To dryness and beyond'- preparation for the dried state and rehydration in vegetative desiccation-tolerant plants. Plant Growth Regul., 24, 193–201, DOI 10.1023/A:1005863015130.

Ötvös E., Kozák I.O., Fekete J., Sharma V.K., Tuba Z. (2004). Atmospheric deposition of polycyclic aromatic hydrocarbons (PAHs) in mosses (*Hypnum cupressiforme*) in Hungary. Sci. Tot. Environ., 330, 89-99, DOI 10.1016/j.scitotenv.2004.02.019.

Proctor M.C.F. (2000). The Bryophyte Paradox: tolerance of desiccation, evasion of drought. Plant Ecol., 151(1), 41-49, DOI 10.1023/A:1026517920852.

Ravindra K., Sokhi R., Van Grieken R. (2008). Atmospheric polycyclic aromatic hydrocarbons: Source attribution, emission factors and regulation. Atmos. Environ., 42, 2895–2921, DOI 10.1016/j.atmosenv.2007.12.010.

Seel W.E., Baker N.R., Lee J.A. (1992). Analysis of the decrease in photosynthesis on desiccation of mosses from xeric and hydric environments. Physiol. Plant., 86, 451-458, DOI 10.1111/j.1399-3054.1992.tb01343.x

Sorbo S., Aprile G., Strumia S., Castaldo Cobianchi R., Leone A., Basile A. (2008). Trace element accumulation in Pseudevernia furfuracea (L.) Zopf exposed in Italy's so called Triangle of Death. Sci. Tot. Environ., 407, 647–654, DOI 10.1016/j.scitotenv.2008.07.071.

Spagnuolo V., Figlioli F., De Nicola F., Capozzi F., Giordano S. (2017). Tracking the route of phenanthrene uptake in mosses: an experimental trial. Sci. Total Environ., 575, 1066-1073, DOI 10.1016/j.scitotenv.2016.09.174.

Spagnuolo V., Giordano S., Pérez-Llamazares A., Ares A., Carballeira A., Fernández J.A., Aboal J.R. (2013). Distinguishing metal bioconcentration from particulate matter in moss tissue: Testing methods of removing particles attached to the moss surface. Sci. Total Environ., 463–464, 727-733, DOI 10.1016/j.scitotenv.2013.05.061.

Terzaghi E., Zacchello G., Scacchi M., Raspa G., Jones K.C., Cerabolini B., Di Guardo A. (2015). Towards more ecologically realistic scenarios of plant uptake modelling for chemicals: PAHs in a small forest. Sci.Tot. Environ., 505, 329–337, DOI 10.1016/j.scitotenv.2014.09.108.

Thomas W. (1986). Representativity of mosses as biomonitor organisms for the accumulation of environmental chemicals in plants and soils. Ecotoxicol. Environ. Saf., 11 (3), 339-346, DOI 10.1016/0147-6513(86)90106-5.

Tretiach M., Adamo P., Bargagli R., Baruffo L., Carletti L., Crisafulli P., Giordano S., Modenesi P., Orlando S., Pittao E. (2007). Lichen and moss bags as monitoring devices in urban areas. Part I: Influence of exposure on vitality. Environ. Pollut.,146, 380-391, DOI 1016/j.envpol.2006.03.046.

Tuba Z., Csintalan Z., Proctor M.C.F.(1996). Photosynthetic responses of a moss, Tortula ruralis ssp. ruralis, and the lichens Cladonia convoluta and C. furcata to water deficit and short periods of desiccation: a baseline study at present-day CO2 concentration. New Phytol., 133, 353-361, DOI 10.1111/j.1469-8137.1996.tb01902.x

# Chapter 5

# Multi-elemental profile and enviromagnetic analysis of moss transplants exposed indoors and outdoors in Italy and Belgium

**Maria Cristina Sorrentino[1], Karen Wuyts [2], Steven Joosen[3], Valentine K. Mubiana [3], Simonetta Giordano [1], Roeland Samson[2], Fiore Capozzi [1]*, Valeria Spagnuolo [1]**

*[1]Department of Biology, University of Naplesi Federico II, Campus Monte S. Angelo, Via Cinthia 4, 80126 Napoli, Italy*
*[2]Department of Bioscience Engineering, University of Antwerp, Campus Groenenborgerlaan 171, 2020 Antwerp, Belgium*
*[3]Department of Biology, University of Antwerp, Campus Groenenborgerlaan 171, 2020 Antwerp, Belgium*

**Abstract**

Air pollution represents one of the major concerns worldwide, fueled by the increasing urbanization and related PM production worsening air quality in open air as well as in confined environments. In the present work, exposure to atmospheric metal pollution was investigated in 20 paired indoor (I)-outdoor (O) sites located in two urban areas of Italy and Belgium, by chemical (ICP-MS) and magnetic (saturation isothermal remanent magnetization, SIRM) analyses of *Hypnum cupressiforme* moss exposed in bags. After 12 weeks, the elemental profiles of the moss material exposed in the two countries largely overlapped, except for some elements which specifically accumulated in Belgium (Ag, As, Cd, Mo, Pb and Sb) and in Italy (Ca, Mg, Co, Cr, Sr, Ti and U). Element concentrations were higher in moss exposed outdoors, with the Italian sites mostly showing a terrigenous footprint, and the Belgian sites mostly affected by elements of environmental concern. The Indoor/Outdoor ratios (mostly lower than 0.75) indicated indoor pollution as strongly affected by outdoor pollution, although specific elements could be of indoor origin or magnified in indoor environments (e.g., Al, Ag, Cd and Co). In line with the chemical analysis, the SIRM signal was significantly higher in outdoor than indoor moss material. A positive, significant correlation was observed between SIRM and several accumulated elements indicating SIRM analysis as a powerful tool to predict the level of metal pollution. Moss bags were confirmed as a useful and versatile tool to highlight metal contamination even in confined environments, an essential prerogative in the perspective of the evaluation of the total exposure risk for humans to these pollutants.

**Key words:** air metal pollution; *Hypnum cupressiforme*; indoor pollution; SIRM analysis; moss bags.

*Corresponding author: fiore.capozzi@unina.it

## 1. Introduction

During the last three decades, the World is experiencing an extraordinary growth, especially in the urban human population, which is expected to increase 2.3% per year up to 2030 (Brockherhoff, 2000; United Nations, 2018; UNFPA, 2004). Population growth coupled with rapid economic development involves an increase in energy consumption and in environmental pollution (Gurjar et al., 2012). This growing urbanization, and related particulate matter (PM) emission, has detrimental consequences for urban air quality (Hofman et al., 2017; Iodice et al., 2016; Lee et al., 2020).

Urban atmospheric pollution levels vary both spatially and temporally, depending on the distance from pollution sources, city topology, traffic intensity and its dynamics, meteorological conditions and the day-by-day, or even within-day, fluctuations; therefore, air quality assessment is intrinsically challenging because it must consider both spatial and temporal dynamics (Iodice et al., 2016).

Many researchers have been using biological material for air quality monitoring, in particular PM pollution (e.g., Conti and Cecchetti, 2001; Kardel et al., 2010, 2011; Giordano et al., 2013; Vuković et al., 2015a), as the direct measurement of atmospheric PM concentration is expensive and practically impossible at high spatial resolution (Kardel et al., 2018). Among biomonitors, plants play an important role in urban environments, due to their applicative versatility; in fact, the possibility of using both plants already present at the area of interest and transplants, allows to realize very flexible experimental designs, which can well fit to various topological features and can elucidate both spatial and temporal dynamics of airborne pollutants (Jiang et al., 2018; Iodice et al., 2016). Urban environments can be considered a multiphase system, in which continuous exchanges exist among their components (i.e., air, soil, plants, water bodies). They embrace both outside locations (i.e., parks, roads, industrial and commercial settlements) and the indoor environments, where people live and spend most time, also due to the quickly changing mobility habits imposed by the recent Covid-19 pandemic. There is a lack of knowledge in this regard, since most published papers investigating air pollution quality indoors are based on active samplers (e.g., Huang et al., 2007; Miler and Gosar, 2019). The transplant approach has been applied to detect metal indoor pollution in some previous works (Al-Radady et al., 1993, 1994; Motyka et al., 2013), as well as outdoor metal pollution near houses (Rivera et al., 2011). A comparison between indoor and outdoor pollution, to try disentangling the specific contamination sources at the same sites, was attempted in only very few works (Canha et al., 2014; Capozzi et al., 2019; Zechmeister et al., 2020). Previous

works carried out both by biomonitors and monitoring devices, evidenced that indoor environment is largely affected by outdoors (e.g., Capozzi et al., 2019) and that habits may influence indoor pollution (e.g., Liu et al., 2018).

Magnetic measurements of biological material, mainly by saturation isothermal remanent magnetization (SIRM) have been increasingly used as a simple, robust and cost-effective method to investigate the load of PM deposited on plant biomonitors and predict atmospheric metal pollution (Hofman et al., 2017). Particularly the combination of magnetic analyses with chemical analysis techniques on exposed matrices provides insight into PM composition and creates opportunities for source apportionment and PM source profiling (Kardel et al., 2018; Castanheiro et al., 2020). SIRM was already successful applied in moss bags exposed outdoors (e.g., Vuković et al., 2015a), but, to our knowledge, the only magnetic analysis on biological matrices exposed indoors was performed by Van Dyck et al. (2019), who measured SIRM in strawberry plant leaves exposed in houses; however, no chemical analysis and outdoor comparison was carried out.

The aim of this work is to disentangle indoor/outdoor contamination sources and to investigate the influence of home habits and meteorology on the dependence of indoor pollution on outdoor pollution, by using SIRM and chemical analysis of moss transplants. Therefore, the use of SIRM (combined to chemical analysis) on moss transplants exposed in paired indoor/outdoor sites represents the novelty of the present work. A further innovation is the discussion of the meteorological variables as factors affecting indoor pollution.

Based on all above, i) we investigated, by chemical and magnetic analyses of exposed moss bags, atmospheric metal inputs in paired indoor-outdoor sites; ii) we verified, under the hypothesis that meteorology can affect the results of this comparison, the effectiveness of the methodology in the urban areas of two European countries, Italy and Belgium, characterized by different climate conditions (Mediterranean vs. temperate maritime); iii) we verified the consistency of the SIRM signal to predict metal accumulation in moss also in indoor environment.

## 2 Materials and Methods

### 2.1 Moss material, study area and exposure design

The moss *Hypnum cupressiforme* Hedw. collected in Italy at the Taburno-Camposauro Regional Park (1000 m a.s.l. - 41.105094° N, 14.593559° E) was used as plant material for the

experiment here described. For moss and bags preparation, the procedure reported in Capozzi et al (2016) was followed.

The study areas included the metropolitan area of Naples in the Campania region (south Italy), featured by a Mediterranean climate, and the region of Flanders (north Belgium), characterized by a temperate maritime climate. The experimental design for both countries involved the selection of ten urban sites, each consisting of one pair of indoor /outdoor environments (Table S1), yielding 20 exposure locations per country, and 40 in total. All Italian sites were located in Naples and labelled as NAP, while the Belgian sites were located in the cities of Antwerp (8), Ghent (1) and Lier (1) and were labelled as ANT. All the houses, selected on a voluntary basis, were located between 0 and 50 m from the closest vehicle-accessible street.

Table S1 – Site coordinates and supplementary variables characterizing indoor environments. Legend - Smokers: presence (1) or absence (0); Traffic in neighboring streets (low to high level, 1 to 3); Fireplace: presence (1) or absence (0); Building material: tuff (t), reinforced concrete (c), brick (b); Residence time: daily hours spent at home on average (up to 12h, 1, 12-18h, 2, 18-24h, 3); Ventilation: natural (a), only conditioned (b), combined (c); B/H: balcony and windows/house surface ratio (%)

| Sites | Latitude (N) | Longitude (E) | Smokers | Traffic | Fireplace | Building | Res. Time | Ventilation | W/H (%) | Balconies | Windows | surface |
|---|---|---|---|---|---|---|---|---|---|---|---|---|
| **ANT1** | 51.051515° | 3.660243° | 0 | 2 | 0 | b | 1 | c | 9% | 2 | 4 | 120 |
| **ANT2** | 51.134642° | 4.573090° | 0 | 2 | 0 | b | 2 | a | 3% | 1 | 1 | 130 |
| **ANT4** | 51.187171° | 4.393914° | 0 | 2 | 0 | b | 1 | c | 18% | 2 | 7 | 85 |
| **ANT5** | 51.214389° | 4.455977° | 0 | 3 | 0 | b | 2 | a | 14% | 1 | 6 | 85 |
| **ANT6** | 51.013136° | 4.467899° | 0 | 1 | 0 | c | 1 | a | 7% | 9 | 0 | 340 |
| **ANT7** | 51.185541° | 4.424307° | 0 | 2 | 0 | b | 1 | a | 10% | 1 | 4 | 89 |
| **ANT8** | 51.198290° | 4.430117° | 0 | 2 | 0 | b | 1 | a | 19% | 1 | 10 | 90 |
| **ANT9** | 51.209980° | 4.423611° | 0 | 3 | 0 | b | 1 | a | 4% | 0 | 2 | 85 |
| **ANT10** | 51.176678° | 4.346181° | 0 | 2 | 1 | b | 2 | a | 11% | 1 | 13 | 200 |
| **NAP1** | 40.846921° | 14.331294° | 0 | 2 | 1 | b | 2 | a | 9% | 8 | 0 | 180 |
| **NAP2** | 40.832139° | 14.206328° | 0 | 2 | 0 | c | 3 | c | 13% | 4 | 2 | 100 |
| **NAP3** | 40.860015° | 14.218848° | 0 | 2 | 0 | c | 2 | a | 15% | 6 | 0 | 79 |
| **NAP4** | 40.872807° | 14.237239° | 0 | 2 | 0 | c | 3 | a | 13% | 5 | 4 | 140 |
| **NAP5** | 40.844195° | 14.221569° | 1 | 3 | 0 | c | 1 | c | 12% | 4 | 2 | 110 |
| **NAP6** | 40.845079° | 14.241730° | 0 | 1 | 0 | t | 1 | a | 18% | 9 | 0 | 100 |
| **NAP7** | 40.838587° | 14.233176° | 0 | 2 | 0 | c | 3 | a | 17% | 10 | 0 | 120 |
| **NAP8** | 40.833406° | 14.231941° | 0 | 3 | 0 | t | 2 | a | 5% | 4 | 3 | 270 |
| **NAP9** | 40.862502° | 14.267587° | 1 | 2 | 0 | t | 2 | c | 11% | 8 | 0 | 150 |
| **NAP10** | 40.859425° | 14.248278° | 1 | 3 | 0 | t | 2 | a | 8% | 5 | 0 | 132 |

At each exposure location, moss bags were simultaneously exposed in triplicate (each bag containing 500 mg moss) for a 12-weeks period (March-June 2019). Indoors, the bags were exposed in the bedroom or living room, at 2 m above the floor. Outdoors, the moss-bags were exposed at the first to third floor (according to Capozzi et al., 2016), fixed to a stick placed on the windows facing the street side with no protection against rain or wind. Overall, 60 moss bags were employed for each country: 30 exposed indoors and 30 outdoors. Unexposed additional moss samples (n=4) were used as control (labeled as BL), to assess the pre-exposure element contents.

Meteorological conditions, as well as PM and gaseous pollutants recorded in the two study areas were considered in the present study (Table S2). For NAP sites, these data were obtained by the Regional Agency for Environmental Protection. As for the ANT sites, meteorological data were provided by the Royal Meteorological Institute of Belgium (www.meteo.be), while air quality data from an urban background air quality monitoring station (42R801, Plantin en Moretuslei, Antwerp, operated by the Flanders Environment Agency) were obtained from the Belgian Interregional Environment Agency (IRCEL - CELINE; www.irceline.be)

To take into consideration the different lifestyle running in the selected houses, a questionnaire was proposed to people involved in the study, regarding the presence of smokers, the number of windows and the house surface area, heating, ventilation system (natural, i.e., air flux through opened windows, vs. conditioned ventilation), residence time (i.e., how many hours per day people stay on average at home) and traffic in neighboring streets (Table S1). Due to the loss of moss bags in one site of Flanders (ANT 3), all the analyses are based on 19 sites.

Table S2. Data on the weather condition and aero-dispersed pollutants in Naples (NAP) and Flanders (ANT) during the exposure period. *Data reported as monthly averages. Meteorological data for ANT are provided by the Royal Meteorological Institute of Belgium for the reference station at Ukkel (www.meteo.be); air quality data (mean ± SD hourly concentrations) are provided by Belgian Interregional Environment Agency (IRCEL - CELINE; www.irceline.be) from the urban background air quality monitoring station 42R801 (Plantin en Moretuslei, Antwerp). Meteorological and aero-dispersed pollutants data for NAP were provided by the Campania Region and by the Regional Agency for Environmental protection. (http://www.agricoltura.regione.campania.it/meteo/agrometeo.htm and https://www.arpacampania.it/qualita-dell-aria).

| | NAP | | | | ANT | | | |
|---|---|---|---|---|---|---|---|---|
| | **March** | **April** | **May** | **June** | **March** | **April** | **May** | **June** |
| | **Weather condition** | | | | | | | |
| **Mean Temperature* (°C)** | 12.9 | 14.9 | 15.7 | 25.3 | 8.5 | 11.0 | 11.9 | 18.5 |
| **Relative humidity* (%)** | 66 | 66 | 74 | 62 | 78 | 66 | 73 | 72 |
| **Wind speed* (km $h^{-1}$)** | 12.2 | 9.9 | 10.0 | 8.5 | 16.2 | 11.9 | 10.4 | 11.2 |
| **Rainy days** | 7 | 13 | 17 | 2 | 18 | 8 | 18 | 12 |
| **Rain amount (mm)** | 26.0 | 71.2 | 32.4 | 18.3 | 85.5 | 36.0 | 55.0 | 98.1 |
| | **Pollutants*** | | | | | | | |
| **$NO_2$ µg/$m^3$** | 51±31 | 55±29 | 44±21 | 53±31 | 30±18 | 34±18 | 26±15 | 25±14 |
| **PM10 µg/$m^3$** | 26±20 | 22±14 | 20±10 | 37±20 | 26 ±17 | 32±16 | 24±13 | 23±12 |
| **PM2.5 µg/$m^3$** | 13±9 | 12±9 | 9±6 | 19±9 | 15±14 | 19±13 | 15±12 | 12±8 |

## 2.2 Magnetic analysis

After exposure, the moss bags were transported to the lab in plastic bags and were dried in oven (Memmert) at 40 °C for 72 h. The three replicates were taken for each exposure site and weighed to verify eventual material loss. The moss was tightly packed in transparent film to avoid any possible movement during the analysis and placed inside a plastic container with a volume of 6.7 $cm^3$.

All the samples were individually magnetized in a direct current (DC) field of 1 T with a Molspin pulse magnetizer (Molspin Ltd, UK) (Kardel et al., 2011, Hofman et al., 2017). Immediately after, the isothermal remanent magnetization (IRM) of the samples (A $m^{-1}$) was measured twice using a JR-6 spinner magnetometer (AGICO, Czech Republic) with high sensitivity (2.4 $10^{-6}$ A $m^{-1}$). The instrument was calibrated with a calibration standard and the

measured values were corrected for the sample holder with blanks of pots with a similar amount of cling film. Based on Hofman et al. (2017) this IRM at 1 T is taken to be the saturation isothermal remanent magnetization (SIRM) of each measured sample. The methodology is described in detail by Castanheiro et al. (2020). The SIRM was normalized for post-exposure moss dry mass (g) and the size of the plastic container, obtaining mass-normalized SIRM values in $10^{-6}$ A $m^2$ $kg^{-1}$.

### 2.3 Chemical analysis

The concentrations of 30 elements (Al, Ag, As, Be, Ca, Cd, Co, Cr, Cu, Fe, Hg, K, Mg, Mn, Mo, Na, Ni, Pb, Pd, Rb, Rh, Sb, Se, Si, Sr, Ti, Tl, U, V, Zn) were determined using HR-ICP-MS, except for Ca, K, Mg and Na which required the use of ICP-OES (inductively coupled plasma optical emission spectrometry). Following the non-destructive SIRM measurements, the mosses were recovered and weighed before proceeding to acid digestion in glass tubes with 2 ml of $HNO_3$ and 6 ml of HCl at 100°C, over-night. After this step, 0.5 ml of $H_2O_2$ was added for digestion into a microwave digester (Discover SP-D, CEM). Parameters used for digestion were temperature 180°C, ramp time 5 minutes and hold time 5 minutes. The digested solution was transferred from glass to plastic tubes and deionized water was added until the volume of 40 ml. For quality control of the analysis, the certified reference plant material (Certified Reference Material BCR® – 679, white cabbage) was analyzed in parallel with samples. For the elements indicated in the certified material, the percentages of recovery were in the range of acceptability, specifically from 80% to 105% (Ca 99.63%, Cd 80.15%, Cr 84.80%, Cu 91.55%, Fe 95.13%, Mg 89.28%, Mn 92 %, Ni 99.35%, Sr 85.69%, Zn 88.49%), and below 80% for As (60.42%). The data were normalized considering the dilution factor and the mass of each sample.

### 2.4 Data Analyses

The data were processed following these steps: 1) assessment of element enrichment in the exposed moss; 2) exploratory Principal Component Analysis (PCA) in order to highlight the general trend provided by the data; 3) Generalized Linear Model (GLM) applied to each moss element content and to the SIRM to distinguish among the different factors (Country and Environment, as specified below); T-test and GLM were also applied on the PCA location scores and T-test also to assess the differences between the I/O ratios; 4) In order to assess the degree of correlation between moss element contents exposed in the two environments and between the SIRM data with element contents, we applied the Spearman's rank correlation test.

The threshold to determine element accumulation in each sample was fixed in the limit of quantification of the technique (LOQT), calculated from the initial concentrations as follows: xCi + 2sCi, where xCi is the mean value of the initial concentration in unexposed moss samples (n = 4) for each element determined, and sCi is the corresponding standard deviation (Couto et al., 2004 as modified in Ares et al., 2015). We performed Principal Component Analysis (PCA) to explore the elemental composition of moss samples and the SIRM signal in relation to different environments and sites. Environmental descriptors (i.e., building material, presence of fireplace and smokers, residence time, ratio between balcony area and home surface, traffic load and ventilation type) characterizing the indoor sites were plotted as supplementary variables.

A general linearized model (GLM) was applied to each moss element content and to the SIRM (considered as dependent variable) to test the main and the interactive effects of country (fixed factor, two levels "ANT" and "NAP") and environments (fixed factor, two levels "Indoor" or "Outdoor"). T-test and GLM were applied on the PCA location scores (i.e., the first 3 factors for indoor samples; the first 2 factors for outdoor samples and the first two factors of the PCA in Figure 1 for which we maintained the same design previously described for the GLMs applied to element content and SIRM). The Spearman's rank correlation coefficient was calculated to assess the correlation between moss element contents exposed in the two environments and between the SIRM data with element contents. T-test was also used to assess the significance of the differences between the I/O ratios in the two countries for each element. Because of the multiple comparisons, we used false discovery rate (FDR) adjusted p-values using Benjamini-Hochberg's correction. Basic statistics and normalization of the data were processed using Microsoft Excel, statistical tests were performed using STATISTICA software ver. 8.0 (StatSoft, Inc. 2008).

## 3 Results

### 3.1 SIRM

The saturation isothermal remanent magnetization (SIRM) was on average 3141 ±183 μA $m^2$ $kg^{-1}$in pre-exposed moss and 4316 ±169 in exposed moss samples, the latter ranging between 3724 μA $m^2$ $kg^{-1}$ (ANT7-IN) and 6495 μA $m^2$ $kg^{-1}$ (NAP1-OUT) (Table 1). The SIRM signals in indoor and outdoor environments were generally comparable in order of magnitude, but I/O ratios of SIRM ranged between 0.61 and 1.23 and indoor and outdoor SIRM values did not significantly correlate (p=0.491 for all locations, 0.122 for NAP and 0.570 for ANT).

Nonetheless, the GLM applied to the SIRM data revealed a significant effect of both fixed factors (p= 0.030 and p=0.002 for country and environment, respectively) but not of their interaction (p=0.220). Specifically, both environments in NAP sites showed on average SIRM values significantly higher than ANT ones. With an average I/O ratio of 0.94, the outdoor sites were characterized by values higher than the corresponding indoor sites, regardless of the country. Outdoor SIRM was not significantly influenced by estimated traffic class (p=0.517), while indoor SIRM was marginally significantly affected by traffic class (p=0.053), but not by the presence of smokers or by ventilation. The I/O ratio on SIRM could not be explained by country (p=0.668) or any of the variables from the questionnaire (p>0.05). Significant correlations were observed both indoors and outdoors between SIRM and several accumulated elements (Table 2), among which the highly magnetizable Co, Ni and Cu.

Table 1 – Mean ± standard deviation (n=3) of the SIRM values ($\mu A\ m^2\ kg^{-1}$) for each site. The SIRM value for the pre-exposed moss was: 3141±183 (n=4).

| | IN | OUT | | IN | OUT |
|---|---|---|---|---|---|
| ANT1 | 4713 ± 107 | 4501 ± 83 | NAP1 | 3931 ± 80 | 6495 ± 259 |
| ANT2 | 4920 ± 131 | 4345 ± 162 | NAP2 | 3756 ± 142 | 4986 ± 165 |
| ANT3 | - | - | NAP3 | 4698 ± 118 | 5761 ± 320 |
| ANT4 | 3996 ± 112 | 4054 ± 161 | NAP4 | 4162 ± 239 | 5818 ± 182 |
| ANT5 | 5121 ± 268 | 5098 ± 202 | NAP5 | 4341 ± 87 | 5050 ± 148 |
| ANT6 | 5287 ± 128 | 4945 ± 247 | NAP6 | 5173 ± 219 | 4267 ± 392 |
| ANT7 | 3724 ± 240 | 5314 ± 134 | NAP7 | 5568 ± 101 | 4600 ± 195 |
| ANT8 | 3855 ± 116 | 4612 ± 69 | NAP8 | 6141 ± 283 | 5008 ± 283 |
| ANT9 | 4627 ± 103 | 4452 ± 196 | NAP9 | 4291 ± 128 | 5166 ± 187 |
| ANT10 | 4905 ± 138 | 6351 ± 102 | NAP10 | 4972 ± 316 | 5245 ± 132 |

Table 2 - Correlation between accumulated elements and SIRM; R is Spearman correlation coefficient and p indicates significance level. Significant correlation and relative p value highlighted in red.

| | ANT | | | | NAP | | | |
|---|---|---|---|---|---|---|---|---|
| | IN | | OUT | | IN | | OUT | |
| | R* | p | R | p | R | p | R | p |
| **Al** | 0.565 | 0.002 | 0.556 | 0.003 | 0.352 | 0.057 | 0.430 | 0.018 |
| **Ag** | 0.496 | 0.008 | 0.457 | 0.017 | 0.503 | 0.005 | 0.161 | 0.395 |
| **Ca** | -0.016 | 0.935 | 0.054 | 0.790 | -0.123 | 0.516 | 0.470 | 0.009 |
| **Cd** | 0.297 | 0.132 | 0.425 | 0.027 | 0.152 | 0.423 | -0.057 | 0.766 |
| **Co** | 0.789 | <0.001 | 0.566 | 0.002 | 0.576 | 0.001 | 0.375 | 0.041 |
| **Cu** | 0.555 | 0.003 | 0.418 | 0.030 | 0.628 | <0.001 | 0.229 | 0.224 |
| **Mg** | 0.708 | <0.001 | 0.468 | 0.014 | 0.518 | 0.003 | 0.479 | 0.007 |
| **Mn** | 0.651 | <0.001 | 0.468 | 0.014 | 0.079 | 0.677 | 0.629 | <0.001 |
| **Ni** | 0.691 | <0.001 | 0.473 | 0.013 | 0.712 | 0.000 | 0.320 | 0.085 |
| **Pb** | 0.480 | 0.011 | 0.415 | 0.032 | 0.543 | 0.002 | 0.459 | 0.011 |
| **Sb** | 0.719 | <0.001 | 0.422 | 0.028 | 0.698 | 0.000 | -0.204 | 0.281 |
| **Si** | -0.255 | 0.199 | 0.216 | 0.280 | 0.031 | 0.871 | 0.200 | 0.289 |
| **Sr** | 0.621 | 0.001 | 0.411 | 0.033 | 0.373 | 0.043 | 0.497 | 0.005 |
| **Ti** | 0.069 | 0.732 | 0.228 | 0.253 | 0.251 | 0.181 | 0.087 | 0.649 |
| **U** | 0.537 | 0.004 | 0.640 | <0.001 | 0.631 | <0.001 | 0.331 | 0.074 |
| **Zn** | 0.009 | 0.964 | 0.268 | 0.177 | 0.426 | 0.019 | 0.319 | 0.086 |

### 3.2 Element analysis

The chemical contents of moss exposed at each site (Table S3) highlighted that post-exposure contents were overall higher in mosses exposed outdoors in both countries.

Table S3 –Mean (n=3) and SD of the chemical contents (mg $Kg^{-1}$ DW) of unexposed moss (T0; n=4) and post-exposure moss (n=3) from each of the exposure sites in Antwerp (ANT) and Naples (NAP), indoors (IN) and outdoors (OUT)

| SITE | STATISTIC | Al | Ag | As | Be | Ca | Cd | Co | Cr | Cu | Fe | Hg | K | Mg | Mo | Mn | Na | Ni | Pb | Pd | Rb | Rh | Sb | Se | Si | Sr | Ti | Tl | U | V | Zn |
|---|---|---|---|---|---|---|---|---|---|---|---|---|---|---|---|---|---|---|---|---|---|---|---|---|---|---|---|---|---|---|---|
| **T0** | Mean | 5587 | 0.05 | 0.87 | 0.51 | 1874 | 0.06 | 0.82 | 2.38 | 10.63 | 2150 | 0.12 | 1849 | 887 | 0.32 | 56 | 8258 | 2.40 | 4.37 | 0.01 | 6.94 | 0.00 | 0.31 | 0.59 | 1922 | 18 | 23 | 0 | 0 | 7 | 24 |
| | SD | 171 | 0.01 | 0.04 | 0.08 | 100 | 0.02 | 0.04 | 0.05 | 0.12 | 59 | 0.00 | 70 | 45 | 0.02 | 1 | 349 | 0.09 | 0.21 | 0.00 | 0.45 | 0.00 | 0.02 | 0.02 | 54 | 1 | 1 | 0 | 0 | 0 | 2 |
| | LOQt | 5929 | 0.07 | 0.95 | 0.67 | 2074 | 0.10 | 0.91 | 2.48 | 10.87 | 2269 | 0.13 | 1988 | 977 | 0.36 | 57 | 8956 | 2.58 | 4.80 | 0.02 | 7.83 | 0.00 | 0.36 | 0.63 | 2030 | 20 | 24 | 0 | 0 | 8 | 27 |
| ANT1-IN | Mean | 6170 | 0.04 | 0.85 | 0.28 | 2068 | 0.03 | 1.45 | 2.09 | 9.40 | 2067 | 0.11 | 1999 | 967 | 0.27 | 54 | 8605 | 2.37 | 3.87 | 0.01 | 3.67 | 0.00 | 0.25 | 0.53 | 2259 | 14 | 25 | 0 | 0 | 6 | 22 |
| | SD | 2100 | 0.01 | 0.12 | 0.07 | 187 | 0.02 | 1.10 | 0.26 | 0.21 | 312 | 0.01 | 144 | 91 | 0.05 | 6 | 328 | 0.05 | 0.23 | 0.01 | 0.65 | 0.00 | 0.03 | 0.53 | 49 | 1 | 1 | 0 | 0 | 1 | 1 |
| ANT1-OUT | Mean | 5756 | 0.17 | 0.88 | 0.21 | 3601 | 0.06 | 0.97 | 2.37 | 15.20 | 2265 | 0.10 | 1695 | 1201 | 0.38 | 64 | 5379 | 2.55 | 6.03 | 0.00 | 2.38 | 0.00 | 1.51 | 0.19 | 2562 | 16 | 29 | 0 | 0 | 6 | 141 |
| | SD | 948 | 0.02 | 0.14 | 0.10 | 254 | 0.03 | 0.13 | 0.77 | 0.43 | 533 | 0.01 | 134 | 86 | 0.04 | 6 | 221 | 0.29 | 0.21 | 0.01 | 1.14 | 0.00 | 0.17 | 0.33 | 442 | 2 | 4 | 0 | 0 | 2 | 34 |
| ANT2-IN | Mean | 5696 | 0.05 | 0.82 | 0.31 | 1982 | 0.04 | 0.70 | 1.69 | 8.53 | 1856 | 0.10 | 1919 | 913 | 0.27 | 48 | 8341 | 2.10 | 3.75 | 0.01 | 3.59 | 0.00 | 0.26 | 0.05 | 1987 | 14 | 22 | 0 | 0 | 5 | 20 |
| | SD | 1431 | 0.01 | 0.06 | 0.02 | 266 | 0.02 | 0.05 | 0.07 | 0.22 | 24 | 0.01 | 155 | 106 | 0.01 | 0 | 509 | 0.19 | 0.36 | 0.01 | 0.23 | 0.00 | 0.02 | 0.09 | 76 | 1 | 1 | 0 | 0 | 0 | 1 |
| ANT2-OUT | Mean | 4745 | 0.05 | 0.81 | 0.22 | 3354 | 0.12 | 0.84 | 2.32 | 15.45 | 1978 | 0.10 | 1598 | 1127 | 0.31 | 58 | 4740 | 3.01 | 9.52 | 0.00 | 1.65 | 0.00 | 1.46 | 0.00 | 2596 | 16 | 26 | 0 | 0 | 5 | 90 |
| | SD | 411 | 0.01 | 0.13 | 0.01 | 365 | 0.02 | 0.04 | 0.47 | 1.01 | 123 | 0.00 | 73 | 38 | 0.07 | 1 | 611 | 0.69 | 0.83 | 0.01 | 0.83 | 0.00 | 0.29 | 0.00 | 35 | 0 | 0 | 0 | 0 | 0 | 31 |
| ANT4-IN | Mean | 6337 | 0.04 | 0.81 | 0.26 | 1822 | 0.03 | 0.74 | 1.68 | 9.12 | 1865 | 0.11 | 1742 | 828 | 0.25 | 48 | 7321 | 2.21 | 3.89 | 0.00 | 2.44 | 0.00 | 0.24 | 0.01 | 2367 | 15 | 25 | 0 | 0 | 5 | 22 |
| | SD | 2996 | 0.00 | 0.28 | 0.10 | 445 | 0.02 | 0.19 | 0.59 | 0.73 | 539 | 0.04 | 303 | 187 | 0.05 | 12 | 802 | 0.35 | 0.77 | 0.00 | 1.57 | 0.00 | 0.04 | 0.03 | 235 | 4 | 2 | 0 | 0 | 2 | 1 |
| ANT4-OUT | Mean | 5992 | 0.18 | 1.23 | 0.23 | 5052 | 0.56 | 1.26 | 2.39 | 18.18 | 2168 | 0.10 | 1711 | 1129 | 0.27 | 58 | 4187 | 3.11 | 15.75 | 0.01 | 1.76 | 0.00 | 1.80 | 0.00 | 2643 | 18 | 28 | 0 | 0 | 5 | 50 |
| | SD | 1811 | 0.03 | 0.20 | 0.11 | 2498 | 0.48 | 0.15 | 0.30 | 3.08 | 749 | 0.01 | 602 | 105 | 0.00 | 15 | 1612 | 0.31 | 5.71 | 0.01 | 1.88 | 0.00 | 0.32 | 0.00 | 218 | 2 | 4 | 0 | 0 | 2 | 13 |
| ANT5-IN | Mean | 7136 | 0.04 | 0.97 | 0.38 | 1971 | 0.05 | 0.82 | 1.80 | 9.15 | 2117 | 0.11 | 2004 | 977 | 0.29 | 55 | 8142 | 2.21 | 4.23 | 0.01 | 3.73 | 0.00 | 0.33 | 0.00 | 2438 | 18 | 26 | 0 | 0 | 6 | 21 |
| | SD | 273 | 0.01 | 0.16 | 0.13 | 136 | 0.01 | 0.14 | 0.39 | 0.51 | 517 | 0.01 | 86 | 45 | 0.03 | 13 | 670 | 0.29 | 0.50 | 0.00 | 0.99 | 0.00 | 0.06 | 0.00 | 252 | 2 | 1 | 0 | 0 | 1 | 1 |
| ANT5-OUT | Mean | 6442 | 0.10 | 0.92 | 0.21 | 3308 | 0.18 | 0.92 | 2.35 | 20.86 | 2226 | 0.11 | 1856 | 1152 | 0.56 | 61 | 6547 | 2.66 | 12.34 | 0.01 | 1.53 | 0.00 | 2.93 | 0.00 | 2708 | 23 | 28 | 0 | 0 | 5 | 93 |
| | SD | 1702 | 0.02 | 0.07 | 0.04 | 173 | 0.05 | 0.10 | 0.55 | 1.28 | 373 | 0.01 | 228 | 93 | 0.08 | 10 | 1278 | 0.13 | 0.50 | 0.01 | 1.29 | 0.00 | 0.72 | 0.00 | 52 | 3 | 1 | 0 | 0 | 1 | 10 |
| ANT6-IN | Mean | 6317 | 0.03 | 0.71 | 0.22 | 2344 | 0.03 | 0.65 | 1.71 | 8.25 | 1979 | 0.10 | 1879 | 894 | 0.20 | 54 | 8128 | 1.85 | 4.67 | 0.00 | 1.95 | 0.00 | 0.22 | 0.05 | 2458 | 18 | 26 | 0 | 0 | 5 | 21 |
| | SD | 714 | 0.01 | 0.12 | 0.05 | 473 | 0.02 | 0.07 | 0.33 | 0.49 | 267 | 0.01 | 111 | 46 | 0.03 | 6 | 194 | 0.16 | 0.19 | 0.00 | 1.49 | 0.00 | 0.03 | 0.09 | 414 | 1 | 3 | 0 | 0 | 1 | 0 |
| ANT6-OUT | Mean | 6661 | 0.06 | 0.66 | 0.17 | 2918 | 0.09 | 0.69 | 1.88 | 12.03 | 1872 | 0.08 | 1535 | 1062 | 0.18 | 55 | 4673 | 2.26 | 8.12 | 0.01 | 0.42 | 0.00 | 1.48 | 0.00 | 2775 | 16 | 28 | 0 | 0 | 4 | 34 |
| | SD | 1348 | 0.01 | 0.07 | 0.04 | 214 | 0.01 | 0.04 | 0.06 | 0.81 | 76 | 0.00 | 13 | 43 | 0.01 | 4 | 152 | 0.21 | 0.53 | 0.01 | 0.10 | 0.00 | 0.38 | 0.00 | 267 | 0 | 3 | 0 | 0 | 0 | 1 |
| ANT7-IN | Mean | 5979 | 0.03 | 0.72 | 0.29 | 2017 | 0.04 | 0.69 | 1.71 | 8.20 | 2042 | 0.10 | 1801 | 864 | 0.21 | 55 | 7415 | 1.88 | 4.76 | 0.01 | 4.01 | 0.00 | 0.24 | 0.23 | 2255 | 17 | 28 | 0 | 0 | 5 | 19 |
| | SD | 969 | 0.00 | 0.14 | 0.04 | 451 | 0.02 | 0.11 | 0.39 | 0.29 | 465 | 0.01 | 209 | 119 | 0.04 | 8 | 594 | 0.24 | 0.45 | 0.01 | 0.74 | 0.00 | 0.03 | 0.25 | 702 | 1 | 8 | 0 | 0 | 1 | 1 |
| ANT7-OUT | Mean | 7023 | 0.08 | 0.91 | 0.23 | 2467 | 0.10 | 0.68 | 1.68 | 13.29 | 1779 | 0.11 | 2003 | 1000 | 0.32 | 50 | 7894 | 2.13 | 7.71 | 0.01 | 2.46 | 0.00 | 2.05 | 0.00 | 2427 | 17 | 25 | 0 | 0 | 5 | 31 |
| | SD | 1038 | 0.01 | 0.11 | 0.02 | 181 | 0.03 | 0.08 | 0.20 | 1.36 | 149 | 0.01 | 169 | 100 | 0.02 | 4 | 408 | 0.14 | 0.77 | 0.01 | 0.29 | 0.00 | 0.27 | 0.00 | 180 | 1 | 2 | 0 | 0 | 0 | 1 |
| ANT8-IN | Mean | 8189 | 0.03 | 0.58 | 0.22 | 2290 | 0.03 | 0.62 | 1.41 | 7.86 | 1650 | 0.09 | 1830 | 895 | 0.23 | 46 | 7713 | 1.78 | 4.06 | 0.01 | 3.02 | 0.00 | 0.24 | 0.00 | 2504 | 15 | 26 | 0 | 0 | 4 | 19 |
| | SD | 2788 | 0.02 | 0.10 | 0.12 | 514 | 0.01 | 0.15 | 0.24 | 0.33 | 286 | 0.01 | 177 | 134 | 0.04 | 3 | 286 | 0.31 | 0.30 | 0.01 | 0.53 | 0.00 | 0.03 | 0.00 | 362 | 1 | 3 | 0 | 0 | 1 | 0 |
| ANT8-OUT | Mean | 8232 | 0.12 | 0.64 | 0.17 | 11314 | 1.27 | 0.71 | 2.06 | 16.19 | 2019 | 0.08 | 853 | 1086 | 0.18 | 49 | 661 | 2.60 | 13.96 | 0.01 | 0.52 | 0.00 | 1.32 | 0.00 | 3340 | 26 | 38 | 0 | 0 | 4 | 61 |
| | SD | 1124 | 0.01 | 0.09 | 0.11 | 2407 | 0.47 | 0.07 | 0.44 | 2.05 | 490 | 0.01 | 343 | 190 | 0.02 | 11 | 910 | 0.09 | 1.76 | 0.01 | 0.17 | 0.00 | 0.32 | 0.00 | 758 | 3 | 13 | 0 | 0 | 2 | 14 |
| ANT9-IN | Mean | 6858 | 0.03 | 0.63 | 0.24 | 1820 | 0.04 | 0.61 | 1.50 | 7.98 | 1674 | 0.10 | 1770 | 810 | 0.22 | 44 | 7724 | 1.81 | 3.75 | 0.01 | 2.32 | 0.00 | 0.21 | 0.00 | 2351 | 13 | 23 | 0 | 0 | 4 | 19 |
| | SD | 526 | 0.00 | 0.03 | 0.04 | 122 | 0.02 | 0.04 | 0.04 | 0.25 | 122 | 0.01 | 129 | 57 | 0.03 | 2 | 434 | 0.05 | 0.27 | 0.00 | 0.20 | 0.00 | 0.02 | 0.00 | 180 | 1 | 1 | 0 | 0 | 1 | 2 |
| ANT9-OUT | Mean | 7448 | 0.04 | 0.57 | 0.25 | 1942 | 0.04 | 0.63 | 2.35 | 8.62 | 1794 | 0.10 | 1790 | 853 | 0.35 | 49 | 7792 | 2.24 | 3.92 | 0.00 | 2.16 | 0.00 | 0.26 | 0.00 | 2463 | 12 | 24 | 0 | 0 | 5 | 22 |
| | SD | 955 | 0.01 | 0.09 | 0.02 | 148 | 0.04 | 0.04 | 0.73 | 0.55 | 144 | 0.01 | 111 | 36 | 0.20 | 3 | 469 | 0.69 | 0.27 | 0.00 | 0.30 | 0.00 | 0.02 | 0.00 | 171 | 1 | 1 | 0 | 0 | 0 | 1 |
| ANT10-IN | Mean | 7693 | 0.04 | 0.53 | 0.28 | 1957 | 0.03 | 0.61 | 1.20 | 7.95 | 1405 | 0.10 | 1816 | 839 | 0.24 | 39 | 7926 | 1.77 | 3.55 | 0.01 | 2.12 | 0.00 | 0.23 | 0.00 | 2466 | 12 | 23 | 0 | 0 | 4 | 18 |
| | SD | 2439 | 0.00 | 0.18 | 0.05 | 268 | 0.01 | 0.10 | 0.09 | 0.47 | 81 | 0.01 | 175 | 94 | 0.03 | 2 | 773 | 0.21 | 0.43 | 0.01 | 0.87 | 0.00 | 0.04 | 0.00 | 316 | 2 | 1 | 0 | 0 | 0 | 0 |
| ANT10-OUT | Mean | 11426 | 1.39 | 5.80 | 0.35 | 2831 | 2.38 | 1.45 | 2.93 | 50.37 | 2469 | 0.16 | 1899 | 1017 | 0.42 | 66 | 5505 | 8.40 | 139.57 | 0.04 | 2.66 | 0.01 | 12.44 | 0.00 | 2892 | 16 | 26 | 0 | 0 | 7 | 137 |
| | SD | 1615 | 0.21 | 0.94 | 0.06 | 483 | 0.16 | 0.17 | 0.44 | 4.47 | 402 | 0.01 | 190 | 200 | 0.02 | 9 | 444 | 0.98 | 19.17 | 0.01 | 0.85 | 0.00 | 1.21 | 0.00 | 799 | 2 | 6 | 0 | 0 | 1 | 9 |

| SITE | STATISTIC | Al | Ag | As | Be | Ca | Cd | Co | Cr | Cu | Fe | Hg | K | Mg | Mo | Mn | Na | Ni | Pb | Pd | Rb | Rh | Sb | Se | Si | Sr | Ti | Tl | U | V | Zn |
|---|---|---|---|---|---|---|---|---|---|---|---|---|---|---|---|---|---|---|---|---|---|---|---|---|---|---|---|---|---|---|---|
| NAP1-IN | Mean | 7367 | 0.04 | 0.52 | 0.23 | 3731 | 0.07 | 0.92 | 1.77 | 8.21 | 1579 | 0.09 | 1832 | 879 | 0.22 | 43 | 7775 | 1.90 | 3.75 | 0.01 | 1.98 | 0.00 | 0.23 | 0.00 | 2985 | 16 | 26 | 0.19 | 0.22 | 4 | 20 |
| | SD | 1074 | 0.00 | 0.03 | 0.02 | 2287 | 0.09 | 0.55 | 0.71 | 0.33 | 228 | 0.00 | 81 | 21 | 0.02 | 3 | 270 | 0.12 | 0.48 | 0.00 | 0.58 | 0.00 | 0.02 | 0.00 | 453 | 4 | 2 | 0.00 | 0.03 | 1 | 1 |
| NAP1-OUT | Mean | 10003 | 0.035 | 0.455 | 0.182 | 18618 | 0.031 | 0.913 | 2.218 | 16 | 1927 | 0.085 | 2229 | 2698 | 0.154 | 56 | 4284 | 2.618 | 6.474 | 0.009 | 0.146 | 1E-03 | 1.15 | 0 | 3593 | 24 | 42 | 0.178 | 0.283 | 4 | 55 |
| | SD | 1288 | 0.03 | 0.26 | 0.14 | 5593 | 0.01 | 0.09 | 0.38 | 1.39 | 236 | 0.01 | 881 | 900 | 0.04 | 5 | 2295 | 0.21 | 0.53 | 0.01 | 0.01 | 0.00 | 0.14 | 0.00 | 242 | 1 | 5 | 0.01 | 0.00 | 1 | 18 |
| NAP2-IN | Mean | 8547 | 0.03 | 0.46 | 0.15 | 2348 | 0.05 | 0.73 | 1.53 | 8.96 | 1561 | 0.08 | 1825 | 836 | 0.17 | 45 | 7962 | 2.03 | 3.85 | 0.01 | 2.94 | 0.00 | 0.16 | 0.00 | 2481 | 15 | 22 | 0.14 | 0.25 | 4 | 22 |
| | SD | 509 | 0.01 | 0.23 | 0.06 | 681 | 0.02 | 0.12 | 0.16 | 0.40 | 33 | 0.02 | 162 | 64 | 0.07 | 3 | 912 | 0.16 | 0.10 | 0.01 | 0.20 | 0.00 | 0.06 | 0.00 | 384 | 2 | 3 | 0.04 | 0.02 | 0 | 2 |
| NAP2-OUT | Mean | 9227 | 0.02 | 0.19 | 0.13 | 2968 | 0.03 | 0.77 | 1.53 | 10.48 | 1609 | 0.07 | 1579 | 1004 | 0.12 | 44 | 5442 | 2.27 | 5.00 | 0.00 | 2.22 | 0.00 | 0.89 | 0.00 | 2276 | 16 | 24 | 0.14 | 0.25 | 4 | 44 |
| | SD | 1381 | 0.01 | 0.11 | 0.12 | 385 | 0.02 | 0.04 | 0.19 | 0.50 | 105 | 0.03 | 171 | 32 | 0.07 | 3 | 620 | 0.11 | 0.34 | 0.00 | 0.70 | 0.00 | 0.33 | 0.00 | 163 | 1 | 2 | 0.04 | 0.00 | 1 | 17 |
| NAP3-IN | Mean | 18256 | 0.04 | 0.46 | 0.25 | 2057 | 0.05 | 0.74 | 1.66 | 9.35 | 1747 | 0.10 | 1989 | 918 | 0.25 | 49 | 8481 | 2.19 | 3.93 | 0.01 | 3.40 | 0.00 | 0.25 | 0.00 | 4762 | 14 | 25 | 0.19 | 0.25 | 5 | 21 |
| | SD | 6556 | 0.00 | 0.19 | 0.05 | 195 | 0.01 | 0.02 | 0.09 | 0.12 | 96 | 0.01 | 70 | 29 | 0.01 | 2 | 448 | 0.05 | 0.26 | 0.00 | 0.25 | 0.00 | 0.01 | 0.00 | 1416 | 1 | 2 | 0.00 | 0.00 | 0 | 0 |
| NAP3-OUT | Mean | 24743 | 0.05 | 0.52 | 0.30 | 11288 | 0.03 | 1.10 | 3.37 | 18.09 | 2563 | 0.08 | 1837 | 1883 | 0.24 | 66 | 1225 | 3.06 | 7.07 | 0.02 | 2.22 | 0.00 | 1.24 | 0.00 | 6188 | 29 | 28 | 0.19 | 0.30 | 6 | 37 |
| | SD | 6074 | 0.01 | 0.09 | 0.04 | 1372 | 0.02 | 0.10 | 0.58 | 1.38 | 349 | 0.00 | 224 | 98 | 0.02 | 8 | 389 | 0.20 | 0.43 | 0.02 | 0.25 | 0.00 | 0.10 | 0.00 | 1571 | 5 | 2 | 0.02 | 0.02 | 1 | 2 |
| NAP4-IN | Mean | 17527 | 0.03 | 0.26 | 0.19 | 2242 | 0.01 | 0.66 | 1.64 | 8.66 | 1928 | 0.10 | 1708 | 808 | 0.29 | 54 | 7206 | 2.00 | 3.77 | 0.01 | 3.89 | 0.00 | 0.21 | 0.00 | 5733 | 15 | 31 | 0.20 | 0.25 | 5 | 20 |
| | SD | 3985 | 0.01 | 0.07 | 0.05 | 654 | 0.01 | 0.08 | 0.56 | 0.56 | 209 | 0.00 | 15 | 44 | 0.15 | 7 | 146 | 0.28 | 0.07 | 0.01 | 0.75 | 0.00 | 0.02 | 0.00 | 664 | 1 | 8 | 0.03 | 0.01 | 2 | 0 |
| NAP4-OUT | Mean | 13488 | 0.05 | 0.20 | 0.28 | 5132 | 0.04 | 0.95 | 2.28 | 16.03 | 1966 | 0.09 | 1622 | 1441 | 0.30 | 53 | 4268 | 2.76 | 6.22 | 0.02 | 2.69 | 0.00 | 1.56 | 0.00 | 3359 | 21 | 29 | 0.21 | 0.26 | 4 | 34 |
| | SD | 1947 | 0.01 | 0.10 | 0.03 | 452 | 0.01 | 0.04 | 0.76 | 0.47 | 436 | 0.01 | 137 | 45 | 0.05 | 10 | 592 | 0.06 | 0.23 | 0.01 | 0.44 | 0.00 | 0.32 | 0.00 | 454 | 0 | 1 | 0.01 | 0.00 | 2 | 3 |
| NAP5-IN | Mean | 10527 | 0.03 | 0.05 | 0.14 | 1769 | 0.03 | 0.76 | 0.18 | 9.87 | 1158 | 0.08 | 1720 | 797 | 0.21 | 32 | 7326 | 2.33 | 4.13 | 0.00 | 3.58 | 0.00 | 0.22 | 0.00 | 3461 | 15 | 27 | 0.18 | 0.27 | 2 | 23 |
| | SD | 1713 | 0.01 | 0.02 | 0.05 | 22 | 0.02 | 0.11 | 0.11 | 1.12 | 65 | 0.00 | 21 | 11 | 0.02 | 4 | 163 | 0.27 | 0.63 | 0.00 | 0.92 | 0.00 | 0.02 | 0.00 | 409 | 2 | 1 | 0.02 | 0.05 | 1 | 3 |
| NAP5-OUT | Mean | 17999 | 0.02 | 0.13 | 0.12 | 2876 | 0.05 | 1.12 | 0.20 | 14.14 | 1158 | 0.05 | 1863 | 998 | 0.14 | 33 | 6899 | 2.95 | 6.23 | 0.00 | 4.35 | 0.00 | 1.88 | 0.00 | 4455 | 21 | 21 | 0.11 | 0.36 | 3 | 34 |
| | SD | 8326 | 0.02 | 0.05 | 0.14 | 487 | 0.01 | 0.45 | 0.16 | 1.17 | 330 | 0.04 | 320 | 174 | 0.13 | 11 | 662 | 0.70 | 1.09 | 0.00 | 3.15 | 0.00 | 1.65 | 0.00 | 627 | 4 | 19 | 0.10 | 0.11 | 1 | 2 |
| NAP6-IN | Mean | 10557 | 0.03 | 0.20 | 0.20 | 2385 | 0.04 | 2.67 | 1.00 | 10.97 | 1309 | 0.08 | 1858 | 879 | 0.22 | 38 | 7349 | 2.63 | 4.93 | 0.01 | 4.21 | 0.00 | 0.22 | 0.06 | 3066 | 17 | 30 | 0.19 | 0.31 | 3 | 25 |
| | SD | 1343 | 0.01 | 0.12 | 0.02 | 416 | 0.01 | 3.10 | 0.41 | 0.53 | 350 | 0.01 | 55 | 44 | 0.02 | 12 | 488 | 0.43 | 0.13 | 0.01 | 1.74 | 0.00 | 0.00 | 0.11 | 395 | 3 | 4 | 0.02 | 0.02 | 0 | 1 |
| NAP6-OUT | Mean | 11634 | 0.05 | 0.05 | 0.19 | 4086 | 0.10 | 1.08 | 0.56 | 17.34 | 1320 | 0.08 | 1601 | 1311 | 0.19 | 37 | 4359 | 3.23 | 6.93 | 0.01 | 3.34 | 0.00 | 1.96 | 0.00 | 3578 | 22 | 30 | 0.19 | 0.31 | 1 | 37 |
| | SD | 2493 | 0.01 | 0.03 | 0.09 | 327 | 0.06 | 0.14 | 0.18 | 0.18 | 222 | 0.01 | 178 | 51 | 0.01 | 7 | 333 | 0.38 | 0.14 | 0.01 | 1.20 | 0.00 | 0.91 | 0.00 | 493 | 2 | 2 | 0.03 | 0.03 | 1 | 4 |
| NAP7-IN | Mean | 10728 | 0.06 | 0.06 | 0.22 | 2235 | 0.06 | 0.96 | 0.58 | 11.55 | 1225 | 0.09 | 1851 | 868 | 0.23 | 34 | 7655 | 2.63 | 4.95 | 0.01 | 4.56 | 0.00 | 0.25 | 0.00 | 3246 | 17 | 27 | 0.19 | 0.31 | 2 | 25 |
| | SD | 426 | 0.01 | 0.04 | 0.02 | 118 | 0.02 | 0.10 | 0.50 | 0.36 | 222 | 0.01 | 97 | 40 | 0.02 | 6 | 541 | 0.12 | 0.18 | 0.01 | 0.53 | 0.00 | 0.02 | 0.00 | 246 | 1 | 0 | 0.01 | 0.02 | 0 | 0 |
| NAP7-OUT | Mean | 9853 | 0.04 | 0.05 | 0.16 | 2991 | 0.05 | 0.92 | 0.84 | 13.28 | 1384 | 0.08 | 1774 | 1003 | 0.22 | 38 | 6548 | 2.70 | 5.09 | 0.00 | 3.74 | 0.00 | 1.04 | 0.00 | 3254 | 17 | 27 | 0.17 | 0.28 | 2 | 29 |
| | SD | 543 | 0.01 | 0.00 | 0.04 | 334 | 0.02 | 0.05 | 0.28 | 0.58 | 162 | 0.00 | 171 | 107 | 0.01 | 4 | 910 | 0.11 | 0.25 | 0.01 | 0.33 | 0.00 | 0.11 | 0.00 | 179 | 2 | 2 | 0.01 | 0.02 | 0 | 1 |
| NAP8-IN | Mean | 13434 | 0.05 | 0.12 | 0.26 | 2123 | 0.04 | 1.05 | 0.43 | 11.65 | 1599 | 0.09 | 1892 | 902 | 0.23 | 45 | 7667 | 3.92 | 4.74 | 0.01 | 4.56 | 0.00 | 0.25 | 0.00 | 3631 | 17 | 29 | 0.19 | 0.31 | 3 | 26 |
| | SD | 240 | 0.01 | 0.12 | 0.04 | 108 | 0.01 | 0.08 | 0.26 | 0.30 | 237 | 0.00 | 44 | 18 | 0.01 | 5 | 156 | 0.75 | 0.22 | 0.01 | 0.59 | 0.00 | 0.01 | 0.00 | 159 | 0 | 2 | 0.01 | 0.01 | 0 | 1 |
| NAP8-OUT | Mean | 13881 | 0.10 | 0.07 | 0.20 | 6710 | 0.06 | 2.64 | 1.99 | 31.45 | 1877 | 0.08 | 1475 | 2016 | 0.47 | 48 | 3308 | 3.83 | 6.99 | 0.01 | 3.15 | 0.00 | 2.03 | 0.00 | 3696 | 28 | 29 | 0.18 | 0.31 | 3 | 48 |
| | SD | 2770 | 0.02 | 0.02 | 0.03 | 922 | 0.02 | 2.27 | 1.52 | 1.13 | 538 | 0.01 | 294 | 179 | 0.04 | 11 | 983 | 0.06 | 0.67 | 0.01 | 1.18 | 0.00 | 0.36 | 0.00 | 161 | 1 | 1 | 0.02 | 0.04 | 2 | 2 |
| NAP9-IN | Mean | 11118 | 0.03 | 0.07 | 0.18 | 2371 | 0.04 | 0.88 | 1.12 | 10.99 | 1410 | 0.08 | 1789 | 860 | 0.20 | 38 | 7356 | 2.53 | 4.38 | 0.01 | 3.39 | 0.00 | 0.22 | 0.00 | 3637 | 16 | 32 | 0.17 | 0.28 | 4 | 25 |
| | SD | 560 | 0.01 | 0.05 | 0.06 | 447 | 0.01 | 0.04 | 0.08 | 0.39 | 266 | 0.01 | 75 | 30 | 0.02 | 8 | 373 | 0.23 | 0.28 | 0.01 | 0.90 | 0.00 | 0.02 | 0.00 | 385 | 1 | 3 | 0.00 | 0.02 | 1 | 1 |
| NAP9-OUT | Mean | 14934 | 0.08 | 0.12 | 0.26 | 6165 | 0.06 | 1.23 | 2.04 | 22.67 | 2267 | 0.09 | 1655 | 1501 | 0.26 | 64 | 4530 | 3.57 | 7.31 | 0.01 | 3.49 | 0.00 | 1.71 | 0.00 | 4212 | 23 | 31 | 0.19 | 0.31 | 5 | 42 |
| | SD | 4328 | 0.01 | 0.08 | 0.10 | 496 | 0.01 | 0.21 | 0.70 | 0.11 | 357 | 0.00 | 292 | 231 | 0.05 | 8 | 984 | 0.56 | 0.79 | 0.01 | 1.73 | 0.00 | 0.44 | 0.00 | 313 | 3 | 2 | 0.02 | 0.03 | 1 | 1 |
| NAP10-IN | Mean | 27694 | 0.05 | 0.05 | 0.27 | 2044 | 0.06 | 0.96 | 0.56 | 11.41 | 1596 | 0.09 | 1880 | 876 | 0.25 | 43 | 7948 | 2.66 | 4.61 | 0.01 | 4.97 | 0.00 | 0.24 | 0.00 | 6697 | 17 | 26 | 0.20 | 0.30 | 2 | 26 |
| | SD | 18632 | 0.00 | 0.01 | 0.10 | 141 | 0.02 | 0.13 | 0.05 | 0.30 | 163 | 0.00 | 146 | 106 | 0.02 | 4 | 250 | 0.26 | 0.37 | 0.01 | 0.45 | 0.00 | 0.03 | 0.00 | 3998 | 1 | 3 | 0.04 | 0.04 | 1 | 0 |
| NAP10-OUT | Mean | 20355 | 0.11 | 0.097 | 0.36 | 7591 | 0.061 | 1.46 | 5.167 | 37.26 | 2801 | 0.105 | 1871 | 2102 | 0.522 | 72 | 4170 | 4.462 | 12.13 | 0.032 | 4.42 | 0.001 | 2.389 | 0 | 5814 | 34 | 34 | 0.226 | 0.351 | 5 | 63 |
| | SD | 5804 | 0.01 | 0.05 | 0.12 | 716 | 0.03 | 0.26 | 1.81 | 7.01 | 339 | 0.02 | 485 | 282 | 0.15 | 8 | 2023 | 0.82 | 1.83 | 0.02 | 1.40 | 0.00 | 0.74 | 0.00 | 1329 | 3.79 | 6.18 | 0.05 | 0.07 | 2 | 8 |

Among terrigenous elements, Al ranged between 4744 mg $kg^{-1}$(ANT2-OUT) and 27694 mg $kg^{-1}$ (NAP10-IN). Among the elements of environmental concern, Ni ranged between 1.77 mg $kg^{-1}$ (ANT10-IN) and 8.4 mg $g^{-1}$ (ANT10-OUT), and Pb ranged between 3.55 mg $kg^{-1}$ (ANT10-IN) and 140 mg $kg^{-1}$ (ANT10-OUT). Elemental accumulation (expressed as percent of sites in which the element was significantly accumulated (i.e., higher than the LOQT) for each environment (indoor/outdoor) is reported in Table 3. Only five elements (Be, Rb, Se, Tl and V) never accumulated in the moss-bags. Most of the other elements accumulated in both countries, especially outdoors (16 out of 30) with very high accumulation percentages; but some elements accumulated specifically in one country: Ag, As, Cd, Hg, Mo, and Mn in ANT; Cr, Sr and U in NAP (Table 3).

Table 3 - Elemental accumulation (in %) for each site typology in which each element significantly accumulated.

| Location | Environment | Al | Ag | As | Be | Ca | Cd | Co | Cr | Cu | Fe | Hg | K | Mg | Mo | Mn |
|---|---|---|---|---|---|---|---|---|---|---|---|---|---|---|---|---|
| **ANT** | **Out** | 70 | 70 | 20 | 0 | 90 | 60 | 50 | 10 | 90 | 10 | 10 | 10 | 90 | 40 | 60 |
| | **In** | 90 | 0 | 10 | 0 | 20 | 0 | 20 | 0 | 0 | 0 | 0 | 30 | 10 | 0 | 0 |
| **NAP** | **Out** | 100 | 30 | 0 | 0 | 100 | 10 | 90 | 20 | 90 | 20 | 0 | 10 | 100 | 20 | 30 |
| | **In** | 100 | 0 | 0 | 0 | 70 | 0 | 50 | 0 | 50 | 0 | 0 | 10 | 0 | 0 | 0 |
| | | **Na** | **Ni** | **Pb** | **Pd** | **Rb** | **Rh** | **Sb** | **Se** | **Si** | **Sr** | **Ti** | **Tl** | **U** | **V** | **Zn** |
| **ANT** | **Out** | 0 | 50 | 90 | 10 | 0 | 20 | 90 | 0 | 100 | 20 | 90 | 0 | 10 | 0 | 90 |
| | **In** | 0 | 0 | 0 | 0 | 0 | 10 | 0 | 0 | 90 | 0 | 70 | 0 | 20 | 0 | 0 |
| **NAP** | **Out** | 0 | 90 | 100 | 20 | 0 | 30 | 100 | 0 | 100 | 80 | 80 | 0 | 50 | 0 | 100 |
| | **In** | 0 | 40 | 20 | 0 | 0 | 10 | 0 | 0 | 100 | 0 | 90 | 0 | 30 | 0 | 0 |

### 3.3 Multi-elemental analyses

Following the PCA based on the 16 accumulated elements and SIRM data of all sites (Figure 1), the first two axes explained about 64% of the total variance. Along the first factor (41% of the total variance), a significant effect of the environment ($p=2.6\ 10^{-4}$ according to GLM analysis applied on the score of this factor) was observed. In fact, according to Tukey's post-hoc test ANT indoor sites were significantly different from all outdoor sites ($p<0.05$). Along the second axis (23%), a significant effect of the interaction between country and environment factors was observed ($p<0.026$ according to GLM analysis applied on the score of this factor); according to Tukey's post-hoc test, NAP outdoor sites were significantly different from all the ANT sites ($p<0.05$).

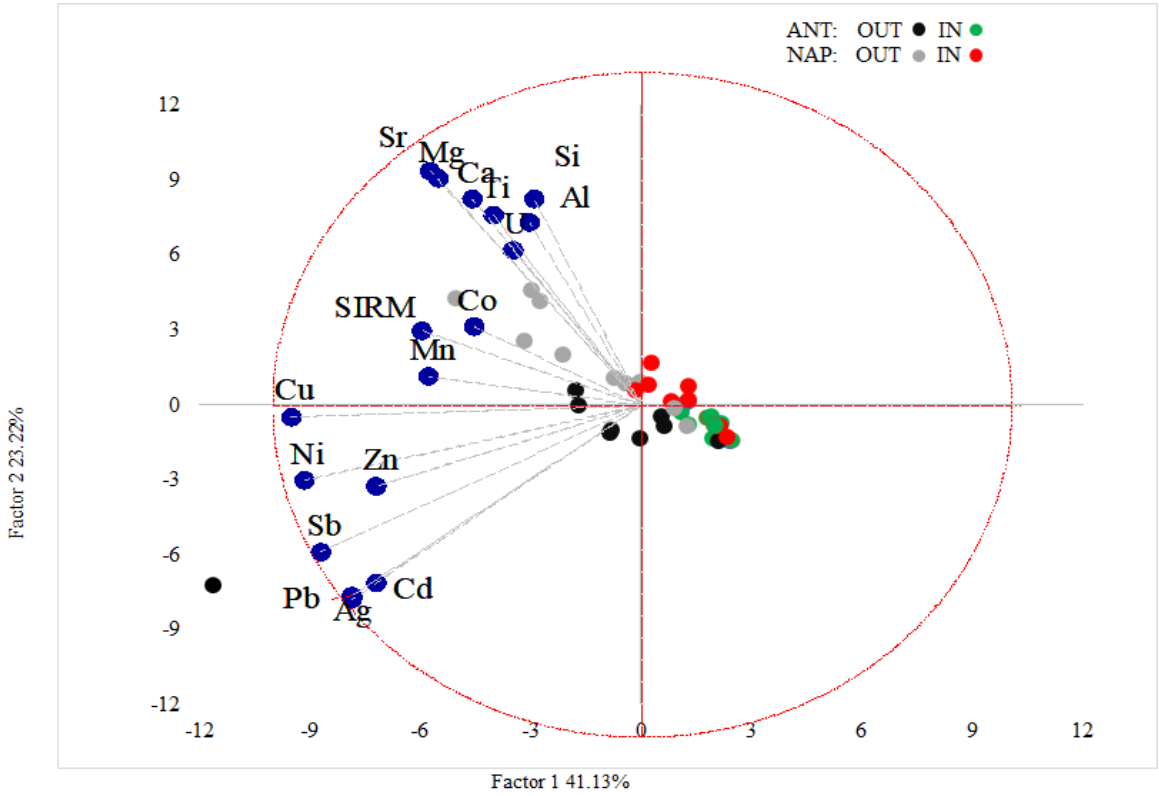


Figure 1 - Biplot of the first and second factor following PCA based on the 16 accumulated elements and SIRM, found in mosses in the outdoor and indoor environments in both Naples (NAP) and Antwerp (ANT).

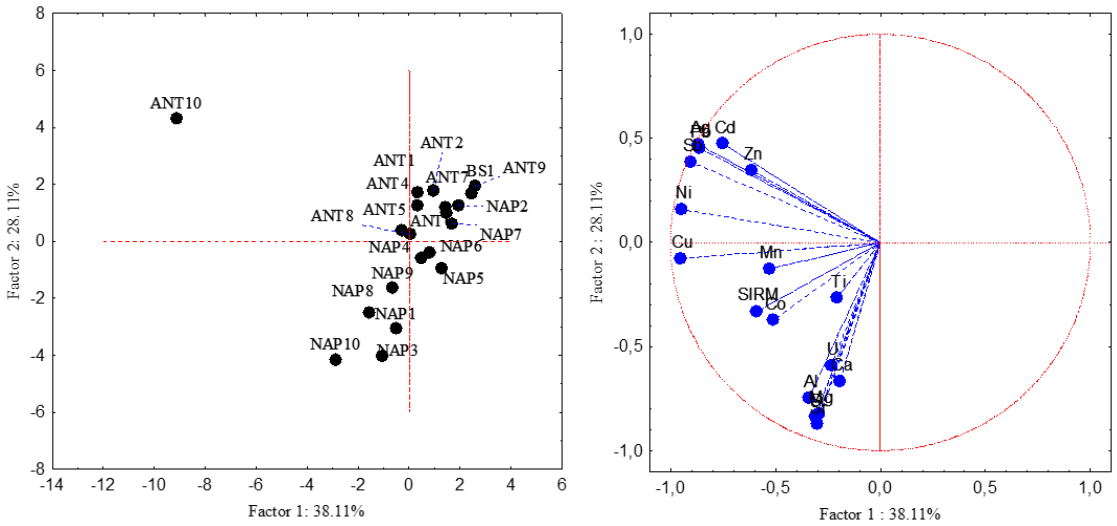


Figure 2 - Biplot of first and second factor following PCA based on the 16 accumulated elements and SIRM, found in mosses exposed outdoors in Naples (NAP) and Antwerp (ANT).

The first two factors of the PCA based on the 16 accumulated elements found in mosses in the outdoor environment explained overall almost 70% of the total variance (Fig. 2). The first axis (38.11%) had high factor loadings for Ag, Cd, Cu, Ni, Pb, Sb and Zn, elements of environmental concern. The site ANT10 was indicated as the most distinct from the other outdoor sites by metal pollution. Along this axis, the two countries were significantly different ($p<0.05$ according to t-test applied on the location score of this factor), and some sites clustered with the background site BS (i.e., pre-exposure moss).

Along the second axis (28.11% of the total variance), which related with concentrations of Ca, Mg, Al, Si and U, no significant effect of country was observed ($p>0.05$ according to t-test applied on the score of this factor). The vectors of the elements of environmental concern were pointed toward ANT sites, while most terrigenous element vectors pointed toward NAP sites; the SIRM vector fell in between the two groups of elements.

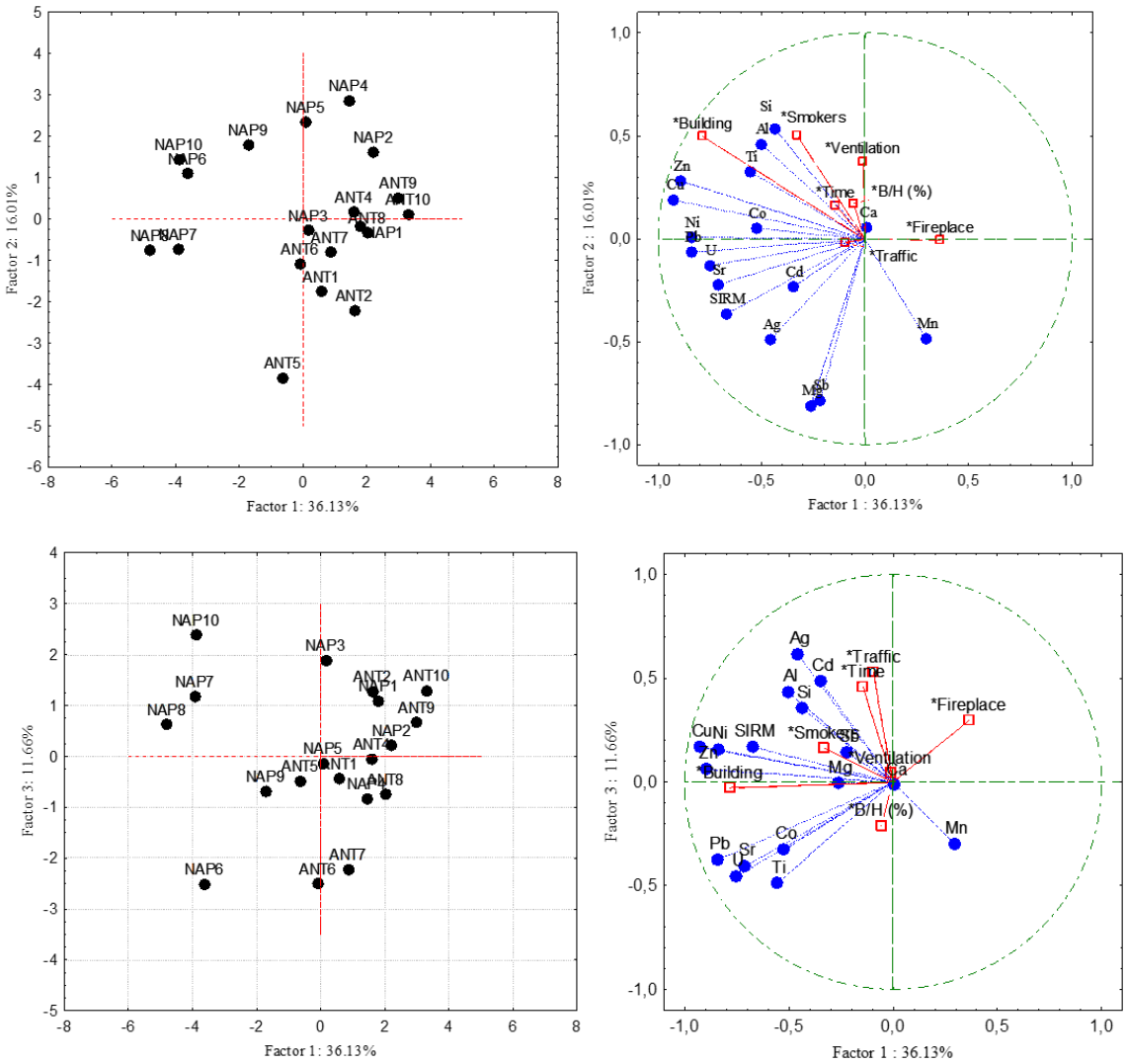


Figure 3. Biplot of (a) first and second factor and (b) first and third factor following PCA based on the 16 accumulated elements and SIRM, found in mosses in the indoor environment in both Naples (NAP) and Antwerp (ANT). *Supplementary variables (see M&M).

The PCA of indoor environments (Fig. 3) showed that most NAP sites were significantly separated from ANT sites along the first axis accounting for about 36% of the total variance ($p<0.05$). Further separation occurred between NAP and ANT along the second axis ($p<0.05$ according to t-test applied on the score of this factor) but not the third axis ($p>0.05$ according to t-test applied on the score of this factor), explaining about 16% and 12% of the total variance, respectively. The SIRM and most element vectors pointed toward NAP sites. The Supplementary variables (see supplementary material Table S2) primarily affecting indoor element pollution were the building material (mainly tuff in NAP and brick in ANT), the presence of smokers, the ventilation system, and the presence of fireplaces; secondly, the building material, the level of traffic in the neighborhood, the presence of fireplaces and the residence time spent at home by inhabitants (shorter in ANT than in NAP). Among the home habits only the residence time was significantly different between the two cities ($p=0.03$). No

significant relationship was found between PCA scores (Three main axes) and the supplementary variables of Table S2.

Element concentrations normalized to the maximum value (Table S4) highlights that the Flanders sites were largely homogeneous, with element loads ranging between 4 and 5 indoor and 4 and 7 outdoor, except for site ANT10-OUT, showing the highest load (12) and 6 elements out of 16, having the maximum value. In Naples, some maximum values were also recorded in indoor environments, Co in NAP6 and Al and Si in NAP10. Additionally, although few maximum values (1 to 3) were recorded outdoors in Naples, some sites (NAP 1, 3, 8, and 10 OUT) showed high element loads (i.e., 8 or 9). This is due to some element normalized concentrations near to 1 (e.g., Al and Mn in NAP3, Co in NAP8). These values close to 1 contribute to the high total load despite the absence, or the low number, of maximal concentrations. Differently from ANT10, outdoor sites of the metropolitan area of Naples showed essentially a terrigenous footprint, since Al, Ca, Mg, Mn, Si, Sr and Ti were most abundant.

Table S4 - Element concentrations normalized to the maximum value as observed for all sites, for the 16 accumulated elements found in moss material at each site. Σ All: count of all maximum values (i.e. "1") for each site; Total Load: sum of all the normalized values for each site.

| | | Al | Ag | Ca | Cd | Co | Cu | Mg | Mn | Ni | Pb | Sb | Si | Sr | Ti | U | Zn | Σ All | Total Load |
|---|---|---|---|---|---|---|---|---|---|---|---|---|---|---|---|---|---|---|---|
| ANT 1 | IN | 0.22 | 0.03 | 0.11 | 0.01 | 0.54 | 0.19 | 0.36 | 0.75 | 0.28 | 0.03 | 0.02 | 0.34 | 0.41 | 0.59 | 0.76 | 0.16 | 0 | 5 |
| ANT 2 | IN | 0.21 | 0.04 | 0.11 | 0.02 | 0.26 | 0.17 | 0.34 | 0.66 | 0.25 | 0.03 | 0.02 | 0.30 | 0.43 | 0.53 | 0.70 | 0.14 | 0 | 4 |
| ANT 4 | IN | 0.23 | 0.03 | 0.10 | 0.01 | 0.28 | 0.18 | 0.31 | 0.67 | 0.26 | 0.03 | 0.02 | 0.35 | 0.43 | 0.60 | 0.71 | 0.16 | 0 | 4 |
| ANT 5 | IN | 0.26 | 0.03 | 0.11 | 0.02 | 0.31 | 0.18 | 0.36 | 0.77 | 0.26 | 0.03 | 0.03 | 0.36 | 0.54 | 0.63 | 0.77 | 0.15 | 0 | 5 |
| ANT 6 | IN | 0.23 | 0.02 | 0.13 | 0.01 | 0.24 | 0.16 | 0.33 | 0.74 | 0.22 | 0.03 | 0.02 | 0.37 | 0.52 | 0.63 | 0.92 | 0.15 | 0 | 5 |
| ANT 7 | IN | 0.22 | 0.03 | 0.11 | 0.02 | 0.26 | 0.16 | 0.32 | 0.76 | 0.22 | 0.03 | 0.02 | 0.34 | 0.50 | 0.66 | 0.85 | 0.14 | 0 | 5 |
| ANT 8 | IN | 0.30 | 0.02 | 0.12 | 0.01 | 0.23 | 0.16 | 0.33 | 0.64 | 0.21 | 0.03 | 0.02 | 0.37 | 0.44 | 0.63 | 0.76 | 0.14 | 0 | 4 |
| ANT 9 | IN | 0.25 | 0.02 | 0.10 | 0.02 | 0.23 | 0.16 | 0.30 | 0.61 | 0.21 | 0.03 | 0.02 | 0.35 | 0.38 | 0.55 | 0.70 | 0.14 | 0 | 4 |
| ANT 10 | IN | 0.28 | 0.03 | 0.11 | 0.01 | 0.23 | 0.16 | 0.31 | 0.54 | 0.21 | 0.03 | 0.02 | 0.37 | 0.36 | 0.55 | 0.64 | 0.13 | 0 | 4 |
| ANT 1 | OUT | 0.21 | 0.12 | 0.19 | 0.03 | 0.36 | 0.30 | 0.45 | 0.89 | 0.30 | 0.04 | 0.12 | 0.38 | 0.48 | 0.68 | 0.68 | 1.00 | 1 | 6 |
| ANT 2 | OUT | 0.17 | 0.04 | 0.18 | 0.05 | 0.31 | 0.31 | 0.42 | 0.81 | 0.36 | 0.07 | 0.12 | 0.39 | 0.46 | 0.61 | 0.68 | 0.64 | 0 | 6 |
| ANT 4 | OUT | 0.22 | 0.13 | 0.27 | 0.24 | 0.47 | 0.36 | 0.42 | 0.80 | 0.37 | 0.11 | 0.15 | 0.39 | 0.55 | 0.66 | 0.72 | 0.35 | 0 | 6 |
| ANT 5 | OUT | 0.23 | 0.07 | 0.18 | 0.08 | 0.35 | 0.41 | 0.43 | 0.85 | 0.32 | 0.09 | 0.24 | 0.40 | 0.67 | 0.68 | 0.92 | 0.66 | 0 | 7 |
| ANT 6 | OUT | 0.24 | 0.04 | 0.16 | 0.04 | 0.26 | 0.24 | 0.39 | 0.76 | 0.27 | 0.06 | 0.12 | 0.41 | 0.49 | 0.67 | 0.77 | 0.24 | 0 | 5 |
| ANT 7 | OUT | 0.25 | 0.06 | 0.13 | 0.04 | 0.26 | 0.26 | 0.37 | 0.70 | 0.25 | 0.06 | 0.16 | 0.36 | 0.49 | 0.59 | 0.79 | 0.22 | 0 | 5 |
| ANT 8 | OUT | 0.30 | 0.09 | 0.61 | 0.54 | 0.26 | 0.32 | 0.40 | 0.68 | 0.31 | 0.10 | 0.11 | 0.50 | 0.76 | 0.90 | 0.68 | 0.43 | 0 | 7 |
| ANT 9 | OUT | 0.27 | 0.03 | 0.10 | 0.02 | 0.24 | 0.17 | 0.32 | 0.67 | 0.27 | 0.03 | 0.02 | 0.37 | 0.36 | 0.56 | 0.67 | 0.15 | 0 | 4 |
| ANT 10 | OUT | 0.41 | 1.00 | 0.15 | 1.00 | 0.54 | 1.00 | 0.38 | 0.92 | 1.00 | 1.00 | 1.00 | 0.43 | 0.47 | 0.61 | 0.77 | 0.97 | 6 | 12 |
| NAP 1 | IN | 0.27 | 0.03 | 0.20 | 0.03 | 0.34 | 0.16 | 0.33 | 0.60 | 0.23 | 0.03 | 0.02 | 0.45 | 0.47 | 0.61 | 0.62 | 0.14 | 0 | 5 |
| NAP 2 | IN | 0.31 | 0.02 | 0.13 | 0.02 | 0.27 | 0.18 | 0.31 | 0.62 | 0.24 | 0.03 | 0.01 | 0.37 | 0.44 | 0.52 | 0.70 | 0.16 | 0 | 4 |
| NAP 3 | IN | 0.66 | 0.03 | 0.11 | 0.02 | 0.28 | 0.19 | 0.34 | 0.68 | 0.26 | 0.03 | 0.02 | 0.71 | 0.41 | 0.60 | 0.71 | 0.15 | 0 | 5 |
| NAP 4 | IN | 0.63 | 0.02 | 0.12 | 0.01 | 0.25 | 0.17 | 0.30 | 0.75 | 0.24 | 0.03 | 0.02 | 0.86 | 0.45 | 0.73 | 0.69 | 0.14 | 0 | 5 |
| NAP 5 | IN | 0.38 | 0.02 | 0.10 | 0.01 | 0.28 | 0.20 | 0.30 | 0.45 | 0.28 | 0.03 | 0.02 | 0.52 | 0.44 | 0.65 | 0.76 | 0.16 | 0 | 5 |
| NAP 6 | IN | 0.38 | 0.02 | 0.13 | 0.02 | 1.00 | 0.22 | 0.33 | 0.53 | 0.31 | 0.04 | 0.02 | 0.46 | 0.51 | 0.71 | 0.88 | 0.18 | 1 | 6 |
| NAP 7 | IN | 0.39 | 0.04 | 0.12 | 0.02 | 0.36 | 0.23 | 0.32 | 0.48 | 0.31 | 0.04 | 0.02 | 0.48 | 0.51 | 0.64 | 0.86 | 0.18 | 0 | 5 |
| NAP 8 | IN | 0.49 | 0.04 | 0.11 | 0.02 | 0.39 | 0.23 | 0.33 | 0.62 | 0.47 | 0.03 | 0.02 | 0.54 | 0.50 | 0.68 | 0.87 | 0.18 | 0 | 6 |
| NAP 9 | IN | 0.40 | 0.02 | 0.13 | 0.02 | 0.33 | 0.22 | 0.32 | 0.53 | 0.30 | 0.03 | 0.02 | 0.54 | 0.48 | 0.75 | 0.77 | 0.18 | 0 | 5 |
| NAP 10 | IN | 1.00 | 0.03 | 0.11 | 0.03 | 0.36 | 0.23 | 0.32 | 0.59 | 0.32 | 0.03 | 0.02 | 1.00 | 0.49 | 0.61 | 0.84 | 0.19 | 2 | 6 |
| NAP 1 | OUT | 0.36 | 0.03 | 1.00 | 0.01 | 0.34 | 0.31 | 1.00 | 0.77 | 0.31 | 0.05 | 0.09 | 0.54 | 0.70 | 1.00 | 0.79 | 0.39 | 3 | 8 |
| NAP 2 | OUT | 0.33 | 0.01 | 0.16 | 0.01 | 0.29 | 0.21 | 0.37 | 0.61 | 0.27 | 0.04 | 0.07 | 0.34 | 0.48 | 0.56 | 0.71 | 0.31 | 0 | 5 |
| NAP 3 | OUT | 0.89 | 0.04 | 0.61 | 0.01 | 0.41 | 0.36 | 0.70 | 0.92 | 0.36 | 0.05 | 0.10 | 0.92 | 0.86 | 0.67 | 0.83 | 0.26 | 0 | 8 |
| NAP 4 | OUT | 0.49 | 0.04 | 0.28 | 0.02 | 0.36 | 0.32 | 0.53 | 0.74 | 0.33 | 0.04 | 0.13 | 0.50 | 0.62 | 0.70 | 0.72 | 0.24 | 0 | 6 |
| NAP 5 | OUT | 0.65 | 0.01 | 0.15 | 0.02 | 0.42 | 0.28 | 0.37 | 0.46 | 0.35 | 0.04 | 0.15 | 0.67 | 0.61 | 0.50 | 1.00 | 0.24 | 1 | 6 |
| NAP 6 | OUT | 0.42 | 0.04 | 0.22 | 0.04 | 0.40 | 0.34 | 0.49 | 0.52 | 0.39 | 0.05 | 0.16 | 0.53 | 0.65 | 0.72 | 0.86 | 0.27 | 0 | 6 |
| NAP 7 | OUT | 0.36 | 0.03 | 0.16 | 0.02 | 0.34 | 0.26 | 0.37 | 0.52 | 0.32 | 0.04 | 0.08 | 0.49 | 0.51 | 0.64 | 0.78 | 0.21 | 0 | 5 |
| NAP 8 | OUT | 0.50 | 0.07 | 0.36 | 0.03 | 0.99 | 0.62 | 0.75 | 0.67 | 0.46 | 0.05 | 0.16 | 0.55 | 0.82 | 0.69 | 0.88 | 0.34 | 0 | 8 |
| NAP 9 | OUT | 0.54 | 0.06 | 0.33 | 0.02 | 0.46 | 0.45 | 0.56 | 0.89 | 0.43 | 0.05 | 0.14 | 0.63 | 0.69 | 0.74 | 0.88 | 0.30 | 0 | 7 |
| NAP 10 | OUT | 0.73 | 0.08 | 0.41 | 0.03 | 0.55 | 0.74 | 0.78 | 1.00 | 0.53 | 0.09 | 0.19 | 0.87 | 1.00 | 0.80 | 0.98 | 0.45 | 2 | 9 |

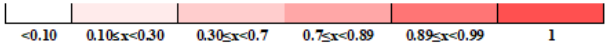

Based on the GLM results (Fig. 4), Ag, Ca, Cd, Mg, Pb, Si, Sr and Zn were significantly affected by the main effects and their interaction; Mn, Ti and U by the country and environment; Al and Si were affected only by country (higher in NAP both indoors and outdoors); Cu, Ni and Sb only by the environment (higher outdoors in both countries); the element Co was not affected by country and environment. For almost all elements, the concentrations measured indoors were lower than outdoors, except for Al, Si and Co, since they did not show a significant effect of the environment. Marked differences between outdoor (higher) and indoor (lower) element concentrations were observed more frequently in Antwerp than in Naples (e.g., Cd, Pb and Zn).

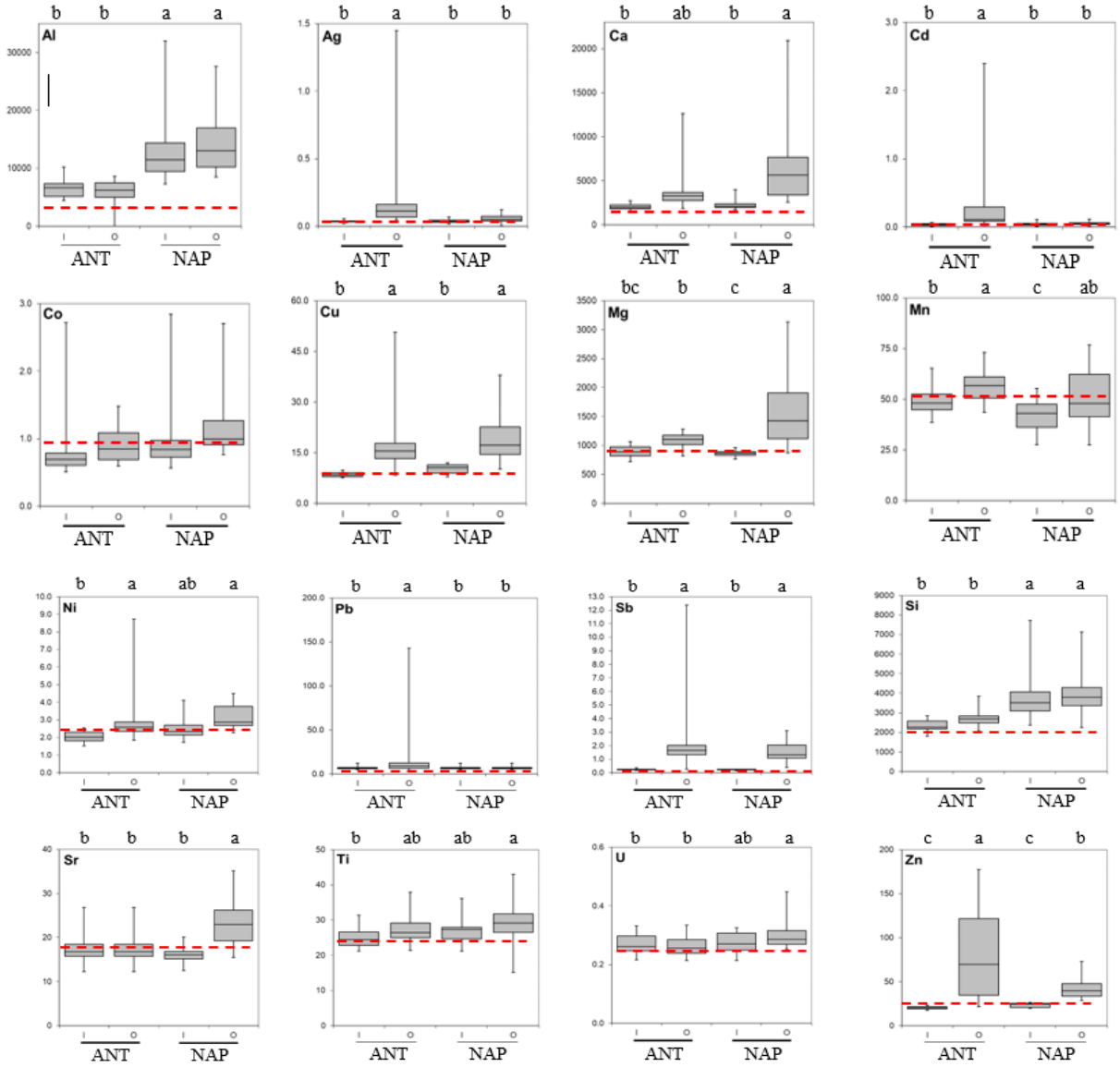


Figure. 4 - Boxplots of element concentrations (mg $kg^{-1}$) in the moss exposed in Indoor and Outdoor environments in Flanders (ANT) and Italy (NAP). The red dashed line represents the LOQT. BOX: inside band = median; extremities = 1st and 3rd quartiles; whiskers = MIN and MAX. Different letters indicate significant differences according to Tukey's test, $p<0.05$.

### 3.4 Comparison of pollution sources between indoor and outdoor environments

The elements Al, Si, Ni, Co and Ca significantly correlated between indoor and outdoor environments over the entire data set ($n=19$, $p<0.05$ according to Spearman's $\rho$ correlation test). When considering only the ANT sites, significant correlations occurred between in and outdoors for Al and Si, and for Al, Ni, and Si in the NAP sites.

With most of the indoor/outdoor (I/O) ratios being below 0.75 (Table 4), it is confirmed that most elements largely accumulated outdoors in both countries; however, in some sites in the metropolitan area of Naples specific elements were found higher indoors (e.g., Al, Ag, Cd). The I/O ratio was significantly different between the two countries only for Mg (Mg was present mainly outdoors in NAP but in ANT).

Table 4 – I/O ratio, expressing the ratio between the indoor and outdoor moss-accumulated element concentrations. First row: elements; first column: site codes. Pink values > 1.25; Green values < 0.75. See the text for details.

| | Al | Ag | Ca | Cd | Co | Cu | Mg* | Mn | Ni | Pb | Sb | Si | Sr | Ti | U | Zn |
|---|---|---|---|---|---|---|---|---|---|---|---|---|---|---|---|---|
| **ANT_1** | 1.07 | 0.22 | 0.57 | 0.48 | 1.50 | 0.62 | 0.80 | 0.84 | 0.93 | 0.64 | 0.17 | 0.88 | 0.84 | 0.86 | 1.11 | 0.16 |
| **ANT_2** | 1.20 | 0.89 | 0.59 | 0.38 | 0.84 | 0.55 | 0.81 | 0.82 | 0.70 | 0.39 | 0.18 | 0.77 | 0.93 | 0.87 | 1.03 | 0.22 |
| **ANT_4** | 1.06 | 0.20 | 0.36 | 0.06 | 0.58 | 0.50 | 0.73 | 0.83 | 0.71 | 0.25 | 0.13 | 0.90 | 0.79 | 0.91 | 0.99 | 0.44 |
| **ANT_5** | 1.11 | 0.40 | 0.60 | 0.26 | 0.89 | 0.44 | 0.85 | 0.90 | 0.83 | 0.34 | 0.11 | 0.90 | 0.81 | 0.92 | 0.83 | 0.22 |
| **ANT_6** | 0.95 | 0.49 | 0.80 | 0.34 | 0.93 | 0.69 | 0.84 | 0.97 | 0.82 | 0.57 | 0.15 | 0.89 | 1.07 | 0.94 | 1.19 | 0.61 |
| **ANT_7** | 0.85 | 0.44 | 0.82 | 0.38 | 1.01 | 0.62 | 0.86 | 1.08 | 0.88 | 0.62 | 0.12 | 0.93 | 1.02 | 1.13 | 1.08 | 0.61 |
| **ANT_8** | 0.99 | 0.28 | 0.20 | 0.03 | 0.88 | 0.49 | 0.82 | 0.94 | 0.69 | 0.29 | 0.18 | 0.75 | 0.58 | 0.70 | 1.12 | 0.32 |
| **ANT_9** | 0.92 | 0.76 | 0.94 | 1.06 | 0.96 | 0.93 | 0.95 | 0.90 | 0.80 | 0.96 | 0.84 | 0.95 | 1.04 | 0.98 | 1.05 | 0.88 |
| **ANT_10** | 0.67 | 0.03 | 0.69 | 0.01 | 0.42 | 0.16 | 0.82 | 0.59 | 0.21 | 0.03 | 0.02 | 0.85 | 0.77 | 0.90 | 0.83 | 0.13 |
| **NAP_1** | 0.74 | 1.05 | 0.20 | 2.33 | 1.01 | 0.52 | 0.33 | 0.78 | 0.73 | 0.58 | 0.20 | 0.83 | 0.67 | 0.61 | 0.78 | 0.36 |
| **NAP_2** | 0.93 | 1.76 | 0.79 | 1.39 | 0.95 | 0.86 | 0.83 | 1.01 | 0.90 | 0.77 | 0.18 | 1.09 | 0.91 | 0.91 | 0.98 | 0.50 |
| **NAP_3** | 0.74 | 0.80 | 0.18 | 1.44 | 0.67 | 0.52 | 0.49 | 0.74 | 0.72 | 0.56 | 0.20 | 0.77 | 0.48 | 0.90 | 0.86 | 0.57 |
| **NAP_4** | 1.30 | 0.49 | 0.44 | 0.30 | 0.70 | 0.54 | 0.56 | 1.01 | 0.73 | 0.61 | 0.13 | 1.71 | 0.72 | 1.04 | 0.96 | 0.61 |
| **NAP_5** | 0.58 | 1.38 | 0.62 | 0.66 | 0.67 | 0.70 | 0.80 | 0.97 | 0.79 | 0.66 | 0.12 | 0.78 | 0.71 | 1.30 | 0.76 | 0.69 |
| **NAP_6** | 0.91 | 0.54 | 0.58 | 0.37 | 2.48 | 0.63 | 0.67 | 1.02 | 0.81 | 0.71 | 0.11 | 0.86 | 0.78 | 0.99 | 1.02 | 0.67 |
| **NAP_7** | 1.09 | 1.45 | 0.75 | 1.22 | 1.04 | 0.87 | 0.87 | 0.91 | 0.97 | 0.97 | 0.24 | 1.00 | 1.00 | 1.00 | 1.11 | 0.87 |
| **NAP_8** | 0.97 | 0.50 | 0.32 | 0.73 | 0.40 | 0.37 | 0.45 | 0.93 | 1.02 | 0.68 | 0.12 | 0.98 | 0.61 | 0.99 | 0.99 | 0.53 |
| **NAP_9** | 0.74 | 0.38 | 0.38 | 0.73 | 0.71 | 0.48 | 0.57 | 0.60 | 0.71 | 0.60 | 0.13 | 0.86 | 0.70 | 1.01 | 0.88 | 0.60 |
| **NAP_10** | 1.36 | 0.42 | 0.27 | 0.99 | 0.66 | 0.31 | 0.42 | 0.59 | 0.60 | 0.38 | 0.10 | 1.15 | 0.49 | 0.76 | 0.85 | 0.41 |

* Significant differences between the I/O ratios of the two countries in relation to each element according to t-test. $p<0.01$

## 4 Discussion

### 4.1 SIRM as metal pollution proxy

The concept of environmental magnetism as a proxy for air pollution monitoring was first reported based on the analysis of soils, sediments, or even street or roof dust in an urban context, as urban soils are often inaccessible due to buildings and roads (e.g. Muxworthy et al., 2003; Wang et al., 2012) and also for the analysis of biological materials, as leaves, trunk and branch bark, lichens, mosses and animal and human tissue (see Hofman et al. 2017 for a review). A correlation was observed by Hunt et al. (1984) between the saturation isothermal remanent magnetization (SIRM) and the metal component of atmospheric PM, suggesting the use of magnetic parameters to help identify metal-containing PM sources. Since also many plant species can intercept and retain PM (e.g., Di Palma et al., 2017) several authors in recent years investigated magnetic properties of plant leaves or mosses to predict the level of metal pollution in the atmosphere (Hofman et al., 2017; Vuković et al. 2014, 2015 a and b).

SIRM analysis was already applied to moss transplants in biomonitoring of air quality (Salo et al., 2012 and 2014; Vuković et al., 2015a and b) in experiments carried out in open air. Salo et al. (2012), analyzing 22 sites in Finland, found SIRM values between 112 (urban forest), and 917 mA $m^2 kg^{-1}$ (major urban road of Turku City center), which is substantially lower than the post-exposure values in this study (3724 to 6495 μA $m^2$ $kg^{-1}$). However, the different biomonitor species (*Sphagnum papillosum*), and the diverse experimental design (urban forest and passive biomonitoring vs urban sites and active biomonitoring), make a comparison of results hard. Vuković et al. (2015a) used the same moss species as this present study did, i.e., *Hypnum cupressiforme*, exposed in bags in 153 sites of Belgrade, characterized by different land uses. The authors found SIRM post-exposure values ranging between 670 and 4780, with a mean value of 1970 μA $m^2$ $kg^{-1}$. These values are generally lower than those measured in the present experiment, but they can be considered in a good agreement, taking into account the different exposure periods (8 weeks vs. 12 weeks in the present experiment). Our SIRM values were more homogeneous, probably due to the homogeneity of the studied sites (all urban sites). When comparing indoor with outdoor SIRM values, no relationship occurred, suggesting that outdoor PM exposure does not necessarily relate with the one indoors and so indoor measurements are essential to evaluate the exposure to PM indoors. The ratio of I/O could not be explained by country, which points to the absence of a meteorological effect (e.g., rain and wind) on the outdoor SIRM-indoor SIRM relation. A difference in PM sources indoors and outdoors was implied by the different relationships between SIRM and metal content indoors and outdoors. Moreover, differently from Vuković et al. (2015a), who found high correlations with Cr, Cu and Fe, only a significant correlation with Cu (Spearman R: 0.47, $p<0.05$) was observed in the present work (since in our case Cr and Fe did not accumulate). The lack of significant Cr and Fe accumulation could be due to the different emission sources insisting over the study areas. Maher et al. (2008) and Castanheiro et al. (2016) established significant correlations of SIRM values measured on the leaves with Fe and Pb, and the latter authors also with Zn and to a lesser extent Cd and Mn. In the present study, a significant positive correlation of the SIRM values with Pb and Zn was evidenced (Table 4).

Finally, the significant difference in SIRM values recorded between indoor and outdoor moss in both countries, even with magnetizable elements like Co and Ni, indicates the enviromagnetic approach as a powerful tool to predict metal pollution also in indoor environments.

**4.2 Indoor/outdoor elemental pollution**

**A**ll the elaborations indicate that elements accumulated indoors represent a subset of those found outdoors. There are few articles investigating air pollution indoors; therefore, proper comparisons are hardly feasible. As for element accumulation, Pekey et al. (2010) found in the PM collected on filters exposed in a Turkish city, both indoors and outdoors, a noticeable accumulation of Ca, K, S and Si. These results are partly consistent with ours, specifically for Ca and Si. The lower accumulation of K in our moss samples was likely due to the low number of smokers among the people living at the selected houses (only in two apartments out of 19, Table S1), as K is released into a confined environment especially from smoke of cigarettes (Na et al., 2004). Canha et al. (2014) investigated metal pollution by lichen transplants in different Portuguese schools, located in urban and rural areas, and found accumulation values generally lower than those here calculated, sometimes lower than those measured in pre-exposed lichens. These discrepancies could partly depend on the different exposure time of the bags (12 weeks in the present experiment vs. 8 weeks in theirs). Another factor explaining the results obtained by Canha et al. (2014) could be the use of lichen instead of moss in the transplants. It is reported, indeed, that airborne elements are mostly linked to PM and in this form adhere to the biomonitoring surface; consequently, the amount of PM intercepted and retained by biomonitors depends on their surface to mass ratio, which is higher in mosses compared to lichens (Capozzi et al., 2020; Tretiach et al., 2007). Similarly, lower element concentrations than those measured in the present work were generally found in the moss *Pleurozium schreberi* (Willd. Ex Brid) Mitt. (Zechmeister et al., 2020) exposed in paired indoor-outdoor sites in Girona (Spain). In this case the authors also applied an exposure period of 8 weeks. We have chosen an exposure period of 12 weeks based on the hypothesis that indoor pollution level is lower than outdoors, and therefore longer exposure periods are needed to obtain measurable concentrations. According to our results, 12 weeks seem a sufficient exposure time to detect indoor element pollution.

Analysis of the normalized contents suggested that the outdoor environments of both countries were largely similar, with some exceptions of sites and elements. As for ANT10 outdoor, showing the highest load of elements (Table 4), Castanheiro et al. (2016) found in the same area particles deposited on leaves enriched in Pb and Cu and, to a lesser extent, in Zn and Cd. In this site, located at 400 m from an industrial area (a non-ferrous metallurgical industry and a cement industry) in the south of Antwerp city, several elements of environmental concern were found in the present study at the highest concentrations, such as Cd, Cu, Ni, Pb and Sb, in addition to Ag, suggesting it as the most polluted site. Moreover, the presence of Zn in outdoor ANT sites could be due to organic matter degradation in urban parks near the study area; Zn is

a micronutrient, therefore, it is commonly found in fertilizers and organic matter (Montalvo et al., 2016). However, Zn has also been identified in Flanders as related with traffic-emitted pollutants, such as elemental carbon, Cu, Cr and Fe (Vercauteren et al., 2011). Uranium, especially abundant in outdoor NAP sites, is considered a lithological marker of the Vesuvian soils, while Co and Mg, also abundant in NAP outdoor sites, can be attributed to igneous rocks, widely spread throughout the Campania region including the metropolitan area of Naples (De Vivo et al., 2006).

According to Alloway et al. (2013), Co and Mn (here abundant mainly at ANT sites) naturally occur in soils and rocks even if they can be produced by a wide range of industrial wastes and urban processes (Yoshizawa and Ohzuku, 2007) and due to their toxicity (USEPA 2015), they are potentially dangerous for ecosystems.

Both normalized contents and GLM analysis evidenced a marked difference between indoor and outdoor environments, especially in ANT. Although no significant correlation was found between indoor PCA scores and supplementary variables, the different lifestyle, specifically the shorter residence time (mostly 8-12 h) declared by the inhabitants in ANT, could explain this result. In fact, it can be hypothesized that if people stay at home only in the night hours, they tend to open the windows less frequently, with a reduced exchange with outside air. A similar result was observed in a previous work (Capozzi et al., 2019). This result could also depend on the different meteorological conditions recorded in the two areas: as suggested by Canha et al. (2014), in countries with warm and moderate climate, such as south European countries, natural ventilation indoors through opening the windows is generally applied all day long, which results in accumulation and magnification of pollutants, and therefore, higher levels of exposure to contaminants for humans. Meteorological data recorded in the exposure period (Table S2) highlighted lower temperatures, higher number of rainy days, and low levels of PM, at least in June, in ANT compared to NAP, suggesting a high level of erosion and dust resuspension in NAP, in line with the higher level of outdoor element contamination found in this area.

### 4.3 Disentangling metal pollution sources between indoor and outdoor environments

The I/O ratio allows to establish the outer/internal source for elements; even if according to Chen and Zhao (2011) values higher than 1 are routinely considered as indicators of internal source and values lower than 1 as indicators of outdoor origin, we prefer to keep the 0.75-1.25 range as a precautionary buffer interval indicating a mixed origin for a given element. The I/O ratio assumes considerable importance, if read in the light of the correlation between the indoor and outdoor concentrations, of each element. In fact, the existence of this correlation supports

the idea of a common origin, likely outdoor origin for the elements (Al, Si, Ni, Co and Ca, in our case). In the absence of this correlation and when I/O ratio is higher than 1.25, an indoor source can be hypothesized for a given element. This condition occurred in some sites for Cd and Ti; Cd can be released by building materials (Davis et al., 2001), whereas Ti could derive by combustion processes, including cooking and heating systems (Habre et al., 2014). For those elements showing significant indoor-outdoor correlation and higher concentration in indoor moss (as observed in some sites for Al, Si and Co), progressive indoor accumulation due to a repeated entrance from outdoors (magnification) could be a conceivable explanation. In papers investigating indoor metal pollution by active samplers (e.g., Miler and Gosar, 2019; Pekey et al., 2010), element concentrations are expressed in mg per volume of air; therefore, a direct comparison between element concentrations is not feasible and the only parameter useful for comparison is the non-dimensional I/O ratio. In both the above mentioned articles, according to the I/O ratio, the authors found that metal-bearing particles were more abundant outdoors than indoors, consolidating our findings. In the recent paper by Zechmeister et al. (2020), in which elemental pollution was assessed indoors and outdoors by *Pleurozium schreberi* transplants in 20 paired sites in Girona (Spain), the authors found I/O ratio values lower than 1, for all elements analyzed except Cd, suggesting the presence of an indoor source for this element. It is reported that Cd can be easily released by building materials, including wall paints (Davis et al., 2001), so that the exposure of the moss in frames in contact with the wall could have resulted in an enrichment of Cd in the moss. Finally, in a previous paper carried out in Campania region, south Italy, Capozzi et al. (2019) found in some sites an indoor accumulation of Cr, Ni and V, elements probably released from household furnishings and cleaning products. Among these elements, only Ni was found in four NAP indoor sites (Table 1); the discrepancy observed could depend on the different apartments here selected or different cleaning products and furnishings employed.

**Conclusions**

This article explored the potential of moss transplants to disentangle the airborne metal-pollution sources between indoor and outdoor environments, in two European areas characterized by different climate conditions. In addition, for the first time, SIRM was successfully tested as a proxy to investigate indoor metal pollution. SIRM proved to be a low-expensive and low-time consuming tool to evaluate the level of elemental pollution even indoors. Furthermore, being a non-destructive technique, it allows to measure the magnetic properties and the content of elements on the same plant sample.

It was confirmed that outdoor pollution is the major source of indoor pollution, but in some cases domestic sources seem to be more important than outdoor environmental sources. Among variables concerning people's lifestyle, in addition to known pollution fonts, like traffic and fireplaces, other factors can modulate indoor pollution level; particularly, the residence time could have a relevant role in the magnification of pollutants found indoors. Twelve weeks seem to be a sufficient exposure time for the biomonitoring of indoor environments. Notwithstanding, due to the recent application of the moss-bags methodology in indoor environments, a dedicated study to find the best exposure time and condition should be organized to provide useful information for a shared harmonized protocol. Overall, moss bags proved a useful and versatile tool to highlight the contamination differences between the indoor and outdoor environments and can flank other non-biological methods, such as filter cartridges and PM samplers, used for the same purpose.

**Acknowledgements** We are grateful to all the volunteers who participated in the experiment by providing their homes and the information about their habits filling the questionnaires. Founds: This work was partly financed by the University of Naples Federico II (PhD founds, M.C.S.) and Dipartimento di Biologia (Resp. V.S.)

## References

Alloway, B.J., 2013. Sources of heavy metals and metalloids in soils, in: Alloway B. (eds) Heavy metals in soils. Environmental Pollution, Springer, Dordrecht. https://doi.org/10.1007/978-94-007-4470-7_2.

Al-Radady, A.S., Davies, B.E., French, M.J., 1993. A new design of moss bag to monitor metal deposition both indoors and outdoors. Sci. Total Environ. 133, 275-283. https://doi.org/10.1016/0048-9697(93)90249-6.

Al-Radady, A.S., Davies, B.E., French, M.J., 1994 Distribution of lead inside the home: case studies in the North of England. Sci. Total Environ. 145, 143-156. https://doi.org/10.1016/0048-9697(94)90305-0.

Ares, A., Aboal, J.R., Carballeira, A., Fernandez, J.A., 2015. Do moss bags containing devitalized *Sphagnum denticulatum* reflect heavy metal concentrations in bulk deposition? Ecol. Indic. 50, 90-98. https://doi.org/10.1016/j.ecolind.2014.10.030.

Brockerhoff, M., 2000. An urbanizing world. Popul. Bull. 55 (3)

Canha, N., Almeida, S.M., Freitas, M.C., Wolterbeek, H.T., 2014. Indoor and outdoor biomonitoring using lichens at urban and rural primary schools. J. Tox. Env. Health. Part A, 77, 14-16, 900-915, https://doi.org/10.1080/15287394.2014.911130

Castanheiro, A., Hofman, J., Nuyts, G., Joosen, S., Spassov, S., Blust, R., Lenaerts, S., De Wael, K., Samson, R., 2020. Leaf accumulation of atmospheric dust: Biomagnetic, morphological and elemental evaluation using SEM, ED-XRF and HR-ICP-MS. Atmos. Environ. 221, 117082 https://doi.org/10.1016/J.ATMOSENV.2019.117082

Castanheiro, A., Samson, R., De Wael, K., 2016. Magnetic- and particle-based techniques to investigate metal deposition on urban green. Sci. Total Environ. 571, 594–602. http://dx.doi.org/10.1016/j.scitotenv.2016.07.026

Capozzi, F., Giordano, S., Aboal, J.R., Adamo, P., Bargagli, R., Boquete, T., Di Palma, A., Real, C., Reski, R., Spagnuolo, V., Steinbauer, K., Tretiach, M., Varela, Z., Zechmeister, H., Fernandez, J.A., 2016. Best options for the exposure of traditional and innovative moss bags: a systematic evaluation in three European countries. Environ. Pollut. 214, 362-373. https://doi.org/10.1016/j.envpol.2016.04.043

Capozzi, F., Di Palma, A., Adamo, P., Sorrentino, M.C., Giordano, S., Spagnuolo, V., 2019. Indoor vs. outdoor airborne element array: a novel approach using moss bags to explore possible pollution sources. Environ. Pollut., 249, 566-572, https://doi.org/10.1016/J.ENVPOL.2019.03.012.

Capozzi, F., Sorrentino, M.C., Di Palma, A., Mele, F., Arena, C., Adamo, P., Spagnuolo, V., Giordano, S., 2020. Implication of vitality, seasonality and specific leaf area on PAH uptake in moss and lichen transplanted in bags. Ecol. Indic. 108, 105727, https://doi.org/10.1016/j.ecolind.2019.105727.

Chen, C., Zhao, B., 2011. Review of relationship between indoor and outdoor particles: I/O ratio, infiltration factor and penetration factor. Atmos. Environ. 45, 275-288.

Conti, M.E., Cecchetti, G., 2001. Biological monitoring: lichens as bioindicators of air pollution assessment — a review. Environ. Pollut. 114, 471-492. https://doi.org/10.1016/S0269-7491(00)00224-4.

Couto, J.A., Aboal, J.R., Fernández, J.A., Carballeira, A., 2004. A new method for testing the sensitivity of active biomonitoring: an example of its application to a terrestrial moss. Chemosphere, 57, 303-308.
https://doi.org/10.1016/j.chemosphere.2004.05.036.

Davis, A.P., Shokouhian, M., Ni, S., 2001. Loading estimates of lead, copper, cadmium, and zinc in urban runoff from specific sources. Chemosphere 44, 997-1009. doi.org/10.1016/S0045-6535(00)00561-0

De Vivo, B., Cicchella, D., Lima, A., Albanese, S., 2006. Atlante geochimico ambientale dei suoli dell'area urbana e della Provincia di Napoli. Ed. ARACNE, Roma. pp. 315. ISBN: 88-548-0563-7

Di Palma, A., Capozzi, F., Spagnuolo, V., Adamo, P., Giordano, S., 2017. Atmospheric particulate matter intercepted by moss-bags: Relations to moss trace element uptake and land use. Chemosphere, 176, 361–368.

Giordano, S., Adamo, P., Spagnuolo, V., Tretiach, M., Bargagli, R., 2013. Accumulation of airborne trace elements in mosses, lichens and synthetic materials exposed at urban

monitoring stations: Towards a harmonisation of the moss-bag technique. Chemosphere. 90, 292-299. https://doi.org/10.1016/j.chemosphere.2012.07.006.

Gurjar B, Nagpure AS, Singh TP, 2012. Air quality in megacities. http://www.eoearth.org/view/article/149934.

Hofman, J., Maher, B., Adrian, A., Muxworthy, R., Wuyts, K., Castanheiro, A., Samson, R., 2017. Biomagnetic monitoring of atmospheric pollution: a review of magnetic signatures from biological sensors. Environ. Sci. Technol. 51, 6648−6664 https://doi.org/10.1021/acs.est.7b00832.

Habre, R., Coull, B., Moshier, E., Godbold, J., Grunin, A., Nath, A., Castro, W., Schachter, N., Rohr, A., Kattan, M., Spengler, J., Koutrakis, P., 2014. Sources of indoor air pollution in New York City residences of asthmatic children. J. Exp. Sci. Env. Epid. 24, 269–278. https://doi.org/10.1038/jes.2013.74.

Huang, H., Lee, S., Cao, J., Zou, C., Chen, X., Fan, S., 2007. Characteristics of indoor/outdoor PM2.5 and elemental components in generic urban, roadside and industrial plant areas of Guangzhou City, China. J. Environ. Sci. 19, 35-43. https://doi.org/10.1016/S1001-0742(07)60006-0.

Hunt, A., Jones, J., Oldfield, F., 1984. Magnetic measurements and heavy metals in atmospheric particulates of anthropogenic origin. Sci. Total Environ. 33, 129-139. https://doi.org/10.1016/0048-9697(84)90387-5.

Iodice, P., Adamo, P., Capozzi, F., Di Palma, A., Senatore, A., Spagnuolo, V., Giordano, S., 2016. Air pollution monitoring using emission inventories combined with the moss bag approach. Sci. Total Environ. 541, 1410-1419. https://doi.org/10.1016/j.scitotenv.2015.10.034.

Jiang, Y., Fan, M., Hu, R., Zhao, J., Wu, Y., 2018. Mosses are better than leaves of vascular plants in monitoring atmospheric heavy metal pollution in urban areas. Int. J. Environ. Res. Public Health. 15, 1105.

Kardel, F., Wuyts, K., Babanezhad, M., Vitharana, U.W.A., Wuytack, T., Potters, G., Samson, R., 2010. Assessing urban habitat quality based on specific leaf area and stomatal characteristics of *Plantago lanceolata* L. Environ. Pollut. 158, 788-794. https://doi.org/10.1016/j.envpol.2009.10.006.

Kardel, F., Wuyts, K., Maher, B.A., Hansard, R., Samson, R., 2011. Leaf saturation isothermal remanent magnetization (SIRM) as a proxy for particulate matter monitoring: Inter-species differences and in-season variation. Atmos. Environ. 45, 5164-5171. https://doi.org/10.1016/j.atmosenv.2011.06.025.

Kardel, F., Wuyts, K., De Wael, K., Samson, R., 2018. Biomonitoring of atmospheric particulate pollution via chemical composition and magnetic properties of roadside tree leaves. Environ. Sci. Pollut. Res. 25, 25994–26004. https://doi.org/10.1007/s11356-018-2592-z.

Lee, B.X.Y., Hadibarata, T., Yuniarto, A., 2020. Phytoremediation Mechanisms in Air Pollution Control: a Review. Water Air Soil Pollut. 231, 437. https://doi.org/10.1007/s11270-020-04813-6

Liu, J., Dai, X., Li, X., Jia, S., Pei, J., Sun, Y., Lai, D., Shen, X., Sun, H., Yin, H., Huang, K., Tan, H., Gao, Y., Jian, Y., 2018. Indoor air quality and occupants' ventilation habits in China: Seasonal measurement and long-term monitoring, Building and Environment 142, 119-129. doi: 10.1016/j.buildenv.2018.06.002.

Maher, B.A., Moore, C., Matzka, J., 2008. Spatial variation in vehicle-derived metal pollution identified by magnetic and elemental analysis of roadside tree leaves. Atmos. Environ. 42, 364−373.

Miler, M., Gosar, M., 2019. Assessment of contribution of metal pollution sources to attic and household dust in Pb-polluted area. Indoor Air. 29,487–498. DOI: 10.1111/ina.12548.

Montalvo, D., Degryse, F., da Silva, R.C., Baird, R., McLaughlin, M.J., 2016. Agronomic effectiveness of zinc sources as micronutrient fertilizer. In: (D.L. Sparks Ed.) Advances in Agronomy, 139. Pp. 215-267. Elsevier. Doi.org/10.1016/bs.agron.2016.05.004.

Motyka, O., Macečková, B., Seidlerová, J., 2013. Indoor biomonitoring of particle related pollution: trace element concentration in an office environment. Conference Paper Nanocom 2013; 16-18 October 2013, Brno, Czech Republic, EU.

Muxworthy, A. R., Matzka, J., Fernández Davila, A., Petersen, N., 2003. Magnetic signature of daily sampled urban atmospheric particles. Atmos. Environ. 37, 4163-4169, https://doi.org/10.1016/S1352-2310(03)00500-4.

Rivera, M., Zechmeister, H., Medina-Ramón, M., Basagaña, X., Foraster, M., Bouso, L., Moreno, T., Solanas, P., Ramos, R., Köllensperger, G., Deltell, A., Vizcaya, D., Künzli, N., 2011, Monitoring of heavy metal concentrations in home outdoor air using moss bags. Environ. Pollut. 159, 954-962. https://doi.org/10.1016/j.envpol.2010.12.004.

Pekey, B., Bozkurt, Z. B., Pekey, H., Doğan, G., Zararsız, A., Efe, N., Tuncel, G., 2010. Indoor/outdoor concentrations and elemental composition of PM10/PM2.5 in urban/industrial areas of Kocaeli City, Turkey. Indoor Air. 20, 112–125. doi:10.1111/j.1600-0668.2009.00628.x.

Salo, H., Bućko, M.S., Vaahtovuo, E., Limo, J., Mäkinen, J., Pesonen, L.J., 2012. Biomonitoring of air pollution in SW Finland by magnetic and chemical measurements of moss bags and lichens. J. Geochem. Explor. 115, 69–81.

Salo, H., Mäkinen, J., 2014. Magnetic biomonitoring by moss bags for industry-derived air pollution in SW Finland. Atmos. Environ. 97, 19–27.

Tretiach, M., Adamo, P., Bargagli, R., Baruffo, L., Carletti, L., Crisafulli, P., Giordano, S., Modenesi, P., Orlando, S., Pittao, E., 2007. Lichen and moss bags as monitoring devices in urban areas. Part I: influence of exposure on vitality. Environ. Pollut. 146, 380-39.

Van Dyck, L., Bentouhami, H., Koch, K., Samson, R., Weyler, J., 2019. Exposure to indoor ferromagnetic particulate matter monitored by strawberry plants and the occurrence of acute respiratory events in adults. Int. J. Environ. Res. Public Health, 16, 4823. https://doi.org/10.3390/ijerph16234823

Vercauteren, J., Matheeussen, C., Wauters, E., Roekens, E., van Grieken, R., Krata, A., Makarovska, Y., Maenhaut, W., Chi, X., Geypens, B., 2011. Chemkar PM10: An extensive look at the local differences in chemical composition of PM10 in Flanders, Belgium. Atmos. Environ. 45, 108-116. https://doi.org/10.1016/j.atmosenv.2010.09.040.

Vuković, G., Urošević, M.A., Razumenić, I., Kuzmanoski, M., Pergal, M., Škrivanj, S., Popović, A., 2014. Air quality in urban parking garages (PM10, major and trace elements, PAHs): instrumental measurements vs. active moss biomonitoring. Atmos. Environ. 85, 31-40.

Vuković, G., Urošević, M.A., Goryainova, Z., Pergal, M., Škrivanj, S., Samson, R., Popović, A., 2015a. Active moss biomonitoring for extensive screening of urban air pollution: magnetic and chemical analyses. Sci. Total Environ. 521, 200-210.

Vuković, G., Aničić Urošević, M., Tomašević, M., Samson, R., Popović, A., 2015b. Biomagnetic monitoring of urban air pollution using moss bags (*Sphagnum girgensohnii*). Ecol. Ind. 52, 40-47, https://doi.org/10.1016/j.ecolind.2014.11.018.

Wang, G., Oldfield, F., Xia, D., Chen, F., Liu, X., Zhang, W., 2012. Magnetic properties and correlation with heavy metals in urban street dust: A case study from the city of Lanzhou, China. Atmos. Environ. 46, 289-298. https://doi.org/10.1016/j.atmosenv.2011.09.059.

Yoshizawa, H., T Ohzuku, T., 2007. An application of lithium cobalt nickel manganese oxide to high-power and high-energy density lithium-ion batteries. J. Power Sources 174, 813-817.

Zechmeister, H.G., Rivera, M., Köllensperger, G., Marrugat J., Künzli, N., 2020. Indoor monitoring of heavy metals and NO2 using active monitoring by moss and Palmes diffusion tubes. Environ. Sci. Eur. 32, 156 https://doi.org/10.1186/s12302-020-00439-x.

**Sitografy**

https://www.unfpa.org/publications/unfpa-annual-report-2004
https://population.un.org/wup/Publications/Files/WUP2018-Report.pdf
https://www.meteo.be
https://www.irceline.be

# Chapter 6

## Mobile biomonitoring as an innovative tool to estimate personal exposure to atmospheric pollution: a new perspective for the moss-bag approach.

**Maria Cristina Sorrentino[1], Fiore Capozzi[1], Karen Wuyts[2], Steven Joosen[3], Valentine K. Mubiana[3], Simonetta Giordano[1], Roeland Samson[2], Valeria Spagnuolo[*1]**

*[1]Dipartimento di Biologia, Università degli Studi di Napoli Federico II, Campus Monte S. Angelo, Via Cinthia 4, 80126 Napoli, Italy*
*[2]Department of Bioscience Engineering, University of Antwerp, Campus Groenenborgerlaan 171, 2020 Antwerp, Belgium*
*[3]Department of Biology, University of Antwerp, Campus Groenenborgerlaan 171, 2020 Antwerp, Belgium*

Key words: *Hypnum cupressiforme*; air biomonitoring; elemental pollution; SIRM

**Abstract**

In this work we tested by magnetic and chemical analysis for the first time the potential of moving moss-bags, fixed to bicycles, to intercept particulate matter (PM) and linked metal(loid)s. Seven volunteers carried three moss bags for fifty days while commuting by bicycle in the urban area of Antwerp, Belgium. In addition, one bike with moss-bags was equipped with mobile PM samplers and travelled along four routes: urban, industrial, green route and the total path, carrying three moss-bags at each route. The saturation isothermal remanent magnetization (SIRM) signal and chemical composition (assessed by ICP-MS) of the moss indicated that the industrial route was the most polluted. Element fluxes (i.e., the ratio between element daily uptake and the specific leaf area) could discriminate among the different land uses; particularly, they were significantly higher in the industrial route for Ag, As, Cd and Pb; significantly lowest in the green route for As and Pb; comparable for all accumulated elements along most urban routes. A comparison with a previous experiment carried out in the same study area using similar moss bags at static exposure points, showed that the element fluxes were significantly higher in the mobile system. Finally, PM amounts measured along the four routes were consistent with element fluxes. Chemical analysis highlighted a noticeable variability in elemental content among replicas, suggesting that longer exposure times and the use of analytical replicas could provide more homogeneous and reliable data.

## 1. Introduction

Air pollution is defined as the presence of harmful or poisonous substances in the Earth's atmosphere, causing adverse effects on human health and ecosystems (Archibald et al., 2017). In fact, air pollution also affects animals, plants, and ecological resources including water and soils (Brunekreef and Holgate, 2002; Duan et al., 2017). The WHO global conference on air pollution and health reported that over 4 million people died of air pollution every year and that about 91% of the world's population live in places exceeding the thresholds reported by the WHO air quality guidelines. These latter fixed the limits for 24-h exposure to PM 2.5 and PM 10 at 25 and 50 μg $m^{-3}$, respectively, but limits imposed by the national legislations are indeed more tolerant; for example, the limit for 24-h exposure to PM 2.5 is of 35 μg $m^{-3}$ in USA and 75 μg $m^{-3}$ in China (Wei et al 2017). A wide body of literature have demonstrated that PM can determine the onset of diseases regardless its chemical composition, but also as carrier of toxicants and pathogens (e.g., Oves et al., 2012; Pope et al., 2002; Sanità di Toppi et al., 2020). Especially in urban areas, air pollution levels undergo fluctuations in space and time due to the coexistence of different pollution sources and their constant or intermittent emissions; consequently, the evaluation of air quality is intrinsically complicated. Since the measurements of PM concentration directly in the atmosphere (i.e., through automatic devices) is very expensive and practically impossible at high spatial resolution (Kardel et al., 2018), many researchers use biomonitors to detect airborne pollutants, and particularly PM (Conti and Cecchetti 2001; Kardel et al. 2010, 2011). Due to their intrinsic properties (e.g., sessile organisms, wide surface exposed to atmosphere…) plants are particularly suited as biomonitors of airborne pollutants. Accordingly, recent literature demonstrated that the elemental contents measured in mosses transplanted in bags is significantly correlated with amounts of PM entrapped (Di Palma et al., 2017).

In biomonitoring, chemical analysis of the plant tissues can be profitably integrated with magnetic measures, since these latter are sample-conservative, and require low costs and less time. Enviro-magnetic analysis of atmospheric PM by SIRM (saturation isothermal remanent magnetization) was employed since the 80s (Hunt et al., 1984), but only in the last decades, this approach revealed its efficacy for monitoring air quality through the analysis of soil, sediments, and road dust (e.g., Goddu et al., 2004). Since many plants can intercept and retain PM, several authors in recent years have studied the magnetic properties of vascular plant leaves and mosses to predict the level of metal pollution in the atmosphere (e.g., Kapper et al., 2020; Vuković et al., 2015). This approach also provided useful information in biomonitoring of indoor environments by moss-bags (Sorrentino et al., submitted).

Moss and lichen-bags have been valuably used in biomonitoring of air quality, but while their efficacy in bioaccumulation of pollutants (e.g., metals, metalloids, PAHs) is well known when they are exposed in open air and fixed positions, poor data exist on their potential ability in other exposure conditions. For example, few data are available on pollutant bioaccumulation by bags exposed indoors (Canha et al., 2014; Capozzi et al., 2019; Sorrentino et al., submitted; Zechmeister et al., 2020); and, to our knowledge, no data have been published so far on moss bags exposed in moving systems. These data are of fundamental importance for a global evaluation of the risk level related to the exposure to airborne pollutants. In many cities people reach their workplace or school by bikes or motorcycles to escape vehicular traffic and overcrowded public transport. Over the past year, due to the Covid 19 pandemic, we have seen a surge in the sale of bicycles, pedal assisted electric bikes, electric mopeds, and scooters to avoid the crowded wagons of the subway.

Based on all of the above reported, the aim and novelty of this work was to test by magnetic and chemical analysis by ICP-MS the potentiality of mobile moss-bags fixed to bicycles to intercept airborne metal(loid)s. Taking into account the proved sensitivity of moss-bags to discriminate different levels of airborne pollutants even between relatively close areas (Capozzi et al., 2016a), we hypothesized that moss-bags can be profitably used for the biomonitoring of air quality in moving systems; therefore, in this pilot work we aimed to provide answers to the following questions:

i) Can the "mobile" moss-bags accumulate airborne elements and what are, if any, the criticisms to be considered to customize the moss-bag technique to the moving exposure condition? ii) Can the mobile bags discriminate among different land uses routes? iii) Is it possible to estimate the magnitude of the exposure to metal pollution in mobile systems, in comparison with fixed position?

The results are discussed in a methodological view to provide a first guideline to this new approach.

## 2. Materials and Methods

### 2.1 Moss material, study area and experimental design

For the present study, the moss *Hypnum cupressiforme* Hedw. was chosen as plant material, collected in Italy at the Taburno-Camposauro Regional Park (1000 m s.l.m. - Lat. N 41.105094°,

Long. E 14.593559°); the preparation of moss and bags followed the description reported in Sorrentino et al. (submitted).

In parallel, two experimental designs were carried out in and around the city of Antwerp (N 51.22°, E 4.40°) in the Flanders region (northern Belgium) during the period of March-June 2019. The first design involved six volunteer cyclists who carried three moss-bags each on their bicycles (hereafter named 1U to 6U) on their daily commute to work through urban areas for 50 days (Table S1). In the second, a single volunteer rode with a bicycle on four routes in selected areas in and around the city for 22 days, carrying three moss bags for each route. Specifically, the four routes in the city of Antwerp were chosen covering areas characterized by different land uses (Fig. 1): i) an urban area in the city center of Antwerp along heavily trafficked motorway, ring and national roads and street canyons (7U); ii) an industrial route in the Hoboken area , in the southern outskirts of Antwerp city, where there are non-ferrous metallurgical plants and a cement industry (7I); iii) a green route in Kruibeke, a small community south-east of Antwerp, on the left bank of the Scheldt river through agricultural and green areas (7G); iv) a fourth route (7T) was represented by the complete path including the three routes above described and all the connecting streets among them. For each route, the three bags were attached to the handlebar of the bike by means of a nylon rope at three different heights, about 15 cm apart from each other, figure 2.


Figure 2 - The arrangement of the bicycle hosting the bags in triplicate. Bag position: proximal - P; middle - M; distal - D.

Table S1. For each route travelled by the six volunteers (1U to 6U), the total distance traveled (km) with moss exposed on their bikes, the total exposure time (h) of the moss bags, and the average speed (km/h).

| | Route (km) | Exposure time (h) | Average speed (km/h) |
|---|---|---|---|
| 1U | 300 | 25 | 12 |
| 2U | 297 | 22 | 13.5 |
| 3U | 310 | 25 | 12.4 |
| 4U | 180 | 13 | 13.8 |
| 5U | 1700 | 93 | 18.3 |
| 6U | 340 | 22 | 15.4 |

The 7th bicycle was equipped with four triplets of bags, each to be exposed during a specific route, and then covered. This bicycle was also equipped with a PM sampler (Nova SDS01) measuring the amount of PM 2.5 and PM 10 (1 minute frequency) with the inlet attached at the same height as the exposed moss bags.

Each volunteer exposed the moss bags during the journey, took note of the date and time of the start / end of the exposure, and covered the moss bags with plastic bags at the end of each route, to avoid further element accumulation while bags stayed in fixed position.

**2.2 SIRM analysis**

SIRM analysis was carried out according to Sorrentino et al. (submitted). After exposure, the moss bags were dried in an oven (Memmert) at 40 °C for 72 h. Then, all moss samples (three replicas for each route plus 4 unexposed moss samples as controls) were weighed and tightly packed in transparent film to avoid any possible movement during the analysis and placed inside the appropriate plastic container.

All the samples were individually magnetized in a direct current (DC) field of 800 mT with a Molspin pulse magnetizer (Molspin Ltd, UK) (Kardel et al., 2011, Hofman et al., 2017). Immediately after, the remanent magnetization of the samples (A $m^{-1}$) was measured twice using a JR-6 spinner magnetometer (AGICO, Czech Republic) with high sensitivity (2.4 $10^{-6}$ A $m^{-1}$). The instrument was calibrated with a standard and the measured values were corrected for the sample holder containing a similar amount of cling film. The methodology is described in detail by Castanheiro et al. (2020). The SIRM was normalized for post-exposure moss dry mass (g) and the size of the plastic container, obtaining mass-normalized SIRM values, expressed in $10^{-6}$ A $m^2$ $kg^{-1}$.

### 2.3 Chemical analysis

Chemical analysis was performed following Sorrentino et al. (submitted). In brief, in each moss sample, the concentration of 28 elements (Al, Ag, As, Be, Ca, Cd, Co, Cr, Cu, Fe, Hg, K, Mg, Mn, Mo, Na, Ni, Pb, Pd, Rb, Sb, Si, Sr, Ti, Tl, U, V, Zn) were measured by HR-ICP-MS or ICP-OES (for Ca, K, Mg and Na). Moss samples were weighed and acid-digested in glass tubes with 2 ml of $HNO_3$ and 6 ml of HCl at 100°C, over-night. After this step, 0.5 ml of $H_2O_2$ was added for digestion into a microwave digester (Discover SP-D, CEM). Digestion was carried out at 180°C, ramp time 5 minutes and hold time 5 minutes. The digested solution was transferred to plastic tubes and added deionized water until 40 ml. Elements were considered accumulated when their post-exposure concentration was higher than the pre-exposure concentration + 2*SD (Couto et al., 2004 as modified in Ares et al., 2015). For quality control of the analysis, the certified reference plant material (Certified Reference Material BCR® – 679, white cabbage) was analyzed in parallel with samples. For the elements indicated in the certified material, the percentages of recovery were in the range of acceptability, specifically from 80% to 105% (Ca 99.63%, Cd 80.15%, Cr 84.80%, Cu 91.55%, Fe 95.13%, Mg 89.28%, Mn 92 %, Ni 99.35%, Sr 85.69%, Zn 88.49%), and below 80% for As (60.42%). The data were normalized considering the dilution factor and the mass of each sample.

### 2.4 PM sampling

The bicycle of the volunteer 7 (who moved along urban, green, industrial and total routes) was equipped with PM sampler for PM 2.5 and PM 10 (Nova SDS01, PM 2.5 and PM 10). This sampler measured every minute the amount of PM during each route. Based on the annotation of the starting and ending times of each route, the PM values measured every day could be assigned to a specific route.

## 2.5 Data analyses

Raw data of SIRM and elements were processed by excel to calculate mean values and standard deviation. The threshold to determine element accumulation in each sample was fixed in the limit of quantification of the technique (LOQT), calculated from the initial concentrations as follows: xCi + 2sCi, where xCi is the mean value of the initial concentration in unexposed moss samples (n = 4) for each element determined, and sCi is the corresponding standard deviation (Couto et al., 2004 as modified in Ares et al., 2015).

The daily flux for each element was calculated according to Capozzi et al., 2020, using the following formula:

$\Theta DF=[M]acc*(2*SLA*d)^{-1}$

where ΘDF is the deposition flux [µg $m^{-2}$ $d^{-1}$]; [M]acc is the concentration of each element (expressed as µg $kg^{-1}$) accumulated during the exposure period, obtained by subtracting the pollutant concentration found in pre-exposure moss from that measured after the exposure; SLA = specific leaf area, i.e. fresh leaf area ($m^2$)/dry weight (kg); d is the exposure time expressed in days.

Spearman Rank Order Correlation was performed to assess the correlation between the element accumulation and the SIRM signal. Also, an ANOVA was carried out to check for significant differences in elemental fluxes and SRIM data (these latter normalized for the exposure time) among all the routes.

The T-test for independent samples was used to compare element accumulation by bike vs fixed position (Sorrentino et al., submitted) in the same study area on a total of seven urban sites and seven routes (n=21, both for fixed and for mobile bags). For the multiple comparisons, we used false discovery rate (FDR) adjusted p-values using the Benjamini-Hochberg's correction.

To compare the PM values to the element data, elemental fluxes were normalized to each maximum value (i.e., between 0 and 1) to equally weigh all the elements. Then, normalized fluxes of each element were summed to obtain total normalized flux calculated at each route to be compared to the averaged PM 10 and PM 2.5 amount. To test the significance among replicas (proximal, middle, and distal bags) exposed along the different routes the elemental contents were scored between 1 to 3, according to their lower-higher element content measured in each sample, and summed in each bag class (i.e., proximal, middle, and distal) to express the level of total element load for each class. The difference between bag classes was tested by ANOVA.

## 3. Results

### 3.1 SIRM analysis

The SIRM value of the unexposed moss was 3141 μA $m^2$ $kg^{-1}$ ± 183 (n=4, Table 1). The SIRM values of the exposed mosses ranged between the value of 2283 μA $m^2$ $kg^{-1}$ (lower than unexposed moss) recorded at 2U route, and 4498 μA $m^2$ $kg^{-1}$ measured at 7I route.

Table 1. SIRM values (μA $m^2$ $kg^{-1}$) for unexposed moss (mean and standard deviation SD; n=4) and for each replica, mean replica value (n=3) and SD for exposed moss. For route codes, see the text.

| | SIRM value | Mean | SD | CV |
|---|---|---|---|---|
| **BL (n=4)** | | 3141 | 183 | 0.06 |
| **U1.1** | 2813 | | | |
| **U1.2** | 2456 | | | |
| **U1.3** | 2663 | 2644 | 179 | 0.07 |
| **U2.1** | 2258 | | | |
| **U2.2** | 2370 | | | |
| **U2.3** | 2220 | 2283 | 78 | 0.03 |
| **U3.1** | 3639 | | | |
| **U3.2** | 3826 | | | |
| **U3.3** | 3432 | 3632 | 197 | 0.05 |
| **U4.1** | 3601 | | | |
| **U4.2** | 3789 | | | |
| **U4.3** | 3696 | 3695 | 94 | 0.03 |
| **U5.1** | 4059 | | | |
| **U5.2** | 4095 | | | |
| **U5.3** | 3841 | 3998 | 137 | 0.03 |
| **U6.1** | 3264 | | | |
| **U6.2** | 3216 | | | |
| **U6.3** | 3283 | 3254 | 35 | 0.01 |
| **U7.1** | 3116 | | | |
| **U7.2** | 3065 | | | |
| **U7.3** | 3002 | 3061 | 57 | 0.02 |
| **I7.1** | 4733 | | | |
| **I7.2** | 4510 | | | |
| **I7.3** | 4251 | 4498 | 241 | 0.05 |
| **G7.1** | 4051 | | | |
| **G7.2** | 3923 | | | |
| **G7.3** | 3951 | 3975 | 67 | 0.02 |
| **T7.1** | 4493 | | | |
| **T7.2** | 4065 | | | |
| **T7.3** | 3917 | 4159 | 299 | 0.07 |

The SIRM data were always consistent in the three moss replicas exposed at each route. The mean SIRM value, once subtracted from the pre-exposure value, was positive at all routes apart from 1U, 2U and 7U, with the highest value recorded at 7I. ANOVA based on SIRM values

normalized on the exposure times, h indicated a significant difference ($p<0.05$) among the magnetic signals measured in the different land uses with I>G>U. A positive, significant correlation was found between the SIRM signal and some elements (Table 2), including the magnetizable Co and Ni.

Table 2. Correlation coefficient, t-value, and p-value of the relationship between SIRM and elements of the exposed moss.

| | R | t(N-2) | P |
|---|---|---|---|
| Ag | 0.609 | 4.071 | 0.000 |
| As | 0.582 | 3.789 | 0.000 |
| Cd | 0.607 | 4.038 | 0.000 |
| Co | 0.509 | 3.131 | 0.004 |
| Hg | 0.494 | 3.007 | 0.005 |
| Ni | 0.451 | 2.673 | 0.012 |
| Pb | 0.638 | 4.392 | 0.000 |

### 3.2 Chemical analysis: element accumulation and flux

Element concentrations in each moss sample, mean values, and standard deviations, are reported in Table S2 and Table S3. Elemental concentration found in each replica (Table S2) evidenced a great variability among samples carried along the same route. This is especially evident for Ag, K, Mg and Mo. The more proximal bag sometimes did not accumulate a given element (according to our criterion, see M&M), even when the other two bags did. The proximal bags showed a significantly lower total element load compared to the middle and distal bags (Fig. 3). Of the 28 elements examined, 10 elements (Be, Cu, Fe, Mn, Pd, Rb, Sr, Tl, U and V) never accumulated in a moss replica (i.e., these elements did not pass the fixed threshold); Al, Ca, Co, Mg, and Mo accumulated in some replicas, but the mean value (n=3) for each route does not fulfill the accumulation threshold (LOQt; criterion). All the other elements accumulated in the moss bags at least along one of the routes, with a minimum of 3 elements at the route 2U (Sb, Si and Ti) and a maximum of 10 elements (Ag, As, Cd, Hg, Ni, Pb, Sb, Si, Ti and Zn) at 7T route. The most accumulated elements were Si and Ti, found in 10 routes out of 10; Sb, in 9 routes; Ni, in 6 routes.

Table S2. Mean element content (µg $Kg^{-1}$ DW) in pre-exposed moss (BL) and standard deviation (SD); LOQT (limit of quantification of the technique; see the text for details); element content in each moss sample. Concentrations higher than LOQT are marked in light pink. All element concentrations and LOQT are expressed as µg $Kg^{-1}$ DW.

| | | Ag | Al | As | Ca | Cd | Co | Cr | Hg | K | Mg | Mo | Na | Ni | Pb | Si | Sb | Ti | Zn |
|---|---|---|---|---|---|---|---|---|---|---|---|---|---|---|---|---|---|---|---|
| BL | mean (n=4) | 0.045 | 5817 | 0.873 | 2097 | 0.065 | 0.823 | 2.380 | 0.117 | 1849 | 887 | 0.293 | 8258 | 2.40 | 4.37 | 1922 | 0.275 | 23.1 | 23.8 |
| | SD | 0.015 | 481 | 0.037 | 284 | 0.015 | 0.043 | 0.048 | 0.005 | 70 | 45 | 0.065 | 349 | 0.09 | 0.21 | 54 | 0.067 | 0.6 | 1.8 |
| | **LOQT** | 0.076 | 6779 | 0.948 | 2665 | 0.096 | 0.909 | 2.477 | 0.127 | 1988 | 977 | 0.423 | 8956 | 2.58 | 4.80 | 2030 | 0.408 | 24.3 | 27.5 |
| | **1U** | 0.047 | 5422 | 0.790 | 1783 | 0.043 | 0.605 | 2.397 | 0.087 | 1994 | 809 | 0.446 | 8790 | 2.86 | 4.57 | 2575 | 1.603 | 30.2 | 25.7 |
| | **1U** | 0.034 | 5303 | 0.918 | 3267 | 0.057 | 0.458 | 1.495 | 0.100 | 2104 | 904 | 0.342 | 8729 | 2.60 | 4.27 | 3049 | 2.465 | 47.8 | 27.3 |
| | **1U** | 0.023 | 4915 | 0.884 | 1800 | 0.011 | 0.571 | 1.727 | 0.087 | 1856 | 812 | 0.193 | 8553 | 2.26 | 3.74 | 2544 | 1.228 | 27.1 | 24.3 |
| | **2U** | 0.053 | 4855 | 0.661 | 1838 | 0.021 | 0.500 | 1.649 | 0.086 | 1836 | 829 | 0.187 | 8736 | 2.10 | 3.71 | 2532 | 0.887 | 30.4 | 23.8 |
| | **2U** | 0.030 | 5445 | 0.787 | 2567 | 0.027 | 0.581 | 1.765 | 0.084 | 1896 | 883 | 0.200 | 8407 | 2.06 | 3.89 | 2861 | 0.874 | 32.4 | 24.3 |
| | **2U** | 0.042 | 5855 | 0.829 | 1826 | 0.048 | 0.656 | 1.799 | 0.097 | 1836 | 848 | 0.229 | 8228 | 2.33 | 4.12 | 2712 | 0.687 | 28.0 | 25.1 |
| | **3U** | 0.038 | 5988 | 0.816 | 1564 | 0.077 | 0.671 | 2.150 | 0.104 | 1664 | 771 | 0.274 | 7519 | 2.38 | 3.95 | 2515 | 0.333 | 25.1 | 29.2 |
| | **3U** | 0.072 | 5622 | 0.836 | 2405 | 0.035 | 0.618 | 1.494 | 0.092 | 1748 | 810 | 0.226 | 7659 | 2.10 | 4.09 | 2721 | 0.330 | 31.5 | 22.9 |
| | **3U** | 0.032 | 5243 | 0.766 | 1656 | 0.023 | 0.695 | 1.952 | 0.101 | 1753 | 819 | 0.228 | 8230 | 2.28 | 3.78 | 2387 | 0.271 | 24.2 | 22.5 |
| | **4U** | 0.170 | 5221 | 0.930 | 2328 | 0.096 | 0.817 | 2.251 | 0.115 | 4174 | 1037 | 0.327 | 11329 | 4.46 | 4.42 | 2213 | 2.593 | 24.5 | 34.0 |
| | **4U** | 0.046 | 4744 | 0.731 | 2008 | 0.013 | 0.680 | 1.826 | 0.099 | 2422 | 969 | 0.266 | 9118 | 2.59 | 3.78 | 2690 | 2.967 | 31.8 | 27.8 |
| | **4U** | 0.034 | 6097 | 0.740 | 1762 | 0.032 | 0.667 | 1.967 | 0.100 | 1962 | 844 | 0.227 | 8578 | 2.33 | 3.87 | 2152 | 1.730 | 22.6 | 26.1 |
| | **5U** | 0.086 | 4739 | 0.918 | 2509 | 0.020 | 0.728 | 2.497 | 0.095 | 2194 | 1074 | 0.457 | 9041 | 2.62 | 4.88 | 2691 | 2.978 | 31.0 | 40.6 |
| | **5U** | 0.078 | 4115 | 0.629 | 2416 | 0.039 | 0.487 | 2.438 | 0.081 | 1829 | 938 | 0.360 | 7632 | 2.98 | 4.06 | 2785 | 2.076 | 35.9 | 42.0 |
| | **5U** | 0.044 | 5466 | 0.869 | 1924 | 0.033 | 0.731 | 2.272 | 0.101 | 1930 | 909 | 0.282 | 8276 | 2.69 | 4.09 | 2511 | 1.948 | 27.2 | 32.8 |
| | **6U** | 0.094 | 5922 | 0.916 | 2165 | 0.044 | 0.815 | 3.812 | 0.114 | 2268 | 1026 | 0.448 | 9425 | 5.82 | 4.62 | 2029 | 1.968 | 23.5 | 33.0 |
| | **6U** | 0.049 | 4803 | 0.779 | 1853 | 0.074 | 0.644 | 1.713 | 0.101 | 1991 | 838 | 0.267 | 8474 | 2.37 | 4.07 | 2349 | 2.179 | 24.2 | 28.4 |
| | **6U** | 0.054 | 5064 | 0.773 | 1954 | 0.026 | 0.645 | 2.192 | 0.099 | 1952 | 905 | 0.229 | 8598 | 2.59 | 4.04 | 2480 | 2.228 | 27.0 | 28.0 |
| | **7U** | 0.036 | 4582 | 1.088 | 2054 | 0.042 | 0.577 | 1.708 | 0.091 | 1834 | 859 | 0.173 | 8099 | 2.29 | 4.91 | 3091 | 1.734 | 38.1 | 26.2 |
| | **7U** | 0.047 | 4077 | 0.896 | 1773 | 0.036 | 0.598 | 1.542 | 0.101 | 1854 | 836 | 0.198 | 8141 | 2.31 | 4.10 | 2445 | 1.190 | 26.7 | 23.1 |
| | **7U** | 0.051 | 6737 | 0.860 | 2189 | 0.057 | 0.713 | 2.067 | 0.113 | 2032 | 951 | 0.252 | 8860 | 2.37 | 4.08 | 2256 | 0.614 | 25.5 | 22.8 |
| | **7I** | 0.334 | 4102 | 2.619 | 1260 | 0.199 | 0.468 | 1.226 | 0.094 | 1386 | 565 | 0.156 | 6220 | 3.61 | 14.46 | 1921 | 1.666 | 20.8 | 19.1 |
| | **7I** | 0.277 | 5901 | 2.710 | 1883 | 0.113 | 0.821 | 1.597 | 0.126 | 2062 | 1007 | 0.225 | 8556 | 4.36 | 16.63 | 2727 | 1.565 | 32.5 | 26.4 |
| | **7I** | 0.287 | 8082 | 2.555 | 1867 | 0.141 | 0.916 | 1.592 | 0.118 | 2067 | 1003 | 0.217 | 8367 | 4.09 | 13.98 | 2791 | 1.410 | 31.1 | 25.8 |
| | **7G** | 0.042 | 7126 | 1.075 | 1907 | 0.060 | 0.821 | 1.658 | 0.112 | 1933 | 912 | 0.253 | 7774 | 2.50 | 4.69 | 2477 | 0.533 | 26.5 | 23.0 |
| | **7G** | 0.081 | 6725 | 1.122 | 1774 | 0.047 | 0.701 | 1.630 | 0.091 | 1894 | 911 | 0.207 | 8127 | 2.26 | 4.70 | 2762 | 0.386 | 29.1 | 22.1 |
| | **7G** | 0.046 | 4765 | 0.977 | 1679 | 0.061 | 0.601 | 1.376 | 0.096 | 1858 | 864 | 0.184 | 8482 | 2.12 | 4.40 | 2700 | 0.352 | 26.1 | 21.9 |
| | **7T** | 0.431 | 5385 | 5.285 | 2012 | 0.464 | 0.855 | 1.940 | 0.151 | 1931 | 909 | 0.296 | 8163 | 6.62 | 27.15 | 2579 | 2.792 | 27.6 | 32.6 |
| | **7T** | 0.296 | 6205 | 4.974 | 1980 | 0.294 | 0.919 | 1.933 | 0.139 | 1767 | 869 | 0.305 | 7344 | 6.97 | 19.75 | 2715 | 2.580 | 28.8 | 30.7 |
| | **7T** | 0.289 | 5156 | 4.743 | 1956 | 0.317 | 0.731 | 1.810 | 0.128 | 2047 | 943 | 0.230 | 8918 | 6.40 | 18.80 | 2737 | 2.395 | 33.3 | 31.8 |

Table S3. Mean element concentrations and SD (n=3, mg $Kg^{-1}$) measured for each route at the end of experiment; the element content and the standard deviation of the pre-exposed moss is indicated as BL (baseline).

| | Ag | Al | As | Be | Ca | Cd | Co | Cr | Cu | Fe | Hg | K | Mg | Mn |
|---|---|---|---|---|---|---|---|---|---|---|---|---|---|---|
| BL | 0.04±0.01 | 5817±480 | 0.87±0.03 | 0.46±0.1 | 2096±283 | 0.06±0.01 | 0.82±0.04 | 2.38±0.04 | 13.6±6.02 | 2150±59.4 | 0.11±0.00 | 1848±69.6 | 886±44.9 | 55.6±0.85 |
| 1U | 0.03±0.01 | 5213±264 | 0.86±0.06 | 0.2±0.11 | 2283±851 | 0.03±0.02 | 0.54±0.07 | 1.87±0.46 | 11.4±0.42 | 1567±95.5 | 0.09±0.00 | 1984±124 | 841±54 | 42.9±1.89 |
| 2U | 0.04±0.01 | 5385±502 | 0.75±0.08 | 0.11±0.06 | 2076±424 | 0.03±0.01 | 0.57±0.07 | 1.73±0.07 | 10.1±0.13 | 1636±134 | 0.08±0.00 | 1855±34.4 | 853±27.3 | 42.8±2.7 |
| 3U | 0.04±0.02 | 5617±372 | 0.8±0.03 | 0.22±0.02 | 1875±461 | 0.04±0.02 | 0.66±0.03 | 1.86±0.33 | 10.1±0.38 | 1767±213 | 0.09±0.00 | 1722±49.9 | 799±25.6 | 46.3±5.63 |
| 4U | 0.08±0.07 | 5353±686 | 0.8±0.11 | 0.26±0.05 | 2032±283 | 0.04±0.04 | 0.72±0.08 | 2.01±0.21 | 15.3±5.85 | 1814±84.6 | 0.1±0.00 | 2852±1167 | 949±98.1 | 47.1±1.41 |
| 5U | 0.06±0.02 | 4773±676 | 0.8±0.15 | 0.18±0.09 | 2282±314 | 0.03±0.00 | 0.64±0.14 | 2.4±0.11 | 21±2.71 | 1849±253 | 0.09±0.01 | 1984±188 | 973±88 | 46.4±4.87 |
| 6U | 0.06±0.02 | 5262±585 | 0.82±0.08 | 0.2±0.03 | 1990±158 | 0.04±0.02 | 0.7±0.09 | 2.57±1.1 | 12.6±1.59 | 1900±300 | 0.1±0.00 | 2070±172 | 923±95.4 | 49.6±3.89 |
| 7U | 0.04±0.00 | 5132±1412 | 0.94±0.12 | 0.18±0.11 | 2005±211 | 0.04±0.01 | 0.62±0.07 | 1.77±0.26 | 10.4±0.47 | 1746±176 | 0.1±0.01 | 1906±109 | 881±61 | 44.1±2.65 |
| 7I | 0.29±0.03 | 6028±1993 | 2.62±0.07 | 0.21±0.08 | 1670±355 | 0.15±0.04 | 0.73±0.23 | 1.47±0.21 | 15.8±1.29 | 1739±463 | 0.11±0.01 | 1838±391 | 858±253 | 42.1±11.1 |
| 7G | 0.05±0.02 | 6205±1263 | 1.05±0.07 | 0.18±0.02 | 1786±114 | 0.05±0.00 | 0.7±0.11 | 1.55±0.15 | 9.78±0.26 | 1719±200 | 0.09±0.01 | 1894±37.4 | 895±27.4 | 43.1±4.19 |
| 7T | 0.33±0.07 | 5582±551 | 5±0.27 | 0.15±0.00 | 1982±28.3 | 0.35±0.09 | 0.83±0.09 | 1.89±0.07 | 22.8±1.31 | 1921±72.4 | 0.13±0.01 | 1914±140 | 907±37 | 49.7±3.19 |

| | Mo | Na | Ni | Pd | Pb | Rb | Si | Sb | Sr | Ti | Tl | U | V | Zn |
|---|---|---|---|---|---|---|---|---|---|---|---|---|---|---|
| BL | 0.29±0.06 | 8257±349 | 2.4±0.08 | BDL | 4.36±0.21 | 6.93±0.44 | 1922±53.8 | 0.27±0.06 | 17.7±0.87 | 23.1±0.56 | 0.18±0.04 | 0.27±0.01 | 7.28±0.28 | 23.7±1.83 |
| 1U | 0.32±0.12 | 8690±122 | 2.57±0.3 | BDL | 4.19±0.42 | 3.24±0.29 | 2722±282 | 1.76±0.63 | 15.5±3.18 | 35±11.10 | 0.17±0.04 | 0.22±0.01 | 4.05±0.87 | 25.7±1.52 |
| 2U | 0.2±0.02 | 8456±257 | 2.16±0.14 | BDL | 3.9±0.2 | 1.86±0.98 | 2701±164 | 0.81±0.11 | 12.9±1.29 | 30.2±2.21 | 0.16±0.00 | 0.22±0.03 | 4.53±0.33 | 24.4±0.64 |
| 3U | 0.24±0.02 | 7802±376 | 2.25±0.14 | BDL | 3.93±0.15 | 2.56±1.09 | 2541±168 | 0.31±0.03 | 12.2±0.92 | 26.9±3.96 | 0.17±0.01 | 0.24±0.00 | 5.1±0.85 | 24.8±3.72 |
| 4U | 0.27±0.05 | 9674±1457 | 3.12±1.15 | BDL | 4.02±0.34 | 3.11±1.34 | 2351±294 | 2.42±0.63 | 11.5±0.85 | 26.2±4.86 | 0.17±0.01 | 0.24±0.00 | 5.33±0.52 | 29.2±4.16 |
| 5U | 0.36±0.08 | 8316±705 | 2.76±0.19 | BDL | 4.34±0.46 | 2.07±0.36 | 2662±139 | 2.33±0.56 | 10.9±1.00 | 31.3±4.37 | 0.16±0.02 | 0.21±0.02 | 4.99±1.47 | 38.4±4.96 |
| 6U | 0.31±0.11 | 8832±516 | 3.59±1.93 | BDL | 4.24±0.32 | 2.61±0.96 | 2254±284 | 2.12±0.13 | 10.7±0.68 | 24.8±1.83 | 0.17±0.00 | 0.23±0.00 | 5.43±1.23 | 29.7±2.78 |
| 7U | 0.2±0.04 | 8366±427 | 2.32±0.04 | BDL | 4.36±0.47 | 1.76±0.77 | 2597±437 | 1.17±0.56 | 10.7±1.04 | 30.1±6.98 | 0.16±0.01 | 0.22±0.02 | 4.15±1.01 | 24±1.86 |
| 7I | 0.19±0.03 | 7714±1297 | 4.02±0.37 | BDL | 15±1.41 | 1.69±1.06 | 2479±484 | 1.54±0.12 | 10.4±2.9 | 28.1±6.37 | 0.17±0.03 | 0.23±0.06 | 4.13±1.05 | 23.8±4.06 |
| 7G | 0.21±0.03 | 8127±353 | 2.29±0.19 | BDL | 4.59±0.17 | 2.48±0.81 | 2646±150 | 0.42±0.09 | 12±1.25 | 27.2±1.64 | 0.18±0.02 | 0.23±0.01 | 4.12±0.57 | 22.3±0.57 |
| 7T | 0.27±0.04 | 8141±787 | 6.66±0.28 | BDL | 21.9±4.57 | 2.01±0.75 | 2676±85.7 | 2.58±0.19 | 13±1.21 | 29.8±3.00 | 0.19±0.01 | 0.25±0.01 | 4.68±0.39 | 31.6±0.92 |

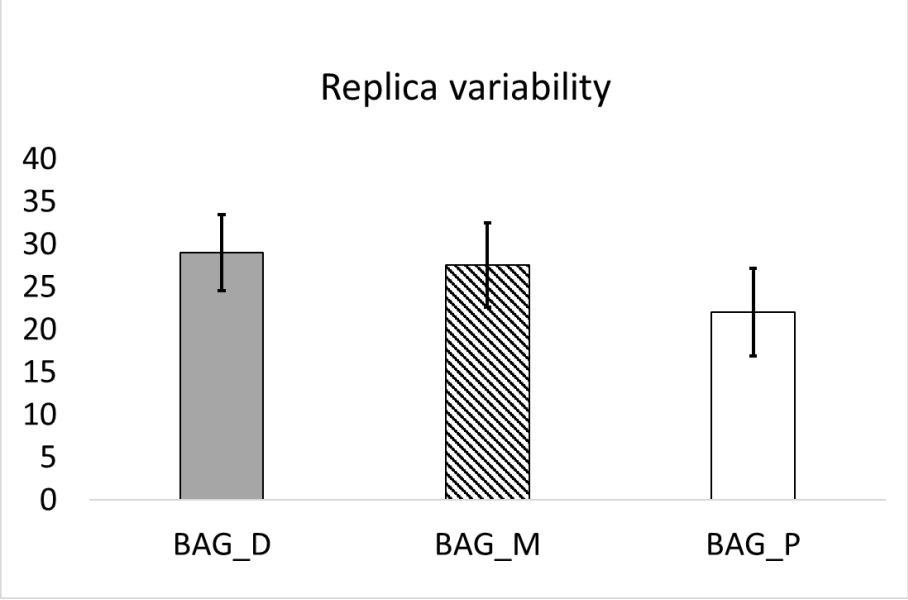


Figure 3. – Total element load for each bag position (proximal: P; middle: M; distal: D). Replicas were scored based on their element content between 1 and 3, where 3 represents the highest content and 1 the lowest. The scores of each element were summed to obtain total element load (y axis) and the means values were compared by ANOVA. * $p<0.05$ according to Tuckey's post-hoc test.

Apart from the route 7T, including 7U, 7I, 7G and connecting paths, where the moss-bags were exposed for the longest time, several elements of environmental concern (As, Cd, Ni and Pb) showed the highest concentrations in 7I (Tables S2 and S3); however, because of the high

overlap of the accumulation signal among the routes (see standard deviations), only for As Cd and Pb there was a significant difference between 7I and the other site typology. It is worth noting that these elements had generally low concentration at 7G, a route embedded in a green area, in which high concentrations of terrigenous elements, as Al and Si were measured.

The element fluxes (Table S4) reflected the trend of element accumulations along each route. Specifically, they highlighted element daily fluxes rather homogeneous along U routes, except for 4U, showing higher fluxes for Na, K, and Sb (the highest, Fig. 4), compared to the other U routes. In agreement with elemental contents, flux was highest in 7I (significantly higher for Ag, As, Cd and Pb)

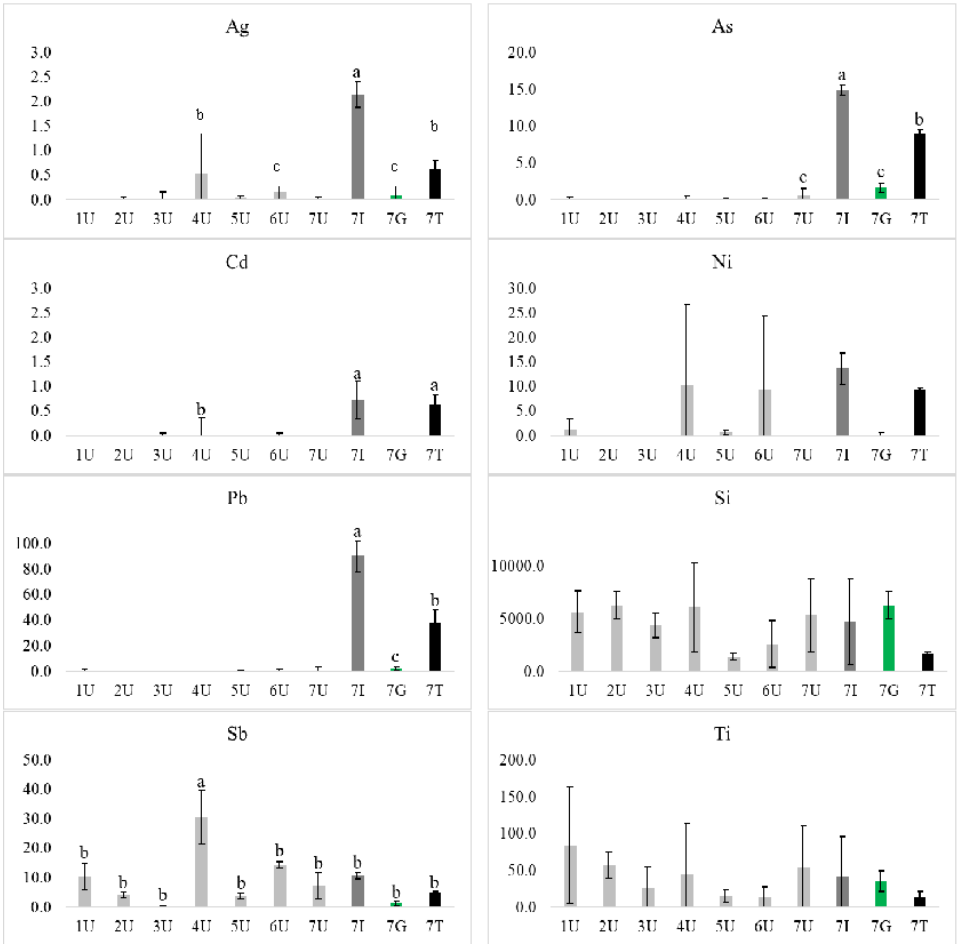


Figure 4 – Daily deposition flux (µg $m^{-2}$ $d^{-1}$) for several accumulated elements measured at each route. Different letters indicate significant differences between routes ($p<0.05$).

Table S4. Daily deposition flux (μg $m^{-2}$ $d^{-1}$) of accumulated elements along each route. Different letters indicate significant differences according to Tukey's post-hoc test ($p<0.05$)

| | Ag | As | Cd | Cr | Hg | K | Na | Ni | Pb | Si | Sb | Ti | Zn |
|---|---|---|---|---|---|---|---|---|---|---|---|---|---|
| **1U** | 0.009e | 0.194d | 0 | 0.122b | 0 | 967c | 3078b | 2.351c | 1.436c | 5691b | 10.60b | 84.62a | 14.14c |
| **2U** | 0.059d | 0 | 0 | 0 | 0 | 379d | 2535c | 0 | 0 | 6297b | 4.37c | 57.61b | 5.15d |
| **3U** | 0.190c | 0 | 0.083d | 0 | 0 | 0 | 0 | 0 | 0 | 4401c | 0.40d | 26.86c | 38.14b |
| **4U** | 0.886b | 0.798c | 0.438c | 0 | 0 | 14278a | 20154a | 15.952a | 0.730c | 6106b | 30.65a | 71.43a | 77.87a |
| **5U** | 0.069d | 0.084d | 0 | 0.166b | 0 | 405d | 762 | 0.689d | 0.967c | 1408d | 3.92c | 15.70d | 27.95b |
| **6U** | 0.160c | 0.333d | 0.067d | 11.192a | 0 | 1732b | 4489b | 14.087a | 1.953c | 2599d | 14.46b | 13.60d | 46.94b |
| **7U** | 0.028e | 0.937c | 0 | 0 | 0 | 743c | 4759b | 0 | 4.272c | 5333c | 7.15b | 55.00b | 18.78c |
| **7I** | 2.147a | 14.855a | 0.727a | 0 | 0.039b | 1826b | 1726c | 13.707a | 90.200a | 7083a | 10.77b | 73.45a | 19.89c |
| **7G** | 0.155c | 1.603c | 0 | 0 | 0 | 401d | 1946c | 0.823d | 1.963c | 6296b | 1.29c | 35.51c | 0 |
| **7T** | 0.635b | 8.948b | 0.636b | 0 | 0.048a | 304d | 1432c | 9.236b | 38.007b | 1636d | 5.02c | 14.65d | 17.13c |

### 3.3 Comparison between moving and static moss-bags

A comparison for the element accumulated in bags exposed in fixed positions or in bike in the urban area of Antwerp (data from Sorrentino et al., submitted), was carried out by averaging data obtained for the seven U routes, and data from bags exposed in fixed position in urban environment, for the same element. This comparison highlighted fluxes significantly higher for moss exposed in bikes compared to moss exposed in fixed position, for the elements Mg, Sb, Si, Ti and Zn (Fig. 5). The boxplots also evidenced heterogeneity of replicas in moss samples exposed in bikes.

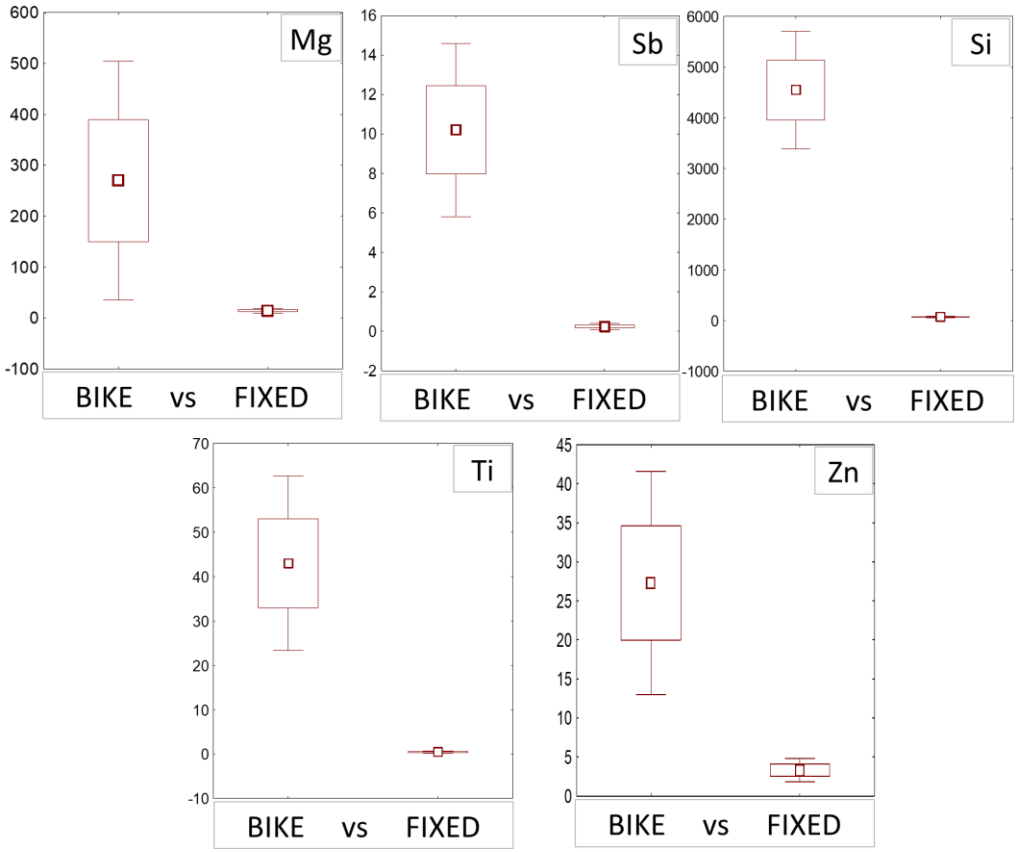


Figure 5. Comparison between fluxes (y axis; µg $m^{-2}$ $d^{-1}$) calculated in mosses exposed by bike and in fixed position (n=21), both in urban environments in Antwerp. Square: Mean; box: Mean±SE; Whiskers: Mean±1.96*SE. For all the comparisons $p<0.05$, according to the T-test for independent samples.

Both chemical mean content (Table S3) and daily flux of specific elements (Fig. 5) evidenced a large variability measured in the three moss replicas, especially for terrigenous elements (Si and Ti). Nevertheless, a decreasing trend of the element content was generally observed passing from the distal to the proximal bag of each triplet (i.e., the proximal bag generally up-took lower amounts).

### 3.4 Particulate matter

Average values of daily PM10 and PM2.5 (expressed in $\mu g/m^3$) recorded along each route were significantly correlated according to Spearman's rank correlation test ($p<0.05$). For both PM fractions, the maximum amounts were found along the I route, followed by U, T and G routes. The comparison between PM and element data (i.e., summation of normalized fluxes calculated for each element along each route typology; Table 3) indicated a similar trend between the two data sets (i.e., element fluxes and PM significantly correlated according to Spearman's rank correlation test, $p<0.05$).

Table 3. Summation of normalized fluxes, PM 10 and PM 2.5 ($\mu g/m^3$)

| | ∑ Normalized fluxes | PM 10 | PM 2.5 |
|---|---|---|---|
| U | 6.815 | 23.348 | 9.746 |
| I | 10.475 | 25.910 | 9.947 |
| G | 2.287 | 20.351 | 3.050 |
| T | 5.692 | 21.906 | 9.051 |

### Discussion

The ability of the moss bags to entrap airborne pollutants from mobile sources, for example car or aircraft engines, was already known (e.g., Giordano et al., 2010; Turgut et al., 2019). Also, the idea of mobile monitoring as an innovative tool providing valuable insights into personal exposure to atmospheric pollution is already reported in the literature. Hofman et al. (2017) investigated indeed, the exposure of a cyclist to black carbon, ultrafine particles, and heavy metals deposited on filters, and found that the exposure was significantly higher (while the cyclist commuted) along vehicle trafficked routes than bicycle highway route. However, the different experimental designs, the different methodology, as well as the different analyses carried out do not allow any comparison with the present biomonitoring study.

Our work demonstrated, for the first time, the feasibility of the moss bags to take up airborne elements while carried by bicycles. The results however, highlighted a wide variance of the elemental content among replicas; specifically, element concentrations seemed affected by the bag position (with a lower, although not statistically different, element content generally found in the proximal bag). To escape replica variability in elemental content, and gain more reliable results, the exposure protocol should be reconsidered; we applied a system equal to bags exposed in fixed position, i.e., three bags suspended at three different heights along a nylon thread, as in the protocol for exposure at fixed positions. It could be likely that in these conditions the bags can shield mutually, due to displacement of air produced while moving, influencing the uptake. Also, the proximal bag could face a wind too fast, determining the formation of a boundary layer. As a consequence, the air could pass externally to the proximal bag, without crossing the sample, impeding or reducing the PM interception and entrapment, which could explain the lower element content often found in this bag. To reduce replica variability, a single larger moss bag, possibly a flat or spherical bag could be more appropriate and moss material could be homogenized before dividing it in three analytical replicas. It is noticeable that the heterogeneity of the chemical data set (Table S2) found no match in the SIRM data, in which replicas were always consistent with each other and between - replica variance was low. This could depend on the different target of the two techniques, being ICP-MS aimed at quantifying all elements analyzed, whereas SIRM is sensitive only to magnetizable elements (Fe, Co and Ni), which represent a subset of the analyzed elements, and could eventually be co-transported. This consideration could also explain why different scores of the pollution levels characterizing the land-uses were observed based on SIRM and ICP-MS data, although the industrial area resulted the most impacted according to both analyses.

A large variability in element content was even observed in bags exposed along all U routes, at parity of exposure time (i.e., about 24h). It is likely that the very short exposure time, compared to any other biomonitoring study based on fixed bags, could be responsible for the heterogeneity found. The exposure time could play an important role for data homogenization and could represent a key factor for the reliability of the technique (Capozzi et al., 2016b); in fact, where the elemental input was stronger, i.e., along the 7I route, a clear signal was observed, specifically for elements of environmental concern, like As, Cd, Ni, Pb and Sb. These elements accumulated in the 7I route and 7T route, the latter of course as the effect of the contribution of the industrial route to the

total path. It is likely that longer exposure times could provide more accurate data, giving information on the pollution level along each route and emphasizing the differences related to the land use. However, the fact that element concentrations, fluxes and even PM levels provided a similar trend with the highest elemental load measured at I route, followed by U routes, T route and the lowest at G route, indicates that the method is sensitive to the different land uses. It is worth noting that Al accumulated only along G route, together with Si and Ti; these elements, regarded as markers of terrigenous inputs, could derive by road dust resuspension occurring while bicycling along the unpaved path, even if further investigations, possibly with higher exposure times and higher number of green and industrial routes, are needed to reach a steady conclusion.

Although significant differences were observed between routes and elements, we did not present ANOVA results for element contents or accumulation, since they are affected by the different exposure time. Therefore, we prefer to discuss ANOVA analysis on flux data, which are normalized on the exposure time (i.e., daily based) for all the elements and routes. The formula of element flux, developed in a previous work (Capozzi et al., 2020), depends on the specific leaf area, which is considered constant in each species, and on the exposure time; therefore, this parameter can be profitably used when moss bags filled with the same species are exposed for different times, even in different conditions. Taking advantage of the above, we compared fluxes calculated for this experimental design, with fluxes calculated for bags filled with *H. cupressiforme* moss and exposed in open air and fixed position in the same study area (i.e., Antwerp city; Sorrentino et al., 2021). The comparison showed that the fluxes of elements in the "mobile bags" were significantly higher than element fluxes measured in "fixed bags" for five elements. This result agrees with literature data; García-Seoane et al. (2019), observed that wind could increase the element uptake in moss bags filled by *Sphagnum palustre* L.; the authors found indeed that metal uptake capacity for As, Cu, Fe, Pb and V in the moss bags attached to weathervanes was higher than in the moss bags attached to static poles. In our case, the magnitude of element fluxes while bicycling was about 10 to 25 folds higher than in fixed position, for several elements in the tested industrial area. All the results based on the comparison between static and moving bags suggest an increased risk of personal exposure to atmospheric pollution while moving (bikes): just as movement implies a major air volume passing through the bags, it aslo implies a higher volume of air inhaled by the cyclist, and therefore, a greater accumulation of pollutants.

However, these results should be considered with caution and verified by further experiments over longer periods, based on higher numbers of exposure points and routes.

## 4. Conclusions

This work encourages further studies based on the moss-bag technique for air biomonitoring with mobile systems (bicycles or even motorcycles) since it highlights the capacity of this device to uptake airborne pollutants even when exposed while travelling. However, some critical issues have arisen that lead to reconsidering the exposure conditions to obtain more reliable results. Specifically, the importance of the exposure times and the possibility to adopt analytical replicas instead of experimental ones, could be studied in depth, with the aim to understand the mechanisms under the high replica variability in element contents observed in this work. Although different pollution levels were highlighted among the land uses investigated in this pilot work, a fine tuning of the methodology could bring to a better sensitivity in case of more continuous gradient of pollution. SIRM signal of exposed moss samples represents a fast and robust methodology to gain information about airborne element pollution, even in moving systems. In general, both SIRM and element fluxes of exposed mosses, as well as PM concentrations measured in the atmosphere indicated the industrial route as the most polluted and the green route as the area having the lowest level of pollution. Further, the comparison between pollution level measured in static and moving bags in terms of element fluxes, indicates that the magnitude of the exposure is significantly higher in moving systems than in fixed positions, at parity of land use. Mobile biomonitoring by SIRM and ICP-MS of moss transplants seems a promising approach that could provide new outcomes, or a broader application, in the evaluation of the total personal exposure to air pollution.

## References

Archibald, A. T., Folberth, G., Wade, D. C., and Scott, D., 2017. A world avoided: impacts of changes in anthropogenic emissions on the burden and effects of air pollutants in Europe and North America. Farad. Discuss. doi: 10.1039/C7FD00004A

Ares, A., Aboal, J.R., Carballeira, A., Fernandez, J.A., 2015. Do moss bags containing devitalized *Sphagnum denticulatum* reflect heavy metal concentrations in bulk deposition? Ecol. Indic. 50, 90-98. https://doi.org/10.1016/j.ecolind.2014.10.030.

Brunekreef, B., Holgate, S. T., 2002. Air pollution and health. The Lancet. 360, 1233-1242, https://doi.org/10.1016/S0140-6736(02)11274-8.

Canha, N., Almeida, S. M., Freitas, M. C., Wolterbeek, H. T., 2014 Indoor and outdoor biomonitoring using lichens at urban and rural primary schools. J. Tox.Env. Health. Part A, 77, 14-16, 900-915, https://doi.org/10.1080/15287394.2014.911130

Capozzi, F., Giordano, S., Di Palma, A., Spagnuolo, V., De Nicola, F., Adamo, P., 2016a. Biomonitoring of atmospheric pollution by moss bags: discriminating urbanrural structure in a fragmented landscape. Chemosphere 149, 211-218.

Capozzi, F., Giordano, S., Aboal, J.R., Adamo, P., Bargagli, R., Boquete, T., Di Palma, A., Real, C., Reski, R., Spagnuolo, V., Steinbauer, K., Tretiach, M., Varela, Z., Zechmeister, H., Fernández, J.A. 2016b. Best options for the exposure of traditional and innovative moss bags: A systematic evaluation in three European countries. Environ. Pollut. 214, 362-373, https://doi.org/10.1016/j.envpol.2016.04.043.

Capozzi, F., Di Palma, A., Adamo, P., Sorrentino, M.C., Giordano, S., Spagnuolo, V., 2019. Indoor vs. outdoor airborne element array: a novel approach using moss bags to explore possible pollution sources. Environ. Pollut., 249, 566-572, https://doi.org/10.1016/J.ENVPOL.2019.03.012.

Capozzi, F., Sorrentino, M.C., Di Palma, A., Mele, F., Arena, C., Adamo, P., Spagnuolo, V., Giordano, S., 2020. Implication of vitality, seasonality and specific leaf area on PAH uptake in moss and lichen transplanted in bags. Ecol. Indic. 108, 105727, https://doi.org/10.1016/j.ecolind.2019.105727.

Castanheiro, A., Hofman, J., Nuyts, G., Joosen, S., Spassov, S., Blust, R., Lenaerts, S., De Wael, K., Samson, R., 2020. Leaf accumulation of atmospheric dust: Biomagnetic,

morphological and elemental evaluation using SEM, ED-XRF and HR-ICP-MS. Atmos. Environ. 221, 117082 https://doi.org/10.1016/J.ATMOSENV.2019.117082

Conti, M.E., Cecchetti, G., 2001. Biological monitoring: lichens as bioindicators of air pollution assessment — a review. Environ. Pollut. 114, 471-492. https://doi.org/10.1016/S0269-7491(00)00224-4.

Couto, J.A., Aboal, J.R., Fernández, J.A., Carballeira, A., 2004. A new method for testing the sensitivity of active biomonitoring: an example of its application to a terrestrial moss. Chemosphere, 57, 303-308. https://doi.org/10.1016/j.chemosphere.2004.05.036.

Di Palma, A., Capozzi, F., Spagnuolo, V., Adamo, P., Giordano, S., 2017. Atmospheric particulate matter intercepted by moss-bags: Relations to moss trace element uptake and land use. Chemosphere, 176, 361–368.

Duan, K., Sun, G., Zhang, Y., Yahya, K., Wang, K., Madden, J. M., Caldwell, P. V., Cohen, E.C., McNulty, S.G. (2017). Impact of air pollution induced climate change on water availability and ecosystem productivity in the conterminous United States. Climatic Change, 140, 259–272 DOI 10.1007/s10584-016-1850-7

García-Seoane, R., Fernández, J.A., Chilà, A., Aboa, J.R., 2019. Improving the uptake of pollutants in moss bags: The wind effect. Ecol. Ind. 107, 105577. https://doi.org/10.1016/j.ecolind.2019.105577.

Giordano, S., Adamo, P., Spagnuolo, V., Vaglieco, B. M. 2010 Instrumental and bio-monitoring of heavy metal and nanoparticle emissions from diesel engine exhaust in controlled environment.

J. Environ. Sci, 22, 1357-1363.

https://doi.org/10.1016/S1001-0742(09)60262-X.

Goddu, S. R., Appel, E., Jordanova, D., Wehland, F., 2004. Magnetic properties of road dust from Visakhapatnam (India)−−relationship to industrial pollution and road traffic. Physics and Chemistry of the Earth, Parts A/B/C, 29, 985−995.

Hofman, J., Maher, B., Adrian, A., Muxworthy, R., Wuyts, K., Castanheiro, A., Samson, R., 2017. Biomagnetic monitoring of atmospheric pollution: a review of magnetic signatures from biological sensors. Environ. Sci. Technol. 51, 6648−6664 https://doi.org/10.1021/acs.est.7b00832.

Hunt, A., Jones, J., Oldfield, F., 1984. Magnetic measurements and heavy metals in atmospheric particulates of anthropogenic origin. Sci. Total Environ. 33, 129-139. https://doi.org/10.1016/0048-9697(84)90387-5.

Kapper, K.L., Bautista, F., Goguitchaishvili, A., Bógalo, M.F., Cejudo-Ruíz, R., Cervantes, S.M. 2020. The use and misuse of magnetic methods to monitor environmental pollution in urban areas. Boletín Soc. Geológica Mex., 72, 1–44

Kardel, F., Wuyts, K., Babanezhad, M., Vitharana, U.W.A., Wuytack, T., Potters, G., Samson, R., 2010. Assessing urban habitat quality based on specific leaf area and stomatal characteristics of Plantago lanceolata L., Environ. Pollut. 158, 788-794. https://doi.org/10.1016/j.envpol.2009.10.006.

Kardel, F., Wuyts, K., Maher, B.A., Hansard, R., Samson, R., 2011. Leaf saturation isothermal remanent magnetization (SIRM) as a proxy for particulate matter monitoring: Inter-species differences and in-season variation. Atmos. Environ. 45, 5164-5171. https://doi.org/10.1016/j.atmosenv.2011.06.025.

Kardel, F., Wuyts, K., De Wael, K., Samson, R., 2018. Biomonitoring of atmospheric particulate pollution via chemical composition and magnetic properties of roadside tree leaves. Environ. Sci. Pollut. Res. 25, 25994–26004. https://doi.org/10.1007/s11356-018-2592-z.

Oves, M., Khan, M.S., Zaidi, A., Ahmad, E. 2012. Soil contamination, nutritive value, and human health risk assessment of heavy metals: an overview. Toxicity of heavy metals to legumes and bioremediation, pp. 1-27

Pope III, C.A., Burnett, R.T., Thun, M.J., Calle E.E., Krewski, D., Ito, K., Thurston, G. D., 2002. Lung Cancer, Cardiopulmonary Mortality, and Long-term Exposure to Fine Particulate Air Pollution. JAMA. 287, 1132–1141. doi:10.1001/jama.287.9.1132

Sanità di Toppi, L., Sanità di Toppi, L., Bellini, E., 2020. Novel coronavirus: how atmospheric particulate affects our environment and health. Challenges, 11, p. 6

Sorrentino, M.C., Wuyts, K., Joosen, S., Mubiana, V. K., Giordano, S., Samson R., Capozzi, F., Spagnuolo V. Multi-elemental profile and enviromagnetic analysis of moss transplants exposed indoors and outdoors in Italy and Belgium. Submitted

Turgut, E. T., Gaga E. O., Jovanović, G., Odabasi, M., Artun G., Ari, A., Urošević, M. A. 2019. Elemental characterization of general aviation aircraft emissions using moss bags. Environ. Sci. Pollut. Res., 26, 26925-26938.

Vuković, G., Aničić Urošević, M., Tomašević, M., Samson, R., Popović, A., 2015. Biomagnetic monitoring of urban air pollution using moss bags (*Sphagnum girgensohnii*). Ecol. Ind. 52, 40-47, https://doi.org/10.1016/j.ecolind.2014.11.018.

Wei, X., Lyu, S., Yu, Y., Wang, Z., Liu, H., Pan, D., Chen, J., 2017. Phylloremediation of air pollutants: exploiting the potential of plant leaves and leaf-associated microbes. Front. Plant. Sci. 8,1-23. https://www.frontiersin.org/articles/10.3389/fpls.2017.01318/full

Zechmeister, H.G., Rivera, M., Köllensperger, G., Marrugat J., Künzli, N., 2020. Indoor monitoring of heavy metals and NO2 using active monitoring by moss and Palmes diffusion tubes. Environ. Sci. Eur. 32, 156 https://doi.org/10.1186/s12302-020-00439-x.

# Conclusions

The present PhD dissertation has examined the relationships between plants and environmental pollutants, particularly heavy metals, and PAHs, highlighting the role of these organisms in the studies concerning both soil phytoremediation and biomonitoring of airborne contaminants. Plant-pollutant interactions are essentially based on absorption and adsorption mechanisms, which play a different role in biomonitoring and phytoremediation.

In soil phytoremediation, pollutants enter plant tissue essentially via root, and therefore absorption prevails on adsorption. This can explain the wide range of effects, which can be studied in plants undergoing phytoremediation experiments. In this respect, the use of a multidisciplinary approach (plant morphology and physiology; chemical analysis) can allow crossing the different data sets, and evaluate them in a global way, which is especially important to formulate realistic hypotheses and verify the results from different points of view, reaching steady conclusions.

In this regard, the doctoral work illustrated in the Chapters 1 to 3 clearly evidences two response patterns observed in cardoon under metal stress. Two cultivars (i.e., Sardo and Siciliano), while being able to accumulate Cd and Pb, exhibit a limited tolerance, displaying several morphophysiological damages, or inadequate responses to face metal-induced stress, in contrast to the most tolerant cultivar, i.e., Spagnolo. In general, the experiments carried out on the industrial soil demonstrate that the three cultivars examined act as hyperaccumulators since their metal contents were overall higher than the promptly available fraction measured in the soil. However, they can be considered as phyto-extractant only for Cd, this heavy metal being the only largely translocated to shoot.

The Spagnolo cardoon shows the best performance under metal stress condition (both grown on contaminated soil and in hydroponics), operating a prompt, multiple response at morphological and physiological levels. This is achieved by balancing structural and functional traits, with a global positive impact on plant tolerance and growth. In other words, the ability of Spagnolo plants to modify leaf structure and physiological traits (stomata number, photosynthesis efficacy, antioxidant power) under heavy metal contamination, to maintain high photosynthetic efficiency, leads to a real resilience of this cultivar to metal stress. In parallel, the work also highlights the existence of common responses and cultivar-specific responses, as well as new parameters, i.e., root hairs

development and stomata modulation, to be used as early proxies in the selection of candidate species for phytoremediation.

In air biomonitoring, pollutant uptake by plants that behave as bioaccumulators, is mainly grounded on passive mechanisms and specific morphological traits; in fact, the pollutants, moving through the atmosphere mostly linked to PM, interact especially with the shoot. A small fraction of pollutants coming into plant tissue via stomata, can enter the plasma membrane, and thus, be absorbed. However, most airborne pollutants are not absorbed, but only adsorbed or remain outside the cell surface; in other words, pollutants do not pass the plasma membrane. Therefore, the accumulation of airborne pollutants in biomonitors largely depend on morphological traits of the biomonitors, such as surface to mass ratio (surface is important for pollutant interception), leaf micromorphology, and leaf or thallus architecture, rather than vitality and metabolic patterns. These considerations are consistent with the results obtained in biomonitoring experiments here presented; particularly, biomonitor vitality does not affect pollutant uptake. Oven devitalization of the plant material represents a way to have ready-to-use samples of moss and lichen, even some time after harvesting. As a further advantage, oven devitalization drops the baseline pollutant content enhancing the sensitivity of the biomaterial, allowing pollutant detection even at low concentration in the environment. Regarding PAHs, in vascular plants these hydrophobic contaminants accumulate in leaf cuticle, but in cryptogams, which lack cuticle, uptake mechanisms were poorly investigated so far. Although in biomonitoring by cryptogams most airborne pollutants are adsorbed on biomonitor surface, PAHs display a different behavior since they move partly in vapor phase, and partly as particles. The work carried out on PAH uptake provides for the first time an overview on PAH accumulation by moss and lichen transplants in relation to vitality and morphological traits of the two biomonitors. The thickness of the thallus is a key trait to preserve low molecular weight (vapor) PAHs and favor their storage. In fact, according to the specific morphological traits, lichen PAH profile after exposure mainly covers 2-4 rings PAHs (vapor and particle phase), whereas moss prevalently accumulates 4-6 rings PAHs (mostly particle phase); hence, their combined use could be appropriate for PAH biomonitoring in anthropized environments. Specific leaf area is an important feature in the analysis of PAH uptake, since it considers both surface and thallus thickness, two key traits to clarify accumulation mechanisms of these pollutants. Biomonitoring studies here presented, focused on airborne elemental pollution, highlight that element accumulation in moss samples exposed in bags may occur both in confined

environments (houses), as well as in dynamic systems (i.e., in moss bags carried by bicycles). Indoor element pollution is qualitatively related to outdoor pollution, but the amount of indoor pollution could be modulated by life habits of inhabitants. Specific indoor sources can be identified when the concentration of an element is greater inside houses (indoor) and there is no correlation between indoor and outdoor concentrations for the same element. Further, for the first time it is demonstrated that moss bags can be valuably used to estimate the magnitude of the exposure to air pollution in mobile systems, also discriminating pollution levels related to the different land uses. However, the adjustment of the exposure protocol (longer exposure times and the use of analytical replicas instead of different samples) could provide more reliable results. Moreover, thanks to the development of a daily flux formula, it is possible to compare the magnitude of the exposure related to different times. Both indoor and mobile biomonitoring by moss transplants seem promising approaches, providing new outcomes in the evaluation of the total personal exposure to elemental air pollution. Finally, the efficacy and versatility of the moss-bag approach in the different exposure conditions here tested, suggest the urgency of an intercalibration between this technique and the air samplers estimating air quality. Once available, these data could allow the use of moss bags to estimate the risk of human exposure to atmospheric pollutants.

# References

Aboal, J.R., Concha-Graña, E., De Nicola, F., Muniategui-Lorenzo, S., López-Mahía, P., Giordano, S., Capozzi, F., Di Palma, A., Reski, R., Zechmeister, H., Martínez-Abaigar, J., Fernández, J.A., 2020. Testing a novel biotechnological passive sampler for monitoring atmospheric PAH pollution. J. Hazard. Mater. 381, 120949. https://doi.org/10.1016/j.jhazmat.2019.120949.

Alloway, B.J., 1995. The origin of heavy metals in soils. In: Alloway BJ (ed) Heavy metals in soils, 2nd edn. Blackie Academic and Professional, Glasgow, pp 38–55.

Al-Qurainy, F., Alameri, A.A., Khan, S.A., 2010. RAPD profile for the assessment of genotoxicity on a medicinal plant; Eruca sativa. J. Med. Plants Res., 4, 579-586.

Arena, C., Figlioli, F., Sorrentino, M.C., Izzo, L.G., Capozzi, F., Giordano, S., Spagnuolo, V., 2017. Ultrastructural, protein and photosynthetic alterations induced by Pb and Cd in *Cynara cardunculus* L., and its potential for phytoremediation. Ecotoxicol. Environ. Safety. 145, 83-89. https://doi.org/10.1016/j.ecoenv.2017.07.015.

Bo, M., Salizzoni, P., Clerico, M., Buccolieri, R. 2017. Assessment of indoor-outdoor particulate matter air pollution: a review. Atmosphere. 8, 136. https://doi.org/10.3390/atmos8080136

Boominathan, R., Doran, P.M. 2003. Cadmium tolerance and antioxidative defenses in hairy roots of the cadmium hyperaccumulator, Thlaspi caerulescens. Biotechnol. Bioeng., 83, 158-167.

Brockerhoff, M., 2000. An urbanizing world. Popul. Bull. 55 (3)

Capozzi, F., Adamo, P., Spagnuolo, V., Giordano, S., 2021. Field comparison between moss and lichen PAHs uptake abilities based on deposition fluxes and diagnostic ratios. Ecol. Ind., 120, 106954, https://doi.org/10.1016/j.ecolind.2020.106954.

Chandra, R., Kang, H., 2016. Mixed heavy metal stress on photosynthesis, transpiration rate, and chlorophyll content in poplar hybrids. Forest. Sci. Technol. 12, 55–61. https://doi.org/10.1080/21580103.2015.1044024

Cunningham, S. D., Berti, W. R., & Huang, J. W., 1995. Phytoremediation of contaminated soils. Trends in Biotechnology, 13, 393–397.

De Agostini, A., Cortis, P., Cogoni, A., 2020. Monitoring of air pollution by moss bags around an oil refinery: a critical evaluation over 16 years. Atmosphere. 11, 272. https://doi.org/10.3390/atmos11030272

Desalme, D., Binet, P., Chiapusio, G., 2013. Challenges in tracing the fate and effects of atmospheric polycyclic aromatic hydrocarbon deposition in vascular plants. Environ Sci Technol. 47 j:3967-81. doi: 10.1021/es304964b.

Di Palma, A., Capozzi, F., Spagnuolo, V., Giordano, S., Adamo, P., 2017. Atmospheric particulate matter intercepted by moss-bags: Relations to moss trace element uptake and land use. Chemosphere, 2017, 361-368. https://doi.org/10.1016/j.chemosphere.2017.02.120.

DoŁęgowska, S., Migaszewski, Z. M., 2011. PAH concentrations in the moss species *Hylocomium splendens* (Hedw.) B.S.G. and *Pleurozium schreberi* (Brid.) Mitt. from the Kielce area (south-central Poland). Ecotoxicol. Environ. Safe. 74, 1636-1644. https://doi.org/10.1016/j.ecoenv.2011.05.011.

García-Seoane, R., Fernández, J.A., Chilà, A., Aboal, J.R., 2019. Improving the uptake of pollutants in moss bags: The wind effect. Ecol. Ind. 107, 105577. https://doi.org/10.1016/j.ecolind.2019.105577

Gurjar, B., Nagpure, A.S., Singh, T.P., 2012. Air quality in megacities. http://www.eoearth.org/view/article/149934.

Fedoroff, N. V., Battisti, D. S., Beachy, R. N., Cooper, P. J. M., Fischhoff, D. A., Hodges, C. N., Knauf, V. C., Lobell, D., Mazur, B. J., Molden, D., Reynolds, M. P., Ronald, P. C., Rosegrant, M. W., Sanchez, P. A., Vonshak, A., Zhu. J.-K., 2010. Radically Rethinking Agriculture for the 21st Century. Science, 327, 833-834 DOI: 10.1126/science.1186834

Foley, J.A., De Fries, R., Asner, G.P., Barford, C., Bonan, G., Carpenter, S.R., Chapin, F.S., Coe, M.T., Daily, G.C., Gibbs, H.K., Helkowski, J.H., Holloway, T., Howard, E.A., Kucharik, C.J., Monfreda, C., Patz, J.A., Prentice, I.C., Ramankutty, N., Snyder, P.K., 2005. Global consequences of land use. Science 309:570–574

Lee, B.X.Y., Hadibarata, T., Yuniarto, A., 2020. Phytoremediation Mechanisms in Air Pollution Control: a Review. Water Air Soil Pollut. 231, 437. https://doi.org/10.1007/s11270-020-04813-6

León, A. M., Palma, J. M., Corpas, F. J., Gómez, M., Romero-Puertas, M. C., Chatterjee, D., Mateos, R. M., del Río, L. A., Sandalio, L. M., 2002. Antioxidative enzymes in cultivars of pepper plants with different sensitivity to cadmium. Plant Physio. Biochem. 40, 813-820. https://doi.org/10.1016/S0981-9428(02)01444-4.

Meggeson, T.P., Hall, N.W., 1999. An investigation into the spatial and temporal distribution of lead, cadmium and zinc in contemporary soils and paleosols in a high arctic and an arctic alpine environment. In: Abstracts of 'European Perspectives on Land Contamination Conference' Soc. of the Chem. Ind., London. Land Contamination and Reclamation 7(4).

Maertens, R. M., Bailey, J., White, P. A., 2004. The mutagenic hazards of settled house dust: a review. Mutation Research/Reviews in Mutation Research. 567, 401-425. https://doi.org/10.1016/j.mrrev.2004.08.004.

Molas, J.,2002. Changes of chloroplast ultrastructure and total chlorophyll concentration in cabbage leaves caused by excess of organic Ni(II) complexes. Environ. Exp. Bot. 47, 115–126. https://doi.org/10. 1016/S0098-8472(01)00116-2

Motuzova, G.V., Minkina, T.M., Karpova, E.A., Barsova, N.U., Mandzhieva, S.S., 2014. Soil contamination with heavy metals as a potential and real risk to the environment. J. Geochem. Explor. 144:241–246

Nedjimi, B., 2021 Phytoremediation: a sustainable environmental technology for heavy metals decontamination. SN Appl. Sci. 3, 286. https://doi.org/10.1007/s42452-021-04301-4

Nriagu, J.O. 1978. The biogeochemistry of Lead in the environment. Pp 18-88. Amsterdam: Elsevier.

Ötvös, E., Kozák, I.O., Fekete, J., Sharma, V.K., Tuba, Z., 2004. Atmospheric deposition of polycyclic aromatic hydrocarbons (PAHs) in mosses (*Hypnum cupressiforme)* in Hungary, Science of The Total Environment, 330, 89-99, https://doi.org/10.1016/j.scitotenv.2004.02.019.

Khan, A., Khan, S., Khan, M.A., Qamar Z., Waqas, M., 2015. The uptake and bioaccumulation of heavy metals by food plants, their effects on plants nutrients, and associated health risk: a review. Environ. Sci. Pollut. Res. 22, 13772–13799. https://doi.org/10.1007/s11356-015-4881-0

Raccuia, S. A., Mainolfi, A., Mandolino, G., & Melilli, M. G. 2004. Genetic diversity in *Cynara cardunculus* revealed by AFLP markers: comparison between cultivars and wild types from Sicily. Plant Breeding, 123, 280-284

Raccuia, S. A., & Melilli, M. G. 2007. Biomass and grain oil yields in *Cynara cardunculus* L. genotypes grown in a Mediterranean environment. Field Crops Research, 101, 187-197.

Raccuia, S. A., & Melilli, M. G. 2010. Seasonal dynamics of biomass, inulin, and water-soluble sugars in roots of *Cynara cardunculus* L. Field crops research, 116, 147-153

Ravindra, K., Sokhi, R., Van Grieken, R. 2008. Atmospheric polycyclic aromatic hydrocarbons: Source attribution, emission factors and regulation. Atmos. Environ. 42, 2895-2921. https://doi.org/10.1016/j.atmosenv.2007.12.010.

Sanità di Toppi, L., Gabbrielli, R., 1999. Response to cadmium in higher plants. Environ. Exp. Bot. 41, 105-130. https://doi.org/10.1016/S0098-8472(98)00058-6.

Sharma, N., Agarwal, A.K., Eastwood, P., Gupta, T., Singh, A.P., 2018. Introduction to air pollution and its control. In: Sharma N., Agarwal A., Eastwood P., Gupta T., Singh A. (eds) Air Pollution and Control. Energy, Environment, and Sustainability. Springer, Singapore. https://doi.org/10.1007/978-981-10-7185-0_1

Sitaras, I.E., Siskos, P.A., 2008. The role of primary and secondary air pollutants in atmospheric pollution: Athens urban area as a case study. Environ Chem Lett 6, 59–69. https://doi.org/10.1007/s10311-007-0123-0

Sorrentino, M.C., Capozzi, F., Giordano, S., Spagnuolo,V., 2017. Genotoxic effect of Pb and Cd on in vitro cultures of *Sphagnum palustre*: An evaluation by ISSR markers. Chemosphere 181, 208-215.

Skórzyńska-Polit, E., Baszyński, T., 1997. Differences in sensitivity of the photosynthetic apparatus in Cd-stressed runner bean plants in relation to their age. Plant Sci. 128, 11–21.

Su, C., Jiang, L.Q., Zhang, W.J., 2014. A review on heavy metal contamination in the soil worldwide: Situation, impact and remediation techniques. Environ. Skep. Crit. 3, 24-38.

Toscano, V., Sollima, L., Genovese, C., Melilli, M. G., & Raccuia, S. A., 2016. Pilot plant system for biodiesel and pellet production from cardoon: technical and economic feasibility. Acta Horticulturae, (1147), 429–442. doi:10.17660/actahortic.2016.1147.60

Thangavel, P., Subhuram, C.V., 2004. Phytoextraction–Role of hyperaccumulators in metal contaminated soils. Proceedings of the Indian National Science Academy. 70, 109–130.

Vuković, G., Urošević, M. A., Razumenić, I., Kuzmanoski, M., Pergal, M., Škrivanj, S., Popović, A., 2014. Air quality in urban parking garages (PM10, major and trace elements, PAHs): Instrumental measurements vs. active moss biomonitoring. Atmos. Environ. 85, 31-40. https://doi.org/10.1016/j.atmosenv.2013.11.053.

Zohary, D. J., Basnizki, 1975. The cultivated artichoke *Cynara scolymus*. Its probable wild ancestors. Econ. Bot, 29, 233-235.

Zhu, J.K., 2016. Abiotic Stress Signaling and Responses in Plants. Cell. 167, 313-324. https://doi.org/10.1016/j.cell.2016.08.029

## Sitografy

https://www.unfpa.org/publications/unfpa-annual-report-2004
https://population.un.org/wup/Publications/Files/WUP2018-Report.pdf
http://www.who.int/mediacentre/news/releases/2014/air-pollution/en/
https://www.mossclone.eu